Genetic manipulation and genetic-based dissection of tumor-specific immunity

Mezzadra, R.

Genetic manipulation and genetic-based dissection of tumor-specific immunity

Proefschrift
ter verkrijging van
de graad van Doctor aan de Universiteit Leiden
op gezag van Rector Magnificus Prof.Mr. C.J.J.M. Stolker,
volgens besluit van het College voor Promoties
te verdedigen op dinsdag 19 februari 2019
klokke 15:00 uur

door
Riccardo Mezzadra

geboren te Milaan
in 1985

Promotor:

Prof.dr. Ton N. Schumacher

Co-supervisor:

Prof.dr. Daniel S. Peeper

Promotiecommissie:

Prof.dr. John B.A.G. Haanen

Prof.dr. Jannie Borst (University of Amsterdam)

Prof.dr. Jacques Neefjes

Prof.dr. Thijn R. Brummelkamp (Utrecht University)

Table of content

Chapter 1

Scope of the thesis

The immune system has evolved to provide protection against pathogens and is composed of two arms, the innate and the adaptive immune system. The innate arm of the immune system can offer a rapid, relatively non-specific, first line of defense that is triggered by pathogen-associated molecular patterns and by endogenous signals that are induced upon tissue damage. The adaptive arm of the immune system, on the contrary, provides a pathogen specific defense, takes longer to become fully activated and can last after an infection has been cleared in order to be quickly reactivated in case of a novel encounter with the same pathogen, providing so-called immunological memory[1]. Cytotoxic T cells, characterized by CD8 expression, constitute a key component of the adaptive arm of the immune system and provide protection by their ability to recognize and eliminate pathogen-infected cells.

The sole determinant of the specificity of a T cell is its T cell receptor (TCR) that is different in every T cell clonotype. TCRs recognize specific combinations of peptide - major histocompatibility complexes (pMHCs)[1]. In the case of cytotoxic T cells, these pMHC complexes are composed of peptide fragments generated by the endogenous antigen presentation machinery (APM) that are bound by MHC class I molecules. In addition to having the capacity to recognize and kill pathogen-infected cells, cytotoxic T cells have the capability of recognizing malignant cells, provided they present peptide-MHC complexes for which a TCR repertoire exists[2-5]. As during their development T cells are educated in order not to recognize "self" peptides, a major class of epitopes that are presented by tumor cells and that can be recognized by tumor-specific T cells in non-virus associated malignancies is represented by neoepitopes that are derived from somatic mutations[6].

Evasion of immune recognition is now broadly acknowledged as one of the hallmarks of cancer development[7], and evidence to support the notion that cytotoxic T cells are an important component of the antitumoral immune response comes from a number of research lines. In particular, seminal work by Schreiber and colleagues demonstrated that mice lacking an adaptive immune system are more susceptible to carcinogen-induced tumors, and that these tumors fail to engraft in immune competent, but not in immunodeficient, hosts upon transplantation[8]. In human cancer, indirect evidence for escape of immune control was obtained by a publication in which analysis of large datasets of tumor exomes and transcriptomes revealed that expression of genes associated with cytolytic activity of T and NK cells is correlated with mutations in the antigen presentation pathway, and that observed a lower frequency than expected of mutations that can give rise to potential neoepitopes[9]. The MHC genes in the human population are highly polymorphic and different MHC alleles have the ability to present distinct series of peptides. For this reason, loss of a single MHC allele will

already reduce the repertoire of peptides that can be presented by a cell. Loss of heterozygosity of MHC has been shown to be a frequent phenomenon during non-small cell lung cancer development[10], consistent with a model in which avoidance of immune-mediated destruction leads to a selective advantage of cancer cells[11].

Direct evidence documenting the capability of the immune system to recognize and eliminate cancer cells is formed by clinical data in which reinvigoration of tumor-specific T cell responses induces tumor regression[11]. Firstly, isolation, *in vitro* expansion and reinfusion of tumor infiltrating lymphocytes (TIL) isolated from melanoma patients has shown durable antitumoral effects in a fraction of patients[12], and at least part of this antitumoral activity was retained when only cytotoxic T cells were administered[13]. Moreover, interference with inhibitory receptors that modulate the activity of T cells, also known as immune checkpoints, has resulted in prolonged clinical benefit in cancer patients. In particular, blockade of CTLA-4, which prevents activating ligands to bind to the costimulatory molecule CD28 on T cells, has resulted in clinical benefit in melanoma patients. Furthermore, blockade of PD-1 signaling, which inhibits T cell activity following TCR triggering, has shown remarkable clinical benefit in multiple types of cancer [14,15]. In line with a role for T cells in these therapies, the number of non-synonymous mutations is a positive predictor of clinical outcome[16-18], and tumors of histological types that are characterized by higher mutational loads generally respond better to agents blocking PD-1 than tumor types that are characterized by limited numbers of genomic aberrations[19]. Furthermore, intratumoral presence of CD8 T cells predicts positive outcome of PD-1 blocking therapies in melanoma[20] and loss of T cell-targeted neoepitopes[21] and defects in antigen presentation mechanism have been associated with resistance[22,23] during T cell-based immunotherapeutic approaches.

Collectively, these data sketch a model in which, for at least a subset of human tumors, evasion of a T cell-based immune response is a positive driver of tumor growth, and for these tumors reversal of this immune evasion can result in clinical benefit. As a second important conclusion that comes from these data, the evidence indicating that tumors may differ in their degree of foreignness, as shown by the correlation between the number of non-synonymous mutations and response to T cell checkpoint blockade, suggests that for a fraction of human cancers insufficient antigens may be present to rely on the endogenous T cell repertoire. Thus, we can identify two conceptually distinct parameters as critically required for a T cell-based antitumor response. First, a tumor-specific T cell repertoire needs to be present. Second, this T cell pool needs to be able to function in the face of a potentially suppressive tumor micro-environment. Both these parameters can now be manipulated in the clinic.

As discussed above, approaches aimed at relieving T cell suppression are one of the most exciting recent developments in oncology[24]. In addition for those patients in which a tumor specific T cell response is lacking, T cells can be genetically redirected towards them, by introducing an exogenous TCR or an artificial receptor (e.g. a chimeric antigen receptor) to confer a desired specificity upon them[25].

This thesis touches upon both these requirements of tumor specific T cell responses, by on the one hand exploring novel technologies for the de novo generation of tumor-specific T cell responses in cases where those are of insufficient magnitude, and, on the other hand, exploiting genetic screening technologies to further understand how tumor cells can escape from T cell-mediated immune response. [24,25]

In **Chapter 2** of this thesis, we discuss how technological advances have been used in recent years to interrogate the TCR repertoire of tumor-infiltrating T cells. Furthermore, we discuss the first studies that employed these techniques for investigating the link between cancer exomes and the intratumoral TCR pool and we discuss how this novel knowledge may potentially be used clinically. We for example propose approaches for personalized TCR gene therapy, and we discuss how this kind of therapy would benefit from non-viral gene transfer systems for T cell modification, such as transposons. Transposon-based gene transfer systems are based on the simultaneous introduction in a cell of a donor DNA sequence, the transposon, and of an enzyme, the transposase, that can catalyze stable integration of the transposon into the genome of the target cells. The use of these non-viral gene transfer systems in primary cells has cost and practicality advantages as compared to viral systems, but also has two main drawbacks in primary T cells, i.e. high toxicity and low gene transfer efficiency.

In **Chapter 3** we propose and evaluate a strategy to obtain cell populations with a high frequency of transposon-modified cells shortly after transfection, by using a traceless selection system. Transposon based modification of cells relies on transient DNA transfection and a large part of the initially transfected cells do not achieve a stable integration. By including a cell surface selection marker in the plasmid expressing the transposase, we were able to select, shortly after transfection, those cells in which the transposase was particularly highly expressed and in which transposition was more likely. A system that, similarly to transposons, relies on transient expression of an auxiliary gene for inducing stable modification in the genome is the CRISPR/Cas9 system. In the same chapter we showed that introduction of a selection system in a plasmid that encodes the Cas9 could be used for selecting those cells that were more likely to undergo CRISPR/Cas9 mediated genome editing. Also, we showed that

the same selection marker can be used to deplete those cells harboring unwanted integration of the plasmid expressing the auxiliary gene, something that may reduce toxicity concerns associated with long-term transposase or Cas9 expression.

In **Chapter 4** we aim to address the second major issue regarding the use of transposons for T cell redirection, which is represented by their high degree of toxicity, likely due to intracellular sensing of plasmid DNA. We design a high throughput, flow-based screen system to interrogate a library of biologically active compounds in an unbiased manner, in order to identify small molecules that would reduce transfection-mediated toxicity. In this way we identify and characterize the effect of a Cdc-25 inhibitor on transposon-transfected T cells. By treating transfected cells with the inhibitor, toxicity of transposon-based gene transfer is to some extent reduced and, as a consequence, gene transfer efficiency is increased.

In **Chapter 5** we introduce the topic of tumor evasion of immune attack by reviewing the literature on the PD-L1 checkpoint. PD-L1 is at this point considered the immunosuppressive molecule of greatest clinical relevance, as blocking antibodies that target either itself or its main ligand, PD-1 have shown durable responses in different types of malignancies. In this chapter we first discuss the role of the PD-1–PD-L1 inhibitory axis in infection and cancer, then we review the successes and limitations of PD-1–PD-L1 targeting agents. Subsequently, we discuss the current understanding of the multilayered regulation of PD-L1 expression and how an improved understanding of PD-L1 regulation (e.g. by identifying those cases in which PD-L1 upregulation is not a consequence of immune pressure but rather a byproduct of certain oncogenic events), can be used both to select those patients that are more likely to respond to PD-1–PD-L1 blocking immunotherapies and to rationally improve current immunotherapeutic approaches.

As recent evidence suggests that increasing the amount of PD-L1 protein on a given cell would result in a more profound suppression of T cell functions[26,27], in **Chapter 6** we aim to investigate PD-L1 regulatory mechanisms. In order to discover potentially undescribed layers of PD-L1 regulation, we perform a flow-based haploid genetic screen for modulators of PD-L1 expression. Among the positive regulators of PD-L1 expression, we identify CMTM6, a transmembrane protein of previously undescribed function, as one of the most prominent hits. We demonstrate that CMTM6 stabilizes PD-L1 in multiple cancer cell systems and in primary dendritic cells. Mechanistically, CMTM6 increases the PD-L1 pool by increasing the half-life of PD-L1 molecules. In order to reveal possible backup mechanisms of CMTM6, we subsequently perform a screen for PD-L1 regulators in CMTM6 deficient cells, and thereby identify CMTM4

as a second regulator. Simultaneous suppression of CMTM6 and CMTM4 expression results in further reduction of PD-L1 levels, and genetic complementation of CMTM6 deficient cells with CMTM4 was sufficient to revert the phenotype. Together with work from Burr and colleagues[28], these data reveal that PD-L1 is present at the cell surface in complex with CMTM6 (and possibly other proteins), and suggest that targeting of CMTM6 may potentially be used to influence the PD-1 – PD-L1 axis.

In **Chapter 7** we aim to reveal cancer cell-intrinsic mechanisms that can alleviate T cell-mediated cytotoxicity, by performing a genome-wide haploid screen for resistance mechanisms to T cell killing. We describe that the main driver of toxicity in HAP1 cells is represented by interferon (IFN)-γ, and we demonstrate that IFN-γ-mediated toxicity causes apoptosis and is associated with induction of a DNA damage response. The toxic effect of IFN-γ in this cell system can be attenuated by interference with SLFN11, a gene whose loss has previously been shown to confer resistance to DNA damaging agents. Interestingly, we observed that in other cell systems, exposure to IFN-γ was not inducing the same degree of toxicity, and in these systems this toxicity was not attenuated by suppression of SLFN11. We therefore concluded that in certain contexts SLFN11 can couple IFN-γ-induced toxicity to the DNA damage response and thereby influence how tumor cells respond to this T cell effector mechanism.

Finally, in **Chapter 8** I start from the work presented in this thesis to pose a series of questions that in my view require a better understanding. Those questions concern the optimal strategies to redirect T cells, how to improve stratification of patients for cancer immunotherapies, how to further understand the role of CMTM6 in PD-L1 regulation, the potentials and limitations of screens in immunotherapy, and the cancer cell-intrinsic role of IFN-γ. For each of these, I firstly briefly discuss the current understanding of the topic, I then try to analyze where the limitations lie in our current knowledge, and I finally suggest how the field may move forward in order to overcome these limitations.

References

1 Murphy, K., Travers, P., Walport, M. & Janeway, C. *Janeway's immunobiology*. (Garland Science, 2012).

2 van der Bruggen, P. *et al.* A gene encoding an antigen recognized by cytolytic T lymphocytes on a human melanoma. *Science (New York, N.Y.)* **254**, 1643-1647 (1991).

3 Wolfel, T. *et al.* A p16INK4a-insensitive CDK4 mutant targeted by cytolytic T lymphocytes in a human melanoma. *Science (New York, N.Y.)* **269**, 1281-1284 (1995).

4 Kvistborg, P. *et al.* TIL therapy broadens the tumor-reactive CD8(+) T cell compartment in melanoma patients. *Oncoimmunology* **1**, 409-418 (2012).

5 van Rooij, N. *et al.* Tumor exome analysis reveals neoantigen-specific T-cell reactivity in an ipilimumab-responsive melanoma. *J Clin Oncol* **31**, e439-442, doi:10.1200/JCO.2012.47.7521 (2013).

6 Schumacher, T. N. & Schreiber, R. D. Neoantigens in cancer immunotherapy. *Science (New York, N.Y.)* **348**, 69-74, doi:10.1126/science.aaa4971 (2015).

7 Hanahan, D. & Weinberg, R. A. Hallmarks of cancer: the next generation. *Cell* **144**, 646-674, doi:10.1016/j.cell.2011.02.013 (2011).

8 Shankaran, V. *et al.* IFNgamma and lymphocytes prevent primary tumour development and shape tumour immunogenicity. *Nature* **410**, 1107-1111, doi:10.1038/35074122 (2001).

9 Rooney, M. S., Shukla, S. A., Wu, C. J., Getz, G. & Hacohen, N. Molecular and genetic properties of tumors associated with local immune cytolytic activity. *Cell* **160**, 48-61, doi:10.1016/j.cell.2014.12.033 (2015).

10 McGranahan, N. *et al.* Allele-Specific HLA Loss and Immune Escape in Lung Cancer Evolution. *Cell* **171**, 1259-1271.e1211, doi:10.1016/j.cell.2017.10.001 (2017).

11 Chen, D. S. & Mellman, I. Oncology meets immunology: the cancer-immunity cycle. *Immunity* **39**, 1-10, doi:10.1016/j.immuni.2013.07.012 (2013).

12 Rosenberg, S. A. *et al.* Durable complete responses in heavily pretreated patients with metastatic melanoma using T-cell transfer immunotherapy. *Clinical cancer research : an official journal of the American Association for Cancer Research* **17**, 4550-4557, doi:10.1158/1078-0432.ccr-11-0116 (2011).

13 Dudley, M. E. *et al.* Randomized Selection Design Trial Evaluating CD8+-Enriched Versus Unselected Tumor-Infiltrating Lymphocytes for Adoptive Cell Therapy for Patients With Melanoma. *Journal of Clinical Oncology* **31**, 2152-2159, doi:10.1200/jco.2012.46.6441 (2013).

14 Hodi, F. S. *et al.* Improved survival with ipilimumab in patients with metastatic melanoma. *The New England journal of medicine* **363**, 711-723, doi:10.1056/NEJMoa1003466 (2010).

15 Topalian, S. L. *et al.* Safety, activity, and immune correlates of anti-PD-1 antibody in cancer. *The New England journal of medicine* **366**, 2443-2454, doi:10.1056/NEJMoa1200690 (2012).

16 Rizvi, N. A. *et al.* Cancer immunology. Mutational landscape determines sensitivity to PD-1 blockade in non-small cell lung cancer. *Science (New York, N.Y.)* **348**, 124-128, doi:10.1126/science.aaa1348 (2015).

17 Snyder, A. *et al.* Genetic basis for clinical response to CTLA-4 blockade in melanoma. *The New England journal of medicine* **371**, 2189-2199, doi:10.1056/NEJMoa1406498 (2014).

18 Hellmann, M. D. *et al.* Tumor Mutational Burden and Efficacy of Nivolumab Monotherapy and in Combination with Ipilimumab in Small-Cell Lung Cancer. *Cancer Cell* **33**, 853-861 e854, doi:10.1016/j.ccell.2018.04.001 (2018).

19 Yarchoan, M., Hopkins, A. & Jaffee, E. M. Tumor Mutational Burden and Response Rate to PD-1 Inhibition. *The New England journal of medicine* **377**, 2500-2501, doi:10.1056/NEJMc1713444 (2017).

20 Tumeh, P. C. *et al.* PD-1 blockade induces responses by inhibiting adaptive immune resistance. *Nature* **515**, 568-571, doi:10.1038/nature13954 (2014).

21 Verdegaal, E. M. *et al.* Neoantigen landscape dynamics during human melanoma-T cell interactions. *Nature* **536**, 91-95, doi:10.1038/nature18945 (2016).

22 Sade-Feldman, M. *et al.* Resistance to checkpoint blockade therapy through inactivation of antigen presentation. *Nat Commun* **8**, 1136, doi:10.1038/s41467-017-01062-w (2017).
23 Zaretsky, J. M. *et al.* Mutations Associated with Acquired Resistance to PD-1 Blockade in Melanoma. *The New England journal of medicine* **375**, 819-829, doi:10.1056/NEJMoa1604958 (2016).
24 Mellman, I., Coukos, G. & Dranoff, G. Cancer immunotherapy comes of age. *Nature* **480**, 480-489, doi:10.1038/nature10673 (2011).
25 June, C. H., Riddell, S. R. & Schumacher, T. N. Adoptive cellular therapy: a race to the finish line. *Sci Transl Med* **7**, 280ps287, doi:10.1126/scitranslmed.aaa3643 (2015).
26 Kataoka, K. *et al.* Aberrant PD-L1 expression through 3'-UTR disruption in multiple cancers. *Nature* **534**, 402-406, doi:10.1038/nature18294 (2016).
27 Noguchi, T. *et al.* Temporally Distinct PD-L1 Expression by Tumor and Host Cells Contributes to Immune Escape. *Cancer Immunol Res* **5**, 106-117, doi:10.1158/2326-6066.CIR-16-0391 (2017).
28 Burr, M. L. *et al.* CMTM6 maintains the expression of PD-L1 and regulates anti-tumour immunity. *Nature* **549**, 101-105, doi:10.1038/nature23643 (2017).

2

Chapter 2

TCR repertoires of intratumoral T-cell subsets

Carsten Linnemann, Riccardo Mezzadra and Ton N. M. Schumacher

Division of Immunology, The Netherlands Cancer Institute (NKI-AVL), Amsterdam, the Netherlands.

Immunol Rev. 2014 Jan;257(1):72-82

Cancer is a genetic disease. The accumulation of genetic mutations within tumor cells leads to changes in their proteome, and it is this change which controls the process of cellular transformation. By the same token, through this process of genetic mutation, a 'cancer anti-genome'[1] is generated that may be recognized by T cells. The spectrum of epitopes that forms the cancer anti-genome includes peptides from genes that are aberrantly expressed within tumor cells, but also the 'neo-antigens' that arise as a direct consequence of somatic mutations within tumor cells. While human tumor types display clear mutational signatures that reflect the underlying mutational process[2], the specific mutations found in any pair of tumors of a given histology are in most cases largely distinct[3]. As such, even tumors of the same histological origin do exhibit highly diverse cancer anti-genomes.

The diversity of human tumors that is seen at the genetic level is paralleled by a strong diversity in the T-cell infiltrates within the tumor lesions. This variability not only concerns the magnitude of the T-cell infiltrate, but also the ratio of different T-cell subsets and their location within the tumor (summarized in[4]). An important unsolved issue here is which factors determine the nature of the T-cell infiltrate in human tumors. Tumor-intrinsic factors that are likely to play a role include the size of the cancer anti-genome and the pro- or anti-inflammatory consequences of the specific mutations within an individual tumor. Tumor-extrinsic factors that could conceivably play a role include patient genotype, possibly including the HLA haplotype, and perhaps even microbiome.

The magnitude and composition of the intratumoral T-cell infiltrate shows a clear correlation with clinical prognosis in a number of human tumor types (summarized in[4]). In particular a fierce infiltration of $CD8^+$ T cells has been shown to correlate with an improved clinical outcome in a number of tumor types. For other T-cell subsets (e.g. Tregs), the data obtained thus far are more ambiguous, possibly in part because of methodological differences.

While the observed correlation between the extent of $CD8^+$ T-cell infiltration (or $CD8^+$ T cell/Treg ratio) and clinical prognosis has often been interpreted as evidence for a role of these $CD8^+$ T cells in tumor control, the evidence is obviously indirect. Indeed, with melanoma as a notable exception[5-7], the evidence that the intratumoral T-cell repertoire is commonly tumor reactive in human cancers is thus far lacking.

On a related note, the analyses of the intratumoral T-cell infiltrates that have thus far been carried out have largely disregarded the T-cell receptor (TCR) repertoire that is expressed by these T cells. The reactivity of the TCRs expressed by intratumoral T cells will critically determine their capacity to interact with other cells in the tumor microenvironment, and because of this, it seems plausible that the TCR repertoire found in intratumoral T-cell subsets may form a prognostic signature or predictive signature in cancer (immuno-) therapies. As such, analysis of the characteristics of the intratumoral TCR repertoire with respect to its (i) diversity; (ii) degree of tumor-reactivity; and (iii) antigen specificity will likely be informative. Moreover, an understanding of how these factors are modulated by immunotherapeutic intervention may provide important insights into the mechanism of action of such therapies.

In this review, we discuss the potential value of new technologies and tools for the analysis of intratumoral TCR repertoires. Furthermore, we provide a perspective on how these recent technological advancements may be exploited to utilize intratumoral TCR repertoires for personalized immunotherapies.

Understanding intratumoral TCR repertoires

Diversity of the intratumoral TCR repertoire

In contrast to TCRα alleles, which in approximately 20% of all T cells are both functionally recombined[8], TCRβ alleles are subjected to strict allelic exclusion. Because of this, TCR β-chain usage can be used as a straightforward means to analyze the diversity of TCR repertoires. Traditionally, such analyses have been performed by flow cytometry using TCR Vβ-segment specific antibodies[9], or by CDR3 size spectratyping[10]. However, the resolution of these approaches is only modest, as TCR clonotypes using the same TCR Vβ-segment or with the same CDR3 length cannot be distinguished. With the development of next generation sequencing (NGS), techniques have been developed that can reveal the nucleotide sequences of all TCRβ CDR3 sequences present within a given T-cell population. Because of the immense read depth that can be achieved, NGS of TCR repertoires allows the quantitative detection of even low-frequency TCR sequences [note that proper filtering to exclude sequence errors[11] is required]. Furthermore, because of the high diversity of the TCRβ CDR3 repertoire, the sequences obtained will in most cases represent individual TCR clonotypes (a noted exception are TCRs sharing a common/public TCR β-chain but distinct TCR α-chains). NGS sequencing of TCRβ CDR3 has first been used in a study that analyzed the TCR distribution among various T-cell compartments in a healthy individual[12]. More recently, the technology has also been implemented to analyze TCR repertoires in disease settings, such as TCR reconstitution upon allogeneic hematopoietic stem cell transplantation[13].

The TCR repertoire diversity of different T-cell subsets (e.g. $CD8^+$ effector T cells) found within different human tumors has not been studied systematically thus far. As exceptions, Sherwood *et al*.[14] assessed the TCR diversity of tumor-infiltrating lymphocytes (TILs) derived from colorectal cancer and compared it to the TCR repertoire of mucosa-infiltrating T cells. This study revealed that the TCR repertoire diversity in colorectal cancer TILs is more restricted compared with TCR repertoires found among mucosal T cells and variable between patients[14]. In another study, the same group analyzed the TCR repertoire of TILs in ovarian cancer, showing them to be largely distinct from circulating T cells[15]. It will be interesting to assess whether the steady-state diversity of intratumoral TCR repertoires correlates with clinical prognosis, and, more importantly, whether (changes in) TCR repertoire diversity among intratumoral T cells may be a predictive marker for a clinical response following immunotherapeutic interventions, such as TIL therapy or T-cell checkpoint blockade. Given the rapid progress in the development of high-throughput sequencing technologies, the use of TCRβ CDR3-sequencing for patient selection would seem a realistic option with regards to time and financial requirements.

Tumor reactivity of the intratumoral TCR repertoire

The analysis of TCR repertoire diversity by bulk TCR gene sequencing reveals the total number of TCRs present in a T-cell population and the extent of clonal dominance within such populations. As outlined above, such data may prove valuable in the context of biomarker identification. Furthermore, because the TCRβ sequences obtained function as genetic barcodes, such information may also be used to describe kinship between different intratumoral T-cell subsets[16]. As a downside, this method does not identify the TCRαβ pairs of individual T cells, implying that the information cannot be utilized to analyze or reconstruct the tumor reactivity or antigen specificity of the intratumoral TCR pool.

Understanding which fraction of intratumoral T cells is reactive to tumor cells and which determinants these cells recognize is of obvious interest. Thus far, the tumor-reactivity of the intratumoral T-cell pool has primarily been assessed in two ways. First, the ability of bulk tumor-resident T cells to recognize HLA-matched allogeneic or (preferably) autologous tumor has been studied in functional assays from the 1980s until today, primarily for melanoma[17-19]. These assays give a straightforward overview of the functional capacity of the T cells on a population level and this type of analysis has inspired the development of TIL therapy[20,21]. Second, in several studies, T-cell clones generated from intratumoral T cells have been utilized to obtain TCR genes that could subsequently be shown to confer tumor reactivity after TCR gene transfer[22-24]. Furthermore, TCRs obtained in this fashion have been utilized in the first clinical studies of TCR gene therapy[25,26].

As a downside to these approaches, both these strategies will not capture the activity of T cells that do carry a tumor-reactive TCR but have been rendered anergic. Furthermore, since these studies commonly utilized *in vitro* expanded T-cell material, they are restricted to those T cells that can expand *in vitro*, thereby likely resulting in a significant bias or even precluding analysis altogether (e.g. for tumor types for which such T-cell expansion cannot be achieved). Therefore, while these studies have provided ample evidence for the presence of tumor-reactivity within the intratumoral pool of T cells, by their nature they cannot provide an unbiased enumeration of the 'true' fraction of tumor-reactive T cells within human tumors.

To obtain a better understanding of the tumor reactivity within intratumoral TCR repertoires, it would be of value to determine the frequency of tumor-reactive TCRs among different intratumoral T-cell subsets without a requirement for (prolonged) *in vitro* expansion. Toward this goal, we propose to isolate large libraries of TCRαβ gene pairs directly from intratumoral T cells. Identified TCR pairs can then be

introduced in peripheral blood lymphocytes by gene transfer, to allow assessment of autologous tumor recognition independent of the parental T-cell phenotype. Such analyses could be focused on intratumoral $CD8^+$ T cells but may also be of interest for the heterogeneous population of intratumoral $CD4^+$ T-cell subsets, for which studies on tumor-reactivity are particularly limited at this moment. This type of autologous TCR gene transfer experiments would provide insights into several aspects of the intratumoral TCR repertoire. First, in analogy to the analysis of TCR repertoire diversity (see above), the frequency of tumor-reactive TCRs may represent a prognostic or predictive clinical marker. Second and somewhat related, these analyses would establish whether the previously described correlation between tumor infiltrating lymphocyte numbers and clinical prognosis can be explained by the tumor-recognition capacity of the tumor-resident TCR repertoire. Finally, such studies would make it is feasible to explore whether the frequency or diversity of tumor-reactive TCRs found in intratumoral TCR repertoires correlates with the size of the cancer anti-genome, as for instance reflected by the mutational load of tumors.

The isolation of the large TCR libraries that are required for such experiments has become a realistic option following the development of a number of strategies to identify TCRαβ gene pairs[27-29]. First, the sequencing of cDNA generated from single T cells has proven a viable strategy to identify TCRαβ pairs[27,28]. To date, these strategies have not been utilized to dissect intratumoral TCR repertoires, but this will likely prove feasible. In addition, our laboratory has developed an independent method to infer TCRαβ sequences directly from the genome (rather than RNA) of T cells that has already been utilized to recreate TCR pairs from intratumoral T cells. This approach, called 'TCR gene capture' utilizes an RNA-bait library targeting the TCRαβ and TCRβ loci to specifically select and sequence genomic fragments encoding the TCR sequences of T cells[29] (*Fig.* 1).

TCR gene capture has proven a versatile tool to analyze TCR repertoires within intratumoral $CD8^+$ T cells. First, with the goal to identify TCRs that may be used clinically, we have utilized the technique to assemble TCR libraries from single T cells expanded *in vitro* for a short period. Using MHC-multimer selected T cells as input, this resulted in the identification of a large panel of TCRs against shared tumor-antigens (we isolated 21 different TCRs against nine distinct Cancer/Germline antigens). In addition, we isolated a library of 19 different tumor-reactive TCRs from a library of clonal tumor-reactive T-cell populations from a melanoma patient without further knowledge of their antigen specificity. The latter data illustrate that the tumor-reactive TCR repertoire of intratumoral $CD8^+$ T cells can be broad and that it is feasible to rapidly assemble a library of patient-specific tumor-reactive TCRs. Second, since

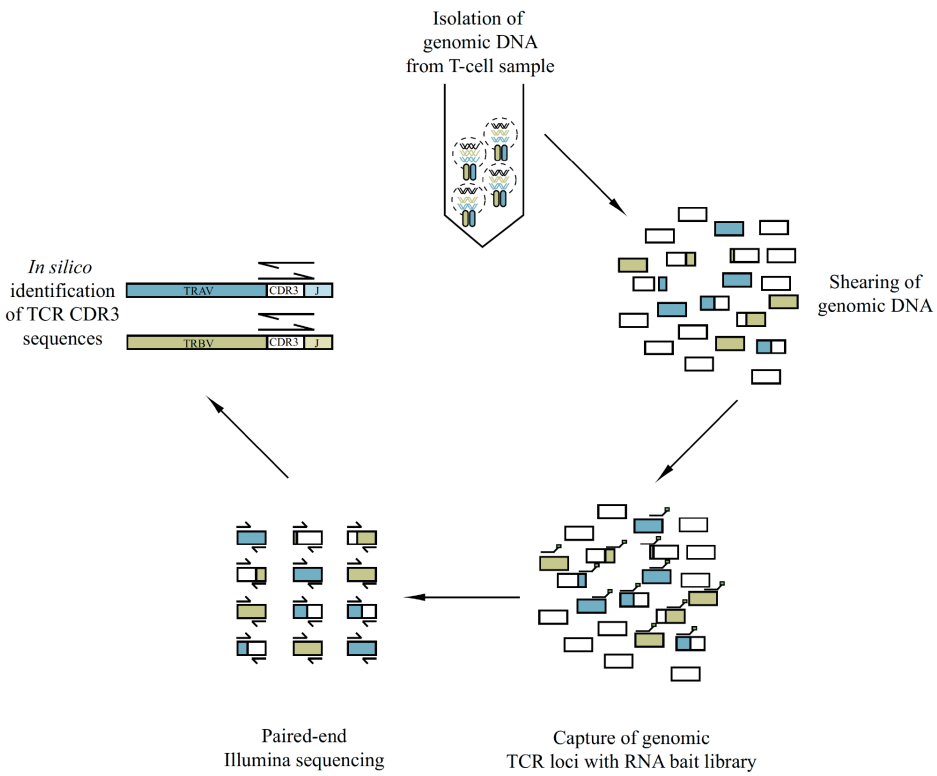

Figure 1: Schematic representation of T-cell receptor (TCR) gene capture approach. Genomic DNA is extracted from (oligo)clonal T-cell populations of interest, the DNA is sheared into small fragments (average length 500 basepairs). Using an RNA-bait library targeting all functional TCR V- and J-segments on both the TCRα and TCRβ loci, all DNA fragments encoding TCR sequences are selected and subsequently analyzed by paired-end Illumina sequencing. Using bioinformatic tools , TCR CDR3 sequences are identified in the resulting sequencing data.

TCR gene capture supplies quantitative read counts for all TCR α- and β-sequences within the sample, TCRαβ pairs can be directly identified within oligoclonal T-cell populations through matching of TCR α- and β-sequences that occur with similar frequency. For polyclonal T-cell populations, such 'frequency-based matching' will be precluded by the occurrence of multiple TCR clonotypes at the same frequency. However, we have successfully unraveled the TCR repertoire of several intratumoral $CD8^+$ T-cell populations specific for shared melanoma antigens (Meloe-1, MAGE-A1, MAGE-10, TAG-1, LAGE-1) by this approach. In these experiments, in which bulk MHC-multimer positive T-cell populations from TILs were used as input for TCR gene capture, the TCR repertoire of the tumor antigen-specific T-cell populations analyzed

commonly was restricted to only 1–5 TCRs. Comparison of the TCR diversity within individual tumor antigen-specific T-cell populations and within the entire tumor-reactive T-cell pool may in future studies perhaps be used to provide a first estimate of the breadth of the antigen repertoire that is recognized.

Using TCR gene capture, it has also proven feasible to identify dominant TCRs within the intratumoral tumor-reactive T-cell population without knowledge of their antigen specificity. Specifically, profiling of the TCR repertoire of three TCRVβ subpopulations among intratumoral, tumor-reactive $CD8^+$ T cells showed that the TCR repertoire in each of these subpopulations was markedly restricted: the two most abundant TCRs comprised at least 75% of all functional TCRαβ CDR3 sequences. This recognition allowed the straightforward identification of tumor-reactive TCRαβ pairs.

Both the recently developed single cell-based approaches and the TCR gene capture strategy described above will be of substantially value to increase our understanding of the intratumoral TCR repertoire in human cancers. Nevertheless, the development of technologies that can sample the repertoire of intratumoral TCRαβ pairs at even greater depth (e.g. revealing the identity of many thousands of TCRαβ pairs) remains an important goal. The recent description of an emulsion-PCR based approach to identify TCRαβ pairs from single cells that are contained within droplets is of interest[30]. While further technical developments will clearly be required to allow an unbiased analysis of TCR repertoires with this type of technology, it does offers the potential to advance capacities for (intratumoral) TCR profiling well beyond the currently available medium-throughput approaches.

Antigen specificity of the intratumoral TCR repertoire

In particular for intratumoral T cells in melanoma, convincing evidence for tumor reactivity is provided by the clinical responses seen in patients that are treated with autologous TIL products. Furthermore, the fact that such clinical responses have also been observed in patients treated with $CD8^+$ enriched TIL cell products[31] maps at least part of the clinically relevant tumor reactivity toward the cytotoxic T-cell subset. At present, our understanding of the critical cancer regression antigens in TIL therapy is limited. A better understanding of the role of different antigens in the clinical responses in patients receiving TIL therapy (or other non-antigen directed immunotherapies, such as blockade of CTLA-4 or PD-1) would possibly enable the 'engineering' of anti-tumor immunity in the large group of patients who do not benefit from current immunotherapies. Because of this, a large effort has been made over past few years to reveal the antigen-specificity of tumor-specific $CD8^+$ T-cell response in patients receiving immunotherapy.

As demonstrated by pioneering work by Altman and Davis[32], fluorescently labeled multimeric pMHC-complexes can be used to detect antigen-specific T cells with high sensitivity and independent of their functional capacities. However, the large-scale screens that are required to assess the antigen specificity of the intratumoral T-cell pool by MHC multimer-based analyses have only become feasible with two subsequent developments: (i) the generation of a high-throughput pipeline to obtain the pMHC collections required for such monitoring and (ii) the design of experimental approaches for multiplexed analysis that allows comprehensive screens to be performed with clinically realistic amounts of biological material.

To obtain very large collections of pMHC-complexes in a high throughput fashion, we have developed (and now routinely use) a peptide exchange technology in which collections of pMHC complexes of interest can be generated in a 1 h procedure[33,34]. This approach is based on the use of pMHC-complexes that carry a peptide ligand that cleaves itself upon UV exposure, and by exposing such conditional pMHC complexes to UV light in the presence of peptide ligands of interest. Peptide exchange technology is now available for around two dozen HLA class I alleles[33-35] (M. Toebes and L. van Dijk personal communication), also through work from the Grotenbreg lab[36]. As a side note, recent work demonstrates that MHC multimer-based detection of antigen-specific T cells is highly sensitive to minor sequence variation between HLA subtypes (M. M. van Buuren, F. E. Dijkgraaf, C. Linnemann, M. Toebes, C. X. L. Chang, J. Y. Mok, M. Nguyen, W. J. E. van Esch, P. Kvistborg, G. M. Grotenbreg and T. N. M. Schumacher, manuscript submitted). The requirement for proper matching between patient HLA alleles and HLA tools used for immunomonitoring that is revealed by these data will make it essential to further expand the HLA-based toolkit in the years to come.

To allow the analysis of T-cell reactivity against many (potential) tumor antigens in MHC-multimer-based screens, both our group and the Davis laboratory have developed the concept of combinatorial MHC-multimer staining[37,38]. In this approach, each pMHC complex is coupled to a unique combination of fluorochromes or more recently lanthanides (see below). The use of such coding schemes then allows one to define the pMHC specificity of individual T cells/TCRs by the combinatorial code that they bind. In addition to offering the possibility of multiplexed analysis, this approach also markedly increases the sensitivity of pMHC-based T-cell detection, enabling the unambiguous detection of low-frequency antigen-specific T-cell populations[38]. The fluorochrome-based combinatorial coding schemes that to date have been used to analyze tumor-specific T-cell responses allow analysis of around 30 T-cell responses within a single sample. Furthermore, as an interesting extension of this approach, Newell and Davis recently demonstrated that the use of combinatorial coding

schemes in MHC multimer mass cytometry can allow multiplexed analysis at an even higher complexity[39].

In recent studies, the combination of UV-mediated peptide exchange and combinatorial coding has been used to study the T cell/TCR repertoire in TIL products used for adoptive T-cell therapy of melanoma patients[40,41]. In work that analyzed T-cell reactivity against a panel of around 150 shared melanoma-associated tumor antigens (TAAs), reactivity patterns in more than 50 TIL products were analyzed. While this work was primarily restricted to the HLA-A2 allele – few shared TAA are known for most other HLA class I alleles – several important conclusions can be drawn from these studies. First, in every TIL culture, an essentially unique pattern of antigen reactivities was found. Furthermore, for the few antigen-TIL product combinations for which this was examined, expression of a given melanocyte differentiation antigen/cancer-germline antigen was generally accompanied by the presence of T cells specific for this epitope, suggesting that tumor antigen expression may in most cases be noted by the immune system (note that a larger data set will certainly be required to test this notion in a rigorous manner). These T-cell monitoring data extend the concept of 'tumor heterogeneity' – described above for tumor genomes and for T-cell infiltrates – to the TCR specificities of the intratumoral $CD8^+$ T-cell pool. A second important observation made in these studies has been that the frequency of antigen-specific T cells that were detected for the shared TAA used in these studies was very low (median of less than 1% for all HLA-A2-restricted T-cell responses detected per TIL product). Even taking into account the fact that T-cell reactivity against the five other possible HLA alleles was not measured, these data suggest that reactivity against shared TAA may only explain part of the composition of clinically used TIL products. As a first explanation for this discrepancy, the fraction of non-tumor reactive 'bystander' TCR specificities in TIL products may in many cases be high. As a second explanation, a large fraction of the tumor-specific TCRs within the intratumoral repertoire may recognize highly patient-specific antigens. Early evidence for a (perhaps small) contribution by bystander cells has been obtained by the detection of low frequencies of CMV and EBV-specific T cells in TIL products. However, the contribution of bystander cells may be addressed in a more definitive manner by the isolation of large TCR libraries from the intratumoral TCR repertoire and their subsequent characterization with regards to tumor-reactivity (see section 'Tumor-reactivity of the intratumoral TCR repertoire'). With respect to the second possibility, the particularly high mutational load of melanoma and other tumors, such as lung cancer, raises the question whether the intratumoral T-cell repertoire could contain a variety of TCRs that recognize neo-antigens derived from tumor-specific mutations, thereby forming a highly personalized, tumor-reactive TCR repertoire.

Recent and exciting studies in animal models by the Sahin and Schreiber groups[42,43] have demonstrated that cancer exome sequencing data may be utilized to analyze T-cell reactivities against neo-antigens formed by tumor-specific mutations. The ability to dissect T-cell reactivity against neo-antigens on the basis of human cancer exome data has now also been demonstrated by others and us. Rosenberg *et al*.[44] have utilized cancer exome sequencing data and recognition of target cells loaded with putative neo-antigens by autologous $CD8^+$ TILs to uncover neo-antigen-specific T-cell reactivity within TIL products. On average, two T-cell responses against neo-antigens were identified in the three patients analyzed. As neo-antigen-specific T-cell reactivity was only analyzed for some of the HLA alleles expressed by these patients, these data suggest that TILs may potentially recognize a series of patient-specific antigens. However, as this study focused on patients that experienced a particularly strong clinical response upon TIL therapy, it is possible that broad neo-antigen-specific T-cell reactivity may not be invariably present in melanoma, and it will be important to extend these studies to address this issue. In parallel work, our group has provided proof of concept for the combination of cancer exome sequencing and MHC-multimer technologies to reveal T-cell responses against patient-specific neo-antigens arising from genomic mutations[45]. Comparison of whole exome sequencing data of a melanoma tumor with that of autologous healthy tissue revealed more than 1000 non-synonymous changes resulting in altered open reading frames. These data were then combined with RNA-expression data to predict potential neo-epitopes for four of the HLA class I alleles expressed by this patient. When TILs from this patient were then screened with a library of MHC-multimers containing these putative T-cell epitopes, two neo-antigen-specific T-cell responses were identified: a low-frequency response against a mutated peptide of ZNF462 gene (0.003% of $CD8^+$ T cells) and a dominant response (3.3% of $CD8^+$ T cells) against a neo-antigen derived from the ATR DNA damage response gene. The magnitude of the T-cell response against the ATR neo-antigen was of a considerably higher magnitude than virtually all of the T-cell responses against shared antigens seen in our previous analyses of TILs[40,41]. While more data are certainly required, these data suggest that (some) T-cell responses against neo-antigens may perhaps be of a higher magnitude than T-cell responses against shared (self) antigens, due to their foreign nature. Comparison of the tumor recognition potential of neo-antigen and shared antigen-specific T cells will also be of importance to address the relative importance of the two antigen classes.

Analysis of peripheral blood samples pre- and post-treatment with anti-CTLA-4 showed an approximately fivefold increase in the frequency of ATR-specific $CD8^+$ T cells upon treatment. This increase in frequency, which coincided with a partial tumor regression within this patient, is consistent with the possibility that the T-

cell response against the mutated ATR peptide may have been therapeutically meaningful, but the evidence is obviously indirect. By the same token, Lu *et al*.[46] used cDNA library screening to reveal a T-cell response against a mutated peptide of PPP1R3B in a metastatic melanoma patient, and could show that a long-term T-cell response against this epitope was present in this patient who experienced a durable complete response after TIL therapy.

The recent studies that have started to link cancer exome data to tumor-specific T-cell responses will likely still only sketch a fraction of the patient-specific intratumoral TCR repertoire. As a first issue, imperfection in epitope predictions will lead investigators to miss neo-antigens, in particular for the less well-studied HLA alleles. Furthermore, in addition to neo-antigens that arise as a consequence of single nucleotide variants or insertions/deletions in known open reading frames, it is highly likely that T-cell epitopes arising from alternative translation events[47,48] will also form part of the patient-specific cancer anti-genome. As precedent for the latter, minor histocompatibility antigens, which bear some similarity with neo-antigens in solid tumors (both generally originate from single nucleotide differences), can also be derived from alternative open reading frames[49,50].

A number of developments can be foreseen that will make the identification of patient-specific antigens recognized by the intratumoral TCR repertoire more efficient. First, an increase in the quality/coverage of sequence data and in particular the quality of epitope predictions will facilitate the identification of neo-antigens. With respect to the latter, especially for the less common HLA-A and -B alleles and for the HLA-C alleles, the quality of prediction algorithms may readily be increased by the generation of more input data. As a less biased approach (that altogether avoids the need to predict T-cell epitopes), systems that allow the efficient expression of the entire set of tumor-specific mutations could be valuable, in particular to identify T-cell epitopes from non-canonical sources (e.g. alternative translation events). Finally, the moment it becomes feasible to (roughly) predict the epitope recognized by a TCR on the basis of TCR sequence data (at present a far removed goal), the combination of intratumoral TCR sequence data and cancer exome data could form a strategy to identify patient-specific antigens in a manner that is altogether independent of immunological analyses.

Utilizing intratumoral TCR repertoires

Both TIL therapy and T-cell checkpoint blockade with anti-CTLA4 or anti-PD1 mAbs induce tumor regression in only a fraction of patients[51-53]. One possible reason for therapy failure could be that in many patients the intratumoral TCR repertoire lacks the capacity to recognize any tumor-expressed antigens. However, in particular for tumors with a high mutational load, such as melanoma, smoking-associated lung cancer, and esophageal cancer[2], the numerous changes in protein-sequences should be expected to lead to T-cell epitopes for which thymus-induced tolerance did not occur. The notion that TCR reactivity against neo-epitopes in such tumors with a high mutational load may be present (perhaps at a low level) but does not suffice for tumor control raises the question whether such TCR repertoires could be exploited by other therapeutic strategies.

The majority of mutations found in melanoma and other tumors with a high-mutational load are 'passenger-mutations' that are unrelated to the cellular transformation process[54]. As such, the vast majority of potential neo-epitopes in these cancers are patient-specific. In addition, for the small fraction of mutations that do occur at an appreciable frequency, the polymorphism in HLA-alleles forms a second variable between tumors. For these two reasons, at best a few neo-antigen/HLA combinations will be sufficiently common within the human population to be targeted by off-the-shelf approaches. Consequently, the therapeutic utilization of mutation-induced tumor antigens is likely to benefit primarily from the development of more personalized treatment strategies. Such personalized treatment strategies could either rely on active immunization (i.e. vaccination) or on passive immunization (i.e. adoptive therapy), and two potential approaches that involve the latter, the use of the patient-specific anti-genome in adoptive therapy, are discussed below.

Antigen-specific TIL therapy?

The T cells present in currently used TIL products are not selected to any substantial extent. Depending of the protocol used, the cell product is either formed by those T cells present in the tumor that were able to grow out *in vitro*, or – in case multiple TIL cultures are initiated that are then tested for tumor recognition – those T cells that stochastically were present in the culture that showed the highest degree of tumor recognition. As a first potential step forward, T-cell products may be generated that are derived from those T cells that were enriched on the basis of autologous tumor recognition. This approach can likely be implemented quite readily in clinical protocols and does not rely on any knowledge on the antigen(s) recognized. An implicit assumption in such a process is that T cells with *in vitro* tumor recognition capacity

differ little amongst themselves in their tumoricidal potential under *in vivo* conditions. As an alternative approach, with the increasing ability to identify (patient-specific) tumor antigens recognized by intratumoral T cells, it may become feasible to develop antigen-defined TIL products. In such a strategy, T cells specific for antigens of interest could be enriched by standard MHC multimer or MHC streptamer technology, the latter offering the advantage of reversibility[55]. Such an approach could be argued to offer increased safety compared with current TIL therapy protocols since selected antigen-specificities will form the majority of the cell product infused into the patient. However, in view of the modest T-cell-mediated toxicity in current TIL therapy, the gain here is at best small. More importantly, the anti-tumor effects of a selected TIL product may potentially be enhanced through a number of mechanisms: depletion of (non-reactive) passenger cells, removal of suppressive T-cell subsets, and increased frequency of highly tumor-reactive T cells[56]. As a potential downside, at the current state of technology development, many T-cell responses within TIL products that are reactive with neo-antigens or other relevant antigens are still not identified. As such, the generation of antigen-specific TIL products will result in a narrowing of the tumor-specific T-cell repertoire, and in particular for highly heterogeneous tumors, such a narrowing could conceivably increase the likelihood of tumor escape. Preclinical studies in which the ability of poly-specific or oligo-specific T-cell products to control growth of autologous tumor is examined will be useful to address these issues.

Autologous TCR gene therapy?

The clinical use of TIL therapy is restricted to those few tumor types for which TILs can reliably be grown. In addition, the cells that are obtained are highly differentiated, which is likely to limit the *in vivo* activity of the cells following transfer. TCR gene therapy offers the possibility to overcome the limitations associated with TIL therapy in terms of expansion potential and functional properties of the T-cell product that is given. Thus far, TCR gene therapy has been used exclusively to target tumor-antigens that are shared between large subgroups of patients. Here, we would like to propose the concept of autologous TCR gene therapy: the transfer of a set of autologous tumor-reactive TCRs into 'young' T cells, to effectively target the patient-specific cancer anti-genome (*Fig.* 2).

The isolation and transfer of a numbers of TCRs on a patient-specific basis in a clinically relevant time frame would have appeared unrealistic a few years ago. However, technical advances make such an approach an increasingly feasible goal now. First, the high-throughput isolation of patient-specific TCRs has become possible with the above-described methods to rapidly identify TCRαβ pairs[27-29]. Second, while the production of clinical-grade retrovirus or lentivirus is involved with

regards to both time and finances, alternative non-viral gene transfer systems can now be used for the stable genetic modification of T cells. Transposon-based approaches, such as the hyperactive Sleeping Beauty transposase[57], have been shown to form suitable systems for T-cell engineering[58]. Furthermore, ongoing work suggests that it is feasible to further develop these systems, to reduce transposon related cytotoxicity (A. Hollenstein and R. Mezzadra, manuscript in preparation) and increase the percentage of gene-modified T cells within the cell product (R. Mezzadra, manuscript in preparation).

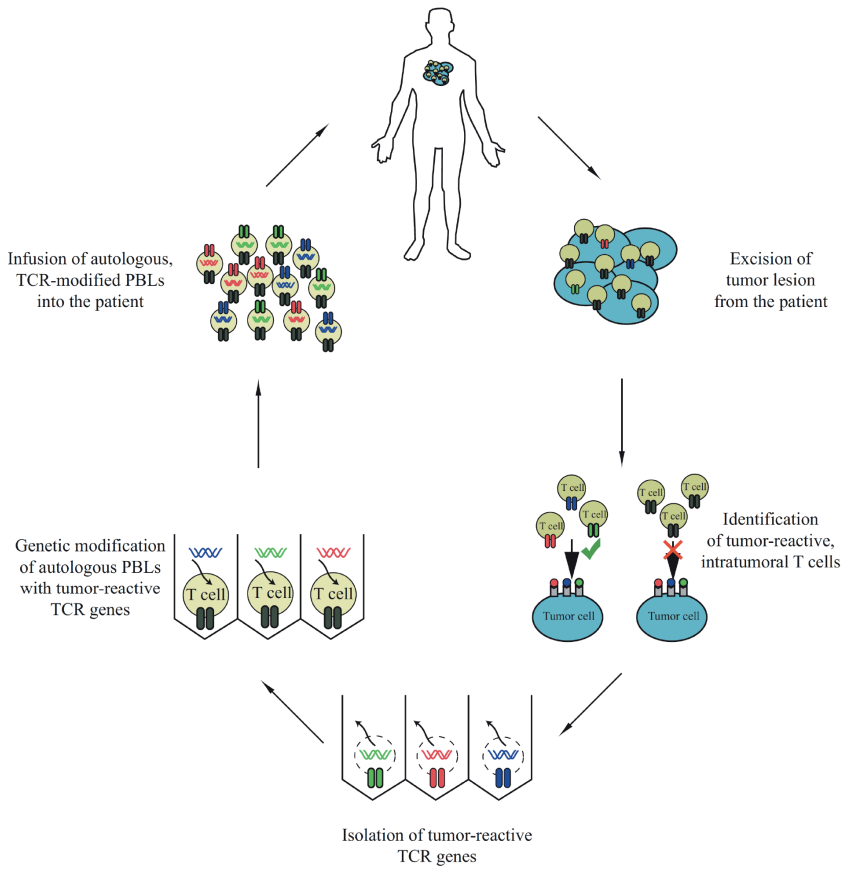

Figure 2: Concept of autologous T-cell receptor (TCR) gene transfer. After excision of a tumor lesion, tumor-reactive intratumoral T cells are identified. Tumor-reactive TCR genes are obtained from such tumor-reactive intratumoral T cells and subsequently utilized for TCR gene transfer into autologous peripheral blood lymphocytes. The resulting tumor-reactive T-cell populations are briefly expanded in vitro and then re-infused into the patient.

For such autologous TCR gene therapy, we consider the simultaneous use of multiple TCRs important to minimize the likelihood of tumor escape, and there is in our view no technical reason why TCR gene therapy should be restricted to a single specificity. The collection of tumor-reactive TCRs that could be used for autologous TCR gene therapy may be generated in a number of different ways. First, a set of TCRs that are reactive with neo-antigens may be created using the tools outlined in this review. Analogous to antigen-specific TIL therapy, this will form a highly safe therapeutic approach since only antigens that are solely expressed within tumor tissue are being targeted.

Second, one could consider the identification of large numbers of autologous tumor-reactive TCRs and their direct use for autologous TCR gene therapy, without knowledge of their antigen specificity. In this way a broad, tumor-reactive TCR repertoire can be utilized that is not restricted by our still limited understanding of the cancer anti-genome. With regards to safety considerations, we note that any TCR transferred in this way will have undergone prior thymic selection in the same individual. Furthermore, with the safety record of transfer of autologous TIL transfer established, there is no *a priori* reason to consider autologous tumor-derived TCR transfer overly risky. Finally, to prevent toxicity due to the 'accidental' engineering of strong T-cell responses against potentially unsafe targets (e.g. some of the MAGE antigens)[59,60], a 'safety-switch' may be co-introduced into the TCR-modified T cells to control their *in vivo* function[61,62].

Concluding remarks

Although it is evident that intratumoral T cells can have the potential to recognize tumor cells, the extent of this tumor recognition and more importantly the specific antigens recognized by intratumoral T cells remain still largely unknown, in particular outside of melanoma. Novel methods for the isolation of TCR genes, allowing the rapid isolation of large TCR libraries from intratumoral T cells, will offer the possibility to assess the antigen-specificity of intratumoral TCRs independent from original (commonly limited) primary material. Furthermore, the availability of such TCR gene libraries may facilitate efforts to locate target epitopes within the cancer anti-genome. The first exploration of these tools suggests that T-cell reactivities against patient-specific, mutated antigens may form an important ingredient of the anti-tumor-potential of the intratumoral TCR repertoire.

Gaining an understanding of the crucial antigen-specificities for cancer regression within intratumoral TCR repertoires could allow the field to improve adoptive T-cell therapies in two ways. First, it may allow the selection/generation of antigen-specific TILs, thereby enabling antigen-directed TIL therapy. Second, it may allow the targeting of the patient-specific cancer anti-genome by autologous TCR gene therapy. Finally, a better understanding of the intratumoral TCR repertoire will also serve to guide the development of active immunotherapies that aim to increase the activity of the tumor-resident T-cell pool.

Acknowledgements

C. L. is a fellow in the PhD Fellowship Program of Boehringer Ingelheim Fonds – Foundation for Basic Research in Biomedicine. T. N. M. S receives grant support from the Dutch Cancer Society (NKI 2009-4282), the FP7 ITN ATTRACT program, and the K. G. Jebsen Center for Cancer Immunotherapy. We thank G. M. Bendle, P. Kvistborg, and M. M. van Buuren for critical discussions. The authors declare no competing financial interests.

References

1 Heemskerk B, Kvistborg P, Schumacher TN. The cancer antigenome. EMBO J 2013;32:194–203.
2 Alexandrov LB, et al. Signatures of mutational processes in human cancer. Nature 2013;500:415–421.
3 Vogelstein B, Papadopoulos N, Velculescu VE, Zhou S, Diaz LA, Jr., Kinzler KW. Cancer genome landscapes. Science 2013;339:1546–1558.
4 Fridman WH, Pages F, Sautes-Fridman C, Galon J. The immune contexture in human tumours: impact on clinical outcome. Nat Rev Cancer 2012;12:298–306.
5 Kawakami Y, et al. Cloning of the gene coding for a shared human melanoma antigen recognized by autologous T cells infiltrating into tumor. Proc Natl Acad Sci USA 1994;91:3515–3519.
6 Kawakami Y, et al. Identification of a human melanoma antigen recognized by tumor-infiltrating lymphocytes associated with in vivo tumor rejection. Proc Natl Acad Sci USA 1994;91:6458–6462.
7 Wang RF, Robbins PF, Kawakami Y, Kang XQ, Rosenberg SA. Identification of a gene encoding a melanoma tumor antigen recognized by HLA-A31-restricted tumor-infiltrating lymphocytes. J Exp Med 1995;181:799–804.
8 Padovan E, Casorati G, Dellabona P, Meyer S, Brockhaus M, Lanzavecchia A. Expression of two T cell receptor alpha chains: dual receptor T cells. Science 1993;262:422–424.
9 Langerak AW, et al. Molecular and flow cytometric analysis of the Vbeta repertoire for clonality assessment in mature TCRalphabeta T-cell proliferations. Blood 2001;98:165–173.
10 Gorski J, et al. Circulating T cell repertoire complexity in normal individuals and bone marrow recipients analyzed by CDR3 size spectratyping. Correlation with immune status. J Immunol 1994;152:5109–5119.
11 Bolotin DA, et al. Next generation sequencing for TCR repertoire profiling: platform-specific features and correction algorithms. Eur J Immunol 2012;42:3073–3083.
12 Robins HS, et al. Comprehensive assessment of T-cell receptor beta-chain diversity in alphabeta T cells. Blood 2009;114:4099–4107.
13 van Heijst JW, et al. Quantitative assessment of T cell repertoire recovery after hematopoietic stem cell transplantation. Nat Med 2013;19:372–377.
14 Sherwood AM, et al. Tumor-infiltrating lymphocytes in colorectal tumors display a diversity of T cell receptor sequences that differ from the T cells in adjacent mucosal tissue. Cancer Immunol Immunother 2013;62:1453–1461.
15 Emerson RO, et al. High-throughput sequencing of T cell receptors reveals a homogeneous repertoire of tumor-infiltrating lymphocytes in ovarian cancer. J Pathol 2013:doi: 10.1002/path.4260.
16 Schumacher TN, Gerlach C, van Heijst JW. Mapping the life histories of T cells. Nat Rev Immunol 2010;10:621–631.
17 Tran KQ, et al. Minimally cultured tumor-infiltrating lymphocytes display optimal characteristics for adoptive cell therapy. J Immunother 2008;31:742–751.
18 Topalian SL, Solomon D, Rosenberg SA. Tumor-specific cytolysis by lymphocytes infiltrating human melanomas. J Immunol 1989;142:3714–3725.
19 Muul LM, Spiess PJ, Director EP, Rosenberg SA. Identification of specific cytolytic immune responses against autologous tumor in humans bearing malignant melanoma. J Immunol 1987;138:989–995.
20 Kradin RL, et al. Tumour-infiltrating lymphocytes and interleukin-2 in treatment of advanced cancer. Lancet 1989;1:577–580.
21 Dudley ME, et al. Cancer regression and autoimmunity in patients after clonal repopulation with antitumor lymphocytes. Science 2002;298:850–854.

22 Johnson LA, et al. Gene transfer of tumor-reactive TCR confers both high avidity and tumor reactivity to nonreactive peripheral blood mononuclear cells and tumor-infiltrating lymphocytes. J Immunol 2006;177:6548–6559.
23 Hughes MS, et al. Transfer of a TCR gene derived from a patient with a marked antitumor response conveys highly active T-cell effector functions. Hum Gene Ther 2005;16:457–472.
24 Cole DJ, et al. Characterization of the functional specificity of a cloned T-cell receptor heterodimer recognizing the MART-1 melanoma antigen. Cancer Res 1995;55:748–752.
25 Morgan RA, et al. Cancer regression in patients after transfer of genetically engineered lymphocytes. Science 2006;314:126–129.
26 Johnson LA, et al. Gene therapy with human and mouse T-cell receptors mediates cancer regression and targets normal tissues expressing cognate antigen. Blood 2009;114:535–546.
27 Dossinger G, et al. MHC multimer-guided and cell culture-independent isolation of functional T cell receptors from single cells facilitates TCR identification for immunotherapy. PLoS ONE 2013;8:e61384.
28 Wang GC, Dash P, McCullers JA, Doherty PC, Thomas PG. T cell receptor alphabeta diversity inversely correlates with pathogen-specific antibody levels in human cytomegalovirus infection. Sci Transl Med 2012;4:128ra142.
29 Linnemann C, et al. High-throughput identification of antigen-specific TCRs by TCR gene capture. Nat Med 2013;19:1534–1541.
30 Turchaninova MA, et al. Pairing of T-cell receptor chains via emulsion PCR. Eur J Immunol 2013;43:2507–2515.
31 Dudley ME, et al. Randomized selection design trial evaluating CD8+-enriched versus unselected tumor-infiltrating lymphocytes for adoptive cell therapy for patients with melanoma. J Clin Oncol 2013;31:2152–2159.
32 Altman JD, et al. Phenotypic analysis of antigen-specific T lymphocytes. Science 1996;274:94–96.
33 Bakker AH, et al. Conditional MHC class I ligands and peptide exchange technology for the human MHC gene products HLA-A1, -A3, -A11, and -B7. Proc Natl Acad Sci USA 2008;105:3825–3830.
34 Toebes M, et al. Design and use of conditional MHC class I ligands. Nat Med 2006;12:246–251.
35 Brackenridge S, et al. An early HIV mutation within an HLA-B*57-restricted T cell epitope abrogates binding to the killer inhibitory receptor 3DL1. J Virol 2011;85:5415–5422.
36 Chang CX, et al. Conditional ligands for Asian HLA variants facilitate the definition of CD8+ T-cell responses in acute and chronic viral diseases. Eur J Immunol 2013;43:1109–1120.
37 Newell EW, Klein LO, Yu W, Davis MM. Simultaneous detection of many T-cell specificities using combinatorial tetramer staining. Nat Methods 2009;6:497–499.
38 Hadrup SR, et al. Parallel detection of antigen-specific T-cell responses by multidimensional encoding of MHC multimers. Nat Methods 2009;6:520–526.
39 Newell EW, Sigal N, Nair N, Kidd BA, Greenberg HB, Davis MM. Combinatorial tetramer staining and mass cytometry analysis facilitate T-cell epitope mapping and characterization. Nat Biotechnol 2013;31:623–629.
40 Kvistborg P, et al. TIL therapy broadens the tumor-reactive CD8(+) T cell compartment in melanoma patients. Oncoimmunology 2012;1:409–418.
41 Andersen RS, et al. Dissection of T-cell antigen specificity in human melanoma. Cancer Res 2012;72:1642–1650.
42 Matsushita H, et al. Cancer exome analysis reveals a T-cell-dependent mechanism of cancer immunoediting. Nature 2012;482:400–404.
43 Castle JC, et al. Exploiting the mutanome for tumor vaccination. Cancer Res 2012;72:1081–1091.

44 Robbins PF, et al. Mining exomic sequencing data to identify mutated antigens recognized by adoptively transferred tumor-reactive T cells. Nat Med 2013;19:747–752.
45 van Rooij N, et al. Tumor exome analysis reveals neoantigen-specific T-cell reactivity in an ipilimumab-responsive melanoma. J Clin Oncol 2013;31:e439–e442.
46 Lu YC, et al. Mutated PPP1R3B is recognized by T cells used to treat a melanoma patient who experienced a durable complete tumor regression. J Immunol 2013;190:6034–6042.
47 Rosenberg SA, et al. Identification of BING-4 cancer antigen translated from an alternative open reading frame of a gene in the extended MHC class II region using lymphocytes from a patient with a durable complete regression following immunotherapy. J Immunol 2002;168:2402–2407.
48 Guilloux Y, et al. A peptide recognized by human cytolytic T lymphocytes on HLA-A2 melanomas is encoded by an intron sequence of the N-acetylglucosaminyltransferase V gene. J Exp Med 1996;183:1173–1183.
49 Torikai H, et al. A novel HLA-A*3303-restricted minor histocompatibility antigen encoded by an unconventional open reading frame of human TMSB4Y gene. J Immunol 2004;173:7046–7054.
50 Tykodi SS, et al. C19orf48 encodes a minor histocompatibility antigen recognized by CD8+ cytotoxic T cells from renal cell carcinoma patients. Clin Cancer Res 2008;14:5260–5269.
51 Hamid O, et al. Safety and tumor responses with lambrolizumab (anti-PD-1) in melanoma. N Engl J Med 2013;369:134–144.
52 Topalian SL, et al. Safety, activity, and immune correlates of anti-PD-1 antibody in cancer. N Engl J Med 2012;366:2443–2454.
53 Hodi FS, et al. Improved survival with ipilimumab in patients with metastatic melanoma. N Engl J Med 2010;363:711–723.
54 Lennerz V, et al. The response of autologous T cells to a human melanoma is dominated by mutated neoantigens. Proc Natl Acad Sci USA 2005;102:16013–16018.
55 Knabel M, et al. Reversible MHC multimer staining for functional isolation of T-cell populations and effective adoptive transfer. Nat Med 2002;8:631–637.
56 de Witte MA, et al. Requirements for effective antitumor responses of TCR transduced T cells. J Immunol 2008;181:5128–5136.
57 Mates L, et al. Molecular evolution of a novel hyperactive Sleeping Beauty transposase enables robust stable gene transfer in vertebrates. Nat Genet 2009;41:753–761.
58 Peng PD, et al. Efficient nonviral Sleeping Beauty transposon-based TCR gene transfer to peripheral blood lymphocytes confers antigen-specific antitumor reactivity. Gene Ther 2009;16:1042–1049.
59 Morgan RA, et al. Cancer regression and neurological toxicity following anti-MAGE-A3 TCR gene therapy. J Immunother 2013;36:133–151.
60 Parkhurst MR, et al. T cells targeting carcinoembryonic antigen can mediate regression of metastatic colorectal cancer but induce severe transient colitis. Mol Ther 2011;19:620–626.
61 de Witte MA, et al. An inducible caspase 9 safety switch can halt cell therapy-induced autoimmune disease. J Immunol 2008;180:6365–6373.
62 Kieback E, Charo J, Sommermeyer D, Blankenstein T, Uckert W. A safeguard eliminates T cell receptor gene-modified autoreactive T cells after adoptive transfer. Proc Natl Acad Sci USA 2008;105:623–628.
63 Bolotin DA, et al. MiTCR: software for T-cell receptor sequencing data analysis. Nat Methods 2013;10:813–814.

Chapter 3

A Traceless Selection: Counter-selection System That Allows Efficient Generation of Transposon and CRISPR-modified T-cell Products

Riccardo Mezzadra[1], Andreas Hollenstein[1,2], Raquel Gomez-Eerland[1], and Ton N Schumacher[1,*]

[1] Division of Immunology, The Netherlands Cancer Institute, Amsterdam, The Netherlands

[2] Present address: Genmab, Utrecht, The Netherlands,

[*] Division of Immunology, The Netherlands Cancer Institute, Plesmanlaan 121, 1066 CX, Amsterdam, The Netherlands. E-mail: t.schumacher@nki.nl

Mol Ther Nucleic Acids. 2016 Mar 22;5:e298

Recent years have seen major breakthroughs in genome-engineering systems, such as transposon-mediated gene delivery systems and CRISPR-Cas9-mediated genome-editing tools. In these systems, transient expression of auxiliary genes is responsible for permanent genomic modification. For both systems, it would be valuable to select for cells that are likely to undergo stable genome modification. Importantly, in particular for clinical applications of genome-engineered cell products, it will also be of importance to remove those cells that, due to random vector integration, display an unwanted stable expression of the auxiliary gene. Here, we develop a traceless selection system that on the one hand allows efficient enrichment of modified cells, and on the other hand can be used to select against cells that retain expression of the auxiliary gene. The value of this system to produce highly enriched-auxiliary gene-free cell products is demonstrated.

Introduction

Over the past few years, a number of novel tools have been developed that greatly facilitate genome engineering, both for research purposes, and for the creation of genome-modified cell therapeutics. Two remarkable examples of this are the molecularly evolved transposon systems[1,2] and the CRISPR system.[3,4,5] Transposon-based gene delivery systems are nonviral systems for gene delivery that are based on the transfection of two plasmids, of which the first encodes the transposase that mediates the integration into the host genome of the transposon sequence that is present within the second. Likewise, the CRISPR system is based on two elements, the Cas9 gene product and the single-guiding RNA (sgRNA) that are together required for genome modification. In this case, the sequence of the sgRNA guides the Cas9 enzyme to a specific spot in the genome where it induces a DNA double strand break. This system can be used to destroy a target open reading frame, exploiting the nonhomologous end joining machinery, or to induce defined genomic alterations, by homology-mediated DNA repair.[6]

Although used for different purposes, in both these systems transient enzymatic activity is required to produce a stable genomic modification. Furthermore, in both cases, continuous expression of this auxiliary gene product is undesirable, because of the possibility of further genomic alterations, an issue that appears of particular importance for the generation of genome-engineered cell therapeutics.[7] One potential strategy to avoid this issue is the use of RNA encoding the auxiliary factor, but in many settings, the use of DNA-encoded auxiliary factors is more convenient in terms of practicality and costs. Furthermore, as the efficiency of both CRISPR and transposon genome modification platforms is variable and can be low in particular in primary cells, we set out to develop a selection system that allows the enrichment of cells undergoing transposase-mediated gene transfer or Cas9-mediated genome editing, and that at the same time avoids the safety risks associated with DNA-encoded transposase or Cas9.

To achieve this, we modified the plasmids encoding either the molecularly enhanced Sleeping Beauty (SB100X) transposase or the Cas9 gene, by the addition of different selection markers. We show that such introduction of selection markers into vectors that encode these auxiliary genes can be used to efficiently select for cells that subsequently undergo stable genome engineering. Furthermore, we show that the same markers can be used to select against cells harboring unwanted subsequent integration of the auxiliary gene. Among the marker systems utilized, the truncated version of the epidermal growth factor receptor (trEGFR)[8] is of particular interest for

clinical applications, as reagents required for cell enrichment are available in clinical grade, and as depletion of cells with prolonged auxiliary gene expression may not only be achieved *in vitro* but also *in vivo*, by application of the EGFR targeting antibody cetuximab. We believe that the method described here can greatly facilitate the clinical application of plasmid-based genome-engineering systems.

Results

Design of a traceless cell selection system

With the aim to develop a "traceless" selection system to, shortly after transfection, enrich cells that are likely to subsequently undergo stable gene modification, we first evaluated the kinetic of expression of two genes expressed from two independent plasmids when simultaneously transfected. To this purpose, we cotransfected a plasmid encoding the Katushka red fluorescent protein plus SB100X transposase ("KPS"), together with a GFP encoding transposon plasmid (Figure 1a) into peripheral blood mononuclear cells (PBMCs) and evaluated fluorochrome expression after 24 hours. Notably, the vast majority of cells either expressed neither of the two fluorochromes or both. Furthermore, flurochrome expression levels in the small fraction of cells that expressed only a single fluorochrome was low (Figure 1b). Thus, as shown long ago for calcium phosphate based transfection, in which DNA aggregates are taken up, also upon electroporation most cells that are successfully transfected receive multiple plasmids. These results suggested that efficient selection of cells that can undergo stable gene modification may be feasible by introduction of a selection marker solely with the plasmid encoding the auxiliary gene product.

To test this possibility, human PBMCs were cotransfected with the KPS plasmid and a transposon plasmid encoding the 1D3 T cell receptor (TCR; Figure 2a). Twenty-four hours after transfection, cells were sorted into populations that displayed either absent-low, intermediate, or bright Katushka expression (Figure 2b,c). Following cell sorting, cells were stimulated with anti-CD3/CD28 beads and cultured for 14 days, and the percentage of 1D3 TCR-positive cells in the different fractions was analyzed by MHC multimer staining and flow cytometry. Only a minor fraction of cells with absent-low Katushka expression shortly after transfection showed expression of the 1D3 TCR at a later time point. Furthermore, 1D3 TCR expression was also only observed in a small percentage of cells with intermediate Katushka expression shortly after transfection. In contrast, stable gene modification was observed in a very high fraction (>90%) of cells that displayed high initial Katushka expression (Figure 2c). These data establish the feasibility of cell enrichment on the basis of auxiliary gene expression, thereby allowing the development of traceless selection systems.

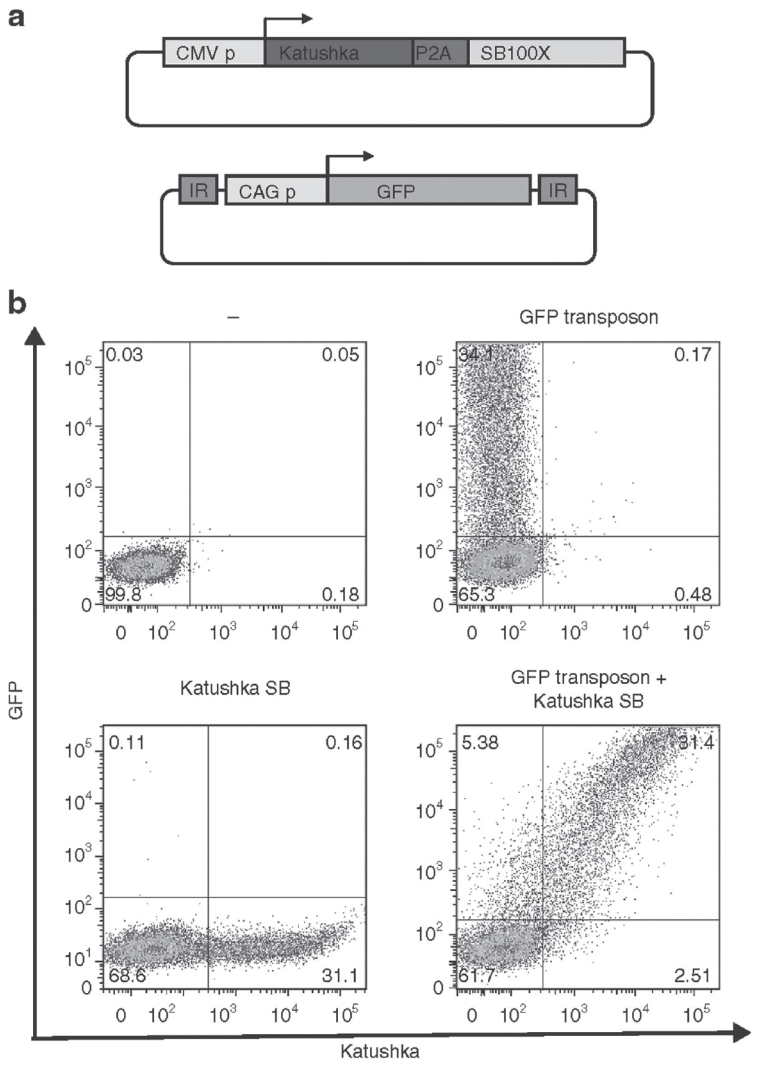

Figure 1: Two vector electroporation dynamics in human peripheral blood mononuclear cells (PBMCs). (a) Vector design. CMV p: immediate-early cytomegalovirus promoter; P2A: porcine teschovirus-1 2A element; SB100X: molecularly evolved sleeping beauty transposase; IR: SB transposon inverted repeat; GFP, enhanced green fluorescent protein. (b) Flow cytometric analysis of human PBMCs transfected with KPS, GFP encoding transposon, or both, 24 hours after transfection. Note that when both vectors are cotransfected (bottom right plot) the large majority of cells either express none or both fluorochromes.

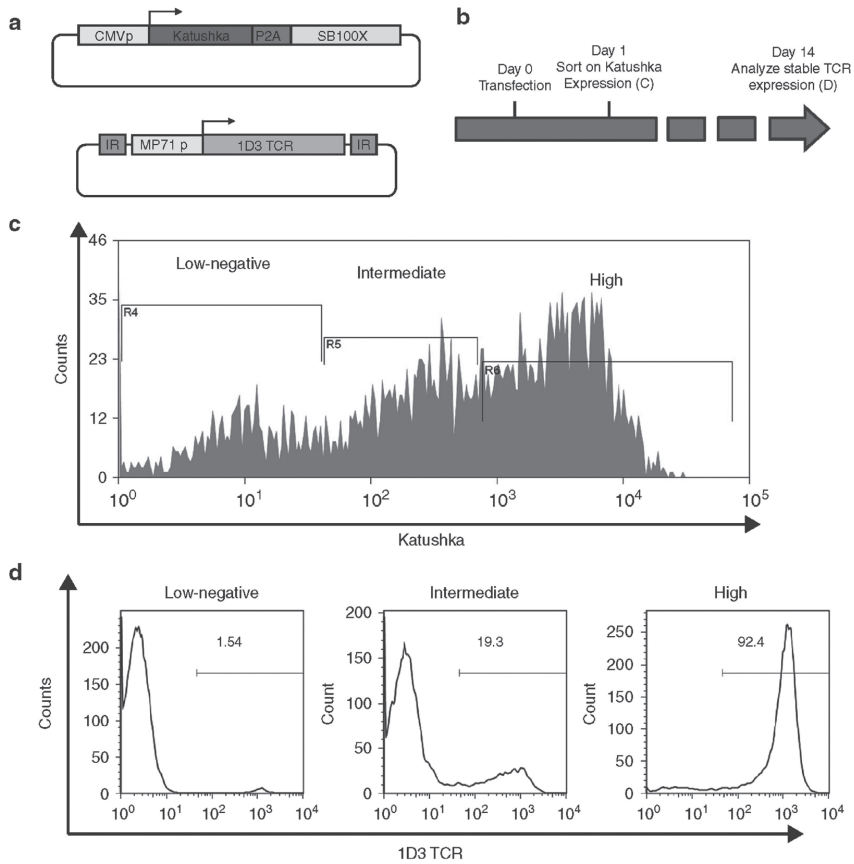

Figure 2: Early enrichment of cells undergoing stable SB transposition. (a) Vectors design. MP71 p: hybrid promoter MP71; 1D3: 1D3 TCR. (b) Schematic experimental time line. Peripheral blood mononuclear cells (PBMCs) were thawed 24 hours prior transfection, transfected and sorted by FACS 24 hours after transfection. Stable gene modification in the indicated fractions was assessed 14 days after transfection. (c) Sorting strategy. Indicated cell populations with either low-negative, intermediate, or high expression levels of Katushka were isolated and cultured in order to analyze stable gene modification efficiency. (d) Stable gene modification efficiency of the indicated cell populations, as established 14 days after transfection. Only cells isolated on the basis of high expression of Katushka show a very high fraction of cells stably expressing the TCR.

Efficient selection of transposon and CRISPRs gene-modified cells on the basis of transient puromycin resistance

Given these results, we aimed to develop a traceless system that allows the efficient selection of cells undergoing genome modifications. Of the available drug resistance systems, puromycin resistance is particularly attractive for this purpose, as puromycin-mediated cell death occurs within days, thereby allowing the selection of cells that carry the auxiliary plasmid episomally for only a limited amount of time. To this

purpose, we generated a vector encoding the SB100X transposase plus the puromycin *N-acetyl-transferase (PAC)* gene (SB100X-IRES-PAC, Figure 3a). Subsequently, HeLa cells were transfected with a GFP encoding transposon plasmid, together with either the SB100X-IRES-PAC plasmid or the parental SB100X plasmid. Twenty-four hours after transfection, parts of the cells transfected with the SB100X-IRES-PAC plasmid were treated with puromycin for a 48-hour time period (Figure 3b). Notably, this brief period of puromycin selection shortly after transfection led to a marked increase in the frequency of cells showing stable transposon-mediated gene integration. Specifically, at day 14 of culture, 94% of the puromycin-treated cells expressed GFP, whereas GFP expression was only observed in 41 and 36% of the cells transfected with either SB100X or SB100X-IRES-PAC (average of three experiments, SB100X-IRES-PAC enriched versus SB100X-IRES-PAC and SB100X-IRES-PAC enriched versus SB100X: both $P < 0.001$; SB100X versus SB100X-IRES-PAC: not significant, Figure 3c,d).

To evaluate whether the same selection system can also be utilized to enhance the efficiency of CRISPR-mediated genome editing, we first generated a set of guiding RNAs (sgRNAs) for the β2 microglobulin (β_2m) gene that is required for cell surface HLA class I expression. HeLa cells were transfected with hCas9 plus sgRNA, and loss of HLA class I expression was evaluated after 5 days. The highest frequency of HLA class I loss that was achieved with this set of sgRNAs was 8.4% (data not shown), indicating that selection of cells that are likely to undergo genome editing could be of value. To evaluate this, we generated a plasmid encoding hCas9 and PAC in an IRES-linked configuration (Figure 3e). We subsequently transfected HeLa cells with the β_2m sgRNA encoding plasmid, together with either the hCas9 plasmid or the hCas9-IRES-PAC plasmid. Twenty-four hours after transfection, cells transfected with the hCas9-IRES-PAC plasmid were either left untreated or exposed to puromycin for 48 hours (Figure 3f). Analysis of HLA class I expression after 10 days of culture demonstrated that puromycin-treated cells contained very high frequencies of cells negative for HLA class I (average of 51%), as compared to cells transfected with the same plasmid system that were not exposed to puromycin (average of 4%), and to cells modified with the standard hCas9 (average of 5%) (average of three experiments, hCas9-IRES-PAC enriched versus hCas9-IRES-PAC, and hCas9-IRES-PAC enriched versus hCas9: both $P < 0.01$; hCas9 versus hCas9-IRES-PAC: not significant, Figure 3g,h). Genome editing was confirmed by analysis of the genomic area targeted by the sgRNA using the Tracking of Indels by Decomposition (TIDE) algorithm, and by sgRNA requirement (Supplementary Figures S1a and S2).[9] Collectively, these data demonstrate that the introduction of fluorescent or drug resistance markers within auxiliary plasmids allows the efficient selection of stably modified cells in a simple, fast and traceless manner, both in the context of transposon-mediated gene transfer and in the context of CRISPR-hCas9-mediated genome editing.

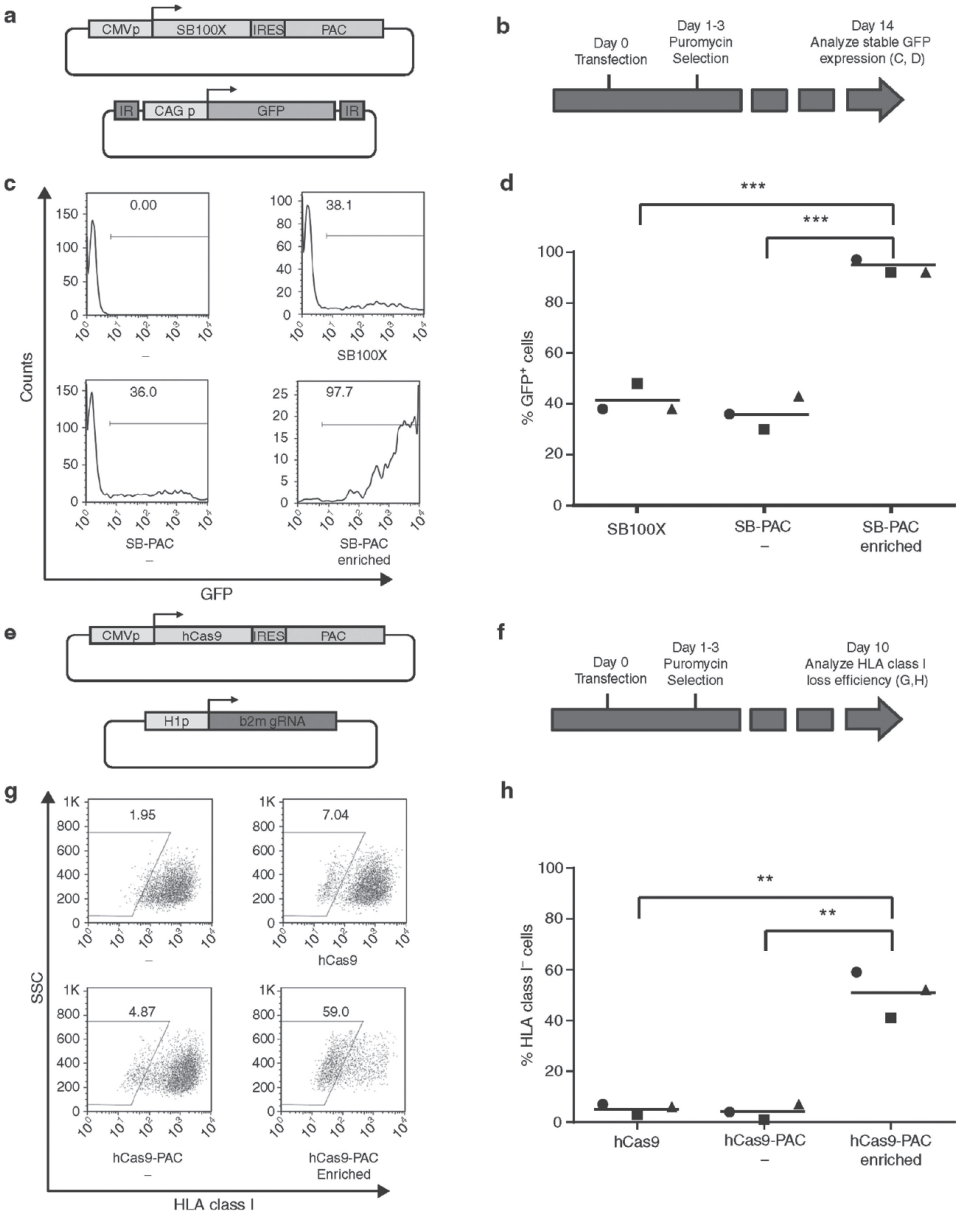
a
CMVp
SB100X
IRES
PAC
IR
CAG p
GFP
IR
b
Day 0
Transfection
Day 1-3
Puromycin
Selection
Day 14
Analyze stable GFP
expression (C, D)
c
0.00
38.1
36.0
97.7
SB100X
SB-PAC
SB-PAC
enriched
Counts
GFP
d
***
***
% GFP+ cells
SB100X
SB-PAC
SB-PAC
enriched
e
CMVp
hCas9
IRES
PAC
H1p
b2m gRNA
f
Day 0
Transfection
Day 1-3
Puromycin
Selection
Day 10
Analyze HLA class I
loss efficiency (G,H)
g
1.95
7.04
4.87
59.0
hCas9
hCas9-PAC
hCas9-PAC
Enriched
SSC
HLA class I
h
**
**
% HLA class I− cells
hCas9
hCas9-PAC
hCas9-PAC
enriched

< Figure 3: Drug selection based enrichment of SB and hCas9 gene-modified cells. (a) Vectors used to evaluate the effect of puromycin selection on stable SB100X transposition. CAG p, chicken β-actin promoter with CMV enhancer; IRES, hepatitis C virus internal ribosome entry site; PAC, puromycin N-acetyl-transferase cassette. (b) Schematic experimental time line. HeLa cells were transfected and, after 24 hours, cultured in the presence of puromycin for 48 hours. 14 days after transfection, stable transposition was assessed by flow cytometry. (c) Flow cytometric analysis of the effect of early puromycin selection on stable GFP transposition. Puromycin-selected cells (bottom right plot) become almost uniformly GFP positive. (d) Summary of three independent SB gene transfer enrichment experiments. In all cases, early puromycin selection leads to very high stable GFP expression (***$P < 0.001$). (e) Vectors used to evaluate the effect of puromycin selection on hCas9-mediated genome editing. hCas9, humanized Cas9; H1p, DNA polymerase III promoter H1; b2m sgRNA, β2M-specific guiding RNA. (f) Schematic experimental time line. HeLa cells were transfected and, after 24 hours, cultured in the presence of puromycin for 48 hours. Fourteen days after transfection, stable HLA class I loss was evaluated by flow cytometry. (g) Flow cytometric analysis of the effect of early puromycin selection on stable HLA class I loss. Puromycin-treated cells (bottom right plot) are highly enriched for HLA class I-negative cells. (h) Summary of three independent hCas9 genome editing enrichment experiments. In all cases, early puromycin selection greatly increases the percentage of cells with stable HLA class I loss (**P value < 0.01).

Efficient selection of transposon gene-modified cells on the basis of transient trEGFR expression

In order to exploit this concept in a clinically applicable format, we generated a vector that encodes the truncated EGFR receptor[8] plus the SB100X transposase in an IRES-linked configuration (SB-IRES-trEGFR). This design offers the advantage that trEGFR expression is modest relative to that of SB100X, ensuring that selection of cells on the basis of trEGFR yields a cell population that expresses high SB100X levels. To test the possibility of enrichment of cells that are likely to undergo stable gene modification on the basis of transient trEGFR expression, PBMCs were electroporated with the 1D3 transposon and SB-IRES-trEGFR vectors, and after 24 hours, trEGFR-expressing cells were isolated by magnetic bead sorting (Figure 4a,b). As a first control, a fraction of the transfected cells was left unsorted and cultured in parallel. As a second control, cells were transfected with the 1D3 transposon in combination with the nonmodified SB100X vector.

Analysis of 1D3 TCR expression 14 days after transfection demonstrated that cell populations isolated on the basis of trEGFR expression showed a very high level of stable TCR gene modification (Figure 4c,d; 71.7 ± 11.7%), with a high recovery of the TCR-modified cell population (51.6 ± 18.7%). By comparison, frequency of cells showing stable 1D3 TCR expression was 18.7 ± 10.8% for cells modified with the same plasmid system that had not undergone cell enrichment, and 24.0 ± 12.0% for cells transfected with the standard SB100x transposon system (SB-IRES-trEGFR enriched

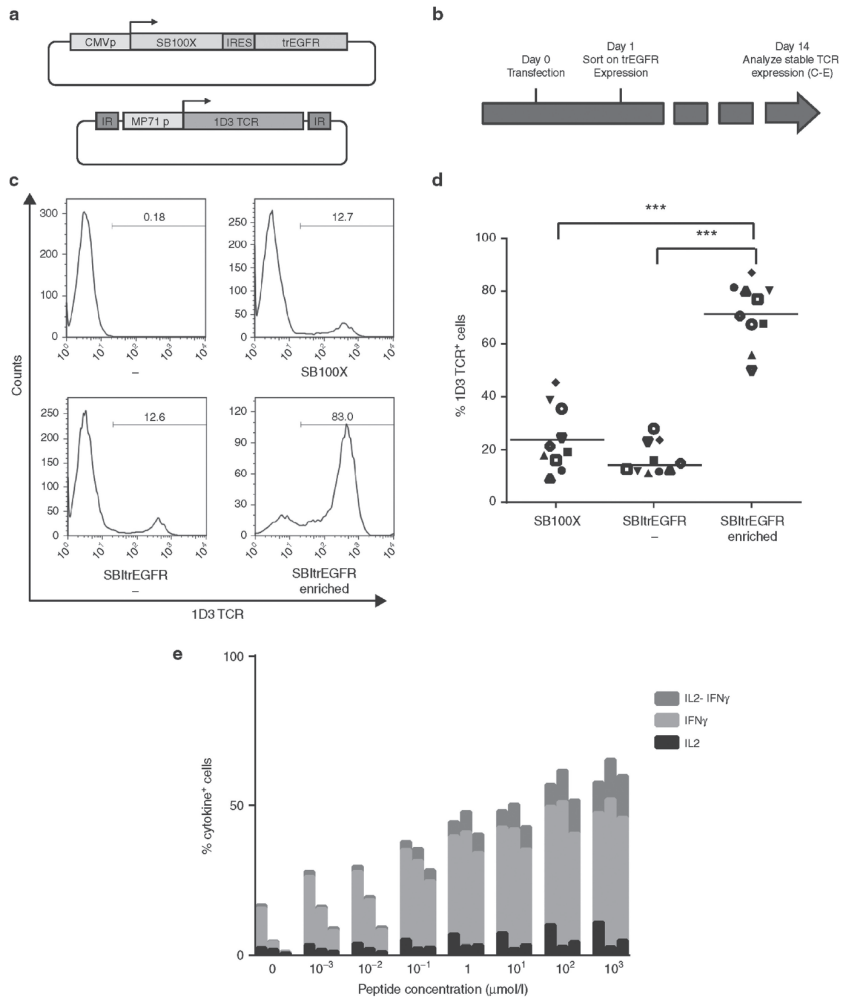

Figure 4: Enrichment of SB gene-modified primary T cells on the basis of transient trEGFR expression. (a) Vectors used. trEGFR: truncated epithelial growth factor receptor. (b) Schematic experimental time line. PBMCs were thawed 24 hours prior to electroporation. Twenty-four hours after transfection, trEGFR cells were magnetically sorted. T cells were cultured for 14 days, and 1D3 TCR stable expression and functionality were evaluated by flow cytometry. (c) Flow cytometric analysis of the effect of early trEGFR selection on stable 1D3 transposition. (d) Summary of ten independent SB gene transfer enrichment experiments, using cells from independent donors. In all cases, early enrichment greatly increases the percentage of stably modified cells (***$P < 0.001$). (e) For each peptide concentration, the percentage of cytokine secreting T cells of TCR redirected T cells is shown. Bars represent SB redirected (left), SBItrEGFR redirected (central), and SBItrEGFR redirected and selected (right). Data were normalized for the percentage 1D3 TCR+ cells.

versus SB-IRES-trEGFR, and SB-IRES-trEGFR enriched versus SB100X: both $P < 0.0001$; SB100X versus SB-IRES-trEGFR: not significant, Figure 4c,d). Furthermore, this increase in the percentage of 1D3 TCR expressing T cells was accompanied by a quantitatively similar increase in the number of gene-modified cells capable of recognizing MART-I_{26-35}-positive target cells, as shown by cytokine secretion assays (Figure 4e).

Efficient selection of CRISPRs genome-edited cells on the basis of episomal expression of truncated EGFR

In order to evaluate the feasibility of enrichment of cells undergoing hCas9 genome modification on the basis of transient trEGFR expression, we first developed an optimal sgRNA specific for the TCR-α constant chain (TRAC) by screening a series of TRAC sgRNAs in Jurkat T cells (data not shown). In addition, a vector encoding the codon optimized truncated EGFR receptor plus hCas9 gene in a P2A-linked configuration (hCas9 P2A cotrEGFR) was developed. Subsequently, activated PBMCs were transfected with hCas9 P2A cotrEGFR and the TRAC sgRNA, and 24 hours after electroporation, trEGFR-expressing cells were isolated by magnetic bead sorting or left untreated (Figure 5a,b). As a second control, cells were transfected with TRAC sgRNA and the standard hCas9 plasmid. Cell populations isolated on the basis of trEGFR expression shortly after transfection showed a high frequency of CD3-negative cells at day 7 after transfection (40.5 ± 9.0%, Figure 5c,d). As a comparison, the frequency of CD3-negative cells was approximately threefold lower in both control conditions (14.7 ± 6.3% for hCas9P2AtrEGFR-transfected cells that were not subjected to enrichment, and 12.5 ± 7.7% for cells transfected with the standard hCas9 system; hCas9 P2A cotrEGFR enriched versus hCas9 P2A cotrEGFR, and hCas9 P2A cotrEGFR enriched versus SB100X: both $P < 0.001$, hCas9 versus hCas9 P2A cotrEGFR: not significant, Figure 5c,d). Cas9-mediated genome editing was again confirmed by sgRNA dependency (Supplementary Figure S1b) and analysis of the genomic area targeted by the sgRNA (Supplementary Figure S3) of both the unselected and the enriched fraction for two donors. Additionally, we performed the same type of analysis on the top three predicted off target sites (Supplementary Table S1 and Supplementary Figure S4). As compared to the background signal seen in untransfected samples, evidence was obtained for off-target editing of one of these sites in one sample, but this was not increased relative to cells transfected with a control Cas9 vector (Supplementary Figure S4).

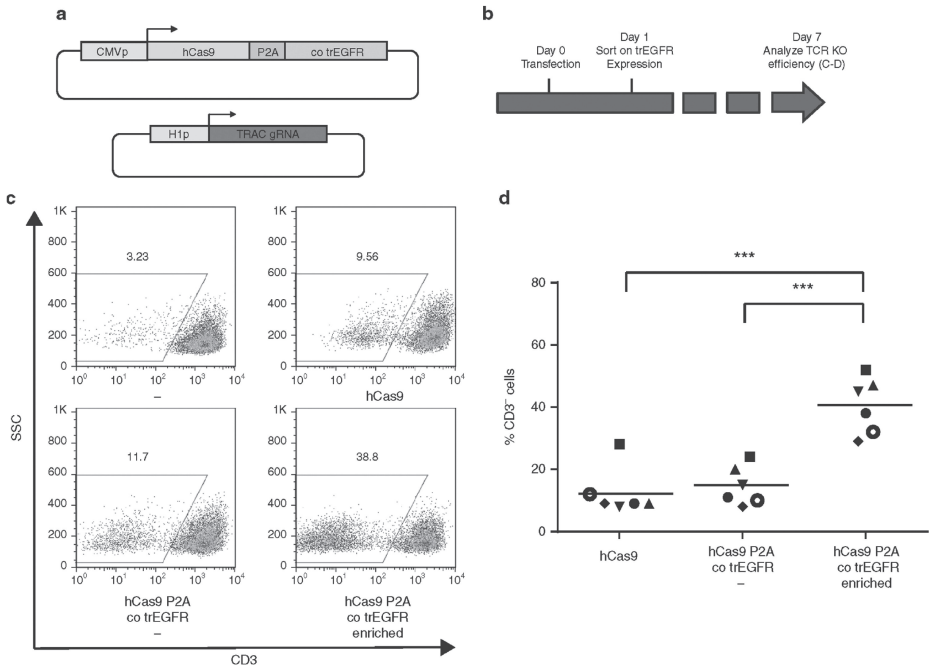

Figure 5: Enrichment of hCas9 genome-edited primary T cells on the basis of transient trEGFR expression. (a) Vectors used. cotrEGFR, codon-optimized truncated epithelial growth factor receptor; TRAC sgRNA, T-cell receptor-α constant-specific guiding RNA. (b) Schematic experimental time line. Peripheral blood mononuclear cells were thawed and activated 2–3 days prior to electroporation. Twenty-four hours after transfection, trEGFR cells were magnetically sorted and cultured. Seven days after transfection, efficiency of stable gene inactivation was evaluated by flow cytometry. (c) Flow cytometric analysis of the effect of early cotrEGFR selection on the efficiency of stable TCR-α gene inactivation. (d) Summary of six independent hCas9 genome-editing enrichment experiments, involving cells from different donors. (***$P < 0.001$).

Efficient counter-selection of cells harboring stable integration of the auxiliary plasmid

A clear advantage of the introduction of selectable surface markers with an auxiliary vector is that it not only allows the positive selection of transfected cells early after gene modification, but also the removal of cells that inadvertently show continuous expression of the auxiliary gene at later time points. In order to evaluate whether cells that continue to express the auxiliary gene after random plasmid integration also show continued expression of the selection marker, we generated a plasmid encoding the puromycin resistance gene product and the trEGFR linked by an IRES element (PAC-IRES-trEGFR, Figure 6a). Jurkat T cells were then transfected with PAC-IRES-trEGFR and 4 days after transfection puromycin was added to select for cells that

had undergone random integration of the auxiliary vector. Following a 30-day culture in the presence of puromycin, cells were analyzed for EGFR expression. This analysis showed a near homogenous (>98%) EGFR positivity (Figure 6b). As this vector design recapitulates the design of enrichment vectors (see Figures 4a and 5a), these data indicate that those cells that would retain expression of transposase or hCas9 after random auxiliary plasmid integration would also retain expression of trEGFR, thereby allowing their subsequent depletion.

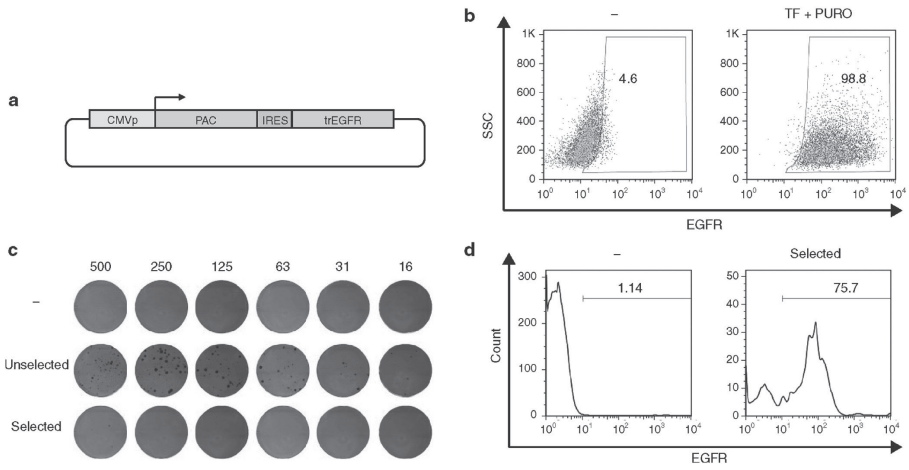

Figure 6: Counter-selection of cells harboring unwanted auxiliary vector integration. (a) Vector used. (b) Flow cytometric analysis of untransfected Jurkat cells and transfected Jurkat cells that were exposed to puromycin selection. Cells resistant to puromycin are almost uniformly positive for EGFR. (c) B16 colony formation by the indicated cell populations. Top: untransfected cells; middle: transfected cells; bottom: transfected cells that were subjected to negative selection. Numbers indicate input cell numbers times 10–3. Note that counter-selection against EGFR expression leads to the formation of only few puromycin-resistant colonies. (d) EGFR expression on untransfected cells (left) and transfected and puromycin selected cells (right). The majority of cells surviving puromycin treatment retain EGFR expression.

To test the efficiency of such depletion, B16 murine melanoma cells (that are negative for cetuximab staining, data not shown) were transfected with PAC-IRES-trEGFR. After 30 days of culture, cells were either magnetically depleted of EGFR-positive cells or left untreated. Subsequently, serial dilutions (5×10^5–15.625×10^3) of depleted, nondepleted, or untransfected cells were plated and cultured in presence of puromycin and, after 10 days, stained with crystal violet. Cells depleted from the EGFR$^+$ fraction formed drastically fewer colonies than the nondepleted control (131 versus 4 colonies for 5×10^5 cells, 82 versus 1 colonies for 2.5×10^5 cells, 65 versus 0 for 1.25×10^5 cells, 38 versus 0 for 62.5×10^4 cells, 19 versus 0 for 31.25×10^4 cells,

and 10 versus 0 for 15.625×10^4 cells (Figure 6c), showing the feasibility of counter-selection of cells harboring unwanted expression of the auxiliary gene. The few cells that did grow out from the EGFR-depleted cell population upon puromycin treatment remained largely EGFR positive, indicating that they potentially may still be targeted by repeated cetuximab exposure (Figure 6d). Since transposase- or Cas9-mediated double-strand DNA breaks that may facilitate aberrant integration were absent in the above setting, we subsequently performed experiments in which, together with PAC-IRES-trEGFR, a GFP encoding transposon and the SB-IRES-trEGFR were cotransfected (Supplementary Figure S5a). Transfected cells were either left unsorted or magnetically sorted for absence or presence of EGFR expression. After 14 days of culture, cells were either magnetically depleted of EGFR-positive cells or left untreated. Serial dilutions (5×10^5–15.625×10^3) of cells from all conditions were plated and cultured for 10 days in presence of puromycin (Supplementary Figure S5b). Importantly, we still were able to counter select 86% of those cells harboring a stable episomal integration (total of 186 versus 25 colonies), showing that the counter-selection is feasible also in a context where double-strand break is induced.

Discussion

Recent years have seen a rapid development in technologies that can be utilized for genome engineering. Two examples of those recently introduced technologies are the molecularly enhanced Sleeping Beauty transposase,[1] that allows nonviral gene transfer with high efficiency and the Cas9-mediated genome editing system, that allows genome editing in a straightforward way.[3,4,5] Both these systems rely on the expression of an auxiliary gene whose activity is required only temporarily for stable genome modification, and for which continued activity is undesirable in clinical use. In this work, we show that, by selecting for cells expressing a selection marker that is coexpressed with the auxiliary gene required for genome modification (*i.e.*, the transposase or the hCas9), it is possible to obtain a cell product that is (i) highly enriched for genome-modified cells, and (ii) depleted of cells with continued auxiliary gene expression.

To our knowledge, this report provides the first strategy that allows the traceless enrichment and counter-selection of gene-modified cells in a single system. With respect to the potential enrichment of genome-edited cells, Kim and colleagues[10,11] have described vectors suitable for enrichment of TALEN and CRISPR genome-edited cells, based on an out-of-frame selection marker downstream of a TALEN or CRISPR recognized site. In this set up, the generation of indels after genome editing of the plasmid has a certain probability to re-establish the correct frame, thereby permitting

cell selection. Although not evaluated in primary cells, data obtained in transformed cell systems demonstrate the feasibility of this approach. However, it does not allow the counter-selection of cells that inadvertently integrate the auxiliary gene. Ran and colleagues[6] have described vectors in which the sgRNA and the hCas9 are linked to a puromycin selection marker, but this system can not be used for counter-selection. Furthermore, the selection'counter-selection strategy we describe in this report is easily translatable to clinical application, as all the necessary reagents are available in clinical grade.

While we have here focused on the use of the truncated EGFR as a clinically useful selection/counter-selection system for the creation of transposon or hCas9 gene-modified cells, it is evident that the same approach may be used for other recently developed marker systems, such CD19 (refs. [12,13]), CD20 (ref. [14]), or RQR8 (ref. [15]). By the same token, while we here demonstrate enrichment of both SB gene-modified cells and hCas9 genome-edited cells, it is apparent that the same strategy can be applied to other transposon gene transfer systems[2] and to other tools for genome editing, such as zinc finger nucleases[16] or TALENs.[17] As a side note, in all these cases, the "traceless" nature of the positive selection system avoids the potential deletion of the gene-modified T cells *in vivo* as a consequence of inadvertent immune recognition, as has for instance been observed for the HSV TK suicide switch.[18]

Materials and methods

Vectors. The pT2-CAGGS-GFP transposon vector, encoding GFP under control of the chicken albumin promoter, and the SB100X transposase vector, encoding the hyperactive SB100X transposase under control of the cytomegalovirus (CMV) promoter were generously provided by Z. Izsvak (Max Delbrück Institute, Berlin, Germany) and have been described previously.[1] The transposon vector encoding the codon-optimized 1D3 T-cell receptor specific for the melanocyte differentiation antigen MART-1 (ref. [19]), under control of the MP71 (ref. [20]) promotor was generated by cloning the corresponding expression cassette[21] between the EcoRI and NotI sites of pT2-HB.[22] To generate the SB P2A Katushka plasmid, the Katushka encoding sequence was amplified by polymerase chain reaction (PCR) with a forward primer containing the P2A sequence and cloned into the ApaI site of the SB100X plasmid. To generate the SB100X IRES PAC plasmid that encodes the PAC enzyme, an IRES PAC cassette was amplified by PCR and cloned into the ApaI site of the SB100X plasmid. To generate the SB100X IRES trEGFR plasmid that encodes the truncated EGFR, an IRES trEGFR cassette was generated and cloned into the ApaI site of the SB100X transposase vector. The hCas9 vector (Addgene plasmid 41815) has been described previously.[5]

The hCas9 IRES PAC plasmid was generated by cloning a PCR amplified IRES PAC fragment into the PmeI site of the hCas9 plasmid. To create the hCas9 P2A codon optimized trEGFR (cotrEGFR) expression cassette, a gene string fragment (Invitrogen, Carlsbad, CA) containing part of hCas9, the P2A element, and the cotrEGFR was cloned between the AscI and PmeI sites of the hCas9 plasmid. The PAC IRES trEGFR plasmid was generated by replacement of the SB100X coding sequence within the SB100X IRES trEGFR vector with the PAC-coding sequence. Guiding RNA (sgRNA) plasmids were ordered as geneblocks (Integrated DNA Technology, Coralville, IA), containing an H1 promoter, the target RNA, and the sgRNA scaffold, and directly cloned into the topo 2.1 vector (Invitrogen). The genomic sequences targeted by the sgRNAs are CGTGAGTAAACCTGAATCTT (β_2m) and CTCGACCAGCTTGACATCAC (TRAC)

Cell culture, transfection, and enrichment. All cell lines were maintained in RPMI (GIBCO, Invitrogen), in the presence of 10% fetal calf serum (FCS; Sigma-Aldrich, St Louis, MO). Tranfection of HeLa and B16 cells was performed using Fugene 6 (Promega, Madison, WI). Adherent cells were seeded 24 hours before transfection into a six-well plate at $1*10^5$ cells/ well, and were transfected using 5 µl of Fugene 6 (Promega) and either 0.5 µg of each plasmid for experiments using hCas9, or 1 µg of plasmid for experiments using PAC IRES trEGFR. Puromycin selection was initiated 24 hours after transfection, for a total of 48 hours at a concentration of 3 µg ml^{-1}.

Jurkat cells were transfected using the Amaxa Nucleofector 4D system (Lonza, Basel, Switzerland), according to the manufacturer's protocol. Briefly, cells were washed once with PBS/0.5% BSA, and for each transfection reaction, 10^6 cells were resuspended in 100 µl nucleofection reagent SE and transferred into a cuvette with 5 µg of plasmid DNA. For transfection, program CL-120 was used. PBMCs, derived from buffy coats from anonymous healthy donors (Sanquin, Amsterdam, The Netherlands) were isolated by Ficoll-Isopaque density centrifugation and cryopreserved in liquid nitrogen.

For DNA electroporation, cells were transfected using the Amaxa Nucleofector 4D system (Lonza), according to the manufacturer's protocol. For transposon experiments, PBMCs were thawed 24 hours prior to nucleofection and cultured in RPMI supplemented with 10% human serum, 50 IU ml^{-1} IL-2 (Novartis, Basel, Switzerland), and 10 ng ml^{-1} IL-15 (Peprotech, Rocky Hill, NJ). On the day of transfection, cells were harvested and washed once with phosphate-buffered saline/0.5% bovine serum albumin. For each transfection reaction, 8×10^6 cells were resuspended in 100 µl nucleofection reagent P3 and transferred into a cuvette together with 5 µg of transposase and 10 µg of transposon vector DNA.

For hCas9 electroporation, cells were activated using Phytohemagglutinin (2 µg ml^{-1}, Biochrom AG, Berlin, Germany). 48–72 hours after activation, cells were harvested and washed once with PBS/0.5% BSA. For each transfection reaction, 5×10^6 cells were resuspended in 100 µl nucleofection reagent P3 and transferred into a cuvette together with 4 µg of hCas9 and 4 µg of sgRNA plasmid DNA. For all experiments involving PBMCs, program EO-115 was used. Following transfection, prewarmed medium was added to the cells, and cells were transferred into a 24-well plate. One day after transfection, trEGFR-expressing cells were purified on an MS column (Miltenyi Biotec, Bergisch Gladbach, Germany) with biotinylated cetuximab and *Strep*-Tactin microbeads (IBA GmbH, Göttingen, Germany), following the manufacturer's instructions. In SB100X transposon experiments, T cells were activated using anti-CD3/CD28 Human T-Activator beads (1 bead/cell, Invitrogen) following selection, and maintained in culture as described above.

Cytokine secretion assay. T2 cells were pulsed with MART-I_{26-35} peptide for 1–2 hours at 37 °C. Subsequently, 0.5×10^6 TCR-modified PBMCs were incubated with 0.5×10^6 peptide-pulsed T2 cells in RPMI containing 10% FCS and 1 µl ml^{-1} Golgiplug (BD Biosciences, San Jose, CA). After a 4- to 5-hour incubation at 37 °C, cells were washed and stained with FITC-labeled anti-CD3- and PerCP-Cy5-labeled anti-CD8, and analyzed for IFN-γ and IL-2 production by intracellular cytokine staining (all antibodies from BD Biosciences).

Statistical analysis and calculation of cell enrichment. Enrichment yield was calculated as (*n* cells pos fraction × TF efficiency pos fraction)/(*n* cells presorting × TF efficiency unsorted). All statistical comparisons were performed using a two-sided student's *t*-test.

Analysis of genome editing. To assess the efficiency of genome editing, genomic DNA was extracted and PCR reactions were performed using Phusion HF polymerase (New England Biolabs) with primer pairs spanning over the sgRNA target site (Supplementary Table S1). PCR products were purified (Illustra GFX PCR DNA purification kit, GE LifeSciences) and Sanger-sequenced. Each sequence chromatogram was analyzed with the online TIDE[9] software (available at http://tide.nki.nl). Off target sites were predicted by using the CRISPR design tool[23] (available at http://crispr.mit.edu).

Acknowledgments

We would like to thank S. Riddell and M. Jensen (University of Washington, USA) for sharing the trEGFR vector system, and Z. Izsvák (Max Delbrück Center for Molecular Medicine, Germany) for sharing the SB100X vector system. This work was supported by the EU FP7 ITN ATTACK and by the EU FP7 project SUPERSIST. R.M. designed, performed, analyzed and interpreted experiments, and wrote the paper. A.H. designed, performed, analyzed, and interpreted experiments. R.G.-E. designed, performed, analyzed, and interpreted experiments. T.N.S supervised the project, designed and interpreted experiments, and wrote the paper. The authors declare no competing financial interests.

References

1 Mates, L. *et al.* Molecular evolution of a novel hyperactive Sleeping Beauty transposase enables robust stable gene transfer in vertebrates. *Nature genetics* **41**, 753-761, doi:10.1038/ng.343 (2009).

2 Yusa, K., Zhou, L., Li, M. A., Bradley, A. & Craig, N. L. A hyperactive piggyBac transposase for mammalian applications. *Proceedings of the National Academy of Sciences of the United States of America* **108**, 1531-1536, doi:10.1073/pnas.1008322108 (2011).

3 Cong, L. *et al.* Multiplex genome engineering using CRISPR/Cas systems. *Science* **339**, 819-823, doi:10.1126/science.1231143 (2013).

4 Jinek, M. *et al.* RNA-programmed genome editing in human cells. *eLife* **2**, e00471, doi:10.7554/eLife.00471 (2013).

5 Mali, P. *et al.* RNA-guided human genome engineering via Cas9. *Science* **339**, 823-826, doi:10.1126/science.1232033 (2013).

6 Ran, F. A. *et al.* Genome engineering using the CRISPR-Cas9 system. *Nature protocols* **8**, 2281-2308, doi:10.1038/nprot.2013.143 (2013).

7 Hackett, P. B., Largaespada, D. A. & Cooper, L. J. A transposon and transposase system for human application. *Molecular therapy : the journal of the American Society of Gene Therapy* **18**, 674-683, doi:10.1038/mt.2010.2 (2010).

8 Wang, X. *et al.* A transgene-encoded cell surface polypeptide for selection, in vivo tracking, and ablation of engineered cells. *Blood* **118**, 1255-1263, doi:10.1182/blood-2011-02-337360 (2011).

9 Brinkman, E. K., Chen, T., Amendola, M. & van Steensel, B. Easy quantitative assessment of genome editing by sequence trace decomposition. *Nucleic acids research* **42**, e168, doi:10.1093/nar/gku936 (2014).

10 Kim, H. *et al.* Surrogate reporters for enrichment of cells with nuclease-induced mutations. *Nature methods* **8**, 941-943, doi:10.1038/nmeth.1733 (2011).

11 Ramakrishna, S. *et al.* Surrogate reporter-based enrichment of cells containing RNA-guided Cas9 nuclease-induced mutations. *Nature communications* **5**, 3378, doi:10.1038/ncomms4378 (2014).

12 Tey, S. K., Dotti, G., Rooney, C. M., Heslop, H. E. & Brenner, M. K. Inducible caspase 9 suicide gene to improve the safety of allodepleted T cells after haploidentical stem cell transplantation. *Biology of blood and marrow transplantation : journal of the American Society for Blood and Marrow Transplantation* **13**, 913-924, doi:10.1016/j.bbmt.2007.04.005 (2007).

13 Di Stasi, A. *et al.* Inducible apoptosis as a safety switch for adoptive cell therapy. *The New England journal of medicine* **365**, 1673-1683, doi:10.1056/NEJMoa1106152 (2011).

14 Serafini, M. *et al.* Characterization of CD20-transduced T lymphocytes as an alternative suicide gene therapy approach for the treatment of graft-versus-host disease. *Human gene therapy* **15**, 63-76, doi:10.1089/10430340460732463 (2004).

15 Philip, B. *et al.* A highly compact epitope-based marker/suicide gene for easier and safer T-cell therapy. *Blood* **124**, 1277-1287, doi:10.1182/blood-2014-01-545020 (2014).

16 Urnov, F. D. *et al.* Highly efficient endogenous human gene correction using designed zinc-finger nucleases. *Nature* **435**, 646-651, doi:10.1038/nature03556 (2005).

17 Christian, M. *et al.* Targeting DNA double-strand breaks with TAL effector nucleases. *Genetics* **186**, 757-761, doi:10.1534/genetics.110.120717 (2010).

18 Bonini, C. *et al.* HSV-TK gene transfer into donor lymphocytes for control of allogeneic graft-versus-leukemia. *Science* **276**, 1719-1724 (1997).

19 Jorritsma, A. *et al.* Selecting highly affine and well-expressed TCRs for gene therapy of melanoma. *Blood* **110**, 3564-3572, doi:10.1182/blood-2007-02-075010 (2007).

20 Engels, B. *et al.* Retroviral vectors for high-level transgene expression in T lymphocytes. *Human gene therapy* **14**, 1155-1168, doi:10.1089/104303403322167993 (2003).

21 Bendle, G. M. *et al.* Lethal graft-versus-host disease in mouse models of T cell receptor gene therapy. *Nature medicine* **16**, 565-570, 561p following 570, doi:10.1038/nm.2128 (2010).
22 Cui, Z., Geurts, A. M., Liu, G., Kaufman, C. D. & Hackett, P. B. Structure-function analysis of the inverted terminal repeats of the sleeping beauty transposon. *Journal of molecular biology* **318**, 1221-1235 (2002).
23 Hsu, P. D. *et al.* DNA targeting specificity of RNA-guided Cas9 nucleases. *Nature biotechnology* **31**, 827-832, doi:10.1038/nbt.2647 (2013).

Supplementary Table 1: gRNA target sites and PCR primer pairs spanning the target sites

gRNA Target site	For	Rev
TRAC On target		
CTCGACCAGCTTGACATCAC	GTGGTGGCAGGGAGGTAACC	CACAGCCTATGTGAGTACTG
TRAC off target 1		
CATGTCCAGGTTGACATCAC	GCTCCTACCCCCTCCATAAG	GACCTGAGGGTCTGGAGTGA
TRAC off target 2		
CATGATCTGCTTGACATCAC	GCAGACACTGCCCATAAGGT	CTGCTTTCTGTCCCATCCTT
TRAC off target 3		
CTAAAGCAGATTGACATCAC	TGAGAAGAGCTGGCCAAAGT	TCTTGTCTCCAAGCCCAGAT
B2M On target		
CGTGAGTAAACCTGAATCTT	TCAATGTCGGATGGATGAAA	AAAATGGAGGTGGCTTGTTG

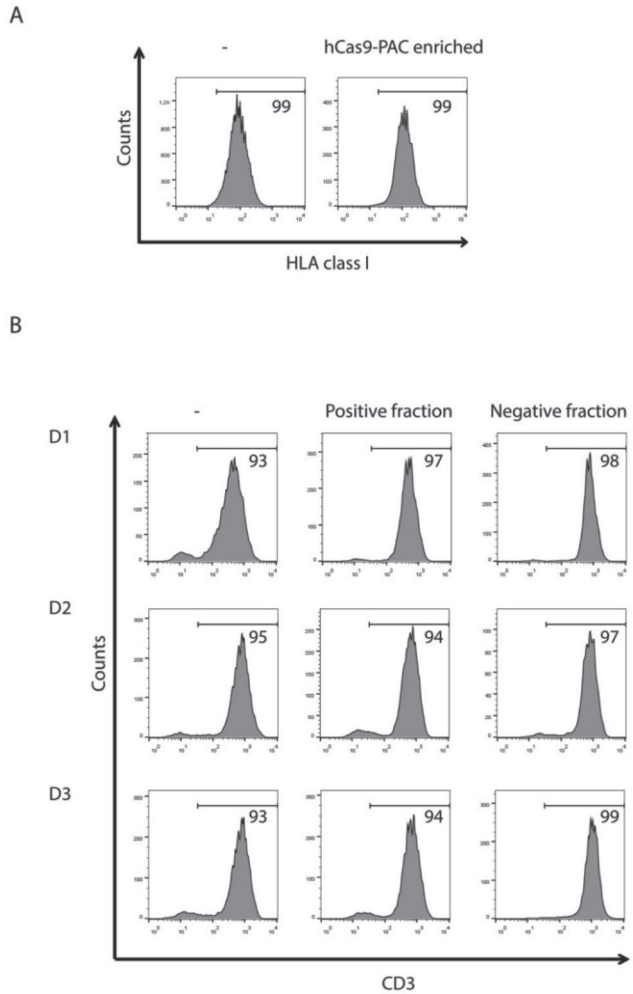

Supplementary figure S1: sgRNA dependency of genome editing.
(a) HeLa cells were transfected with hCas9 IRES PAC without the sgRNA expressing plasmid and treated with puromycin or left untreated. Maintenance of HLA class I in this setting confirms that the HLA class I loss observed in Fig 3 is due to Cas9-mediated genome editing. (b) PBMCs derived from three different donors were activated with PHA and transfected with hCas9 IRES cotrEGFR without the sgRNA expressing plasmid. 24h after transfection, cells were magnetically sorted for trEGFR expression and positive and negative fractions were collected. As compared to untransfected cells, the fraction of CD3-negative cells within the lymphocyte gate is not increased in either the trEGFR positive or trEGFR negative fraction. Numbers in the figures indicate percentage of cells falling in the indicated gates.

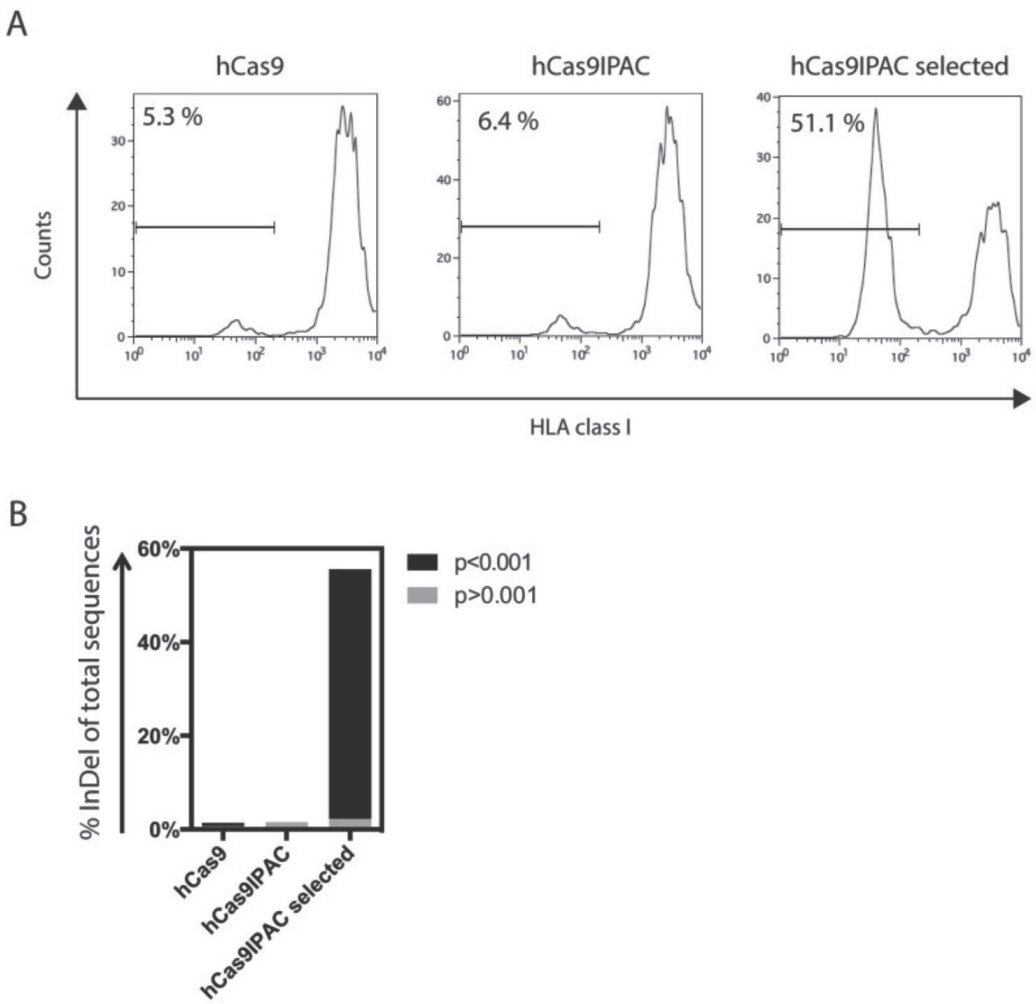

Supplementary figure S2: Analysis of genome editing in HeLa cells.
(a) HeLa cells were transfected with an sgRNA targeting the β2m gene and either the hCas9 or the hCas9 IRES PAC plasmid. Cells transfected with the hCas9 IRES PAC plasmid were either left untreated or treated with puromycin for two days. (b) The frequency of indels created under the three different conditions was assessed by sanger sequencing of PCR product covering the sgRNA targeted site and analysis with the TIDE algorithm. p values indicate the likelihood of the signal of a given indel to be above background. Frequencies of indels with $p<0.001$ or $p>0.001$ (only the former considered significant) were added and are depicted.

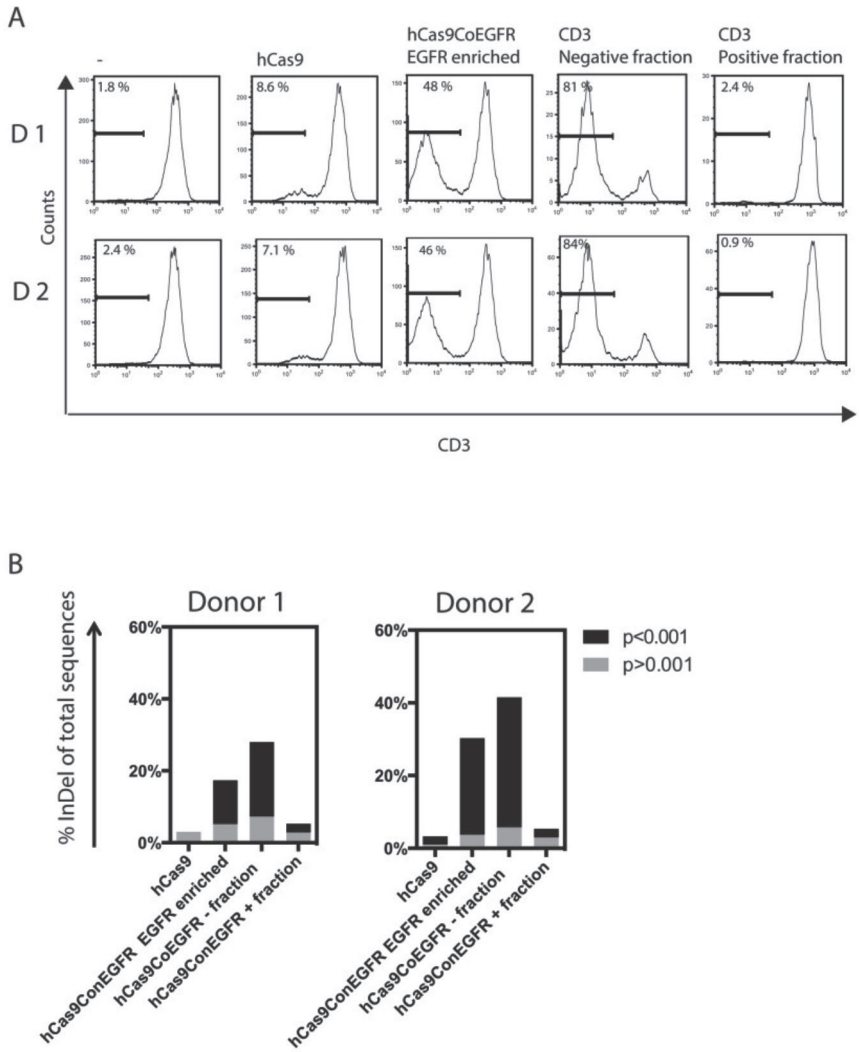

Supplementary figure S3: Analysis of genome editing in PBMCs.
(a) PBMCs from two donors were either left untreated or co-electroporated with a sgRNA targeting the TRAC and either the hCas9 or hCas9 P2A cotrEGFR plasmid. Cells transfected with sgRNA and hCas9 P2A cotrEGFR were magnetically enriched for trEGFR expression. After 10 days of culture, cells previously enriched for trEGFR expression were either left unsorted or magnetically selected for absence or presence of CD3 expression. (b) hCas9, hCas P2A trEGFR enriched, CD3 negative and CD3 positive cells were analysed for the frequency of indels, as described in Suppl. Fig. S2. p values indicate the likelihood of the signal of a given indel to be above background. Frequencies of indels with $p<0.001$ or $p>0.001$ (only the former considered significant) were added and are depicted.

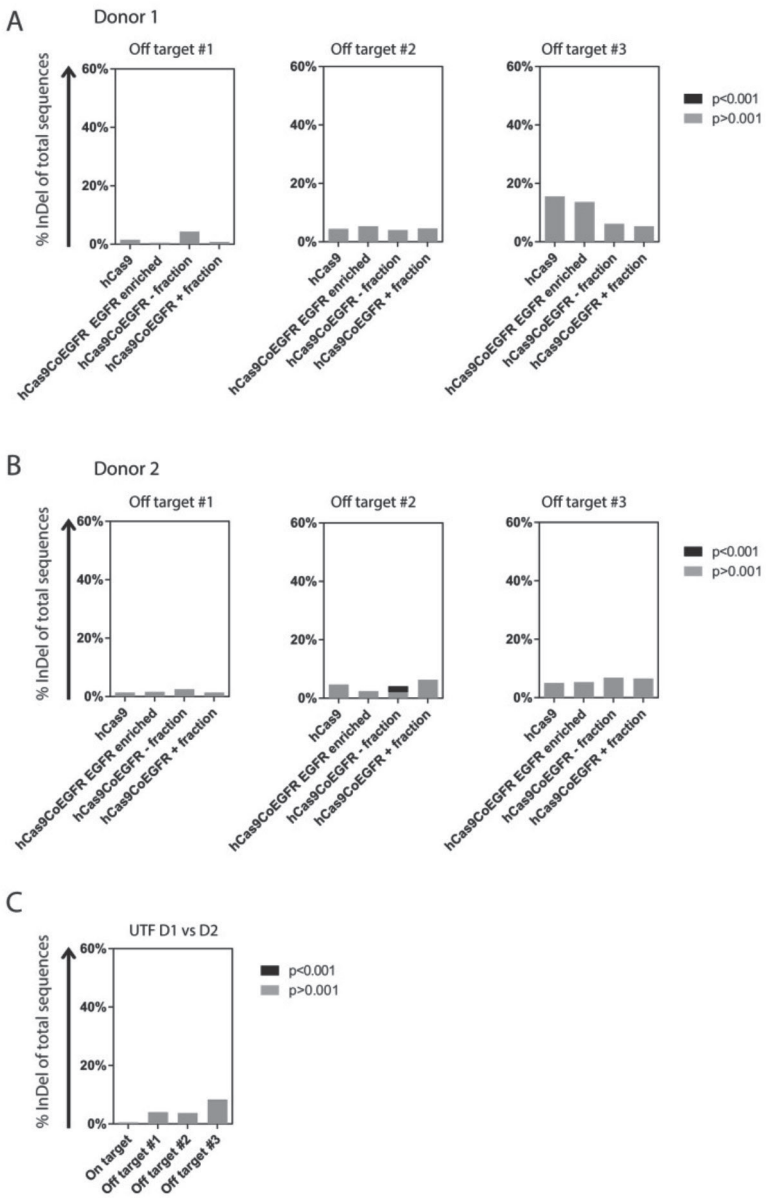

Supplementary figure S4: Analysis of off-target genome editing in PBMCs
Materials of Suppl. Fig. S3 were analysed for the frequency of indels in the top three off-target sites (Table S1). (a) Donor one. (b) Donor two. (c) Comparison between two untransfected samples, used to assess background of the assay. p values indicate the likelihood of the signal of a given indel to be above background. Frequencies of indels with $p<0.001$ or $p>0.001$ (only the former considered significant) were added and are depicted.

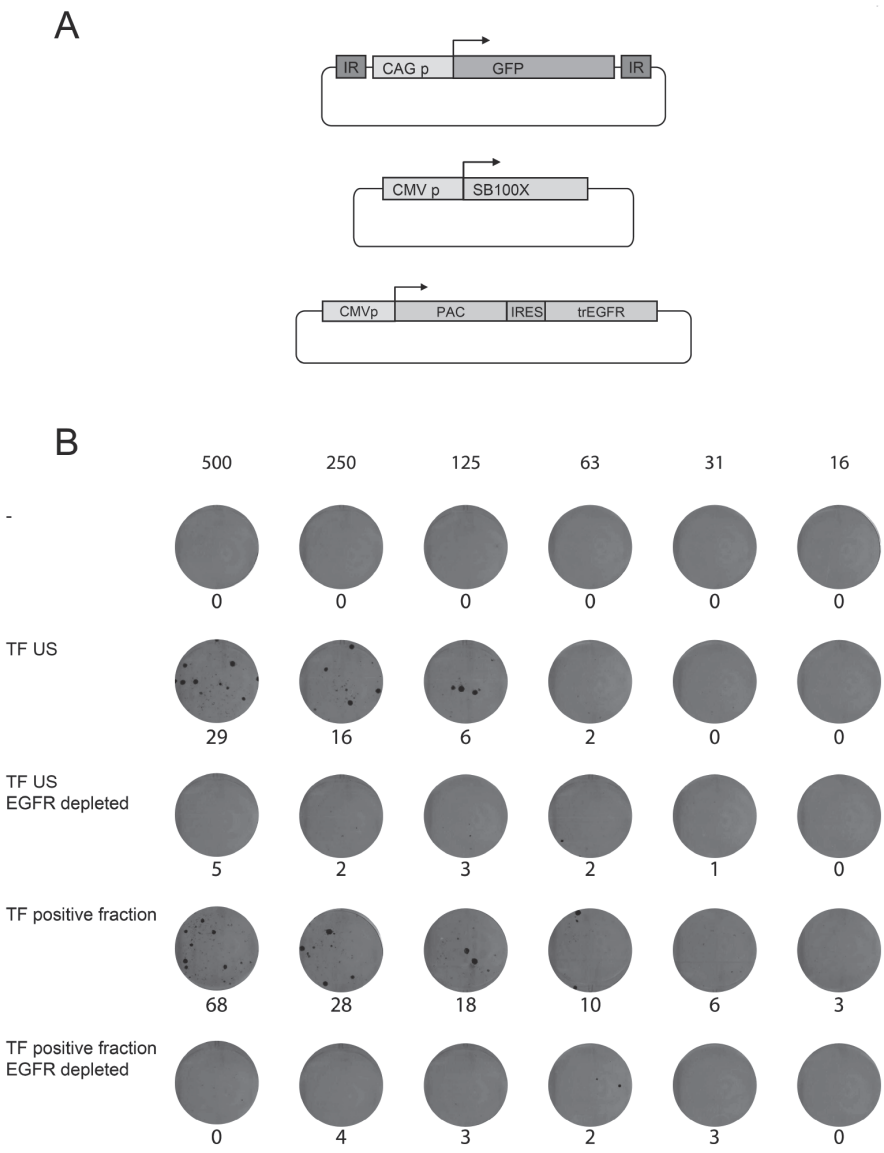

Supplementary figure S5: Counter-selection of cells harbouring unwanted auxiliary vector integrations generated in presence of transposase activity.

(a) Vectors used in the experiment. (b) B16 cells were either left untransfected or transfected ('TF') with the three vectors shown in panel a. Transfected cells were either kept unselected ('US') or magnetically sorted for trEGFR expression ('positive fraction'). After 14 days of culture, samples was either depleted from EGFR positive cells ('EGFR depleted') or left untreated, and serial dilutions of cells were plated and selected with puromycin for 10 days. Numbers on top of the panel indicate input cell numbers times 10-3, numbers below each well indicate the number of colonies observed.

Chapter 4

Cdc25 Inhibitor Improves Transposon-Mediated Gene Modification of Human T Lymphocytes

Andreas Hollenstein[1,#,¶], Riccardo Mezzadra[1,¶], and Ton N. Schumacher[1,*]

[1] Division of Immunology, The Netherlands Cancer Institute, Amsterdam, The Netherlands.

[#] Present address: Genmab, Utrecht, The Netherlands [*]To whom correspondence should be addressed at t.schumacher@nki.nl

[¶] These authors contributed equally

Unpublished

Vectors derived from integrating viruses currently form the gold standard for clinical T cell engineering. An interesting alternative with respect to cost and in particular versatility is represented by non-viral gene delivery systems, such as the Sleeping Beauty transposon-system. At present, the usage of this system is hampered by the high toxicity of the initial plasmid transfection step and lower gene modification efficiency, as compared to viral vector systems. In order to identify small molecule compounds that increase the performance of transposon-based gene modification systems, we conducted a high throughput screen of a library of compounds with defined pharmacological activity. Using this setup, we identified a Cdc25 inhibitor that both improves transfection efficiency and reduces cellular toxicity in human lymphocytes. Inclusion of Cdc25 inhibitor leads to a 60% increase in gene-modified T cells and a 46% increase in cell viability, while leaving phenotype and function of the resulting T cells unaltered. Our results demonstrate that limitations associated with transposon-mediated gene delivery can be pharmacologically mitigated, providing an interesting strategy to facilitate clinical application.

Introduction

Clinical and experimental evidences demonstrate that T cells have the potential to recognize and kill tumor cells. In tumors with a high mutational load, 'neo-antigens' that are formed as a consequence of DNA mutations can lead to a high affinity T cell response[1]. However, in many human tumors, the anti-tumor potential of the endogenous T cell pool is poor, both because the frequency of tumor reactive T cells is low, and because T cells directed against non-mutated tumor-associated self antigens can express low affinity receptors.

Over the past years, compelling preclinical and clinical evidence has been obtained indicating that the lack of antigenicity of such tumors can be overcome by *in vitro* gene modification of T cells with either chimeric antigen receptors or T cell receptors specific for tumor-associated antigens[2-8]. The most broadly used strategy for such T cell engineering relies on the use of integrating lentiviral and retroviral vectors. With now more than 10 years of clinical experience, the risk of adverse events, such as insertional mutagenesis, following viral modification of human T cells appears minimal, and the gene modification efficiencies that can be obtained are generally high. As a significant down side, the time and cost required for the production of clinical grade virus batches is significant, thereby making the flexibility of these systems low.

With the emerging evidence for the clinical activity of receptor-modified T cells[2-8], it has become important to assess the safety and efficacy of CARs and TCRs for a series of different antigens in the coming years. Furthermore, in order to exploit the patient-specific repertoire of tumor-specific TCRs for therapy (discussed in [9]), a highly flexible system for gene transfer will also be required. In this regard, transposon-based gene transfer systems represent an interesting alternative over viral vector systems, as their production is substantially less costly and time-consuming.

Transposon-based gene delivery systems rely on the activity of a transposase enzyme that is able to catalyze the genomic integration of the transposon, a gene expression cassette containing the gene of interest that is flanked by inverted regions (IR). Both the Sleeping Beauty transposon and PiggyBac transposon systems have successfully been used for human T cell modification[10,11] and recently the SB system has been used to generate chimeric antigen receptor-modified T cell products for patient treatment[12]. Furthermore, *in vitro* molecular evolution has led to the generation of hyperactive transposase variants, such as the SB transposase 100X, that yield higher efficiencies of gene transfer[13].

While conceptually appealing, widespread clinical application of transposon-based systems for T cell modification is hindered by two issues: First, introduction of DNA into human T cells leads to significant cell death, and while the required transposase activity may be obtained by transfection of encoding RNA[14], the delivery of the transposon itself in the form of DNA is obligatory. Second, and possibly related to this toxicity, the efficiency of transposon-mediated T cell modification is generally lower than that obtained with virus-based delivery systems.

As the toxicity that is seen upon DNA (but not RNA) transfection is likely to be mediated by the intracellular sensing of incoming DNA, we reasoned that pharmacological modulation may potentially reduce these issues. In order to evaluate this, we established a high throughput screening system in which we tested the effects of more than 1,200 compounds on T cell viability and gene modification efficiency upon SB100X-mediated gene transfer into human peripheral blood mononuclear cells (PBMC). This screen identified the irreversible Cdc25 inhibitor NSC 95397 as a compound that is able to increase both T cell viability and gene modification efficiency upon transposon-mediated gene transfer. Importantly, TCR gene-modified T cells generated in the presence of NSC 95397 show similar activity as compared to untreated cells in terms of specific cell killing and cytokine secretion. To our knowledge, this is the first study demonstrating that the efficiency of transposon-based gene delivery systems can be pharmacologically improved, providing a novel avenue to facilitate clinical application of these gene transfer systems.

Results

A high throughput screen to identify molecules that influence transposon-mediated gene transfer into human T cells

In order to evaluate whether pharmacological modulation can be used to enhance the efficacy of transposon-mediated gene modification, we set up a system to analyse the effects of a library of more than 1,200 compounds with described pharmacological activity (library of pharmaceutically active compound, LOPAC) in a high throughput fashion. To this purpose, T cells were transfected with the SB100X system and distributed over 384 well plates containing the individual compounds (Fig. 1A). 24 h later, T cells were activated and at day 5 following gene modification, cells were evaluated by flow cytometry for viability and transfection efficiency.

This initial LOPAC screen revealed a series of compounds that had a beneficial effect on either cell viability or transgene expression relative to controls (Fig. 1B). To confirm and narrow down the optimal concentration, the effects of the ten compounds

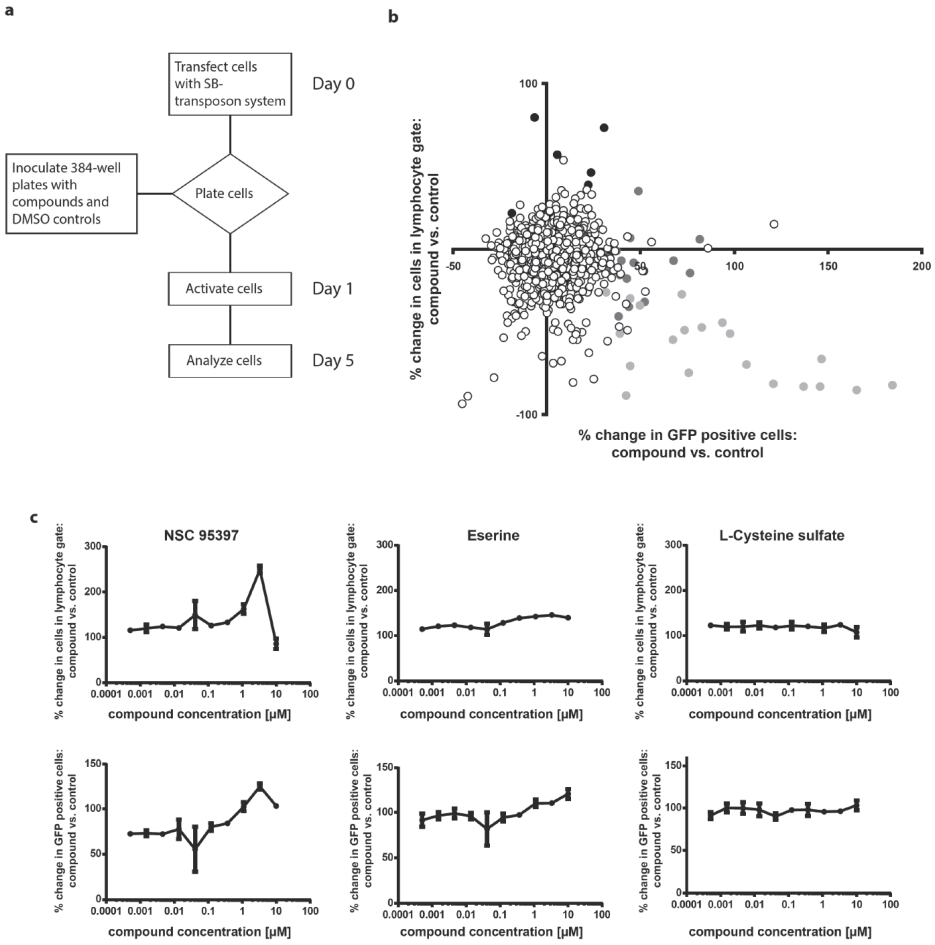

Fig. 1. LOPAC screen and hit validation. a). Experimental scheme of the high throughput compound screen. Frozen PBMCs were thawed, 24h later, cells were electroporated and directly transferred to wells containing individual compounds (1 µM). 24h after electroporation, T cells were stimulated using phytohemagglutinin. Cell viability and transfection efficiency were analyzed by flow cytometry at day 5 after transfection. b). Compound effects on transfection efficiency and cell viability. Dots indicate the effects of individual compounds on viability and transfection efficiency, as compared to untreated transfected cells. Black: significant increase in survival, no significant effect on transfection efficiency. Dark grey significant increase in transfection efficiency, no significant effect on survival. Light grey significant increase in transfection efficiency, significant decrease in survival. c). Compound effect validation. Effect of three hits identified within the primary LOPAC screen on survival (upper panels) and transgene expression (lower panel) of SB100X transfected cells at the indicated concentrations. Of the primary hits, only NSC 95397 showed a statistically significant effect in confirmation experiments.

possessing the highest effect on at least one of the two assessed parameters were evaluated at a series of concentrations (Fig. 1C and data not shown). Of these ten compounds, the irreversible Cdc25 inhibitor NSC 95397 showed the most pronounced effects, with optimal activity at concentrations between 1 – 5 µM. Inhibition of Cdc25 by NSC 95397 has previously been shown to induce cell cycle arrest at the G2/M transition in various cell types, but its effect on T cell expansion has to our knowledge not been reported (see below). The positive effect of NSC 95397 on T cell modification was not restricted to the conditions used for high throughput screening, but was also observed in three independent donors under the standard (larger scale) conditions for SB transposon-mediated gene transfer (Fig. 2). Increased cell viability was both observed when assessed by morphology (fsc/ssc, as performed in the initial screen), and when assessed by propidium iodide staining (data not shown). Specifically, at day six, the fraction of viable cells in samples treated with 5 µM NSC 95397 was on average 34% higher than in non-treated controls (Fig. 2A-B). Treatment with NSC 95397 also had a beneficial effect on the frequency of stable gene modification assessed thirteen days after transfection (Fig. 2C, average increase of 38% at 5 µM).

To evaluate whether the results obtained with these three donors were significant over a large set of experiments, we analysed the effects of NSC 95397 inclusion in a set of technical replicates. The average viability of cells treated with NSC 95397 relative to non-treated controls six days after transfection (n=52) was 146% (Fig. 2E), and the average percentage of cells showing stable transgene expression (n=19) was 160% relative to matched controls (Fig. 2F and table S1). Non-parametric tests comparing viability and stable GFP transgene expression for paired samples in this data set revealed that the effects of NSC 95397 on both viability and transgene expression were highly significant (P-values of 0.0003 and <0.0001, respectively).

As during transposon-mediated gene transfer, both the introduction of foreign DNA into the cells and the subsequent DNA integration event may conceivably lead to a cellular stress response, we explored whether the positive effects of cdc25 inhibiton requires transposase-mediated DNA integration. To assess whether NSC 95397 acts by preventing a DNA damage stress response caused by the transposase-mediated integration event, we determined the effect of NSC 95397 addition when using a catalytically inactive form of the SB transposase (SB-D3). Also in this setting, the improvement in viability at day six relative to control was substantial (Fig. 3A, long term transgene expression not assessed for obvious reasons). This indicates that the positive effect of NSC 95397 is not based on preventing a fatal DNA damage stress response caused by the transposition event, but rather is likely to dampen the adverse effects of DNA introduction.

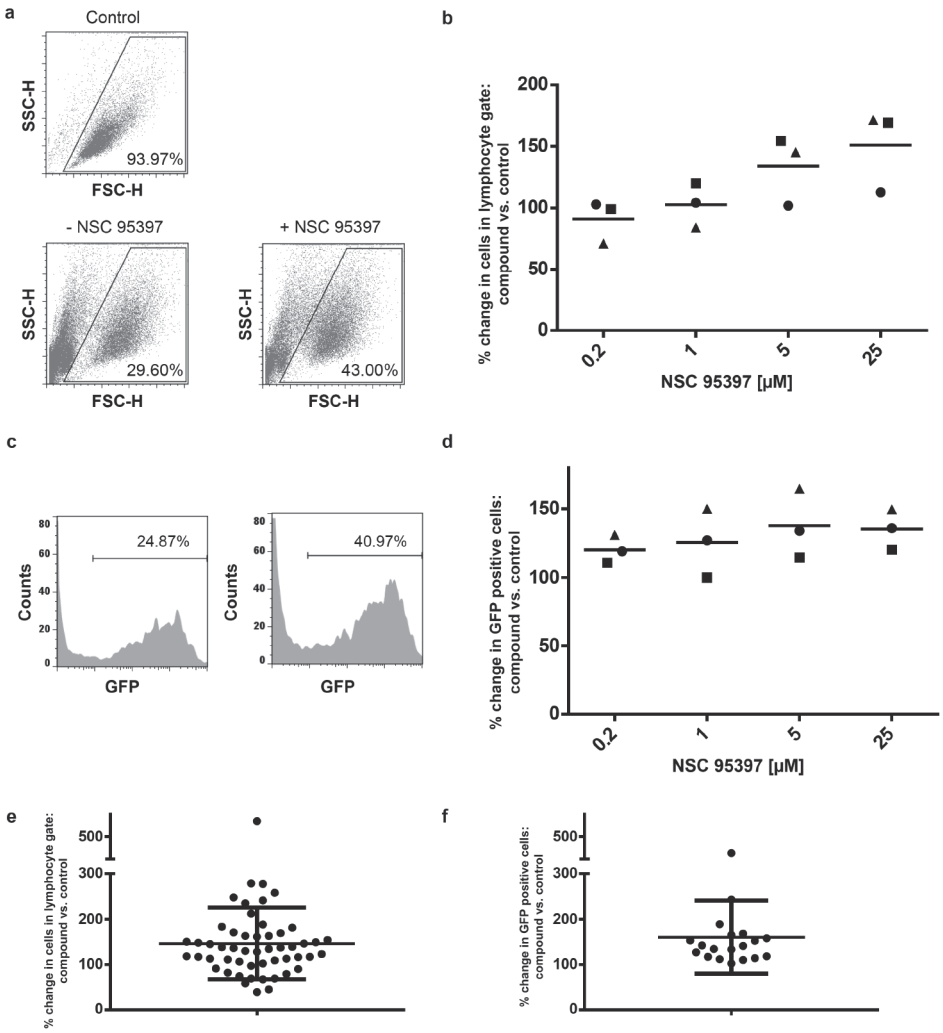

Fig. 2. Effect of NSC 95397 on T cell survival and transfection efficiency. a,b). Effect of the indicated NSC 95397 concentrations on T cell survival upon SB100X mediated T cell modification under standard (large scale) conditions. c,d). Effect of the indicated NSC 95397 concentrations on transfection efficiency upon SB100X mediated T cell modification under standard (large scale) conditions. e,f). Effect of NSC 95397 (5 µM) on T cell survival and transfection upon SB100X mediated T cell modification in a large series of experiments. Effects on both survival (e) and efficiency (f) are significant ($p = 0.0003$ and $p < 0.0001$, respectively).

Effect of NSC 95397 on the PiggyBac (PB) transposon system

To address whether the effects of NSC 95397 are unique to the SB100X transposon system or can be extended to other non-viral gene transfer systems, we compared the efficiency of PiggyBac (PB) transposon-mediated gene transfer in the presence or absence of this compound. In three donors tested, treatment with NSC 95397 increased the fraction of viable cells on day six after transfection on average by approximately 50% (Fig. 3A). Furthermore, while the frequency of stable gene modification using the PB transposon-system is lower than observed for the SB100X-system, the relative improvement obtained by NSC 95397 addition was similar for both systems (Fig. 3A-B).

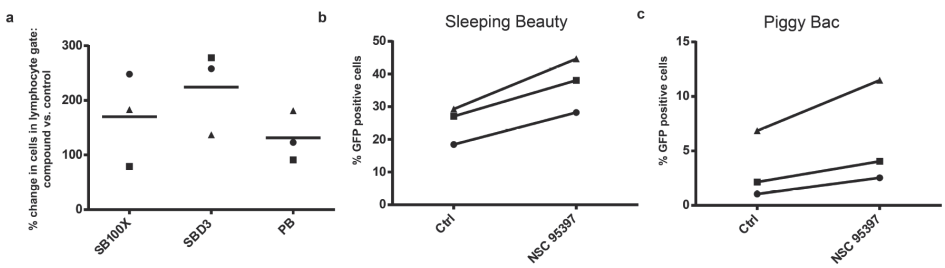

Fig. 3. Effect of NSC95397 addition on different transposon-based gene transfer systems. a). Improvement in human T cell survival upon transfection of PBMCs with SB100X, catalytically inactive SB (SBD3), or PiggyBac by NSC95397 addition. b). Improvement in SB100X mediated gene transfer in human T cells by NSC95397 addition. c). Improvement in PiggyBac-mediated gene transfer in human T cells by NSC95397 addition.

Effect of NSC 95397 on phenotype and functionality of human T cells

To determine whether NSC 95397 treatment influences various aspects of T cell behaviour, transposon modified T cells were generated from three donors. In these experiments, T cells were genetically engineered to express the HLA-A2 restricted, MART-1 specific 1D3 T cell receptor as a clinically relevant transgene [15]. In this small data set, the percentage of transgene expressing cells was not significantly improved by NSC 95397 treatment (data not shown). However, data from a larger series of experiments (n=12) indicates that NSC 95397 also mildly increases the percentage of cells with stable TCR transgene expression (20% increase, $p<0.01$ Fig. S1).

Analysis of the expression of a number of cell surface markers that reflect cell differentiation state (CD62L, CD45RO, CD45RA, CD27) after 13 days of culturing revealed that the differentiation state of T cells exposed to NSC 95793 was comparable to that of untreated transposon-modified T cells (Fig. 4A-B,D). Specifically, in both cases, the majority of T cells consisted of a mixture of cells with effector memory and central memory phenotypes, as based on CD45RA and CD45RO expression. Likewise, the fraction of CD8 positive and negative cells was unaltered by NSC 95793 addition (Fig. 4C).

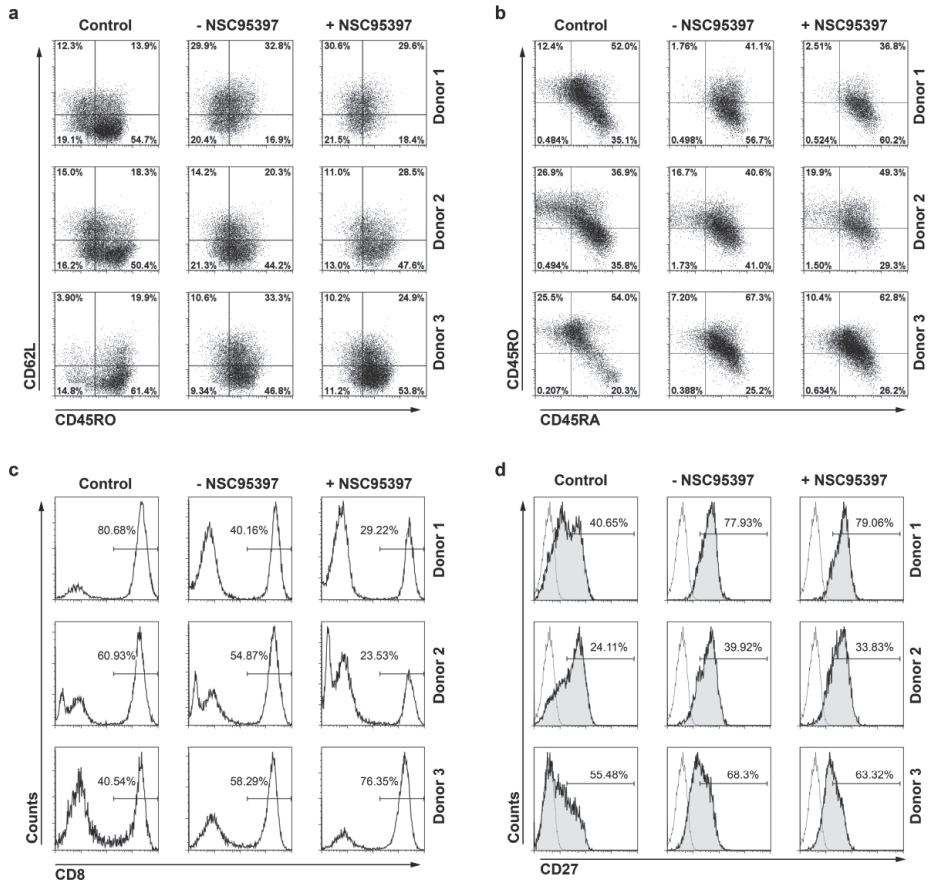

Fig. 4. Unaltered phenoptype of NSC 95397 exposed T cells. Phenotypic characteristics of transfected cells that were either untreated or treated with NSC 95397. Expression of CD45RO and CD62L (a), CD45RO and CD45RA (b), CD8 (c), or CD27 (d) is depicted for NSC 95397 treated and untreated cells, and for untransfected control cells.

To address whether NSC 95397 treatment influences T cell functionality, lymphocytes from those three donors were analyzed for antigen-induced cytokine production and target cell lysis. For T cells from all three donors, the fraction of T cells producing either IL-2, INF-γ, or both were comparable between the two groups over the entire peptide concentration range tested (Fig 5A). To determine lytic capacity, engineered T cells were co-cultured with HLA-A2 positive or negative tumor cell lines expressing MART-1 (in this experiment, T cell receptor expression within the CD8 compartment was near equal for all groups, thereby allowing intergroup comparison). Specific lysis observed upon encounter of relevant tumor cell lines was near identical between the two groups and background activity against an HLA-A2 negative tumor line was equally low (Fig 5B), indicating that also by this criterion, functional activity of NSC 95397 treated cells is fully maintained.

Effect of NSC 95397 on the expansion rate of transposon-modified T cells

In order to generate T cell products for adoptive cell therapy, a shorter *ex vivo* expansion period is considered preferable, as prolonged proliferation biases T cells towards terminal differentiation [16]. To determine whether the enhanced viability of NSC 95397 treated cells translates into an increased expansion capacity, growth curves of transposon-modified T cells from the three donors were generated (Fig. 6A). For all three donors, the fold expansion achieved at day 13 post-transfection was at least three to four times higher for cells treated with NSC 95397 as compared to controls. Importantly the percentage of 1D3 TCR expressing cells was maintained at the same level after 13 days of culturing, showing that there is no growth bias for non-modified T cells in the NSC 95397 treated group (Fig. 6B).

Discussion

At present, retroviral and lentiviral vector systems represent the gold standard for genetic redirection of T cells for adoptive T cell therapy[17]. However, to allow the evaluation of large series of antigen-specific TCRs and CARs, and to assess the potential of personalized TCR gene therapy, alternative systems that allow rapid and cost effective clinical testing of series of receptors would be of value.

Transposon-based systems have significant potential in this respect, as the required GMP grade DNA production is low-cost and rapid, and can easily be performed for multiple transgenes in parallel, without any loss of performances in T cells[18]. At present, the largest obstacle for widespread use of transposon-based systems for human T cell modification is formed by the high cell loss during transfection[19] and

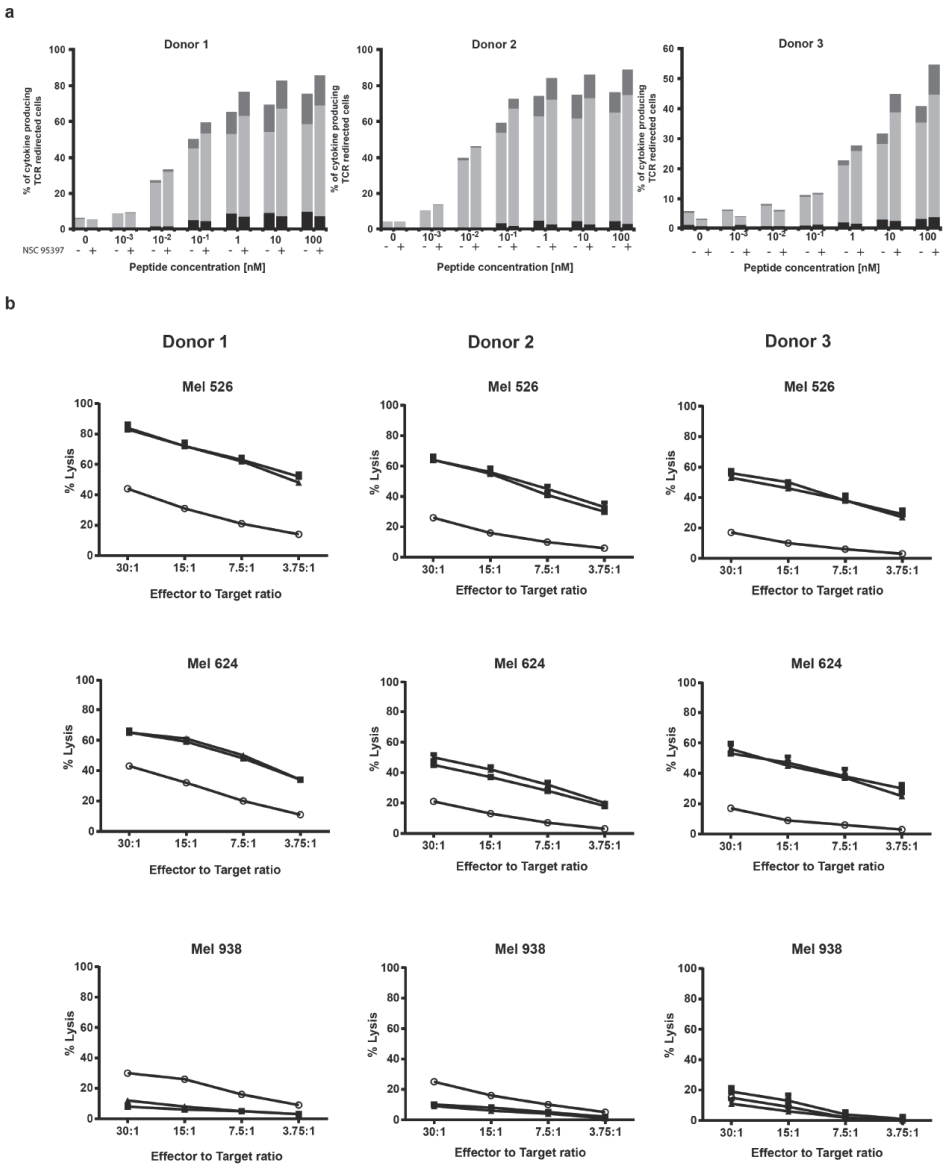

Fig. 5. Cytokine secretion and cytolytic capacity of SB TCR gene modified T cells is maintained upon NSC 95397 exposure. a). PBMC of three different donors were modified with the 1D3 TCR by SB100X-mediated gene transfer. Following cell expansion, the ability of T cells to secrete cytokine upon exposure to T2 cells pulsed with the indicated concentrations of peptide was evaluated. For every peptide concentration, the left and right bar represent untreated samples and NSC 95397 treated samples, respectively. b). PBMC of three different donors were modified with the 1D3 TCR by SB100X-mediated gene transfer (Squares: NSC 95397 treated and transfected; triangles untreated and transfected; open circles: untransfected). Following cell expansion, the lytic capacity of the resulting T cells was evaluated by incubation with relevant (Mel 526 and Mel 624) or control (Mel 938) melanoma lines.

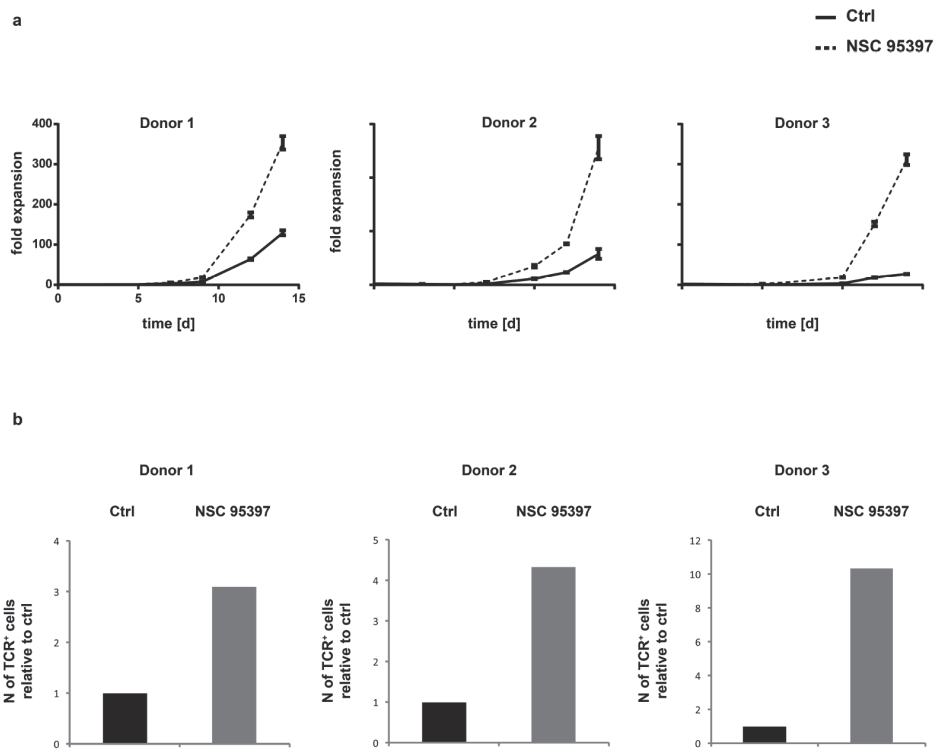

Fig. 6. Improved expansion of NSC 95397 exposed T cells. a) Growth kinetics of NSC 95397 and untreated transfected T cells from three different donors. Cell counts at the indicated time points from the day after transfection show that cells treated with NSC 95397 recover faster from transfection than untreated counterparts. b) Relative fraction of 1D3+ T cells in NSC 95379 treated and untreated transfected T cells.

– possibly because of this – the suboptimal frequency of T cells that stably express the transgene used. In order to mitigate these issues, we here screened a library of 1,280 pharmacologically active compounds for their capacity to improve transposon-mediated gene delivery.

The most significant hit obtained in this screen was the irreversible Cdc25 inhibitor NSC 95397. Under optimized conditions, NSC 95397 addition increased T cell survival at day six after transfection by on average 40% relative to control, and this survival advantage at early time points translated to a very substantial increase in the number of T cells obtained during subsequent culture. The addition of NSC 95397 also led to a significant increase in the percentage of T cells showing stable transgene expression (average increase of 60% relative to control for GFP gene-modified T cells). A possible

explanation for the observation that NSC 95397 addition increases both cell survival and gene modification efficiency is that those cells that take up large amounts of DNA experience higher amount of stress. As such, the cells that are most likely to integrate the transposon are also most likely to benefit from NSC 95397 inclusion. Others have observed that alteration in the cell cycle can impact on Sleeping Beauty transposition[20].

While the effect of NSC 95397 on cell survival was equally pronounced when introducing either a GFP or TCR transgene, the effect on gene modification frequency was more profound for the GFP-encoding than for the TCR-encoding transposon (60%, $p< 0.0001$ relative to control condition versus 20%, $p< 0.01$ relative to control condition). In general, stable gene modification frequencies achieved upon TCR introduction without NSC 95397 addition were higher than for GFP (table S1-2), and also cell recovery was faster. Conceivably, the effect of NSC 95397 addition on gene modification frequency is most profound when utilizing transgenes that are more stressful to cells. This effect may be due to specific motifs within the transgenic DNA sequence or because of the protein encoded. In theory, cellular stress may also be influenced by transgene size. However, as the two transgene cassettes have a similar size (2.7 kb for the GFP vector versus 3.0 kb for the TCR vector), this is excluded as a potential factor here.

Importantly, although the effect of NSC 95397 addition on transfection efficiency is moderate, the combined effect of increased transfection efficiency and faster recovery of cells after transfection allow the production of a clinical grade cell product from at least 5 times less starting material. Furthermore, activity is not restricted to the SB system, but is also observed for the PiggyBac transposon system, making it unlikely that the compound directly interacts with the transposase.

The current data underline the value of unbiased screening, as *a priori*, it would have been difficult to predict the survival benefit of an anti-mitotic drug such as NSC 95397. The data presented here indicate that pharmacological optimization of transposon-mediated gene delivery is feasible, and it is interesting to note that another Cdc25 inhibitor, ARQ 501, has previously been tested in clinical trials. While further mechanistic data are required, the available data suggest that NSC 95397 may increase cell modification efficiency by inhibiting a cell cycle stage dependent pathway that 'senses' incoming DNA. We speculate that with our increased understanding of the molecules that detect incoming DNA[21-23], additional interventions that inactivate this cellular pathway may be developed within the coming years.

Material and Methods

Vectors, transposon-mediated gene modification and cell culture: The transposon vector pT2-CAGGS-GFP, encoding GFP under control of the chicken albumin promoter, and the vectors pCMV-SB100X and pCMV-SB-D3, encoding the hyper active SB100X and inactive variant of the Sleeping Beauty transposase under the control of the CMV promoter, respectively, were generously provided by Z. Izsvak (Max Delbrück Institute) and have been described previously[13]. The transposon vector encoding the codon optimized MART-1 specific T cell receptor 1D3[15] under the control of the MP71[242] promotor was generated by cloning the corresponding expression cassette[25] between the EcoRI and NotI sites of pT2-HB[26]. For experiments involving the PiggyBac transposon-system, the transposase was expressed from a CMV expression plasmid, and GFP was expressed under the control of the chicken albumin promoter from the PiggyBac vector pXL-BacII-GFP, both a kind gift of M. H. Wilson (Baylor College of Medicine).

Melanoma cell lines Mel 526 (HLA-A2$^+$, MART-1$^+$), Mel 624 (HLA-A2$^+$, MART-1$^+$) and Mel 938 (HLA-A2$^-$, MART-1$^+$), and the TAP-deficient T·B cell hybrid T2-A1 (HLA-A1$^+$/A2$^+$) have been described previously[27,28]. All cell lines were maintained in RPMI (GIBCO, Invitrogen, Carlsbad, CA), in the presence of 10% FCS. Peripheral blood mononuclear cells (PBMCs), derived from buffy coats from anonymous healthy donors (Sanquin, Amsterdam, The Netherlands) were isolated by Ficoll-Isopaque density centrifugation and cryopreserved in liquid nitrogen.

For gene transfer, cells were transfected using the Amaxa Nucleofector 4D system (Lonza, Basel, Switzerland), according to the manufacturer's protocol. In brief, PBMCs were thawed one day prior to nucleofection and cultured in RPMI, supplemented with 10% human serum, 50 IU/ml IL-2 (Novartis, Basel, Switzerland) and 10 ng/ml IL-15 (Peprotech, Rocky Hill, NJ). On the day of transfection, cells were harvested and washed once with PBS/ 0.5% BSA. For each transfection reaction, 8 x 10^6 cells were resuspended in 100µl nucleofection reagent P3 and transferred into a cuvette together with 5 µg of transposase and 10 µg of transposon DNA, respectively. For all transfections, program E0-115 was used. Following transfection, prewarmed medium was added to the cells and cells were transferred into a 24-well plate either without compounds, or in the presence of indicated compounds. One day after transfection, T cells were activated using anti-CD3/anti-CD28 Human T-Activator beads, at 1 bead/ cell (Invitrogen, Carlsbad, CA), and maintained in culture as described above. The compound was kept in the culture medium until day 5 post transfection, when it was diluted out by passaging the cells.

LOPAC screen: Compounds that influenced gene modification efficiency and/ or cell viability were identified in 4 consecutive screens, with each screen covering one quarter of the Library of Pharmaceutically Active Compounds (LOPAC^{1280}) (Sigma Aldrich, St Louis, MO). Screens were performed in duplicate, on two identically prepared 348-well plates. 11 x 10^7 cells were transfected with the combination of SB100X transposase vector and the GFP encoding transposon pT2-CAGGS-GFP, as described above. Cells were pooled and subsequently plated into 348-well plates (40µl per well), pre-filled with individual compounds or solvent controls (40µl per well), at a final concentration of 1 µM for each compound. After 24h, T cells were activated by addition of phytohaemagglutinin-L (Biochrom, Berlin, Germany) at 2 µg/ml. Four days after activation, cells were analyzed for viability and GFP expression on a FACSCalibur equipped with a high throughput sampling device (Becton Dickinson, Franklin Lakes, NJ). Compound effects were defined as significant when for both duplicates the change relative to control in either viability or gene expression was larger than twice the standard deviation measured for the solvent controls (n= 32) included in both plates.

Cytokine production and chromium release assays: T2 cells were pulsed with peptides for 1-2 hours at 37°C. Subsequently, 0.5×10^6 TCR-modified PBMCs were incubated with 0.5×10^6 peptide-pulsed T2 cells in RPMI containing 10% FCS and 1µL/mL Golgiplug (BD Biosciences, Basel, Switzerland). After a 4- to 5-hour incubation at 37°C, cells were washed and stained with FITC-labeled anti-CD3 antibody and PerCP-Cy5 labeled anti-CD8 antibody, and analyzed for IFN-γ and IL-2 production by intracellular cytokine staining (all antibodies from BD Biosciences, Basel, Switzerland). For every group, cytokine production was normalized to the percentage of TCR-modified T cells. In order to measure cytotoxic activity of TCR-modified T cells, target cells were labeled with 100 µCi (3.7 MBq) ^{51}Cr (GE healthcare, Little Chalfront, UK) for 1 hour at 37°C. Labeled target cells were incubated with effector cells at the indicated E/T ratios for 4 hours at 37°C in 200 µL RPMI containing 10% FCS. Subsequently, 50 µl of supernatant was transferred onto LumaPlates (Perkin Elmer, Waltham, MO) and analyzed on a TopCount NXT (Perkin Elmer, Waltham, MO).

Flow cytometric analysis: TCR cell surface expression on gene-modified PBMCs was measured by staining with MHC multimers generated through UV-induced peptide exchange [29,30], in combination with allophycocyanin (APC) labeled anti-CD8 (Becton Dickinson, Franklin Lakes, NJ) staining. Phenotypic properties of cells were assessed by staining with FITC-labeled anti-CD62L, PE-labeled anti-CD45RO, APC-labeled anti-CD45RO, and FITC-labeled anti-CD27 antibody (all Becton Dickinson, Franklin Lakes, NJ). For analysis of intracellular cytokine production, cells were stained with PE-

labeled anti-IL2, and APC-labeled anti-INFγ antibody (both Becton Dickinson, Franklin Lakes, NJ). Cells were analyzed using a FACSCalibur (Becton Dickinson, Franklin Lakes, NJ) and data were analyzed with FlowJo 7.6.

Cell expansion analysis: Cells were counted in triplicates at the indicated time points using the CASY cell counting system (Innovatis, Zurich, Switzerland). At each time point, 10^6 cells were placed back into a 24-well plate and kept under standard culture conditions. For each pair of consecutive time points, fold expansion was calculated as (cell count at time point n / cell count at time point n-1), and expansion curves were created by multiplication of consecutive expansion values.

Statistical analysis: Wilcoxon signed-rank tests were used to assess statistical significance of differences in absolute cell numbers and gene modification efficiencies between the indicated groups. Statistical analyses were performed using Prism V6.01.

Acknowledgements

We would like to thank Ben Morris and Boris Rodenko for their assistance in carrying out the LOPAC screen. This work was supported by the EU FP7 ITN ATTACK. The authors declare no conflict of interest.

References

1 Heemskerk, B., Kvistborg, P. & Schumacher, T. N. The cancer antigenome. *The EMBO journal* **32**, 194-203, doi:10.1038/emboj.2012.333 (2013).

2 Morgan, R. A. *et al.* Cancer regression in patients after transfer of genetically engineered lymphocytes. *Science* **314**, 126-129, doi:10.1126/science.1129003 (2006).

3 Johnson, L. A. *et al.* Gene therapy with human and mouse T-cell receptors mediates cancer regression and targets normal tissues expressing cognate antigen. *Blood* **114**, 535-546, doi:blood-2009-03-211714 [pii] 10.1182/blood-2009-03-211714 (2009).

4 Robbins, P. F. *et al.* Tumor regression in patients with metastatic synovial cell sarcoma and melanoma using genetically engineered lymphocytes reactive with NY-ESO-1. *J Clin Oncol* **29**, 917-924, doi:JCO.2010.32.2537 [pii] 10.1200/JCO.2010.32.2537 (2011).

5 Kalos, M. *et al.* T cells with chimeric antigen receptors have potent antitumor effects and can establish memory in patients with advanced leukemia. *Sci Transl Med* **3**, 95ra73, doi:3/95/95ra73 [pii] 10.1126/scitranslmed.3002842 (2011).

6 Porter, D. L., Levine, B. L., Kalos, M., Bagg, A. & June, C. H. Chimeric antigen receptor-modified T cells in chronic lymphoid leukemia. *N Engl J Med* **365**, 725-733, doi:10.1056/NEJMoa1103849 (2011).

7 Grupp, S. A. *et al.* Chimeric antigen receptor-modified T cells for acute lymphoid leukemia. *N Engl J Med* **368**, 1509-1518, doi:10.1056/NEJMoa1215134 (2013).

8 Brentjens, R. J. *et al.* CD19-targeted T cells rapidly induce molecular remissions in adults with chemotherapy-refractory acute lymphoblastic leukemia. *Sci Transl Med* **5**, 177ra138, doi:5/177/177ra38 [pii] 10.1126/scitranslmed.3005930 (2013).

9 Linnemann, C., Mezzadra, R. & Schumacher, T. N. TCR repertoires of intratumoral T-cell subsets. *Immunol Rev* **257**, 72-82, doi:10.1111/imr.12140 (2014).

10 Huang, X. *et al.* Stable gene transfer and expression in human primary T cells by the Sleeping Beauty transposon system. *Blood* **107**, 483-491, doi:2005-05-2133 [pii] 10.1182/blood-2005-05-2133 (2006).

11 Nakazawa, Y. *et al.* Optimization of the PiggyBac transposon system for the sustained genetic modification of human T lymphocytes. *J Immunother* **32**, 826-836, doi:10.1097/CJI.0b013e3181ad762b (2009).

12 Hackett, P. B., Largaespada, D. A. & Cooper, L. J. A transposon and transposase system for human application. *Mol Ther* **18**, 674-683, doi:mt20102 [pii] 10.1038/mt.2010.2 (2010).

13 Mates, L. *et al.* Molecular evolution of a novel hyperactive Sleeping Beauty transposase enables robust stable gene transfer in vertebrates. *Nat Genet* **41**, 753-761, doi:ng.343 [pii] 10.1038/ng.343 (2009).

14 Peng, P. D. *et al.* Efficient nonviral Sleeping Beauty transposon-based TCR gene transfer to peripheral blood lymphocytes confers antigen-specific antitumor reactivity. *Gene Ther* **16**, 1042-1049, doi:10.1038/gt.2009.54 (2009).

15 Jorritsma, A. *et al.* Selecting highly affine and well-expressed TCRs for gene therapy of melanoma. *Blood* **110**, 3564-3572, doi:blood-2007-02-075010 [pii] 10.1182/blood-2007-02-075010 (2007).

16 Dudley, M. E. *et al.* CD8+ enriched "young" tumor infiltrating lymphocytes can mediate regression of metastatic melanoma. *Clin Cancer Res* **16**, 6122-6131, doi:1078-0432.CCR-10-1297 [pii] 10.1158/1078-0432.CCR-10-1297 (2010).

17 Restifo, N. P., Dudley, M. E. & Rosenberg, S. A. Adoptive immunotherapy for cancer: harnessing the T cell response. *Nat Rev Immunol* **12**, 269-281, doi:nri3191 [pii] 10.1038/nri3191 (2012).

18 Field, A. C. *et al.* Comparison of lentiviral and sleeping beauty mediated alphabeta T cell receptor gene transfer. *PloS one* **8**, e68201, doi:10.1371/journal.pone.0068201 (2013).

19 Xue, X. *et al.* Stable gene transfer and expression in cord blood-derived CD34+ hematopoietic stem and progenitor cells by a hyperactive Sleeping Beauty transposon system. *Blood* **114**, 1319-1330, doi:blood-2009-03-210005 [pii] 10.1182/blood-2009-03-210005 (2009).
20 Walisko, O. *et al.* Sleeping Beauty transposase modulates cell-cycle progression through interaction with Miz-1. *Proceedings of the National Academy of Sciences of the United States of America* **103**, 4062-4067, doi:10.1073/pnas.0507683103 (2006).
21 Wu, J. *et al.* Cyclic GMP-AMP is an endogenous second messenger in innate immune signaling by cytosolic DNA. *Science* **339**, 826-830, doi:science.1229963 [pii] 10.1126/science.1229963 (2013).
22 Sun, L., Wu, J., Du, F., Chen, X. & Chen, Z. J. Cyclic GMP-AMP synthase is a cytosolic DNA sensor that activates the type I interferon pathway. *Science* **339**, 786-791, doi:science.1232458 [pii] 10.1126/science.1232458 (2013).
23 Lee, M. N. *et al.* Identification of regulators of the innate immune response to cytosolic DNA and retroviral infection by an integrative approach. *Nat Immunol* **14**, 179-185, doi:10.1038/ni.2509 (2013).
24 Engels, B. *et al.* Retroviral vectors for high-level transgene expression in T lymphocytes. *Hum Gene Ther* **14**, 1155-1168, doi:10.1089/104303403322167993 (2003).
25 Bendle, G. M. *et al.* Lethal graft-versus-host disease in mouse models of T cell receptor gene therapy. *Nat Med* **16**, 565-570, 561p following 570, doi:nm.2128 [pii] 10.1038/nm.2128 (2010).
26 Cui, Z., Geurts, A. M., Liu, G., Kaufman, C. D. & Hackett, P. B. Structure-function analysis of the inverted terminal repeats of the sleeping beauty transposon. *J Mol Biol* **318**, 1221-1235, doi:S0022-2836(02)00237-1 [pii] (2002).
27 Topalian, S. L., Solomon, D. & Rosenberg, S. A. Tumor-specific cytolysis by lymphocytes infiltrating human melanomas. *J Immunol* **142**, 3714-3725 (1989).
28 Salter, R. D., Howell, D. N. & Cresswell, P. Genes regulating HLA class I antigen expression in T-B lymphoblast hybrids. *Immunogenetics* **21**, 235-246 (1985).
29 Rodenko, B. *et al.* Generation of peptide-MHC class I complexes through UV-mediated ligand exchange. *Nat Protoc* **1**, 1120-1132, doi:nprot.2006.121 [pii] 10.1038/nprot.2006.121 (2006).
30 Toebes, M. *et al.* Design and use of conditional MHC class I ligands. *Nat Med* **12**, 246-251, doi:nm1360 [pii] 10.1038/nm1360 (2006).

Table S1: Gene transfer efficiency in GFP gene transfer experiments. Percentages of stably gene modified cells for each experiment are shown.

Untreated	NSC 95397
6,73	31,17
16,44	19,35
15,67	22,22
24,56	28,82
21,86	24,46
26,65	33,77
11,32	17,83
17,99	18,4
25,69	34,43
18,29	20,92
24,87	40,97
37,39	41,31
18,42	28,21
1,04	2,53
27,05	38,06
2,14	4,04
29,29	44,65
6,85	11,48
29,94	39,93

Table S2: Gene transfer efficiency in TCR gene transfer experiments. Percentages of stably gene modified cells for each experiment are shown.

Untreated	NSC 95397
11,09	10,36
5,98	11,5
20,54	24,46
19,36	26,73
36,17	39,36
26,04	32,85
23,72	28,66
24,45	28,29
49,7	65,44
44,42	46,84
23,05	27,37
24,61	24,2

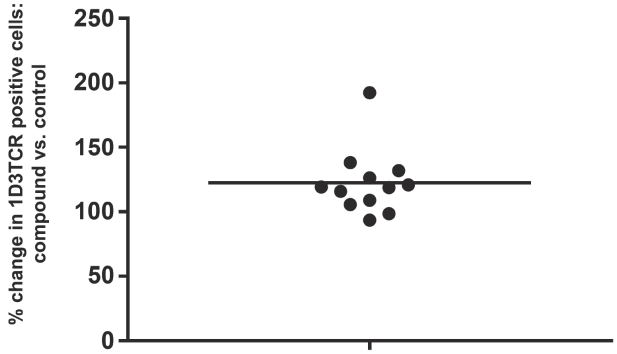

Supplementary Figure 1. Effect of NSC95397 on TCR gene transfer efficiency. Effect of NSC 95397 (5 μM) on SB100X mediated 1D3 TCR modification of human T cells in a large series of experiments ($p<0.01$).

Chapter 5

Regulation and Function of the PD-L1 Checkpoint

Chong Sun[1,2], Riccardo Mezzadra[1,2], Ton N. Schumacher[1,2]

[1] Division of Molecular Oncology & Immunology, Oncode Institute, the Netherlands Cancer Institute, Plesmanlaan 121, 1066 CX Amsterdam, the Netherlands,
[2] These authors contributed equally. Corresponding author t.schumacher@nki.nl

Immunity. 2018 Mar 20;48(3):434-452

Expression of programmed death-ligand 1 (PD-L1) is frequently observed in human cancers. Binding of PD-L1 to its receptor PD-1 on activated T cells inhibits anti-tumor immunity by counteracting T cell-activating signals. Antibody-based PD-1-PD-L1 inhibitors can induce durable tumor remissions in patients with diverse advanced cancers, and thus expression of PD-L1 on tumor cells and other cells in the tumor microenviroment is of major clinical relevance. Here we review the roles of the PD-1-PD-L1 axis in cancer, focusing on recent findings on the mechanisms that regulate PD-L1 expression at the transcriptional, posttranscriptional, and protein level. We place this knowledge in the context of observations in the clinic and discuss how it may inform the design of more precise and effective cancer immune checkpoint therapies.

Introduction

The T cell-based immune system has evolved to recognize and destroy aberrant cells, such as pathogen-infected cells and cancer cells. Detection of such aberrant cells occurs through binding of the T cell receptor (TCR) on T cells to peptide-major histocompatibility complexes (MHC) on target cells. However, the outcome of this interaction is to a very large extent controlled by a series of co-stimulatory and co-inhibitory receptors and their ligands (also known as immune checkpoints). By regulating the quantity and functional activity of antigen-specific T cells, these checkpoint pathways play a critical role in limiting tissue damage and maintenance of self-tolerance.

Among all immune checkpoints, the PD-L1-PD-1 pathway has stood out because of its proven value as a therapeutic target in a large number of malignancies. At present, antibodies targeting the PD-L1-PD-1 axis are being evaluated in more than 1,000 clinical trials and have been approved for cancers including melanoma, non-small cell lung cancer (NSCLC), renal cell carcinoma (RCC), Hodgkin's lymphoma, bladder cancer, head and neck squamous cell carcinoma (HNSCC), Merkel-cell carcinoma, and microsatellite instable-high (MSI-H) or mismatch repair-deficient (dMMR) solid tumors. Despite the considerable improvement in patient outcome that has been achieved with PD-L1-PD-1 blockade, durable responses to these therapies are observed in only a minority of patients and intrinsic therapy resistance is common. In some tumor types, expression of PD-L1 on tumor cells and in the tumor microenvironment has been associated with clinical response, highlighting the need for a better understanding of the processes that regulate PD-L1 expression.

In this review, we first discuss the fundamental biology of the PD-L1-PD-1 immune checkpoint. We then describe the promise and limitations of current anti-PD-L1-PD-1 therapies and the relevance of PD-L1 expression in predicting clinical response. Subsequently, we cover the current understanding of the molecular mechanisms that control such PD-L1 expression. In this section we dissect the complex regulatory network that determines PD-L1 levels into five major components that involve (1) genomic aberrations, (2) inflammatory signaling, (3) oncogenic signaling, (4) microRNA-based control, and (5) posttranslational modulation. Finally, we will discuss how this knowledge may guide further research and potentially be used to design more precise and effective cancer immune checkpoint therapies.

The PD-L1-PD-1 Axis: Structure and Function

Programmed cell death protein 1 (PD-1; also called CD279) is one of the co-inhibitory receptors that is expressed on the surface of antigen-stimulated T cells (Ishida et al., 1992). PD-1 interacts with two ligands, PD-L1 (CD274) and PD-L2 (CD273). Expression of PD-L2 is observed on, for instance, macrophages, DCs, and mast cells. PD-L1 expression can be detected on hematopoietic cells including T cells, B cells, macrophages, dendritic cells (DCs), and mast cells, and non-hematopoietic healthy tissue cells including vascular endothelial cells, keratinocytes, pancreatic islet cells, astrocytes, placenta syncytiotrophoblast cells, and corneal epithelial and endothelial cells. Both PD-L1 and PD-L2 can be expressed by tumor cells and tumor stroma. Engagement of PD-L2 at such tumor sites may potentially contribute to PD-1-mediated T cell inhibition (Yearley et al., 2017). However, to date, there is no compelling evidence indicating that antibodies against PD-1, which block binding to both PD-L1 and PD-L2, show higher clinical activity than antibodies against PD-L1. These data are consistent with a model in which PD-L1 is the dominant inhibitory ligand of PD-1 on T cells in the human tumor microenvironment.

Both PD-1 and PD-L1 are type I transmembrane proteins that belong to the immunoglobulin (Ig) superfamily. PD-1 consists of an Ig-V like extracellular domain, a transmembrane domain, and a cytoplasmic domain that harbors two tyrosine-based signaling motifs (Ishida et al., 1992, Zhang et al., 2004). PD-L1 contains an Ig-V and Ig-C-like extracellular domain, a transmembrane domain, and a short cytoplasmic tail that does not contain canonical signaling motifs (Dong et al., 1999, Keir et al., 2008, Lin et al., 2008). Interactions between the extracellular domains of PD-L1 and PD-1 can induce a conformational change in PD-1 that leads to phosphorylation of the cytoplasmic immunoreceptor tyrosine-based inhibitory motif (ITIM) and the immunoreceptor tyrosine-based switch motif (ITSM) by Src family kinases (Gauen et al., 1994, Straus and Weiss, 1992, Zak et al., 2015). These phosphorylated tyrosine motifs subsequently recruit the SHP-2 and SHP-1 protein tyrosine phosphatases to attenuate T cell-activating signals. While traditionally PD-1 engagement was thought to reduce the strength of the TCR signal itself (Chemnitz et al., 2004, Sheppard et al., 2004, Ugi et al., 1994), recent work suggests that the co-stimulatory receptor CD28, rather than the TCR, may be a primary target for dephosphorylation by the SHP2 phosphatase (Hui et al., 2017). In addition to its interaction with PD-1, PD-L1 can also interact with CD80, which may deliver inhibitory signals to activated T cells (Butte et al., 2007, Park et al., 2010). Engagement of PD-1 by PD-L1 alters the activity of T cells in many ways, inhibiting T cell proliferation, survival, cytokine production, and other effector functions (Butte et al., 2007, Chang et al., 1999, Curiel et al., 2003, Dong et al., 1999, Freeman et al., 2000, Keir et al., 2006, Latchman et al., 2004).

While the effects of checkpoint signaling through PD-1 are reasonably well understood, potential "reverse signaling" through PD-L1 has been explored less, possibly because of the absence of canonical signaling motifs in the short cytoplasmic tail of PD-L1. Nevertheless, some evidence has been obtained for a signaling role of the PD-L1 molecule. First, stimulation of PD-L1 by recombinant PD-1 delivers pro-survival signals to tumor cells, resulting in resistance to Fas- or staurosporine-induced apoptosis (Azuma et al., 2008). Moreover, antibody-based PD-L1 targeting reduces mTOR activity and glycolytic metabolism in tumor cells in the absence of T cells (Chang et al., 2015). Finally, PD-L1 can protect tumor cells from the cytotoxic effects of type I and type II interferons and from cytotoxic T lymphocyte (CTL)-mediated cytolysis with no requirement of PD-1 signaling in T cells (Azuma et al., 2008, Gato-Cañas et al., 2017). While it was shown that the cytoplasmic domain of PD-L1 is critically required for this anti-apoptotic signaling (Azuma et al., 2008), it remains unclear which intracellular factor(s) participate(s) in such proposed signal transduction. In spite of the above data on potential signaling through PD-L1, the current thinking on the mechanism of action of PD-1 and PD-L1 blocking agents focuses to a very large extent on their effects on the activity of PD-1-expressing T cells.

PD-1 Expression in Tolerance, Infection, and Cancer

The PD-L1-PD-1 axis is a critical determinant of physiological immune homeostasis. PD-1-deficient mice of different genetic backgrounds are prone to develop lupus-like autoimmune disease (Nishimura et al., 1999) or fatal autoimmune cardiomyopathy (Nishimura et al., 2001). Similarly, genetic or antibody-based inhibition of PD-1 accelerates diabetes onset in a non-obese diabetic (NOD) background (Ansari et al., 2003, Wang et al., 2005). Moreover, PD-1-deficient mice have altered thymic T cell education (Nishimura et al., 2000) and PD-L1 blockade has been shown to impair fetomaternal tolerance (Guleria et al., 2005). Collectively these data demonstrate a critical role for PD-1 in immune tolerance at various levels. Upon recognition of antigen, T cells rapidly express PD-1 (Agata et al., 1996), and it has been demonstrated that PD-1 expression on recently activated T cells is involved in modulating the strength of the initial T cell response (Honda et al., 2014). Consistent with a role of PD-1 in suppressing T cell activity, inhibition of the PD-1-PD-L1 axis increases immune responses toward pathogens (Erickson et al., 2012, Lázár-Molnár et al., 2008, Liu et al., 2014, Yao et al., 2009).

Chronic infection and cancer are both characterized by the continued presence of antigen-expressing target cells. Work in mouse models of chronic LCMV infection has provided compelling evidence that in such a setting of chronic antigen encounter, T cells progressively lose effector functions, developing into an exhausted (or

dysfunctional) state (Wherry and Kurachi, 2015). Importantly, high expression of PD-1 is one of the defining characteristics of such exhausted T cells (Wherry and Kurachi, 2015). Furthermore, in exhausted T cells, PD-1 has a role in maintenance of the dysfunctional state, both in chronic infection (Barber et al., 2006) and in cancer (Hirano et al., 2005). In human cancers, PD-1-positive T cells in tumors (Gros et al., 2014) and in peripheral blood (Gros et al., 2016) are enriched for tumor reactivity, again consistent with antigen-driven PD-1 expression. However, PD-1 expression can also be induced by other factors, such as IL-10 (Sun et al., 2015) and TGF-β (Park et al., 2016), and "bystander T cells" in mouse tumor models do express intermediate levels of PD-1 (Erkes et al., 2017). Next to its role on T cells, recent data provide evidence for a role of PD-1 on other cell types. In one study, a case was made for a possible role of PD-1 expression on melanoma cells (Kleffel et al., 2015). In addition, blockade of the interaction between PD-1 and PD-L1 has been shown to counteract the activity of immunosuppressive PD-1hi B cells in hepatocellular carcinoma (Zhao et al., 2016). Finally, Gordon et al. (2017) have demonstrated how PD-1 blockade can enhance tumor cell phagocytosis by PD-1+ macrophages. A detailed discussion of PD-1 biology in the context of normal physiology (Sharpe and Pauken, 2018) and T cell exhaustion (Wherry and Kurachi, 2015) is provided elsewhere.

The PD-1-PD-L1 Axis as a Therapeutic Target: Clinical Value and Issues Remaining

Given their role in T cell suppression, PD-1 and PD-L1 have over the past years developed into prominent targets of antibody-based cancer therapeutics. In 2010, the first data were reported on the clinical activity of PD-1-blocking agents in patients with colorectal cancer, melanoma, and renal cell carcinoma, demonstrating an acceptable toxicity profile and providing the first evidence of antitumor activity (Brahmer et al., 2010). Subsequent studies have revealed significant activity of PD-1 blockade in a large variety of cancers, leading to clinical approval for treatment of melanoma (Larkin et al., 2015, Ribas et al., 2015, Robert et al., 2015a, Robert et al., 2015b, Weber et al., 2015, Weber et al., 2017), NSCLC (Antonia et al., 2017, Borghaei et al., 2015, Brahmer et al., 2015, Fehrenbacher et al., 2016, Herbst et al., 2016, Langer et al., 2016, Reck et al., 2016), MSI-H and dMMR cancers (Kok et al., 2017, Le et al., 2017, Le et al., 2015, Overman et al., 2017), RCC (Motzer et al., 2015), Hodgkin's lymphoma (Ansell et al., 2015, Chen et al., 2017b), urothelial carcinoma (Balar et al., 2017a, Balar et al., 2017b, Bellmunt et al., 2017, Patel et al., 2018, Powles et al., 2017, Rosenberg et al., 2016, Sharma et al., 2017b), HNSCC (Ferris et al., 2016, Seiwert et al., 2016), Merkel-cell carcinoma (Kaufman et al., 2016), hepatocellular carcinoma (HCC) (El-Khoueiry et al., 2017), and gastric cancer (Fuchs et al., 2017). On the other hand, in tumor types such as non-MSI colorectal cancer, prostate cancer, ovarian cancer, and breast cancer,

the clinical activity of anti-PD-1-PD-L1 monotherapy is only modest. Furthermore, even in tumor types for which PD-1-PD-L1 blockade is now an approved therapy such as NSCLC, only a fraction of patients shows objective clinical responses (Table 1).

Table 1. Overview of Approved Indications for PD-1 and PD-L1 Blocking Agents

Tumor Type	Target - Antibody	Response Rate	Notes	Reference
Melanoma	PD-1 - nivolumab	CR 3.3%, PR 28.3%	Checkmate-037. Previously treated, PD-L1$^+$ IHC predictive.	Weber et al., 2015
		CR 4%, PR 30%	Checkmate-066. Previously untreated, BRAF wild-type, PD-L1$^+$ IHC predictive.	Robert et al., 2015a
		CR 8.9%, PR 41%	Checkmate-067. Combination with Ipilimumab.	Larkin et al., 2015
		Hazard ratio 0.65 versus ipilimumab adjuvant	Checkmate 238. Stage III and IV, adjuvant therapy after resection. PD-L1$^+$ IHC predictive.	Weber et al., 2017
	PD-1 - pembrolizumab	CR 5-6%, PR 27-29%	Keynote-006. Ipilimumab naive.	Robert et al., 2015b
		CR 2-3%, PR 19-23%	Keynote-002. Ipilimumab refractory.	Ribas et al., 2015
NSCLC	PD-1 - nivolumab	CR 0.7%, PR 19.3%	Checkmate-017. Second line squamous NSCLC, PD-L1$^+$ IHC not predictive.	Brahmer et al., 2015
		CR 1.4%, PR 17.8%	Checkmate-057. Second line non-squamous NSCLC, PD-L1$^+$ IHC predictive.	Borghaei et al., 2015
	PD-1 - pembrolizumab	CR 4%, PR 41%	Keynote-024. PD-L1 > 50%, first line.	Reck et al., 2016
		Hazard ratio 0.53 versus chemotherapy alone	Keynote-021. PD-L1 > 1%, first line, combination with chemotherapy.	Langer et al., 2016
		ORR 18-19% (PD-L1 > 1%), 29-30% (PD-L1 > 50%)	Keynote-010. PD-L1 > 1%. Previously treated.	Herbst et al., 2016
	PD-L1 - atezolizumab	OS 12.6 m versus 9.7 m in chemotherapy arm	POPLAR and OAK. Previously treated. PD-L1$^+$ IHC on tumor and IC predictive.	Fehrenbacher et al., 2016
	PD-L1 - durvalumab	Hazard ratio 0.52 versus placebo	PACIFIC. Stage III, durvalumab after chemotherapy. PD-L1$^+$ IHC not predictive.	Antonia et al., 2017
RCC	PD-1 - nivolumab	ORR 21.5%	Checkmate-025. Progressive patients on or after anti-angiogenic therapies. PD-L1$^+$ IHC not predictive.	Motzer et al., 2015
HNSCC	PD-1 - nivolumab	OS 7.5 m versus 5.1 m for investigator's choice	Checkmate-141. Patients progressing after platinum-based chemotherapy. PD-L1$^+$ IHC predictive.	Ferris et al., 2016
	PD-1 - pembrolizumab	CR 5%, PR 11%	Keynote-012. Patients recurrent on or after chemotherapy. PD-L1$^+$ IHC and IFN-γ-related gene expression predictive.	Seiwert et al., 2016
Urothelial carcinoma	PD-1 - nivolumab	CR 2.6%, PR 17%	Checkmate-275. Patients progressing after chemotherapy.	Sharma et al., 2017b
	PD-1 - pembrolizumab	ORR 21%	Keynote-045. Patients progressing after chemotherapy. PD-L1$^+$ IHC not predictive.	Bellmunt et al., 2017
		ORR 28.6%	Keynote-052. Cisplatin-ineligible patients. PD-L1$^+$ IHC predictive.	Balar et al., 2017a
	PD-L1 - atezolizumab	CR 6.7%, PR 16.8%	NCT02951767. Cisplatin-ineligible patients.	Balar et al., 2017b
		CR 5.5%, PR 9.4%	NCT02108652. Chemotherapy refractory. PD-L1$^+$ IHC on IC predictive.	Rosenberg et al., 2016
	PD-L1 - avelumab	CR 5.6%, PR 10.6% (at 6 months follow-up)	JAVELIN solid tumors. Patients failing platinum-based chemotherapy. Weak predictive value for PD-L1$^+$ IHC.	Patel et al., 2018
	PD-L1 - durvalumab	CR 2.7%, PR 14.3%	NCT01693562. Patients that are progressive, ineligible, or have refused platinum-based chemotherapy. PD-L1$^+$ IHC on tumor and IC predictive.	Powles et al., 2017

Table 1. ***Continued***

Tumor Type	Target - Antibody	Response Rate	Notes	Reference
Merkel cell carcinoma	PD-L1 - avelumab	CR 11.4%, PR 21.6%	JAVELIN Merkel 200. PD-L1 expression and polyomavirus status not predictive.	Kaufman et al., 2016
Hodgkin's lymphoma	PD-1 - nivolumab	CR 14%, PR 55%	Checkmate-039 and Checkmate-205. Patients progressing after autologous HSCT and brentuximab vedotin.	Ansell et al., 2015
	PD-1 - pembrolizumab	CR 22%, PR 47%	Keynote-087. Relapsed or refractory Hodgkin's lymphoma.	Chen et al., 2017b
MSI-H and dMMR CRC	PD-1 - nivolumab	CR 2.7%, PR 30%	Checkmate-142. Patients progressing after or ineligible for chemotherapy.	Overman et al., 2017
MSI-H and dMMR solid tumors	PD-1 - pembrolizumab	ORR 39.6%	NCT-01876511. Patients with no satisfactory alternative treatment options.	Le et al., 2015, 2017
HCC	PD-1 - nivolumab	ORR 14.3%	Checkmate-040. Patients progressing after sorafenib. PD-L1^{+} IHC not predictive.	El-Khoueiry et al., 2017
Gastric cancer	PD-1 - pembrolizumab	ORR 13.3% in PD-L1 positive	Keynote-059. Disease progression after at least two prior lines of therapy.	Fuchs et al., 2017

Table 1: Clinical trials leading to approval, patient subgroups, and predictive value or lack of predictive value of intratumoral PD-L1 expression are indicated where applicable. Abbreviations are as follows: NSCLC, non-small cell lung cancer; RCC, renal cell carcinoma; HNSCC, head and neck squamous cell carcinoma; MSI-H, microsatellite instability high; dMMR, mismatch repair deficient; CRC, colorectal cancer; HCC, hepatocellular carcinoma; CR, complete response; PR, partial response; ORR, overall response rate; OS, overall survival; IHC, immunohistochemistry; IC, immune cells.

The observed heterogeneity in clinical response to PD-1-PD-L1 blockade has led to a major effort to understand which parameters predict clinical response to these therapies. From a conceptual point of view, this question can be divided into two smaller questions. First, is there evidence that the PD-1-PD-L1 inhibitory axis is active in a given tumor? Second, for those tumors in which the PD-1-PD-L1 axis is operational, would blockade of this inhibitory interaction suffice to re-activate the process of tumor cell killing? With respect to the second question, tumor control by T cells is critically dependent on a series of distinct parameters that can be summarized in a "cancer immunogram" that depicts the state of cancer-immune interaction in an individual patient (Blank et al., 2016). In support of this model, the outcome of PD-L1-PD-1 blockade has now been shown to be influenced not only by PD-L1 expression (as discussed in the next section), but also by a series of unrelated parameters that include (1) the "foreignness" of the tumor, (2) the immune status of the patient, (3) the presence and activity of the intratumoral T cell infiltrate, (4) the presence of other inhibitory processes within the tumor, and (5) the sensitivity of tumor cells to tumor-specific T cells at that site.

With respect to the role of tumor foreignness, in most (Goodman et al., 2017, Rizvi et al., 2015, Rosenberg et al., 2016) but not all (Hugo et al., 2016) studies, the number of non-synonymous DNA mutations in human tumors has been shown to correlate

with the likelihood of response to PD-1 axis blocking therapies, consistent with the view that the amount of neoantigens influences the likelihood and/or strength of T cell recognition (Schumacher and Schreiber, 2015). While this correlation has now been described for a series of tumor types, the most compelling evidence for a role of "tumor foreignness" has come from the demonstration that MSI-H tumors, which carry an uncommonly high mutational load, respond particularly well to inhibition of the PD-L1-PD-1 pathway as compared to other tumors of the same histology (Kok et al., 2017, Le et al., 2017, Le et al., 2015).

Several parameters that reflect the general immune status of patients, such as absolute lymphocyte count (ALC), neutrophil to lymphocyte ratio (NLR), and absolute eosinophil count, are also being considered as predictive biomarkers for response to PD-1-PD-L1 blocking therapies. These parameters have previously shown value in predicting response to CTLA-4 blockade. To date, only neutrophil to lymphocyte ratio has shown predictive value in one study that examined response to PD-1-PD-L1 blockade (Bumma et al., 2017). Recently, the frequency of circulating monocytes has also been described as a systemic biomarker to predict response to anti-PD-1 immunotherapy (Krieg et al., 2018).

As a third category of predictive markers, assays that measure accumulation of (clonally expanded) T cells and the activity of such T cells at tumor sites have been shown to be informative. As specific examples, the presence of CD8-positive cells at the tumor invasive margin (Tumeh et al., 2014), clonality of the intratumoral TCR repertoire (Snyder et al., 2017, Tumeh et al., 2014), and a transcriptional signature in which interferon (IFN)-γ-response genes are included (Ayers et al., 2017, Fehrenbacher et al., 2016, Seiwert et al., 2016) all form positive predictive markers. In addition to providing information on intratumoral T cell activity, RNA-seq data have also been utilized to derive a specific transcriptional profile that correlates with lack of response to anti-PD-1 therapies with some of the genes that show increased expression in non-responders, such as IL-10, known to be immunosuppressive (Hugo et al., 2016).

Finally, two classes of predictive markers may be found at the level of tumor cell recognition and tumor cell sensitivity to T cell attack. Specifically, defects in the antigen presentation machinery have been identified in various malignancies (Seliger, 2014). Such defects could lead to both intrinsic and acquired resistance to PD-1-PD-L1 inhibition, and evidence for the latter has already been obtained (Sade-Feldman et al., 2017, Zaretsky et al., 2016). MSI-H tumors should be a useful testing ground to further understand the clinical impact of such alterations, as the beta-2 microglobulin (B2M) gene, a critical component of the HLA class I antigen presentation

pathway, contains microsatellites that are prone to mutation in this class of tumors (Yamamoto et al., 2001). Interestingly, also defects in the IFN-γ receptor pathway have been identified in patients that have developed resistance to PD-1 blocking therapies (Sade-Feldman et al., 2017, Zaretsky et al., 2016). Consistent with this observation, genetic screens have identified inhibition and inactivation of the IFN-γ receptor pathway as a mechanism of resistance of tumor cells to T cell attack, both in vitro (Patel et al., 2017) and in vivo (Manguso et al., 2017). Whether the observed role of the IFN-γ receptor pathway primarily reflects its effect on expression of components of the antigen presentation machinery, or direct cytotoxic or cytostatic effects of IFN-γ receptor signaling in tumor cells, remains to be established.

The Role of PD-L1 Expression in Immunotherapy Response

Expression of PD-L1 within the tumor microenvironment has predictive value for response to monotherapies blocking the PD-L1-PD-1 axis in many studies in melanoma (Robert et al., 2015a, Weber et al., 2017, Weber et al., 2015), NSCLC (Borghaei et al., 2015, Fehrenbacher et al., 2016), and bladder cancer (Rosenberg et al., 2016), but was not predictive in all studies (Motzer et al., 2015, Sharma et al., 2017b). Of note, in certain tumor types, such as bladder cancer (Rosenberg et al., 2016), predictive value is primarily observed for PD-L1 expression on immune infiltrating cells rather than tumor cells, whereas for NSCLC, PD-L1 expression on both immune cells and tumor cells has shown predictive value (Fehrenbacher et al., 2016). These observations have encouraged experimental research to dissect which of the two cell compartments is more relevant in PD-L1-mediated suppression of tumor control. In a first study that aimed to address this issue, Noguchi et al. (2017) took advantage of a murine transplantable sarcoma system in which tumor cells fail to grow in mice treated with PD-1 axis blocking agents. In this setting, selective disruption of PD-L1 on tumor cells resulted in tumor control in most, but not all, animals. Of note, those PD-L1-negative tumors that escaped immune elimination were still sensitive to antibody-mediated PD-L1 blockade, indicating that PD-L1 expression on both cell compartments can play a role under these experimental conditions (Noguchi et al., 2017). In another study, Lau et al. (2017) transplanted either PD-L1-proficient or -deficient tumor cells in either wild-type or PD-L1-deficient mice and observed that absence of PD-L1 from either of the two cell compartments impaired tumor growth, with optimal tumor control being observed when PD-L1 was absent from both cell compartments. In a third report, Juneja et al. (2017) used a similar strategy and implanted either highly immunogenic or mildly immunogenic PD-L1-proficient tumors in either wild-type, PD-L1 plus PD-L2-deficient, or PD-1-deficient mice to dissect once again the role of PD-L1 on the different cell compartments. In these experiments, PD-L1 on non-tumor cells played a dispensable role in case of MC38, the most immunogenic cell line. In

contrast, in case of the less immunogenic cell lines, PD-L1 expression on both the tumor and non-tumor compartment contributed to tumor growth (Juneja et al., 2017). Collectively, these data indicate that PD-L1 expression on both cell compartments can play a role, but that the relative importance of both cell compartments is context dependent. In one of these reports (Juneja et al., 2017), the most immunogenic tumor did not rely on non-autonomous PD-L1 expression, but whether this reflects a causal link between immunogenicity and PD-L1 dependency on different cell compartments has not been assessed. Another parameter that is likely to influence the relative role of PD-L1 on tumor cells and stromal cells is its relative expression level on the two cell compartments. In a recent report, in which loss of the PD-L1 3′ UTR was shown to increase the levels of PD-L1, it was observed that tumor cells with increased PD-L1 protein have a greater suppressive capacity in in vitro and in vivo assays (Kataoka et al., 2016). Consistent with these data, overexpression of PD-L1 on tumor cells has been shown to prevent rejection of two highly immunogenic murine cancer cell lines in immunocompetent hosts (Noguchi et al., 2017). Other contextual factors that should be assessed in future work are the relative abundance of PD-L1+ tumor cells and PD-L1+ stromal cells, the specific type(s) of stromal cells that express the PD-L1 protein, and the role that additional suppressive pathways may play.

With the very rapid increase in clinical studies that evaluate combination immunotherapies, it will be important to also understand the value of PD-L1 as a predictive marker in those settings. In melanoma, combination therapy with anti-PD-1 and anti-CTLA-4 results in a numerical increase in progression-free survival relative to anti-PD-1 monotherapy. Strikingly, the added value of CTLA-4 blockade in this study appeared restricted to those patients with tumors that were PD-L1 negative before start of treatment (Larkin et al., 2015), in line with the model that CTLA-4 blocking therapies broaden the tumor-specific T cell response (Kvistborg et al., 2014). Conceivably, increased tumor-specific T cell reactivity induced by CTLA-4 blockade could in this setting lead to IFN-γ-induced PD-L1 expression, at which point blockade of the PD-1-PD-L1 axis would also become valuable.

In spite of the value of PD-L1 staining as a predictive marker in different tumor types, many PD-L1-positive tumors do not respond, and a fraction of PD-L1-negative tumors do respond to PD-L1-PD-1 blockade (Table 2). Clinical response of seemingly PD-L1-negative tumors may be explained by technical issues (e.g., inadequate sampling of the tumor, or insufficient sensitivity of the detection technique that is used), by a potential role of the PD-L1-PD-1 axis outside of the tumor microenvironment, by the dynamic nature of PD-L1 expression, or by immune cell inhibition through PD-L2. Conversely, absence of clinical response in PD-L1-positive tumors may be explained

by mechanisms described in the prior section, such as loss of tumor cell sensitivity to T cell effector mechanisms, or the presence of additional immunosuppressive mechanisms in the tumor microenvironment, such as TGF-β (Mariathasan et al., 2018). As an alternative explanation, absence of response in PD-L1-positive tumors may occur in settings in which the observed PD-L1 expression is not due to an ongoing immune response but is driven by other mechanisms.

Table 2. Potential Explanations for Discrepencies between Clinical Response to PD-1-PD-L1 Blocking Therapies and Intratumoral PD-L1 Expression

	Clinical Response	
PD-L1 expression	Non responding	Responding
PD-L1 negative		false negative in assays role of PD-L1 outside of the tumor microenvironment dynamic nature of PD-L1 expression role of PD-L2
PD-L1 positive	other suppressive mechanism(s) tumor insensitivity to T cells expression of PD-L1 not due to an ongoing immune response	

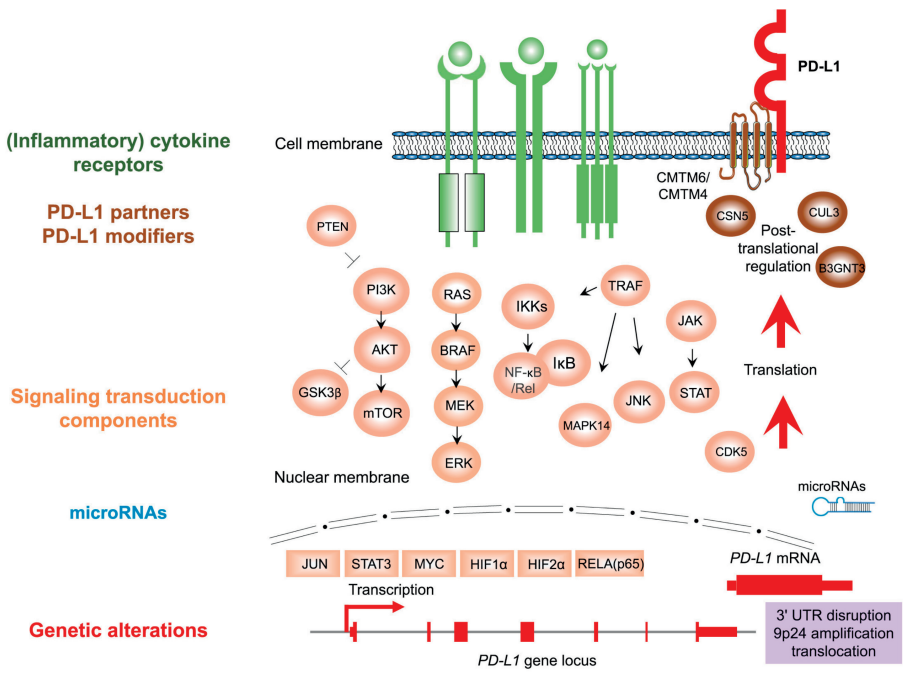

Figure 1: Overview of the Regulatory Mechanisms of PD-L1 Expression. Regulators are color coded by class. Green, (inflammatory) cytokine receptors; orange, signal transduction components; blue, microRNAs; red, genetic alterations; brown, PD-L1 protein partners and modifiers. Directionality ("up" or "down") and references are provided in Table 3.

Given the emerging evidence indicating how PD-L1 levels on different intratumoral cell compartments can influence tumor control and predict treatment response, it is critical to understand how the levels of PD-L1 expression at the cell surface are regulated, and also how this regulation may vary between tumor cells and (different) immune cells. In the next sections, we will discuss the data demonstrating that PD-L1 levels in tumors are regulated in a highly complex manner, with expression being influenced by genomic aberrations, transcriptional control, mRNA stability, oncogenic signaling, and protein stability (Figure 1, Table 3).

Table 3. Regulators of PD-L1

Type	Regulators of PD-L1	Tissue type
Inflammatory signaling	IFN-γ	↑ multiple tumor types (Dong et al., 2002), endothelial cells (Mazanet and Hughes, 2002), glioma (Wintterle et al., 2003), renal tubular epithelial cells (Schoop et al., 2004), colon cancer (Nakazawa et al., 2004), monocytes (Brown et al., 2003), dendritic cells and macrophages (Brown et al., 2003; Kryczek et al., 2008), neutrophils (de Kleijn et al., 2013)
	IFN-α and IFN-β	↑ endothelial cells (Eppihimer et al., 2002), monocytes and dendritic cells (Schreiner et al., 2004), melanoma (Garcia-Diaz et al., 2017)
	TLR4	↑ macrophages (Loke and Allison, 2003), bladder cancer (Qian et al., 2008), monocytes (Huang et al., 2013), dendritic cells (Mezzadra et al., 2017)
	TLR3	↑ dendritic cells (Pulko et al., 2009), endothelial cells (Cole et al., 2011), neuroblastoma (Boes and Meyer-Wentrup, 2015)
	IL-17	↑ monocytes (Zhao et al., 2011), prostate and colon cancer (Wang et al., 2017b)
	IL-10	↑ dendritic cells (Curiel et al., 2003), monocytes (Zhao et al., 2011)
	TNF-α	↑ endothelial cells (Mazanet and Hughes, 2002), myelodysplastic syndrome blasts (Kondo et al., 2010), dendritic cells (Karakhanova et al., 2010), monocytes (Zhao et al., 2011), monocytes (Ou et al., 2012), RCC (Quandt et al., 2014), breast cancer (Lim et al., 2016), prostate and colon cancer (Wang et al., 2017b)
	IL-4	↑ RCC (Quandt et al., 2014)
	IL-1β	↑ dendritic cells (Karakhanova et al., 2010)
	IL-6	↑ dendritic cells (Karakhanova et al., 2010; Kil et al., 2017)
	IL-27	↑ dendritic cells (Karakhanova et al., 2011; Matta et al., 2012), ovarian cancer (Carbotti et al., 2015)
	TGF-β	↑ dendritic cells (Ni et al., 2012; Song et al., 2014), T cells (Baas et al., 2016) ↓ renal tubular epithelial cells (Starke et al., 2007), monocytes (Ou et al., 2012)
	IL-12	↑ endothelial cells (Eppihimer et al., 2002), monocyte-derived macrophages (Xiong et al., 2014) ↓ THP-1-derived macrophages (Xiong et al., 2014)
Oncogenic signaling	MYC	↑ melanoma, NSCLC, HCC, osteosarcoma, leukemia and (mouse) lymphoma (Casey et al.,2016; Atsaves et al., 2017; Wang et al., 2017a)
	HIF1α	↑ breast cancer, prostate cancer (Barsoum et al., 2014), mouse myeloid cells (Noman et al., 2014), NSCLC (Guo et al., 2017)
	HIF2α	↑ RCC (Messai et al., 2016)
	STAT3	↑ lymphoma (Marzec et al., 2008; Atsaves et al., 2017), melanoma (Jiang et al., 2013), HNSCC (Bu et al., 2017)
	RELA	↑ primary monocytes (Huang et al., 2013), melanoma (Gowrishankar et al., 2015), NSCLC (Bouillez et al., 2017), breast cancer (Xue et al., 2017)
	MUC1-C	↑ NSCLC (Bouillez et al., 2017)
	JUN	↑ lymphoma (Green et al., 2012), melanoma (Jiang et al., 2013)
	CDK5	↑ medulloblastoma (Dorand et al., 2016)
	(PTEN loss) PI3K-AKT-mTOR	↑ glioma (Parsa et al., 2007), dendritic cells (Karakhanova et al., 2010), monocytes (Muthumani et al., 2011), CRC (Song et al., 2013), melanoma (Jiang et al., 2013; Atefi et al., 2014; Gowrishankar et al., 2015), NSCLC (Xu et al., 2014; Lastwika et al., 2016; Zhang et al., 2017b), breast cancer (Mittendorf et al., 2014; Yang et al., 2017)
	MEK-ERK	↑ multiple myeloma (Liu et al., 2007), NSCLC (Sumimoto et al., 2016), melanoma (Jiang et al., 2013; Liu et al., 2015), bladder cancer (Qian et al., 2008), lymphoma (Yamamoto et al., 2009), dendritic cells (Karakhanova et al., 2010) ↓ melanoma (Atefi et al., 2014), mouse breast cancer (Loi et al., 2016), NSCLC (Liu et al., 2015)
	MAPK14	↑ multiple myeloma (Liu et al., 2007), bladder cancer (Qian et al., 2008), lymphoma (Yamamoto et al., 2009), dendritic cells (Karakhanova et al., 2010)
	RAS	↑ NSCLC (Sumimoto et al., 2016; Coelho et al., 2017; Chen et al., 2017a; Guo et al., 2017), mouse lung (Lastwika et al., 2016), bronchial epithelial cells (Chen et al., 2017a)
	EGFR	↑ NSCLC (Akbay et al., 2013; Chen et al., 2015; Lin et al., 2015; Zhang et al., 2016; Lastwika et al., 2016; Coelho et al., 2017), bronchial epithelial cells (Akbay et al., 2013), breast cancer (Li et al., 2016), head and neck cancer (Concha-Benavente et al., 2016)
	ALK	↑ lymphoma (Marzec et al., 2008; Yamamoto et al., 2009), NSCLC (Ota et al., 2015; Koh et al., 2015)

Table 3. ***Continued***

Type	Regulators of PD-L1	Tissue type
microRNA	miR-513	↓ cholangiocytes (Gong et al., 2009; Gong et al., 2010)
	miR-155	↓ dermal lymphatic endothelial cells (Yee et al., 2017)
	miR-34a	↓ AML (Wang et al., 2015), NSCLC (Cortez et al., 2015)
	miR-142-5p	↓ pancreatic cancer (Jia et al., 2017)
	miR-93, miR-106b	↓ pancreatic cancer (Cioffi et al., 2017)
	miR-138-5p	↓ CRC (Zhao et al., 2016)
	miR-217	↓ laryngeal cancer (Miao et al., 2017)
	miR-200	↓ NSCLC (Chen et al., 2014; Gibbons et al., 2014), gastric cancer (Xie et al., 2017)
	miR-152	↓ gastric cancer (Xie et al., 2017)
	miR-570	↓ gastric cancer (Wang et al., 2013)
	miR-17-5p	↓ melanoma (Audrito et al., 2017)
	miR-15a, miR-193a, miR-16	↓ malignant pleural mesothelioma (Kao et al., 2017)
	miR-20, miR-21, miR-130b	↑ CRC (Zhu et al., 2014)
	miR-197	↓ NSCLC (Fujita et al., 2015)
Genetic alteration	amplifications	↑ Hodgkin's lymphoma (Green et al., 2010; Roemer et al., 2016), B cell lymphoma (Green et al., 2010; Twa et al., 2014), NSCLC (Ikeda et al., 2016), SCLC (George et al., 2017), squamous cell carcinoma of the oral cavity (Straub et al., 2016), stomach cancer (Cancer Genome Atlas Research Network, 2014)
	translocations	↑ mediastinal large B cell lymphoma (Twa et al., 2014)
	disruption of 3′ UTR region	↑ multiple tumor types, e.g., T cell leukemia, T and B cell lymphoma, stomach adenocarcinoma (Kataoka et al., 2016)
Post-translational regulation	CMTM6	↑ melanoma, NSCLC, CRC, thyroid cancer, dendritic cells, CML-derived cells, pancreatic cancer, breast cancer (Burr et al., 2017; Mezzadra et al., 2017)
	CMTM4	↑ NSCLC, melanoma, CML-derived cells (Mezzadra et al., 2017)
	CDK4	↓ cervical cancer, breast cancer cells (Zhang et al., 2017a)
	GSK3B	↓ breast cancer (Li et al., 2016)
	B3GNT3	↑ breast cancer (Li et al., 2018)
	CSN5	↑ breast cancer (Lim et al., 2016)

Up and down arrows are used to annotate positive and negative regulators of PD-L1s, respectively.

Genetic alterations at the PD-L1 locus

The two ligands of PD-1, PD-L1 and PD-L2, are located on chromosome 9p24.1, only 42 kilobases apart. Over the past years, both amplifications and translocations have been implicated in increasing the levels of PD-L1 in several types of tumors. 9p copy number amplifications were initially shown to occur in cases of Hodgkin's lymphoma and mediastinal large B cell lymphoma and were reported to correlate with increased expression of PD-L1 and PD-L2. Interestingly, janus kinase 2 (JAK2), which is involved in transduction of pro-inflammatory signals known to modulate PD-L1 expression (see below), is also located on chromosome 9p and its amplification was suggested to contribute to increased PD-L1 expression by enhancing IFN-γ receptor signaling (Green et al., 2010). In a subsequent study that analyzed 571 cases of mediastinal large B cell lymphoma, genetic aberrations were also observed frequently, with translocations being identified in 20% of the cases and amplification in 29% of the cases (Twa et al., 2014). Furthermore, in-depth analysis of a larger cohort of Hodgkin's lymphomas showed alterations of the PD-L1 PD-L2 locus in 97% of the cases tested (Roemer et al., 2016). In both of these studies, samples harboring genomic aberrations show increased PD-L1 and PD-L2 expression (Roemer et al., 2016, Twa et al., 2014). Evidence for a functional role of locus amplification in pathogenesis is given by the

fact that Hodgkin's lymphomas respond particularly well to PD-1 blocking agents (Ansell et al., 2015, Armand et al., 2016, Chen et al., 2017b, Younes et al., 2016). It should be noted, though, that these data do not provide conclusive evidence for positive selection of PD-L1, as co-amplification of PD-L2 is generally observed and may also explain the activity of anti-PD-1 therapy. Amplification of the chromosomal portion containing PD-L1, PD-L2, and JAK2 has also been reported in cases of NSCLC, in which they were associated with elevated PD-L1 expression (Ikeda et al., 2016). Similarly, amplifications of 9p24 and focal amplifications of PD-L1 have been described in a small subset of small cell lung cancer patients (George et al., 2017). PD-L1 amplification has likewise been observed in cases of squamous cell carcinoma of the oral cavity (Straub et al., 2016) and in Epstein-Barr virus (EBV)-positive gastric cancer (Cancer Genome Atlas Research Network, 2014).

A series of reports has provided compelling evidence that PD-L1 protein levels are also regulated by microRNAs (miRNA) that bind to the 3′ UTR of the PD-L1 mRNA (reviewed below). In line with a regulatory role of the 3′ UTR of the PD-L1 gene, loss of this gene segment as a consequence of different structural variations has been described in a small fraction of human tumors of diverse histology and correlates with increased PD-L1 expression of those tumors. Furthermore, deletion of the 3′ UTR of the PD-L1 gene by CRISPR Cas9 results in increased PD-L1 mRNA stability in human and murine cells, thereby increasing their resistance to T cell attack in vitro and in vivo (Kataoka et al., 2016). Likewise, in a genetic screen for factors that modulate PD-L1 expression, gene trap vector integrations that result in loss of the 3′ UTR of the PD-L1 gene were enriched in cells with high PD-L1 levels (Mezzadra et al., 2017).

To date, whether tumors with chromosomal aberrations that result in higher PD-L1 expression show an increased response rate to PD-L1-PD-1 blocking agents has not been systematically explored. However, an ovarian cancer patient harboring disruption of the 3′ UTR of PD-L1 was reported as an exceptional responder to PD-1 blockade (Bellone et al., 2018), and chromosomal aberrations of the locus should in future work be explored as a potential biomarker.

Control of PD-L1 Gene Expression through Inflammatory Signaling

Expression of the PD-L1 gene has been shown to be controlled by inflammatory signaling, consistent with the physiological role of the PD-1-PD-L1 axis in suppressing T cell activation. A number of soluble factors produced by immune cells have over the past years been described as inducers of PD-L1. In one of the first reports indicating

that PD-L1 could be employed by tumor cells as a defense mechanism against T cell attack (Dong et al., 2002), regulation of PD-L1 by IFN-γ was described for various tumor types, healthy tissues, and immune cells, and this has been extended in further studies (Brown et al., 2003, de Kleijn et al., 2013, Kryczek et al., 2008, Mazanet and Hughes, 2002, Nakazawa et al., 2004, Schoop et al., 2004, Wintterle et al., 2003). IFN-γ is a pro-inflammatory cytokine that is abundantly produced by T cells upon activation and that is also produced by NK cells. Binding of IFN-γ to its receptor results in signaling through the classical JAK-STAT pathway, preferentially through STAT1, thereby inducing increased expression of a series of transcription factors, called the interferon-responsive factors (IRFs) (Platanias, 2005). Of those factors, IRF1 has been shown to play a central role in the IFN-γ-mediated induction of PD-L1 (Lee et al., 2006). IFN-γ is generally considered the most prominent soluble inducer of PD-L1, and expression of PD-L1 may therefore be viewed as a crude measure of local IFN-γ signaling and T cell activity in most settings. It is important to realize though that the effects of IFN-γ on PD-L1 expression can be context dependent. As an example, some evidence has been obtained suggesting that PD-L1 expression on tumor and immune cells can be differentially regulated. In a sarcoma mouse model, treatment of mice with IFN-γ-blocking antibodies largely abrogated PD-L1 expression on tumor cells but only partially reduced PD-L1 levels on tumor-associated macrophages (Noguchi et al., 2017). Importantly, mutations in JAK1 and JAK2 have been described in tumors that were unresponsive to PD-1 blockade despite a high number of somatic mutations. It is plausible that such tumors do not rely on the PD-L1 pathway to escape immune recognition, but have evolved alternative strategies (Shin et al., 2017).

Next to IFN-γ, type I interferons, i.e., IFN-α and IFN-β, can also induce PD-L1 expression in cultured melanoma cells, endothelial cells, monocytes, and dendritic cells (Eppihimer et al., 2002, Garcia-Diaz et al., 2017, Schreiner et al., 2004). Interestingly, exposure to type I interferons has a much greater effect on PD-L2 than on PD-L1 expression in melanoma cells, highlighting their differential regulation. This study systemically interrogated other signaling pathways that may affect IFN signaling in melanoma, and identified that silencing of MAK14, CRKL, and PI3K greatly impairs IFN-γ-mediated PD-L1 expression in these tumor cell types (Garcia-Diaz et al., 2017).

Interferons are not the only inflammatory stimuli that have been linked to PD-L1 expression. For instance, treatment of macrophages (Loke and Allison, 2003), monocytes (Huang et al., 2013), primary bone marrow-derived dendritic cells (Mezzadra et al., 2017), and bladder cancer cells (Qian et al., 2008) with lipopolysaccharide (LPS) leads to increased PD-L1 expression. LPS signals through toll-like receptor (TLR) 4, and the subsequent induction of nuclear factor kappa-light-chain-enhancer of activated

B cells (NF-κB) results in induction of type I interferons (Lu et al., 2008), possibly explaining the link between LPS exposure and PD-L1 expression. In addition, it has been demonstrated that inhibition of the NF-κB pathway impairs IFN-γ-mediated induction of PD-L1 in melanoma cells in a context in which NF-κB was not directly stimulated, suggesting a crosstalk between the two pathways (Gowrishankar et al., 2015). Similarly, stimulation of TLR3 with polyinosinic-polycytidylic acid (poly(I:C)) was shown to result in increased PD-L1 expression on dendritic cells (Pulko et al., 2009), endothelial cells (Cole et al., 2011), and neuroblastoma cells (Boes and Meyer-Wentrup, 2015). Whether this effect is directly due to TLR3 triggering or is mediated by an autocrine or paracrine factor that is produced upon TLR3 stimulation was not established. Other inflammatory stimuli that have been shown to induce PD-L1 are IL-17 in monocytes (Zhao et al., 2011) and prostate and colon cancer cells (Wang et al., 2017b), IL-10 in dendritic cells and monocytes (Curiel et al., 2003, Zhao et al., 2011), TNF-α in endothelial cells (Mazanet and Hughes, 2002), myelodysplastic syndrome blast cells (Kondo et al., 2010), dendritic cells, monocytes (Ou et al., 2012, Zhao et al., 2011), RCC (Quandt et al., 2014), prostate, breast cancer (Lim et al., 2016), and also colon cancer cells (Wang et al., 2017b), IL-4 in RCC (Quandt et al., 2014), IL-1β in dendritic cells (Karakhanova et al., 2010), IL-6 in dendritic cells (Karakhanova et al., 2010, Kil et al., 2017), and IL-27 in dendritic cells (Karakhanova et al., 2011, Matta et al., 2012) and ovarian cancer cells (Carbotti et al., 2015). Finally, TGF-β, a molecule that is in general considered an anti-inflammatory cytokine, appears to have a context-dependent effect on PD-L1 expression. Specifically, whereas exposure of cultured monocytes (Ou et al., 2012) or tubular epithelial cells (Starke et al., 2007) to TGF-β represses PD-L1 expression, production of TGF-β by CD8 T cells in an in vivo model of pancreatic islet transplantation was shown to be required for sustained expression of PD-L1 by the same cells (Baas et al., 2016), in line with the observation that TGF-β induces PD-L1 expression in dendritic cells in vitro (Ni et al., 2012, Song et al., 2014). Similarly, IL-12-mediated PD-L1 regulation is also context dependent, as it positively regulates PD-L1 in endothelial cells and monocyte-derived macrophages but represses its expression in macrophages derived from the monocytic cell line THP-1 (Xiong et al., 2014). While the data above indicate that PD-L1 expression can be regulated by a substantial number of inflammatory mediators, in many cases it is unclear whether such induction occurs in an indirect manner, for instance via regulation of IFN production. In addition, more data are required to establish (1) in which cell types these different stimuli do or do not alter PD-L1 levels, (2) whether such regulation is also observed in vivo, and (3) what the functional consequences of the altered PD-L1 expression are on local T cell function.

Aberrant Oncogenic Signaling Influences PD-L1 Expression

Alterations in major signaling pathways that control cell survival, proliferation, and differentiation constitute key events in cancer development and maintenance (Hanahan and Weinberg, 2011). In addition to fueling cancer progression in a tumor cell-intrinsic manner, certain oncogenic signaling pathways may also contribute to tumor outgrowth by driving PD-L1 expression, thereby potentially contributing to immune evasion. Findings in this area are of relevance not only because they can highlight mechanisms of PD-L1 gene (dys)regulation, but also because they may offer hypotheses on combinations of immune checkpoint therapies and therapies targeting oncogenic signaling pathways that could be tested clinically. Evidence obtained over the past years demonstrates that oncogenic signaling stemming from altered activity of basal transcription factors, effector components of signaling pathways, and upstream receptors can all influence PD-L1 expression.

A number of oncogenic transcription factors have been identified that directly regulate PD-L1 transcription. Elevated expression of the MYC oncogene contributes to tumorigenesis and is seen in approximately 70% of human cancers (Dang, 2012). Genetic or pharmacological inactivation of MYC has been shown to result in reduced PD-L1 expression in multiple mouse and human tumor cell models including melanoma, NSCLC, leukemia, lymphoma, and HCC (Atsaves et al., 2017, Casey et al., 2016, Wang et al., 2017a). In addition, chromatin immunoprecipitation (ChIP) analysis revealed that MYC binds to the PD-L1 promoter (Casey et al., 2016), indicating that PD-L1 expression can be directly regulated by MYC at the transcriptional level. Consistent with these data, it has been reported that MYC expression positively correlates with PD-L1 expression in NSCLC (Kim et al., 2017). Hypoxia represents a key feature of most tumors, as the expanding tumor mass often outgrows the oxygen supply. Tumors respond to this oxygen deficiency by activating a series of hypoxia-inducible factors (HIFs). As a result of HIF activation, a transcriptional program that promotes angiogenesis and tumor metastasis is initiated (Brown and Wilson, 2004, Liao et al., 2007). In addition, this response can result in increased PD-L1 expression. Specifically, both HIF-1α and HIF-2α have been shown to physically interact with the hypoxia response element (HRE) in the promoter region of PD-L1 (Barsoum et al., 2014, Messai et al., 2016). PD-L1 expression has been shown to be regulated by HIF-1α in mouse melanoma, human breast cancer, prostate cancer, NSCLC cells, and myeloid-derived suppressor cells (MDSCs) (Barsoum et al., 2014, Guo et al., 2017, Koh et al., 2015, Noman et al., 2014), and by HIF-2α in renal cell carcinoma cells (Messai et al., 2016), as shown by perturbation of gene expression. STAT3 is a transcription

factor that promotes cell proliferation, metastasis, and survival. It acts downstream of a variety of growth factors and cytokines and is found to be constitutively active in various cancers (Buettner et al., 2002). Multiple studies indicate that active STAT3 can directly act on the promoter of PD-L1 to increase its expression in human lymphoma and HNSCC cells (Atsaves et al., 2017, Bu et al., 2017, Marzec et al., 2008). Similarly, NF-κB, a family of transcription factors, can be activated in cancers by oncogenic mutations and cytokines produced in the inflammatory microenvironment. It has been reported that inhibition of the NF-κB pathway leads to decreased PD-L1 expression in human NK/T cell lymphomas, melanoma cells, and primary monocytes (Bi et al., 2016, Gowrishankar et al., 2015, Huang et al., 2013). The observed binding of RELA (p65; a subunit of NF-κB) to the PD-L1 promoter in NSCLC cells (in the form of a RELA-MUC1-C complex), monocytes, and breast cancer cells suggests that NF-κB can directly regulate PD-L1 transcription (Bouillez et al., 2017, Huang et al., 2013, Xue et al., 2017). AP-1, a dimeric transcription factor consisting of c-Jun, FOS, MAF, or ATF subunits, is strongly oncogenic (Shaulian and Karin, 2002). Tandem candidate AP-1 binding sites were identified in the first intron of PD-L1, which potentially recruit AP-1 components to elevate PD-L1 transcription in Hodgkin's lymphoma cells (Green et al., 2012). Since EBV-encoded latent membrane protein-1 (LMP1) triggers AP-1 and JAK-STAT activity (Kieser et al., 1997, Chen et al., 2013), EBV infection could conceivably contribute to the increased expression of PD-L1 that is observed in the subset of classical Hodgkin's lymphoma (CHL) in which no 9p24.1 amplification was detected (Green et al., 2012). In line with this, EBV+ CHLs are characterized by relatively higher PD-L1 H scores than their EBV– counterparts, in spite of the similar distribution of 9p24.1 amplification in EBV+ and EBV– CHLs (Roemer et al., 2016), although this difference may also be explained by IFN-γ production upon T cell recognition of EBV antigens. In melanoma cells that have developed resistance to BRAF inhibition, constitutive PD-L1 expression (here defined as PD-L1 expression that is not dependent on external stimuli) can be mediated by both JUN and STAT3, as interference with expression of either one blocked PD-L1 expression (Jiang et al., 2013).

As described above, PD-L1 expression can be induced in various cell types by inflammatory cytokines such as IFN-γ (Chen, 2004, Dong et al., 2002, Eppihimer et al., 2002, Keir et al., 2008). Cyclin-dependent kinase 5 (CDK5), a serine-threonine kinase that is highly expressed in medulloblastoma and many other cancers, can regulate PD-L1 expression through its influence on the IFN-γ-signaling pathway. Mechanistically, CDK5 destabilizes IRF2, a competitive repressor of IRF1, by posttranslational modification of the co-repressor IRF2BP2, and this destabilization then leads to IRF1-mediated induction of PD-L1 (Dorand et al., 2016).

The phosphatidylinositol 3-kinase (PI3K) signaling pathway impacts cancer cell survival, proliferation, metabolism, and mobility. The AKT-mTOR cascade that sits downstream of PI3K can be activated by type I and type II interferons and controls interferon-dependent mRNA translation (Kaur et al., 2008, Lekmine et al., 2004), implying a certain level of cooperation between interferon receptor signaling pathway and AKT-mTOR signaling pathway. In line with this, pharmacological inhibition of PI3K-AKT signaling suppressed IFN-γ-induced PD-L1 expression, while loss of PTEN (a tumor-suppressor gene that negatively regulates PI3K-AKT signaling) strengthens PD-L1 expression in CRC and NSCLC cells (Song et al., 2013, Zhang et al., 2017b). In addition, the PI3K-AKT pathway can regulate PD-L1 expression in an IFN-γ-independent manner in NSCLC, CRC, glioma, breast cancer, and melanoma cells (Atefi et al., 2014, Lastwika et al., 2016, Parsa et al., 2007, Song et al., 2013, Xu et al., 2014), and in melanoma and breast cancer cells, it was suggested that this regulation occurs at least partially by altering PD-L1 mRNA levels (Jiang et al., 2013, Mittendorf et al., 2014). Moreover, PI3K signaling is critically involved in the increase in PD-L1 expression following EGF stimulation in NSCLC cells, 17β-estradiol treatment of estrogen receptor alpha (ERα)-positive breast cancer cells, CpG oligodeoxynucleotide, or poly(I:C) stimulation of dendritic cells, and HIV infection of APCs (Karakhanova et al., 2010, Lastwika et al., 2016, Muthumani et al., 2011, Yang et al., 2017). Finally, some studies have shown that the influence of PI3K inhibition on PD-L1 expression varies substantially across melanoma cells, but the underlying mechanisms have yet to be revealed (Atefi et al., 2014, Gowrishankar et al., 2015).

The MEK-ERK pathway is commonly activated in human cancers, in most cases due to abnormal upstream signaling initiated by amplification or activating mutations in receptor tyrosine kinases, the RAS GTPase, or BRAF (Roberts and Der, 2007). Evidence suggests that MEK-ERK signaling can regulate PD-L1 gene expression through crosstalk with inflammatory signaling. Chemical or genetic suppression of MEK has been shown to inhibit IFN-γ-induced STAT1 phosphorylation and PD-L1 transcription in multiple myeloma cells (Liu et al., 2007). In line with this, activation of MEK-ERK signaling by PMA or by a constitutively active variant of MEK (MEK-DD) increases PD-L1 expression, and this effect can be abolished by MEK inhibition in multiple myeloma cells (Liu et al., 2007, Loi et al., 2016). Similarly, in BRAF mutant melanoma cells that have developed resistance to BRAF inhibition, constitutive PD-L1 expression is elevated in conjunction with the activation of JUN. JUN is a primary target of MAPK signaling and cooperates with STAT3 in transcriptional regulation of PD-L1 expression. It was suggested that suppression of MEK leads to decreased PD-L1 expression through inactivation of JUN and STAT3 in melanoma cells and in several NSCLC cells (Jiang et al., 2013, Sumimoto et al., 2016, Zhang et al., 1999). In

addition, the increased PD-L1 expression seen in multiple myeloma, bladder cancer, lymphoma, and dendritic cells upon stimulation by TLR ligands can be abrogated by MEK inhibition (Karakhanova et al., 2010, Liu et al., 2007, Qian et al., 2008, Yamamoto et al., 2009). Moreover, p38 MAPK, an effector in another MAPK signaling cascade that functions in parallel to the MEK/ERK pathway, also positively regulates PD-L1 expression in multiple myeloma, bladder cancer, lymphoma cells, and dendritic cells (Karakhanova et al., 2010, Qian et al., 2008, Yamamoto et al., 2009).

Activation of KRAS, epidermal growth factor receptor (EGFR), and anaplastic lymphoma kinase (ALK) due to genetic alterations or ligand stimulation can drive PD-L1 expression via their downstream effector pathway(s). In some KRAS mutant NSCLC cells, silencing of KRAS by RNAi decreases ERK activation which in turn can suppress PD-L1 expression (Chen et al., 2017a, Sumimoto et al., 2016). In line with this, ectopic expression of mutant KRAS results in increased PD-L1 expression in bronchial epithelial cells (Chen et al., 2017a). Recently, it was shown that RAS-MEK signaling in part controls expression of PD-L1 in NSCLC cells by modulating the stability of the PD-L1 transcript (Coelho et al., 2017). Activating mutations in EGFR, and also stimulation with EGF, induce PD-L1 expression in bronchial epithelial cells, NSCLC, head and neck cancer (HNC), and breast cancer cells. Consistent with these data, pharmacological inhibition of EGFR reduces constitutive and IFN-γ-induced PD-L1 expression (Akbay et al., 2013, Chen et al., 2015, Concha-Benavente et al., 2016, Lin et al., 2015, Zhang et al., 2016). The increase in PD-L1 expression that occurs as a result of EGFR activation in NSCLC cells can be blocked by rapamycin (Lastwika et al., 2016) and by an ERK inhibitor (Chen et al., 2015), suggesting mTOR- and ERK-dependent regulatory mechanisms. In addition, in different studies in head and neck cancer and NSCLC, evidence was obtained that supports a model in which NF-κB p65, STAT3, and/or JAK2-STAT1 serve as mediators between EGFR signaling and PD-L1 expression (Concha-Benavente et al., 2016, Lin et al., 2015, Zhang et al., 2016).

Finally, oncogenic ALK signaling often results from gene translation or amplification, and the NPM-ALK fusion protein has been shown to promote PD-L1 expression via STAT3 and MEK-ERK in lymphomas (Marzec et al., 2008, Yamamoto et al., 2009). Likewise, in NSCLC cells harboring the EML4-ALK fusion gene, PD-L1 expression is increased by the constitutively active ALK kinase, with ERK, AKT, STAT3, and HIF1α as downstream mediators (Koh et al., 2015, Ota et al., 2015).

While there are now abundant data on the regulation of the PD-L1 gene by a number of signaling pathways that are frequently activated in cancer, a number of aspects remain to be clarified. First, discrepancies with respect to the role of different

signaling components are sometimes observed across studies. Specifically, in contrast to the above-mentioned studies that demonstrate that MEK-ERK signaling positively regulates PD-L1 expression, in two other studies MEK inhibitor treatment had no effect or even increased PD-L1 expression in mouse breast cancer, NSCLC, and melanoma cells (Atefi et al., 2014, Liu et al., 2015, Loi et al., 2016). Moreover, whereas the increased PD-L1 expression upon EGFR activation was in one case shown to be mediated by the AKT-mTOR pathway (Lastwika et al., 2016), in a second study it was shown not to depend on AKT, but on ERK (Chen et al., 2015). These inconsistencies may be explained in several ways. First, inhibition of a major signaling node, such as the MEK-ERK or PI3K-AKT pathway, initiates signaling rewiring through feedback loops and pathway crosstalk to compensate for the perturbations (Sun and Bernards, 2014). Depending on both the specific cell or tissue type used and the duration or the intensity of pathway inhibition, the kinetics and specific type of compensatory signaling can vary. Support for this potential explanation is provided by time-course experiments that show that PD-L1 expression can fluctuate during treatment of KRAS mutant NSCLC cells with either a MEK inhibitor or AKT inhibitor (Lastwika et al., 2016, Minchom et al., 2017). In addition, the effect of the same pathway may vary between cell systems depending on the activity of other pathways. As a somewhat more trivial explanation for the observed discrepancies, the small-molecule kinase inhibitors that are frequently used to assess pathway involvement often have multiple targets. When different inhibitors are used to target the same pathway, a different outcome may result from differential off-target effects (Klaeger et al., 2017). As a second topic that deserves further attention, while the relationship between activity of signaling pathways and expression of PD-L1 has now been documented in many cell systems, it is presently unclear whether the increased PD-L1 expression that is observed acts as a positive selection pressure for pathway activation or is a mere epiphenomenon. As an example, MYC activation leads to increased transcription of a plethora of genes, and enhanced expression of only a part of these is likely to form a driving force in oncogenesis.

miRNA-Mediated PD-L1 mRNA Regulation

In normal physiology, miRNAs function as posttranscriptional regulators of gene expression by mediating target mRNA degradation and/or by inhibiting translation. Recently, the role of miRNAs in regulating PD-L1 expression has been revealed. Such regulation can either involve direct binding to the PD-L1 mRNA, or occur indirectly, by influencing the expression of other PD-L1 regulators. miR-513 was the first miRNA identified as a PD-L1 regulator. miR-513 suppresses PD-L1 at the level of translation by direct binding to the 3′ UTR of PD-L1 mRNA. It was shown that IFN-γ suppresses

miR-513 expression, and enforced expression of miR-513 blocks IFN-γ-induced PD-L1 expression in cholangiocytes (Gong et al., 2009, Gong et al., 2010). In contrast, miR-155 can be induced by TNFα and IFN-γ and suppresses PD-L1 expression at the protein level by direct binding to the 3′ UTR of PD-L1 in human dermal lymphatic endothelial cells (Yee et al., 2017). Together, miR-513 and 155 can be considered a system to fine-tune PD-L1 expression upon IFN-γ signaling. miR-34a, another miRNA that binds to the 3′UTR of PD-L1, has been shown to reduce PD-L1 mRNA levels in AML (Wang et al., 2015) and NSCLC cells (Cortez et al., 2015). In NSCLC, it was suggested that p53 suppresses PD-L1 expression via miR-34 (Cortez et al., 2015, Wang et al., 2015). Moreover, miR-142-5p (Jia et al., 2017), miR-93, and miR-106b (Cioffi et al., 2017) in pancreatic cancer, miR-138-5p (Zhao et al., 2016) in CRC, miR-217 (Miao et al., 2017) in laryngeal cancer, miR-200 (Chen et al., 2014, Gibbons et al., 2014, Xie et al., 2017) in NSCLC and gastric cancer, miR-152 (Xie et al., 2017) and miR-570 (Wang et al., 2013) in gastric cancer, miR-17-5p (Audrito et al., 2017) in melanoma, and miR-15a, miR-193a, and miR-16 (Kao et al., 2017) in malignant pleural mesothelioma have all been identified as suppressors of PD-L1 expression. As discussed above, the structural variations in the 3′ region of the PD-L1 gene that are found in adult T cell leukemia-lymphoma, diffuse large B cell lymphoma, and stomach adenocarcinoma (with variable frequencies ranging from 2%–27%) are known to lead to increased PD-L1 mRNA levels. A role of altered miRNA binding in the observed increase in PD-L1 mRNA levels appears plausible (Kataoka et al., 2016). Next to these direct effects, miRNAs can also influence PD-L1 expression in an indirect manner. Specifically, miR-20, miR-21, and miR-130b repress PTEN, which in turn causes increased PD-L1 expression in CRC (Zhu et al., 2014), and miR-197 suppresses PD-L1 expression via its direct action on the CKS1B-STAT3 cascade in NSCLC (Fujita et al., 2015).

PD-L1 Regulation at the Protein Level

Posttranslational regulation is final mechanism by which the level of PD-L1 expression is modulated, and several regulators of the PD-L1 protein have recently been identified. In two large-scale genetic screens in pancreatic cancer cells and CML-derived haploid cells, CMTM6 was identified as a positive regulator of PD-L1 expression (Burr et al., 2017, Mezzadra et al., 2017). Interference with CMTM6 expression reduces both constitutive and IFN-γ-induced PD-L1 protein expression, with no effect on PD-L1 mRNA levels. This control of PD-L1 levels by CMTM6 has to date been observed in all cell systems tested, including melanoma, NSCLC, breast cancer, pancreatic cancer, thyroid cancer, and CRC, and also LPS-stimulated primary dendritic cells. However, the magnitude of CMTM6-mediated PD-L1 regulation does differ substantially across the cell models tested. A modifier genetic screen in CMTM6-

deficient cells identified CMTM4 as a second PD-L1 regulator. The variable effect size of CMTM6 modulation across cell systems may therefore potentially be explained by differences in CMTM4 levels, but may also point to additional context dependencies. Mechanistically, CMTM6 was shown to bind to PD-L1 and thereby increase its half-life, presumably by preventing ubiquitination and lysosomal degradation during protein recycling. Mass spectrometric analysis suggests that CMTM6 associates with only a limited number of proteins, adding to its attractiveness as a possible target (Burr et al., 2017, Mezzadra et al., 2017). One aspect of the CMTM6-PD-L1 interaction that deserves further attention is whether CMTM6 has additional roles in this complex. Such roles could involve the clustering of PD-L1, allowing PD-L1 co-localization with other proteins, and/or signal transduction in the PD-L1-expressing cell.

As another proposed mechanism of PD-L1 protein regulation, in a study by Zhang et al. (2017a), it was demonstrated that the level of PD-L1 protein fluctuates during the cell cycle and that the cyclin D-CDK4 cascade participates in the regulation of PD-L1 levels in human cervical cancer and breast cancer cells. CDK4 phosphorylates SPOP, which stabilizes the latter by dissociating it from the ubiquitin E3-ligase complex APC/CCdh1. SPOP is an adaptor protein of Cullin 3 (CUL3), which interacts with and serves as an E3 ubiquitin ligase for PD-L1. Thus, CDK4 functions as a negative regulator of PD-L1 expression by indirectly regulating its ubiquitination (Zhang et al., 2017a). Evidence has also been obtained for a possible interaction between glycogen synthase kinase 3b (GSK3b) and non-glycosylated PD-L1 in breast cancer cells, thereby increasing PD-L1 degradation (Li et al., 2016). In addition, glycosylation of PD-L1 appears to influence its interaction with PD-1. Regulation of such glycosylation has been proposed as an additional level of control, but evidence for physiological relevance is presently limited (Li et al., 2018). Finally, evidence has been obtained indicating that, in addition to the role of NF-κB signaling in transcriptional regulation of PD-L1, NF-κB signaling induces expression of COP9 signalosome 5 (CSN5), resulting in increased PD-L1 protein levels in breast cancer cells through removal of ubiquitin chains (Lim et al., 2016).

Comparison of the effect of the different regulatory processes described in the sections above makes it apparent that the effect size of different PD-L1 regulators varies widely. In addition, the role of a given PD-L1 regulator can vary strongly, both between tissues and between tumors. As a straightforward example, whereas some tumors show a very profound increase in PD-L1 levels upon IFN-γ exposure, only a minor induction is observed in other cases. In the coming years, it will be important to understand under which conditions a specific regulatory process contributes to the PD-L1 levels in human cancers in a physiologically meaningful way.

Concluding Remarks

Immunotherapies that target the PD-L1-PD-1 axis have demonstrated unprecedented efficacy in the treatment of a variety of human cancers. Nevertheless, only a proportion of patients show objective responses to treatment, with only a small fraction experiencing complete responses.

PD-L1 expression has undergone extensive assessment with respect to its value as a predictive biomarker of anti-PD-1-PD-L1 therapies (Pitt et al., 2016, Sharma et al., 2017a). As shown in a number of cancer types, patients with PD-L1-positive tumors have a higher objective response rate and improved progression-free survival and overall survival as compared to PD-L1-negative subgroups (Borghaei et al., 2015, Fehrenbacher et al., 2016, Robert et al., 2015a, Rosenberg et al., 2016, Weber et al., 2015, Weber et al., 2017). However, a non-negligible number of exceptions is observed, both with patients in the PD-L1-negative subgroup still benefiting and with patients with PD-L1-positive tumors displaying intrinsic resistance to therapy (Carbognin et al., 2015). A major goal is therefore to improve our ability to predict response to these agents. Such an improvement will certainly come in part from a better understanding of the activity of other inhibitory mechanisms in individual patients (Blank et al., 2016). At the same time, a better understanding of the activity of the PD-1-PD-L1 axis itself in individual tumors can be expected to contribute. Specifically:

- One reason why PD-L1 expression is thought to have information value with respect to outcome upon PD-1-PD-L1 targeting is the fact that PD-L1 expression is frequently driven by IFN-γ exposure. As such, intratumoral PD-L1 expression can be seen as an indirect measure of local T cell activity. A confounder in these analyses, however, is that PD-L1 expression is also regulated by many other mechanisms, thereby reducing its accuracy as a measure of T cell activity. Strategies to distinguish IFN-γ-induced and IFN-γ-independent PD-L1 expression would therefore be of value. A straightforward way to achieve this goal would for instance be the simultaneous measurement of other IFN-γ-induced genes (Seiwert et al., 2016).

- As a second issue, the expression of PD-L1 may potentially increase during PD-1-PD-L1 blockade in some patients, thereby reducing the predictive value of a low pre-treatment PD-L1 expression. Specifically, in a case in which PD-L1 blockade reactivates rare tumor-reactive T cells, the resulting local cytokine secretion can induce multiple positive feedback loops: IFN-γ-induced production of CXCL9 and CXCL10 can promote T cell infiltration, and IFN-γ-induced increases in expression

of components of the antigen presentation machinery can enhance visibility of tumor cells to T cells. The possible occurrence of such feedforward loops makes it important to understand whether PD-1-PD-L1 blockade is or is not likely to spark enhanced T cell reactivity in an individual tumor.

- As a third and slightly related issue, as the ambition should be to understand whether the PD-1-PD-L1 axis is active in the tumor of an individual patient, it is somewhat counterintuitive to solely focus on expression of PD-L1. This issue is all the more important in view of the fact that intratumoral T cells can vary widely in the levels of PD-1 that they express (Thommen and Schumacher, 2018), and the effect of PD-1-PD-L1 axis blockade on T cells with different levels of PD-1 expression are presently ill understood. In addition to the possible joint assessment of expression of PD-L1 and PD-1, it may also be attractive to identify downstream consequences of PD-1 ligation in intratumoral T cells and other PD-1-expressing cells in tumor microenvironment, as a direct strategy to probe the activity of the PD-1-PD-L1 axis.

It is presently unclear whether our increased understanding of PD-L1 regulation will offer novel opportunities for therapeutic intervention. As described above, aberrant cell signaling that results from genetic or epigenetic alterations drive PD-L1 expression in many cancers, and these pathways may be targeted with small molecules to reverse this effect. Whether this will add to the activity of current anti-PD-1-PD-L1 antibodies depends on whether the current agents already fully block checkpoint signaling. Especially at sites of close T cell-tumor cell contact, it would seem possible that newly emerging checkpoint molecules may not be occupied sufficiently fast by antibody to fully prevent ligand binding. By the same token, dual targeting of CMTM6 and PD-L1 may conceivably form a strategy to more efficiently block the PD-1-PD-L1 checkpoint. Specifically, as CMTM6 is constitutively expressed, targeting of this molecule may pro-actively limit IFN-γ-induced adaptive PD-L1 expression by reducing the CMTM6 pool available for PD-L1 stabilization. Finally, the identification of such a bewildering variety of regulatory mechanisms of the PD-L1 checkpoint makes analysis of regulatory pathways that control the expression of other immune checkpoints also a highly attractive research area.

Acknowledgments

We would like to thank Lisette Rozeman, Daniela Thommen, and Christian Blank for valuable discussions. This work was supported by ERC AdG SENSIT (to T.N.S.) and The Cancer Research Institute (CRI) Irvington Postdoctoral Fellowship (to C.S.). We apologize to colleagues whose work was not cited in this review owing to space constraints.

References

Agata, Y., Kawasaki, A., Nishimura, H., Ishida, Y., Tsubata, T., Yagita, H., and Honjo, T. (1996). Expression of the PD-1 antigen on the surface of stimulated mouse T and B lymphocytes. Int. Immunol. 8, 765–772.

Akbay, E.A., Koyama, S., Carretero, J., Altabef, A., Tchaicha, J.H., Christensen, C.L., Mikse, O.R., Cherniack, A.D., Beauchamp, E.M., Pugh, T.J., et al. (2013). Activation of the PD-1 pathway contributes to immune escape in EGFR-driven lung tumors. Cancer Discov. 3, 1355–1363.

Ansari, M.J., Salama, A.D., Chitnis, T., Smith, R.N., Yagita, H., Akiba, H., Yamazaki, T., Azuma, M., Iwai, H., Khoury, S.J., et al. (2003). The programmed death-1 (PD-1) pathway regulates autoimmune diabetes in nonobese diabetic (NOD) mice. J. Exp. Med. 198, 63–69.

Ansell, S.M., Lesokhin, A.M., Borrello, I., Halwani, A., Scott, E.C., Gutierrez, M., Schuster, S.J., Millenson, M.M., Cattry, D., Freeman, G.J., et al. (2015). PD-1 blockade with nivolumab in relapsed or refractory Hodgkin's lymphoma. N. Engl. J. Med. 372, 311–319.

Antonia, S.J., Villegas, A., Daniel, D., Vicente, D., Murakami, S., Hui, R., Yokoi, T., Chiappori, A., Lee, K.H., de Wit, M., et al.; PACIFIC Investigators (2017). Durvalumab after chemoradiotherapy in stage III non-small-cell lung cancer. N. Engl. J. Med. 377, 1919–1929.

Armand, P., Shipp, M.A., Ribrag, V., Michot, J.M., Zinzani, P.L., Kuruvilla, J., Snyder, E.S., Ricart, A.D., Balakumaran, A., Rose, S., and Moskowitz, C.H. (2016).Programmed death-1 blockade with pembrolizumab in patients with classical Hodgkin lymphoma after brentuximab vedotin failure. J. Clin. Oncol. 34, 3733–3739.

Atefi, M., Avramis, E., Lassen, A., Wong, D.J., Robert, L., Foulad, D., Cerniglia, M., Titz, B., Chodon, T., Graeber, T.G., et al. (2014). Effects of MAPK and PI3K pathways on PD-L1 expression in melanoma. Clin. Cancer Res. 20, 3446–3457.

Atsaves, V., Tsesmetzis, N., Chioureas, D., Kis, L., Leventaki, V., Drakos, E., Panaretakis, T., Grander, D., Medeiros, L.J., Young, K.H., and Rassidakis, G.Z. (2017). PD-L1 is commonly expressed and transcriptionally regulated by STAT3 and MYC in ALK-negative anaplastic large-cell lymphoma. Leukemia 31, 1633–1637.

Audrito, V., Serra, S., Stingi, A., Orso, F., Gaudino, F., Bologna, C., Neri, F., Garaffo, G., Nassini, R., Baroni, G., et al. (2017). PD-L1 up-regulation in melanoma increases disease aggressiveness and is mediated through miR-17-5p. Oncotarget 8, 15894–15911.

Ayers, M., Lunceford, J., Nebozhyn, M., Murphy, E., Loboda, A., Kaufman, D.R., Albright, A., Cheng, J.D., Kang, S.P., Shankaran, V., et al. (2017). IFNg-related mRNA profile predicts clinical response to PD-1 blockade. J. Clin. Invest. 127, 2930–2940.

Azuma, T., Yao, S., Zhu, G., Flies, A.S., Flies, S.J., and Chen, L. (2008). B7-H1 is a ubiquitous antiapoptotic receptor on cancer cells. Blood 111, 3635–3643.

Baas, M., Besanc¸on, A., Goncalves, T., Valette, F., Yagita, H., Sawitzki, B., Volk, H.D., Waeckel-Ene´e, E., Rocha, B., Chatenoud, L., and You, S. (2016). TGFb-dependent expression of PD-1 and PD-L1 controls CD8(+) T cell anergy in transplant tolerance. eLife 5, e08133.

Balar, A.V., Castellano, D., O'Donnell, P.H., Grivas, P., Vuky, J., Powles, T., Plimack, E.R., Hahn, N.M., de Wit, R., Pang, L., et al. (2017a). First-line pembrolizumab in cisplatin-ineligible patients with locally advanced and unresectable or metastatic urothelial cancer (KEYNOTE-052): a multicentre, single-arm, phase 2 study. Lancet Oncol. 18, 1483–1492.

Balar, A.V., Galsky, M.D., Rosenberg, J.E., Powles, T., Petrylak, D.P., Bellmunt, J., Loriot, Y., Necchi, A., Hoffman-Censits, J., Perez-Gracia, J.L., et al.; IMvigor210 Study Group (2017b). Atezolizumab as first-line treatment in cisplatin-ineligible patients with locally advanced and metastatic urothelial carcinoma: a single-arm, multicentre, phase 2 trial. Lancet 389, 67–76.

Barber, D.L., Wherry, E.J., Masopust, D., Zhu, B., Allison, J.P., Sharpe, A.H., Freeman, G.J., and Ahmed, R. (2006). Restoring function in exhausted CD8 T cells during chronic viral infection. Nature 439, 682–687.

Barsoum, I.B., Smallwood, C.A., Siemens, D.R., and Graham, C.H. (2014). A mechanism of hypoxia-mediated escape from adaptive immunity in cancer cells. Cancer Res. 74, 665–674.

Bellmunt, J., de Wit, R., Vaughn, D.J., Fradet, Y., Lee, J.L., Fong, L., Vogelzang, N.J., Climent, M.A., Petrylak, D.P., Choueiri, T.K., et al.; KEYNOTE-045 Investigators (2017). Pembrolizumab as second-line therapy for advanced urothelial carcinoma. N. Engl. J. Med. 376, 1015–1026.

Bellone, S., Buza, N., Choi, J., Zammataro, L., Gay, L., Elvin, J.A., Rimm, D.L., Liu, Y., Ratner, E., Schwartz, P.E., and Santin, A.D. (2018). Exceptional response to pembrolizumab in a metastatic, chemotherapy/radiation resistant ovarian cancer patient harboring a CD274/PD-L1-genetic rearrangement. Clin. Cancer Res. Published online January 19, 2018. https://doi.org/10.1158/1078-0432.CCR-17-1805.

Bi, X.W., Wang, H., Zhang, W.W., Wang, J.H., Liu, W.J., Xia, Z.J., Huang, H.Q., Jiang, W.Q., Zhang, Y.J., and Wang, L. (2016). PD-L1 is upregulated by EBV driven LMP1 through NF-kB pathway and correlates with poor prognosis in natural killer/T-cell lymphoma. J. Hematol. Oncol. 9, 109.

Blank, C.U., Haanen, J.B., Ribas, A., and Schumacher, T.N. (2016). CANCER IMMUNOLOGY. The "cancer immunogram". Science 352, 658–660.

Boes, M., and Meyer-Wentrup, F. (2015). TLR3 triggering regulates PD-L1 (CD274) expression in human neuroblastoma cells. Cancer Lett. 361, 49–56.

Borghaei, H., Paz-Ares, L., Horn, L., Spigel, D.R., Steins, M., Ready, N.E., Chow, L.Q., Vokes, E.E., Felip, E., Holgado, E., et al. (2015). Nivolumab versus docetaxel in advanced nonsquamous non-small-cell lung cancer. N. Engl. J. Med. 373, 1627–1639.

Bouillez, A., Rajabi, H., Jin, C., Samur, M., Tagde, A., Alam, M., Hiraki, M., Maeda, T., Hu, X., Adeegbe, D., et al. (2017). MUC1-C integrates PD-L1 induction with repression of immune effectors in non-small-cell lung cancer. Oncogene 36, 4037–4046.

Brahmer, J.R., Drake, C.G., Wollner, I., Powderly, J.D., Picus, J., Sharfman, W.H., Stankevich, E., Pons, A., Salay, T.M., McMiller, T.L., et al. (2010). Phase I study of single-agent anti-programmed death-1 (MDX-1106) in refractory solid tumors: safety, clinical activity, pharmacodynamics, and immunologic correlates. J. Clin. Oncol. 28, 3167–3175.

Brahmer, J., Reckamp, K.L., Baas, P., Crino` , L., Eberhardt, W.E., Poddubskaya, E., Antonia, S., Pluzanski, A., Vokes, E.E., Holgado, E., et al. (2015). Nivolumab versus docetaxel in advanced squamous-cell non-small-cell lung cancer. N. Engl. J. Med. 373, 123–135.

Brown, J.M., and Wilson, W.R. (2004). Exploiting tumour hypoxia in cancer treatment. Nat. Rev. Cancer 4, 437–447.

Brown, J.A., Dorfman, D.M., Ma, F.R., Sullivan, E.L., Munoz, O., Wood, C.R., Greenfield, E.A., and Freeman, G.J. (2003). Blockade of programmed death-1 ligands on dendritic cells enhances T cell activation and cytokine production. J. Immunol. 170, 1257–1266.

Bu, L.L., Yu, G.T., Wu, L., Mao, L., Deng, W.W., Liu, J.F., Kulkarni, A.B., Zhang, W.F., Zhang, L., and Sun, Z.J. (2017). STAT3 induces immunosuppression by upregulating PD-1/PD-L1 in HNSCC. J. Dent. Res. 96, 1027–1034.

Buettner, R., Mora, L.B., and Jove, R. (2002). Activated STAT signaling in human tumors provides novel molecular targets for therapeutic intervention. Clin. Cancer Res. 8, 945–954.

Bumma, N., Jeyakumar, G., Kim, S., Galasso, C., Thakur, M.K., Gadgeel, S.M., Vaishampayan, U.N., and Wozniak, A.J. (2017). Neutrophil lymphocyte ratio (NLR) as a predictive biomarker for PD-1/PD-L1 directed therapy in metastatic non-small cell lung cancer (NSCLC). J. Clin. Oncol. 35, https://doi.org/10. 1200/JCO.2017.35.15_suppl.e20633.

Burr, M.L., Sparbier, C.E., Chan, Y.C., Williamson, J.C., Woods, K., Beavis, P.A., Lam, E.Y.N., Henderson, M.A., Bell, C.C., Stolzenburg, S., et al. (2017). CMTM6 maintains the expression of PD-L1 and regulates anti-tumour immunity. Nature 549, 101–105.

Butte, M.J., Keir, M.E., Phamduy, T.B., Sharpe, A.H., and Freeman, G.J. (2007). Programmed death-1 ligand 1 interacts specifically with the B7-1 costimulatory molecule to inhibit T cell responses. Immunity 27, 111–122.

Cancer Genome Atlas Research Network (2014). Comprehensive molecular characterization of gastric adenocarcinoma. Nature 513, 202–209.

Carbognin, L., Pilotto, S., Milella, M., Vaccaro, V., Brunelli, M., Calio` , A., Cuppone, F., Sperduti, I., Giannarelli, D., Chilosi, M., et al. (2015). Differential activity of nivolumab, pembrolizumab and MPDL3280A according to the tumor expression of programmed death-ligand-1 (PD-L1): sensitivity analysis of trials in melanoma, lung and genitourinary cancers. PLoS ONE 10, e0130142.

Carbotti, G., Barisione, G., Airoldi, I., Mezzanzanica, D., Bagnoli, M., Ferrero, S., Petretto, A., Fabbi, M., and Ferrini, S. (2015). IL-27 induces the expression of IDO and PD-L1 in human cancer cells. Oncotarget 6, 43267–43280.

Casey, S.C., Tong, L., Li, Y., Do, R.,Walz, S., Fitzgerald, K.N., Gouw, A.M., Baylot, V., Gutgemann, I., Eilers, M., and Felsher, D.W. (2016). MYC regulates the antitumor immune response through CD47 and PD-L1. Science 352, 227–231.

Chang, T.T., Jabs, C., Sobel, R.A., Kuchroo, V.K., and Sharpe, A.H. (1999). Studies in B7-deficient mice reveal a critical role for B7 costimulation in both induction and effector phases of experimental autoimmune encephalomyelitis. J. Exp. Med. 190, 733–740.

Chang, C.H., Qiu, J., O'Sullivan, D., Buck, M.D., Noguchi, T., Curtis, J.D., Chen, Q., Gindin, M., Gubin, M.M., van der Windt, G.J., et al. (2015). Metabolic competition in the tumor microenvironment is a driver of cancer progression. Cell 162, 1229–1241.

Chemnitz, J.M., Parry, R.V., Nichols, K.E., June, C.H., and Riley, J.L. (2004). SHP-1 and SHP-2 associate with immunoreceptor tyrosine-based switch motif of programmed death 1 upon primary human T cell stimulation, but only receptor ligation prevents T cell activation. J. Immunol. 173, 945–954.

Chen, L. (2004). Co-inhibitory molecules of the B7-CD28 family in the control of T-cell immunity. Nat. Rev. Immunol. 4, 336–347.

Chen, B.J., Chapuy, B., Ouyang, J., Sun, H.H., Roemer, M.G., Xu, M.L., Yu, H., Fletcher, C.D., Freeman, G.J., Shipp, M.A., and Rodig, S.J. (2013). PD-L1 expression is characteristic of a subset of aggressive B-cell lymphomas and virus-associated malignancies. Clin. Cancer Res. 19, 3462–3473.

Chen, L., Gibbons, D.L., Goswami, S., Cortez, M.A., Ahn, Y.H., Byers, L.A., Zhang, X., Yi, X., Dwyer, D., Lin, W., et al. (2014). Metastasis is regulated via microRNA-200/ZEB1 axis control of tumour cell PD-L1 expression and intratumoral immunosuppression. Nat. Commun. 5, 5241.

Chen, N., Fang, W., Zhan, J., Hong, S., Tang, Y., Kang, S., Zhang, Y., He, X., Zhou, T., Qin, T., et al. (2015). Upregulation of PD-L1 by EGFR activation mediates the immune escape in EGFR-driven NSCLC: implication for optional immune targeted therapy for NSCLC patients with EGFR mutation. J. Thorac. Oncol. 10, 910–923.

Chen, N., Fang, W., Lin, Z., Peng, P., Wang, J., Zhan, J., Hong, S., Huang, J., Liu, L., Sheng, J., et al. (2017a). KRAS mutation-induced upregulation of PD-L1 mediates immune escape in human lung adenocarcinoma. Cancer Immunol. Immunother. 66, 1175–1187.

Chen, R., Zinzani, P.L., Fanale, M.A., Armand, P., Johnson, N.A., Brice, P., Radford, J., Ribrag, V., Molin, D., Vassilakopoulos, T.P., et al.; KEYNOTE-087 (2017b). Phase II study of the efficacy and safety of pembrolizumab for relapsed/refractory classic Hodgkin lymphoma. J. Clin. Oncol. 35, 2125–2132.

Cioffi, M., Trabulo, S.M., Vallespinos, M., Raj, D., Kheir, T.B., Lin, M.L., Begum, J., Baker, A.M., Amgheib, A., Saif, J., et al. (2017). The miR-25-93-106b cluster regulates tumor metastasis and immune evasion via modulation of CXCL12 and PD-L1. Oncotarget 8, 21609–21625.

Coelho, M.A., de Carne´ Tre´ cesson, S., Rana, S., Zecchin, D., Moore, C., Molina-Arcas, M., East, P., Spencer-Dene, B., Nye, E., Barnouin, K., et al. (2017). Oncogenic RAS signaling promotes tumor immunoresistance by stabilizing PD-L1 mRNA. Immunity 47, 1083–1099.e6.

Cole, J.E., Navin, T.J., Cross, A.J., Goddard, M.E., Alexopoulou, L., Mitra, A.T., Davies, A.H., Flavell, R.A., Feldmann, M., and Monaco, C. (2011). Unexpected protective role for Toll-like receptor 3 in the arterial wall. Proc. Natl. Acad. Sci. USA 108, 2372–2377.

Concha-Benavente, F., Srivastava, R.M., Trivedi, S., Lei, Y., Chandran, U., Seethala, R.R., Freeman, G.J., and Ferris, R.L. (2016). Identification of the cellintrinsic and -extrinsic pathways downstream of EGFR and IFNg that induce PD-L1 expression in head and neck cancer. Cancer Res. 76, 1031–1043.

Cortez, M.A., Ivan, C., Valdecanas, D., Wang, X., Peltier, H.J., Ye, Y., Araujo, L., Carbone, D.P., Shilo, K., Giri, D.K., et al. (2015). PDL1 regulation by p53 via miR-34. J. Natl. Cancer Inst. 108, 108.

Curiel, T.J., Wei, S., Dong, H., Alvarez, X., Cheng, P., Mottram, P., Krzysiek, R., Knutson, K.L., Daniel, B., Zimmermann, M.C., et al. (2003). Blockade of B7-H1 improves myeloid dendritic cell-mediated antitumor immunity. Nat.Med. 9, 562–567.

Dang, C.V. (2012). MYC on the path to cancer. Cell 149, 22–35.

de Kleijn, S., Langereis, J.D., Leentjens, J., Kox, M., Netea, M.G., Koenderman, L., Ferwerda, G., Pickkers, P., and Hermans, P.W. (2013). IFN-g-stimulated neutrophils suppress lymphocyte proliferation through expression of PD-L1. PLoS ONE 8, e72249.

Dong, H., Zhu, G., Tamada, K., and Chen, L. (1999). B7-H1, a third member of the B7 family, co-stimulates T-cell proliferation and interleukin-10 secretion. Nat. Med. 5, 1365–1369.

Dong, H., Strome, S.E., Salomao, D.R., Tamura, H., Hirano, F., Flies, D.B., Roche, P.C., Lu, J., Zhu, G., Tamada, K., et al. (2002). Tumor-associated B7-H1 promotes T-cell apoptosis: a potential mechanism of immune evasion. Nat. Med. 8, 793–800.

Dorand, R.D., Nthale, J., Myers, J.T., Barkauskas, D.S., Avril, S., Chirieleison, S.M., Pareek, T.K., Abbott, D.W., Stearns, D.S., Letterio, J.J., et al. (2016). Cdk5 disruption attenuates tumor PD-L1 expression and promotes antitumor immunity. Science 353, 399–403.

El-Khoueiry, A.B., Sangro, B., Yau, T., Crocenzi, T.S., Kudo, M., Hsu, C., Kim, T.Y., Choo, S.P., Trojan, J., Welling, T.H.R., et al. (2017). Nivolumab in patients with advanced hepatocellular carcinoma (CheckMate 040): an open-label, non-comparative, phase 1/2 dose escalation and expansion trial. Lancet 389, 2492–2502.

Eppihimer, M.J., Gunn, J., Freeman, G.J., Greenfield, E.A., Chernova, T., Erickson, J., and Leonard, J.P. (2002). Expression and regulation of the PD-L1 immunoinhibitory molecule on microvascular endothelial cells. Microcirculation 9, 133–145.

Erickson, J.J., Gilchuk, P., Hastings, A.K., Tollefson, S.J., Johnson, M., Downing, M.B., Boyd, K.L., Johnson, J.E., Kim, A.S., Joyce, S., and Williams, J.V. (2012). Viral acute lower respiratory infections impair CD8+ T cells through PD-1. J. Clin. Invest. 122, 2967–2982.

Erkes, D.A., Smith, C.J., Wilski, N.A., Caldeira-Dantas, S., Mohgbeli, T., and Snyder, C.M. (2017). Virus-specific CD8+T cells infiltrate melanoma lesions and retain function independently of PD-1 expression. J. Immunol. 198, 2979–2988.

Fehrenbacher, L., Spira, A., Ballinger, M., Kowanetz, M., Vansteenkiste, J., Mazieres, J., Park, K., Smith, D., Artal-Cortes, A., Lewanski, C., et al.; POPLAR Study Group (2016). Atezolizumab versus docetaxel for patients with previously treated non-small-cell lung cancer (POPLAR): a multicentre, open-label, phase 2 randomised controlled trial. Lancet 387, 1837–1846.

Ferris, R.L., Blumenschein, G., Jr., Fayette, J., Guigay, J., Colevas, A.D., Licitra, L., Harrington, K., Kasper, S., Vokes, E.E., Even, C., et al. (2016). Nivolumab for recurrent squamous-cell carcinoma of the head and neck. N. Engl. J. Med. 375, 1856–1867.

Freeman, G.J., Long, A.J., Iwai, Y., Bourque, K., Chernova, T., Nishimura, H., Fitz, L.J., Malenkovich, N., Okazaki, T., Byrne, M.C., et al. (2000). Engagement of the PD-1 immunoinhibitory receptor by a novel B7 family member leads to negative regulation of lymphocyte activation. J. Exp. Med. 192, 1027–1034.

Fuchs, C.S., Doi, T., Jang, R.W.-J., Muro, K., Satoh, T., Machado, M., Sun, W., Jalal, S.I., Shah, M.A., Metges, J.-P., et al. (2017). KEYNOTE-059 cohort 1: Efficacy and safety of pembrolizumab (pembro) monotherapy in patients with previously treated advanced gastric cancer. J. Clin. Oncol. 35, https://doi.org/10.1200/JCO.2017.35.15_suppl.4003.

Fujita, Y., Yagishita, S., Hagiwara, K., Yoshioka, Y., Kosaka, N., Takeshita, F., Fujiwara, T., Tsuta, K., Nokihara, H., Tamura, T., et al. (2015). The clinical relevance of the miR-197/CKS1B/STAT3-mediated PD-L1 network in chemoresistant non-small-cell lung cancer. Mol. Ther. 23, 717–727.

Garcia-Diaz, A., Shin, D.S., Moreno, B.H., Saco, J., Escuin-Ordinas, H., Rodriguez, G.A., Zaretsky, J.M., Sun, L., Hugo, W., Wang, X., et al. (2017). Interferon receptor signaling pathways regulating PD-L1 and PD-L2 expression. Cell Rep. 19, 1189–1201.

Gato-Canas, M., Zuazo, M., Arasanz, H., Ibanez-Vea, M., Lorenzo, L., Fernandez-Hinojal, G., Vera, R., Smerdou, C., Martisova, E., Arozarena, I., et al. (2017). PDL1 signals through conserved sequence motifs to overcome interferon-mediated cytotoxicity. Cell Rep. 20, 1818–1829.

Gauen, L.K., Zhu, Y., Letourneur, F., Hu, Q., Bolen, J.B., Matis, L.A., Klausner, R.D., and Shaw, A.S. (1994). Interactions of p59fyn and ZAP-70 with T-cell receptor activation motifs: defining the nature of a signalling motif. Mol. Cell. Biol. 14, 3729–3741.

George, J., Saito, M., Tsuta, K., Iwakawa, R., Shiraishi, K., Scheel, A.H., Uchida, S., Watanabe, S.I., Nishikawa, R., Noguchi, M., et al. (2017). Genomic amplification of CD274(PD-L1) in small-cell lung cancer. Clin. Cancer Res. 23, 1220–1226.

Gibbons, D.L., Chen, L., Goswami, S., Cortez, M.A., Ahn, Y.-H., Byers, L.A., Lin, W., Diao, L., Wang, J., Roybal, J., et al. (2014). Regulation of tumor cell PD-L1 expression by microRNA-200 and control of lung cancer metastasis. J. Clin. Oncol. 32, https://doi.org/10.1200/jco.2014.32.15_suppl.8063.

Gong, A.Y., Zhou, R., Hu, G., Li, X., Splinter, P.L., O'Hara, S.P., LaRusso, N.F., Soukup, G.A., Dong, H., and Chen, X.M. (2009). MicroRNA-513 regulates B7-H1 translation and is involved in IFN-gamma-induced B7-H1 expression in cholangiocytes. J. Immunol. 182, 1325–1333.

Gong, A.Y., Zhou, R., Hu, G., Liu, J., Sosnowska, D., Drescher, K.M., Dong,H., and Chen, X.M. (2010). Cryptosporidium parvum induces B7-H1 expression in cholangiocytes by down-regulatingmicroRNA-513. J. Infect. Dis. 201, 160–169.

Goodman, A.M., Kato, S., Bazhenova, L., Patel, S.P., Frampton, G.M., Miller, V., Stephens, P.J., Daniels, G.A., and Kurzrock, R. (2017). Tumor mutational burden as an independent predictor of response to immunotherapy in diverse cancers. Mol. Cancer Ther. 16, 2598–2608.

Gordon, S.R., Maute, R.L., Dulken, B.W., Hutter, G., George, B.M., McCracken, M.N., Gupta, R., Tsai, J.M., Sinha, R., Corey, D., et al. (2017). PD-1 expression by tumour-associated macrophages inhibits phagocytosis and tumour immunity. Nature 545, 495–499.

Gowrishankar, K., Gunatilake, D., Gallagher, S.J., Tiffen, J., Rizos, H., and Hersey, P. (2015). Inducible but not constitutive expression of PD-L1 in human melanoma cells is dependent on activation of NF-kB. PLoS ONE 10, e0123410.

Green, M.R., Monti, S., Rodig, S.J., Juszczynski, P., Currie, T., O'Donnell, E., Chapuy, B., Takeyama, K., Neuberg, D., Golub, T.R., et al. (2010). Integrative analysis reveals selective 9p24.1 amplification, increased PD-1 ligand expression, and further induction via JAK2 in nodular sclerosing Hodgkin lymphoma and primary mediastinal large B-cell lymphoma. Blood 116, 3268–3277.

Green, M.R., Rodig, S., Juszczynski, P., Ouyang, J., Sinha, P., O'Donnell, E., Neuberg, D., and Shipp,M.A. (2012).Constitutive AP-1 activity and EBV infection induce PD-L1 in Hodgkin lymphomas and posttransplant lymphoproliferative disorders: implications for targeted therapy. Clin. Cancer Res. 18, 1611–1618.

Gros, A., Robbins, P.F., Yao, X., Li, Y.F., Turcotte, S., Tran, E., Wunderlich, J.R., Mixon, A., Farid, S., Dudley, M.E., et al. (2014). PD-1 identifies the patient-specific CD8+ tumor-reactive repertoire infiltrating human tumors. J. Clin. Invest. 124, 2246–2259.

Gros, A., Parkhurst, M.R., Tran, E., Pasetto, A., Robbins, P.F., Ilyas, S., Prickett, T.D., Gartner, J.J., Crystal, J.S., Roberts, I.M., et al. (2016). Prospective identification of neoantigen-specific lymphocytes in the peripheral blood of melanoma patients. Nat. Med. 22, 433–438.

Guleria, I., Khosroshahi, A., Ansari, M.J., Habicht, A., Azuma, M., Yagita, H., Noelle, R.J., Coyle, A., Mellor, A.L., Khoury, S.J., and Sayegh, M.H. (2005). A critical role for the programmed death ligand 1 in fetomaternal tolerance. J. Exp. Med. 202, 231–237.

Guo, R., Li, Y., Bai, H., and Wang, J. (2017). KRAS mutants to regulate PDL1 expression through NF-KB and HIF-1a pathways in non-small cell lung cancer cells. J. Clin. Oncol. 35, https://doi.org/10.1200/JCO.2017.35.15_suppl. e20049.

Hanahan, D., and Weinberg, R.A. (2011). Hallmarks of cancer: the next generation. Cell 144, 646–674.

Herbst, R.S., Baas, P., Kim, D.W., Felip, E., Perez-Gracia, J.L., Han, J.Y., Molina, J., Kim, J.H., Arvis, C.D., Ahn, M.J., et al. (2016). Pembrolizumab versus docetaxel for previously treated,PD-L1-positive, advancednon-small-cell lungcancer (KEYNOTE-010): a randomised controlled trial. Lancet 387, 1540–1550.

Hirano, F., Kaneko, K., Tamura, H., Dong, H., Wang, S., Ichikawa, M., Rietz, C., Flies, D.B., Lau, J.S., Zhu, G., et al. (2005). Blockade of B7-H1 and PD-1 by monoclonal antibodies potentiates cancer therapeutic immunity. Cancer Res. 65, 1089–1096.

Honda, T., Egen, J.G., L€ammermann, T., Kastenm€uller, W., Torabi-Parizi, P., and Germain, R.N. (2014). Tuning of antigen sensitivity by T cell receptor dependent negative feedback controls T cell effector function in inflamed tissues. Immunity 40, 235–247.

Huang, G., Wen, Q., Zhao, Y., Gao, Q., and Bai, Y. (2013). NF-kB plays a key role in inducing CD274 expression in human monocytes after lipopolysaccharide treatment. PLoS ONE 8, e61602.

Hugo, W., Zaretsky, J.M., Sun, L., Song, C., Moreno, B.H., Hu-Lieskovan, S., Berent-Maoz, B., Pang, J., Chmielowski, B., Cherry, G., et al. (2016). Genomic and transcriptomic features of response to anti-PD-1 therapy in metastatic melanoma. Cell 165, 35–44.

Hui, E., Cheung, J., Zhu, J., Su, X., Taylor, M.J., Wallweber, H.A., Sasmal, D.K., Huang, J., Kim, J.M., Mellman, I., and Vale, R.D. (2017). T cell costimulatory receptor CD28 is a primary target for PD-1-mediated inhibition. Science 355, 1428–1433.

Ikeda, S., Okamoto, T., Okano, S., Umemoto, Y., Tagawa, T., Morodomi, Y., Kohno, M., Shimamatsu, S., Kitahara, H., Suzuki, Y., et al. (2016). PD-L1 is upregulated by simultaneous amplification of the PD-L1 and JAK2 genes in nonsmall cell lung cancer. J. Thorac. Oncol. 11, 62–71.

Ishida, Y., Agata, Y., Shibahara, K., and Honjo, T. (1992). Induced expression of PD-1, a novel member of the immunoglobulin gene superfamily, upon programmed cell death. EMBO J. 11, 3887–3895.

Jia, L., Xi, Q., Wang, H., Zhang, Z., Liu, H., Cheng, Y., Guo, X., Zhang, J., Zhang, Q., Zhang, L., et al. (2017). miR-142-5p regulates tumor cell PD-L1 expression and enhances anti-tumor immunity. Biochem. Biophys. Res. Commun. 488, 425–431.

Jiang, X., Zhou, J., Giobbie-Hurder, A., Wargo, J., and Hodi, F.S. (2013). The activation of MAPK in melanoma cells resistant to BRAF inhibition promotes PD-L1 expression that is reversible by MEK and PI3K inhibition. Clin. Cancer Res. 19, 598–609.

Juneja, V.R., McGuire, K.A., Manguso, R.T., LaFleur, M.W., Collins, N., Haining, W.N., Freeman, G.J., and Sharpe, A.H. (2017). PD-L1 on tumor cells is sufficient for immune evasion in immunogenic tumors and inhibits CD8 T cell cytotoxicity. J. Exp. Med. 214, 895–904.

Kao, S.C., Cheng, Y.Y., Williams, M., Kirschner, M.B., Madore, J., Lum, T., Sarun, K.H., Linton, A., McCaughan, B., Klebe, S., et al. (2017). Tumor suppressor microRNAs contribute to the regulation of PD-L1 expression in malignant pleural mesothelioma. J. Thorac. Oncol. 12, 1421–1433.

Karakhanova, S., Meisel, S., Ring, S., Mahnke, K., and Enk, A.H. (2010). ERK/p38 MAP-kinases and PI3K are involved in the differential regulation of B7-H1 expression in DC subsets. Eur. J. Immunol. 40, 254–266.

Karakhanova, S., Bedke, T., Enk, A.H., and Mahnke, K. (2011). IL-27 renders DC immunosuppressive by induction of B7-H1. J. Leukoc. Biol. 89, 837–845.

Kataoka, K., Shiraishi, Y., Takeda, Y., Sakata, S., Matsumoto, M., Nagano, S., Maeda, T., Nagata, Y., Kitanaka, A., Mizuno, S., et al. (2016). Aberrant PD-L1 expression through 30-UTR disruption in multiple cancers. Nature 534, 402–406.

Kaufman, H.L., Russell, J., Hamid, O., Bhatia, S., Terheyden, P., D'Angelo, S.P., Shih, K.C., Lebbe´ , C., Linette, G.P., Milella, M., et al. (2016). Avelumab in patients with chemotherapy-refractory metastatic Merkel cell carcinoma: a multicentre, single-group, open-label, phase 2 trial. Lancet Oncol. 17, 1374–1385.

Kaur, S., Sassano, A., Dolniak, B., Joshi, S., Majchrzak-Kita, B., Baker, D.P., Hay, N., Fish, E.N., and Platanias, L.C. (2008). Role of the Akt pathway in mRNA translation of interferon-stimulated genes. Proc. Natl. Acad. Sci. USA 105, 4808–4813.

Keir, M.E., Liang, S.C., Guleria, I., Latchman, Y.E., Qipo, A., Albacker, L.A., Koulmanda, M., Freeman, G.J., Sayegh, M.H., and Sharpe, A.H. (2006). Tissue expression of PD-L1 mediates peripheral T cell tolerance. J. Exp. Med. 203, 883–895.

Keir, M.E., Butte, M.J., Freeman, G.J., and Sharpe, A.H. (2008). PD-1 and its ligands in tolerance and immunity. Annu. Rev. Immunol. 26, 677–704.

Kieser, A., Kilger, E., Gires, O., Ueffing, M., Kolch, W., and Hammerschmidt, W. (1997). Epstein-Barr virus latent membrane protein-1 triggers AP-1 activity via the c-Jun N-terminal kinase cascade. EMBO J. 16, 6478–6485.

Kil, S.H., Estephan, R., Sanchez, J., Zain, J.M., Kadin, M.E., Young, J.W., Rosen, S.T., and Querfeld, C. (2017). PD-L1 is regulated by interferon gamma and interleukin 6 through STAT1 and STAT3 signaling in cutaneous T-cell lymphoma. Blood 130, 1458.

Kim, E.Y., Kim, A., Kim, S.K., and Chang, Y.S. (2017). MYC expression correlates with PD-L1 expression in non-small cell lung cancer. Lung Cancer 110, 63–67.

Klaeger, S., Heinzlmeir, S., Wilhelm, M., Polzer, H., Vick, B., Koenig, P.A., Reinecke, M., Ruprecht, B., Petzoldt, S., Meng, C., et al. (2017). The target landscape of clinical kinase drugs. Science 358, 358.

Kleffel, S., Posch, C., Barthel, S.R., Mueller, H., Schlapbach, C., Guenova, E., Elco, C.P., Lee, N., Juneja, V.R., Zhan, Q., et al. (2015). Melanoma cell-intrinsic PD-1 receptor functions promote tumor growth. Cell 162, 1242–1256.

Koh, J., Jang, J.Y., Keam, B., Kim, S., Kim, M.Y., Go, H., Kim, T.M., Kim, D.W., Kim, C.W., Jeon, Y.K., and Chung, D.H. (2015). EML4-ALK enhances programmed cell death-ligand 1 expression in pulmonary adenocarcinoma via hypoxia-inducible factor (HIF)-1a and STAT3. OncoImmunology 5, e1108514.

Kok, M., Horlings, H.M., Snaebjornsson, P., Chalabi, M., Schumacher, T.N., Blank, C.U., Linn, S.C., and Dieren, J.v. (2017). Profound immunotherapy response in mismatch repair-deficient breast cancer. JCO Precision Oncology 9, 1–3.

Kondo, A., Yamashita, T., Tamura, H., Zhao, W., Tsuji, T., Shimizu, M., Shinya, E., Takahashi, H., Tamada, K., Chen, L., et al. (2010). Interferon-gamma and tumor necrosis factor-alpha induce an immunoinhibitory molecule, B7-H1, via nuclear factor-kappaB activation in blasts in myelodysplastic syndromes. Blood 116, 1124–1131.

Krieg, C., Nowicka, M., Guglietta, S., Schindler, S., Hartmann, F.J., Weber, L.M., Dummer, R., Robinson, M.D., Levesque, M.P., and Becher, B. (2018). High-dimensional single-cell analysis predicts response to anti-PD-1 immunotherapy. Nat. Med. 24, 144–153.

Kryczek, I., Wei, S., Gong, W., Shu, X., Szeliga, W., Vatan, L., Chen, L., Wang, G., and Zou, W. (2008). Cutting edge: IFN-gamma enables APC to promote memory Th17 and abate Th1 cell development. J. Immunol. 181, 5842–5846.

Kvistborg, P., Philips, D., Kelderman, S., Hageman, L., Ottensmeier, C., Joseph-Pietras, D., Welters, M.J., van der Burg, S., Kapiteijn, E., Michielin, O., et al. (2014). Anti-CTLA-4 therapy broadens the melanoma-reactive CD8+ T cell response. Sci. Transl. Med. 6, 254ra128.

Langer, C.J., Gadgeel, S.M., Borghaei, H., Papadimitrakopoulou, V.A., Patnaik, A., Powell, S.F., Gentzler, R.D., Martins, R.G., Stevenson, J.P., Jalal, S.I., et al.; KEYNOTE-021 investigators (2016). Carboplatin and pemetrexed with or without pembrolizumab for advanced, non-squamous non-small-cell lung cancer: a randomised, phase 2 cohort of the open-label KEYNOTE-021 study. Lancet Oncol. 17, 1497–1508.

Larkin, J., Chiarion-Sileni, V., Gonzalez, R., Grob, J.J., Cowey, C.L., Lao, C.D., Schadendorf, D., Dummer, R., Smylie, M., Rutkowski, P., et al. (2015). Combined nivolumab and ipilimumab or monotherapy in untreated melanoma. N. Engl. J. Med. 373, 23–34.

Lastwika, K.J., Wilson, W., 3rd, Li, Q.K., Norris, J., Xu, H., Ghazarian, S.R., Kitagawa, H., Kawabata, S., Taube, J.M., Yao, S., et al. (2016). Control of PD-L1 expression by oncogenic activation of the AKT-mTOR pathway in non-small cell lung cancer. Cancer Res. 76, 227–238.

Latchman, Y.E., Liang, S.C., Wu, Y., Chernova, T., Sobel, R.A., Klemm, M., Kuchroo, V.K., Freeman, G.J., and Sharpe, A.H. (2004). PD-L1-deficient mice show that PD-L1 on T cells, antigen-presenting cells, and host tissues negatively regulates T cells. Proc. Natl. Acad. Sci. USA 101, 10691–10696.

Lau, J., Cheung, J., Navarro, A., Lianoglou, S., Haley, B., Totpal, K., Sanders, L., Koeppen, H., Caplazi, P., McBride, J., et al. (2017). Tumour and host cell PD-L1 is required to mediate suppression of anti-tumour immunity in mice. Nat. Commun. 8, 14572.

Lazar-Molnar, E., Gacser, A., Freeman, G.J., Almo, S.C., Nathenson, S.G., and Nosanchuk, J.D. (2008). The PD-1/PD-L costimulatory pathway critically affects host resistance to the pathogenic fungus Histoplasma capsulatum. Proc. Natl. Acad. Sci. USA 105, 2658–2663.

Le, D.T., Uram, J.N., Wang, H., Bartlett, B.R., Kemberling, H., Eyring, A.D., Skora, A.D., Luber, B.S., Azad, N.S., Laheru, D., et al. (2015). PD-1 blockade in tumors with mismatch-repair deficiency. N. Engl. J. Med. 372, 2509–2520.

Le, D.T., Durham, J.N., Smith, K.N.,Wang, H., Bartlett, B.R., Aulakh, L.K., Lu, S., Kemberling,H., Wilt,C., Luber, B.S., et al. (2017). Mismatch repair deficiency predicts response of solid tumors to PD-1 blockade. Science 357, 409–413.

Lee, S.J., Jang, B.C., Lee, S.W., Yang, Y.I., Suh, S.I., Park, Y.M., Oh, S., Shin, J.G., Yao, S., Chen, L., and Choi, I.H. (2006). Interferon regulatory factor-1 is prerequisite to the constitutive expression and IFN-gamma-induced upregulation of B7-H1 (CD274). FEBS Lett. 580, 755–762.

Lekmine, F., Sassano, A., Uddin, S., Smith, J., Majchrzak, B., Brachmann, S.M., Hay, N., Fish, E.N., and Platanias, L.C. (2004). Interferon-gamma engages the p70 S6 kinase to regulate phosphorylation of the 40S S6 ribosomal protein. Exp. Cell Res. 295, 173–182.

Li,C.W., Lim, S.O., Xia, W., Lee, H.H., Chan, L.C., Kuo, C.W., Khoo, K.H., Chang, S.S., Cha, J.H., Kim, T., et al. (2016). Glycosylation and stabilization of programmed death ligand-1 suppresses T-cell activity. Nat. Commun. 7, 12632.

Li, C.W., Lim, S.O., Chung, E.M., Kim, Y.S., Park, A.H., Yao, J., Cha, J.H., Xia, W., Chan, L.C., Kim, T., et al. (2018). Eradication of triple-negative breast cancer cells by targeting glycosylated PD-L1. Cancer Cell 33, 187–201.e10.

Liao, D., Corle, C., Seagroves, T.N., and Johnson, R.S. (2007). Hypoxia-inducible factor-1alpha is a key regulator of metastasis in a transgenic model of cancer initiation and progression. Cancer Res. 67, 563–572.

Lim, S.O., Li, C.W., Xia, W., Cha, J.H., Chan, L.C., Wu, Y., Chang, S.S., Lin, W.C., Hsu, J.M., Hsu, Y.H., et al. (2016). Deubiquitination and stabilization of PD-L1 by CSN5. Cancer Cell 30, 925–939.

Lin, D.Y., Tanaka, Y., Iwasaki, M., Gittis, A.G., Su, H.P., Mikami, B., Okazaki, T., Honjo, T., Minato, N., and Garboczi, D.N. (2008). The PD-1/PD-L1 complex resembles the antigen-binding Fv domains of antibodies and T cell receptors. Proc. Natl. Acad. Sci. USA 105, 3011–3016.

Lin, K., Cheng, J., Yang, T., Li, Y., and Zhu, B. (2015). EGFR-TKI down-regulates PD-L1 in EGFR mutant NSCLC through inhibiting NF-kB. Biochem. Biophys. Res. Commun. 463, 95–101.

Liu, J., Hamrouni, A., Wolowiec, D., Coiteux, V., Kuliczkowski, K., Hetuin, D., Saudemont, A., and Quesnel, B. (2007). Plasma cells from multiple myeloma patients express B7-H1 (PD-L1) and increase expression after stimulation with IFN-gamma and TLR ligands via a MyD88-, TRAF6-, and MEK-dependent pathway. Blood 110, 296–304.

Liu, J., Zhang, E., Ma, Z., Wu, W., Kosinska, A., Zhang, X., Moller, I., Seiz, P., Glebe, D., Wang, B., et al. (2014). Enhancing virus-specific immunity in vivo by combining therapeutic vaccination and PD-L1 blockade in chronic hepadnaviral infection. PLoS Pathog. 10, e1003856.

Liu, L., Mayes, P.A., Eastman, S., Shi, H., Yadavilli, S., Zhang, T., Yang, J., Seestaller-Wehr, L., Zhang, S.Y., Hopson, C., et al. (2015). The BRAF and MEK inhibitors dabrafenib and trametinib: effects on immune function and in combination with immunomodulatory antibodies targeting PD-1, PD-L1, and CTLA-4. Clin. Cancer Res. 21, 1639–1651.

Loi, S., Dushyanthen, S., Beavis, P.A., Salgado, R., Denkert, C., Savas, P., Combs, S., Rimm, D.L., Giltnane, J.M., Estrada, M.V., et al. (2016). RAS/MAPK activation is associated with reduced tumor-infiltrating lymphocytes in triple-negative breast cancer: therapeutic cooperation between MEK and PD-1/PD-L1 immune checkpoint Inhibitors. Clin. Cancer Res. 22, 1499–1509.

Loke, P., and Allison, J.P. (2003). PD-L1 and PD-L2 are differentially regulated by Th1 and Th2 cells. Proc. Natl. Acad. Sci. USA 100, 5336–5341.

Lu, Y.C., Yeh, W.C., and Ohashi, P.S. (2008). LPS/TLR4 signal transduction pathway. Cytokine 42, 145–151.

Manguso, R.T., Pope, H.W., Zimmer, M.D., Brown, F.D., Yates, K.B., Miller, B.C., Collins, N.B., Bi, K., LaFleur, M.W., Juneja, V.R., et al. (2017). In vivo CRISPR screening identifies Ptpn2 as a cancer immunotherapy target. Nature 547, 413–418.

Mariathasan, S., Turley, S.J., Nickles, D., Castiglioni, A., Yuen, K., Wang, Y., Kadel Iii, E.E., Koeppen, H., Astarita, J.L., Cubas, R., et al. (2018). TGFb attenuates tumour response to PD-L1 blockade by contributing to exclusion of T cells. Nature 554, 544–548.

Marzec, M., Zhang, Q., Goradia, A., Raghunath, P.N., Liu, X., Paessler, M., Wang, H.Y., Wysocka, M., Cheng, M., Ruggeri, B.A., and Wasik, M.A. (2008). Oncogenic kinase NPM/ALK induces through STAT3 expression of immunosuppressive protein CD274 (PD-L1, B7-H1). Proc. Natl. Acad. Sci. USA 105, 20852–20857.

Matta, B.M., Raimondi, G., Rosborough, B.R., Sumpter, T.L., and Thomson, A.W. (2012). IL-27 production and STAT3-dependent upregulation of B7-H1 mediate immune regulatory functions of liver plasmacytoid dendritic cells. J. Immunol. 188, 5227–5237.

Mazanet, M.M., and Hughes, C.C. (2002). B7-H1 is expressed by human endothelial cells and suppresses T cell cytokine synthesis. J. Immunol. 169, 3581–3588.

Messai, Y., Gad, S., Noman, M.Z., Le Teuff, G., Couve, S., Janji, B., Kammerer, S.F., Rioux-Leclerc, N., Hasmim, M., Ferlicot, S., et al. (2016). Renal cell carcinoma programmed death-ligand 1, a new direct target of hypoxia-inducible factor-2 alpha, is regulated by von Hippel-Lindau gene mutation status. Eur. Urol. 70, 623–632.

Mezzadra, R., Sun, C., Jae, L.T., Gomez-Eerland, R., de Vries, E., Wu, W., Logtenberg, M.E.W., Slagter, M., Rozeman, E.A., Hofland, I., et al. (2017). Identification of CMTM6 and CMTM4 as PD-L1 protein regulators. Nature 549, 106–110.

Miao, S., Mao, X., Zhao, S., Song, K., Xiang, C., Lv, Y., Jiang, H., Wang, L., Li, B., Yang, X., et al. (2017). miR-217 inhibits laryngeal cancer metastasis by repressing AEG-1 and PD-L1 expression. Oncotarget 8, 62143–62153.

Minchom, A., Thavasu, P., Ahmad, Z., Stewart, A., Georgiou, A., O'Brien, M.E.R., Popat, S., Bhosle, J., Yap, T.A., de Bono, J., and Banerji, U. (2017). A study of PD-L1 expression in KRAS mutant non-small cell lung cancer cell lines exposed to relevant targeted treatments. PLoS ONE 12, e0186106.

Mittendorf, E.A., Philips, A.V., Meric-Bernstam, F., Qiao, N., Wu, Y., Harrington, S., Su, X.,Wang, Y., Gonzalez-Angulo, A.M., Akcakanat, A., et al. (2014). PD-L1 expression in triple-negative breast cancer. Cancer Immunol. Res. 2, 361–370.

Motzer, R.J., Escudier, B., McDermott, D.F., George, S., Hammers, H.J., Srinivas, S., Tykodi, S.S., Sosman, J.A., Procopio, G., Plimack, E.R., et al.; CheckMate 025 Investigators (2015). Nivolumab versus everolimus in advanced renal-cell carcinoma. N. Engl. J. Med. 373, 1803–1813.

Muthumani, K., Shedlock, D.J., Choo, D.K., Fagone, P., Kawalekar, O.U., Goodman, J., Bian, C.B., Ramanathan, A.A., Atman, P., Tebas, P., et al. (2011). HIV-mediated phosphatidylinositol 3-kinase/serine-threonine kinase activation in APCs leads to programmed death-1 ligand upregulation and suppression of HIV-specific CD8 T cells. J. Immunol. 187, 2932–2943.

Nakazawa, A.,Dotan, I.,Brimnes, J.,Allez, M., Shao, L., Tsushima, F.,Azuma, M., and Mayer, L. (2004). The expression and function of costimulatory molecules B7H and B7-H1 on colonic epithelial cells. Gastroenterology 126, 1347–1357.

Ni, X.Y., Sui, H.X., Liu, Y., Ke, S.Z., Wang, Y.N., and Gao, F.G. (2012). TGF-b of lung cancer microenvironment upregulates B7H1 and GITRL expression in dendritic cells and is associated with regulatory T cell generation. Oncol. Rep. 28, 615–621.

Nishimura, H., Nose, M., Hiai, H., Minato, N., and Honjo, T. (1999). Development of lupus-like autoimmune diseases by disruption of the PD-1 gene encoding an ITIM motif-carrying immunoreceptor. Immunity 11, 141–151.

Nishimura, H., Honjo, T., and Minato, N. (2000). Facilitation of beta selection and modification of positive selection in the thymus of PD-1-deficient mice. J. Exp. Med. 191, 891–898.

Nishimura, H., Okazaki, T., Tanaka, Y., Nakatani, K., Hara, M., Matsumori, A., Sasayama, S., Mizoguchi, A.,Hiai, H.,Minato, N., and Honjo, T. (2001).Autoimmune dilated cardiomyopathy in PD-1 receptor-deficient mice. Science 291, 319–322.

Noguchi, T., Ward, J.P., Gubin, M.M., Arthur, C.D., Lee, S.H., Hundal, J., Selby, M.J., Graziano, R.F., Mardis, E.R., Korman, A.J., and Schreiber, R.D. (2017). Temporally distinct PD-L1 expression by tumor and host cells contributes to immune escape. Cancer Immunol. Res. 5, 106–117.

Noman, M.Z., Desantis, G., Janji, B., Hasmim, M., Karray, S., Dessen, P., Bronte, V., and Chouaib, S. (2014). PD-L1 is a novel direct target of HIF-1a, and its blockade under hypoxia enhanced MDSC-mediated T cell activation. J. Exp. Med. 211, 781–790.

Ota, K., Azuma, K., Kawahara, A., Hattori, S., Iwama, E., Tanizaki, J., Harada, T., Matsumoto, K., Takayama, K., Takamori, S., et al. (2015). Induction of PD-L1 expression by the EML4-ALK oncoprotein and downstream signaling pathways in non-small cell lung cancer. Clin. Cancer Res. 21, 4014–4021.

Ou, J.N., Wiedeman, A.E., and Stevens, A.M. (2012). TNF-a and TGF-b counter-regulate PD-L1 expression on monocytes in systemic lupus erythematosus. Sci. Rep. 2, 295.

Overman, M.J., McDermott, R., Leach, J.L., Lonardi, S., Lenz, H.J., Morse, M.A., Desai, J., Hill, A., Axelson, M., Moss, R.A., et al. (2017). Nivolumab in patients with metastatic DNA mismatch repair-deficient or microsatellite instability-high colorectal cancer (CheckMate 142): an open-label, multicentre, phase 2 study. Lancet Oncol. 18, 1182–1191.

Park, J.J., Omiya, R., Matsumura, Y., Sakoda, Y., Kuramasu, A., Augustine, M.M., Yao, S., Tsushima, F., Narazaki, H., Anand, S., et al. (2010). B7-H1/ CD80 interaction is required for the induction and maintenance of peripheral T-cell tolerance. Blood 116, 1291–1298.

Park, B.V., Freeman, Z.T., Ghasemzadeh, A., Chattergoon, M.A., Rutebemberwa, A., Steigner, J., Winter, M.E., Huynh, T.V., Sebald, S.M., Lee, S.J., et al. (2016). TGFb1-mediated SMAD3 enhances PD-1 expression on antigen-specific T cells in cancer. Cancer Discov. 6, 1366–1381.

Parsa, A.T., Waldron, J.S., Panner, A., Crane, C.A., Parney, I.F., Barry, J.J., Cachola, K.E., Murray, J.C., Tihan, T., Jensen, M.C., et al. (2007). Loss of tumor suppressor PTEN function increases B7-H1 expression and immunoresistance in glioma. Nat. Med. 13, 84–88.

Patel, S.J., Sanjana, N.E., Kishton, R.J., Eidizadeh, A., Vodnala, S.K., Cam, M., Gartner, J.J., Jia, L., Steinberg, S.M., Yamamoto, T.N., et al. (2017). Identification of essential genes for cancer immunotherapy. Nature 548, 537–542.

Patel, M.R., Ellerton, J., Infante, J.R., Agrawal, M., Gordon, M., Aljumaily, R., Britten, C.D., Dirix, L., Lee, K.W., Taylor, M., et al. (2018). Avelumab in metastatic urothelial carcinoma after platinum failure (JAVELIN Solid Tumor): pooled results from two expansion cohorts of an open-label, phase 1 trial. Lancet Oncol. 19, 51–64.

Pitt, J.M., Vetizou, M., Daillere, R., Roberti, M.P., Yamazaki, T., Routy, B., Lepage, P., Boneca, I.G., Chamaillard, M., Kroemer, G., and Zitvogel, L. (2016). Resistance mechanisms to immune-checkpoint blockade in cancer: tumor intrinsic and -extrinsic factors. Immunity 44, 1255–1269.

Platanias, L.C. (2005). Mechanisms of type-I- and type-II-interferon-mediated signalling. Nat. Rev. Immunol. 5, 375–386.

Powles,T., O'Donnell, P.H.,Massard,C., Arkenau, H.T.,Friedlander, T.W., Hoimes, C.J., Lee, J.L., Ong, M., Sridhar, S.S., Vogelzang, N.J., et al. (2017). Efficacy and safety of durvalumab in locally advanced or metastatic urothelial carcinoma: updated results from a phase 1/2 open-label study. JAMA Oncol. 3, e172411.

Pulko, V., Liu, X., Krco, C.J., Harris, K.J., Frigola, X., Kwon, E.D., and Dong, H. (2009). TLR3-stimulated dendritic cells up-regulate B7-H1 expression and influence the magnitude of CD8 T cell responses to tumor vaccination. J. Immunol. 183, 3634–3641.

Qian, Y., Deng, J., Geng, L., Xie, H., Jiang, G., Zhou, L., Wang, Y., Yin, S., Feng, X., Liu, J., et al. (2008). TLR4 signaling induces B7-H1 expression through MAPK pathways in bladder cancer cells. Cancer Invest. 26, 816–821.

Quandt, D., Jasinski-Bergner, S.,M€uller, U., Schulze, B., and Seliger, B. (2014). Synergistic effects of IL-4 and TNFa on the induction of B7-H1 in renal cell carcinoma cells inhibiting allogeneic T cell proliferation. J. Transl. Med. 12, 151.

Reck, M., Rodriguez-Abreu, D., Robinson, A.G., Hui, R., Csoszi, T., Fulop, A., Gottfried, M., Peled, N., Tafreshi, A., Cuffe, S., et al.; KEYNOTE-024 Investigators (2016). Pembrolizumab versus chemotherapy for PD-L1-positive nonsmall-cell lung cancer. N. Engl. J. Med. 375, 1823–1833.

Ribas, A., Puzanov, I., Dummer, R., Schadendorf, D., Hamid, O., Robert, C., Hodi, F.S., Schachter, J., Pavlick, A.C., Lewis, K.D., et al. (2015). Pembrolizumab versus investigator-choice chemotherapy for ipilimumab-refractory melanoma (KEYNOTE-002): a randomised, controlled, phase 2 trial. Lancet Oncol. 16, 908–918.

Rizvi, N.A., Hellmann, M.D., Snyder, A., Kvistborg, P., Makarov, V., Havel, J.J., Lee, W., Yuan, J., Wong, P., Ho, T.S., et al. (2015). Cancer immunology. Mutational landscape determines sensitivity to PD-1 blockade in non-small cell lung cancer. Science 348, 124–128.

Robert, C., Long, G.V., Brady, B., Dutriaux, C., Maio, M., Mortier, L., Hassel, J.C., Rutkowski, P., McNeil, C., Kalinka-Warzocha, E., et al. (2015a). Nivolumab in previously untreated melanoma without BRAF mutation. N. Engl. J. Med. 372, 320–330.

Robert, C., Schachter, J., Long, G.V., Arance, A., Grob, J.J., Mortier, L., Daud, A., Carlino, M.S., McNeil, C., Lotem, M., et al.; KEYNOTE-006 investigators (2015b). Pembrolizumab versus ipilimumab in advanced melanoma. N. Engl. J. Med. 372, 2521–2532.

Roberts, P.J., and Der, C.J. (2007). Targeting the Raf-MEK-ERK mitogen-activated protein kinase cascade for the treatment of cancer. Oncogene 26, 3291–3310.

Roemer, M.G., Advani, R.H., Ligon, A.H., Natkunam, Y., Redd, R.A., Homer, H., Connelly, C.F., Sun, H.H., Daadi, S.E., Freeman, G.J., et al. (2016). PD-L1 and PD-L2 genetic alterations define classical Hodgkin lymphoma and predict outcome. J. Clin. Oncol. 34, 2690–2697.

Rosenberg, J.E., Hoffman-Censits, J., Powles, T., van der Heijden, M.S., Balar, A.V., Necchi, A., Dawson, N., O'Donnell, P.H., Balmanoukian, A., Loriot, Y., et al. (2016). Atezolizumab in patients with locally advanced and metastatic urothelial carcinoma who have progressed following treatment with platinum-based chemotherapy: a single-arm, multicentre, phase 2 trial. Lancet 387, 1909–1920.

Sade-Feldman, M., Jiao, Y.J., Chen, J.H., Rooney, M.S., Barzily-Rokni, M., Eliane, J.P., Bjorgaard, S.L., Hammond, M.R., Vitzthum, H., Blackmon, S.M., et al. (2017). Resistance to checkpoint blockade therapy through inactivation of antigen presentation. Nat. Commun. 8, 1136.

Schoop, R., Wahl, P., Le Hir, M., Heemann, U., Wang, M., and Wuthrich, R.P. (2004). Suppressed T-cell activation by IFN-gamma-induced expression of PD-L1 on renal tubular epithelial cells. Nephrol. Dial. Transplant. 19, 2713–2720.

Schreiner, B., Mitsdoerffer, M., Kieseier, B.C., Chen, L., Hartung, H.P., Weller, M., and Wiendl, H. (2004). Interferon-beta enhances monocyte and dendritic cell expression of B7-H1 (PD-L1), a strong inhibitor of autologous T-cell activation: relevance for the immune modulatory effect in multiple sclerosis. J. Neuroimmunol. 155, 172–182.

Schumacher, T.N., and Schreiber, R.D. (2015). Neoantigens in cancer immunotherapy. Science 348, 69–74.

Seiwert, T.Y., Burtness, B., Mehra, R., Weiss, J., Berger, R., Eder, J.P., Heath, K., McClanahan, T., Lunceford, J., Gause, C., et al. (2016). Safety and clinical activity of pembrolizumab for treatment of recurrent or metastatic squamous cell carcinoma of the head and neck (KEYNOTE-012): an open-label, multicentre, phase 1b trial. Lancet Oncol. 17, 956–965.

Seliger, B. (2014). The link between MHC class I abnormalities of tumors, oncogenes, tumor suppressor genes, and transcription factors. J. Immunotoxicol. 11, 308–310.

Sharma, P., Hu-Lieskovan, S., Wargo, J.A., and Ribas, A. (2017a). Primary, adaptive, and acquired resistance to cancer immunotherapy. Cell 168, 707–723.

Sharma, P., Retz, M., Siefker-Radtke, A., Baron, A., Necchi, A., Bedke, J., Plimack, E.R., Vaena, D., Grimm, M.O., Bracarda, S., et al. (2017b). Nivolumab in metastatic urothelial carcinoma after platinum therapy (CheckMate 275): a multicentre, single-arm, phase 2 trial. Lancet Oncol. 18, 312–322.

Sharpe, A.H., and Pauken, K.E. (2018). The diverse functions of the PD1 inhibitory pathway. Nat. Rev. Immunol. 18, 153–167.

Shaulian, E., and Karin, M. (2002). AP-1 as a regulator of cell life and death. Nat. Cell Biol. 4, E131–E136.

Sheppard, K.A., Fitz, L.J., Lee, J.M., Benander, C., George, J.A., Wooters, J., Qiu, Y., Jussif, J.M., Carter, L.L., Wood, C.R., and Chaudhary, D. (2004). PD-1 inhibits T-cell receptor induced phosphorylation of the ZAP70/CD3zeta signalosome and downstream signaling to PKCtheta. FEBS Lett. 574, 37–41.

Shin, D.S., Zaretsky, J.M., Escuin-Ordinas, H., Garcia-Diaz, A., Hu-Lieskovan, S., Kalbasi, A., Grasso, C.S., Hugo, W., Sandoval, S., Torrejon, D.Y., et al. (2017). Primary resistance to PD-1 blockade mediated by JAK1/2 mutations. Cancer Discov. 7, 188–201.

Snyder, A., Nathanson, T., Funt, S.A., Ahuja, A., Buros Novik, J., Hellmann, M.D., Chang, E., Aksoy, B.A., Al-Ahmadie, H., Yusko, E., et al. (2017). Contribution of systemic and somatic factors to clinical response and resistance to PD-L1 blockade in urothelial cancer: An exploratory multi-omic analysis. PLoS Med. 14, e1002309.

Song, M., Chen, D., Lu, B., Wang, C., Zhang, J., Huang, L., Wang, X., Timmons, C.L., Hu, J., Liu, B., et al. (2013). PTEN loss increases PD-L1 protein expression and affects the correlation between PD-L1 expression and clinical parameters in colorectal cancer. PLoS ONE 8, e65821.

Song, S., Yuan, P.,Wu,H., Chen, J., Fu, J., Li, P., Lu, J., andWei,W. (2014). Dendritic cells with an increased PD-L1 by TGF-b induce T cell anergy for the cytotoxicity of hepatocellular carcinoma cells. Int. Immunopharmacol. 20, 117–123.

Starke, A., Wuthrich, R.P., and Waeckerle-Men, Y. (2007). TGF-beta treatment modulates PD-L1 and CD40 expression in proximal renal tubular epithelial cells and enhances CD8 cytotoxic T-cell responses. Nephron, Exp. Nephrol. 107, e22–e29.

Straub, M., Drecoll, E., Pfarr, N., Weichert, W., Langer, R., Hapfelmeier, A., Gotz, C., Wolff, K.D., Kolk, A., and Specht, K. (2016). CD274/PD-L1 gene amplification and PD-L1 protein expression are common events in squamous cell carcinoma of the oral cavity. Oncotarget 7, 12024–12034.

Straus, D.B., and Weiss, A. (1992). Genetic evidence for the involvement of the lck tyrosine kinase in signal transduction through the T cell antigen receptor. Cell 70, 585–593.

Sumimoto, H., Takano, A., Teramoto, K., and Daigo, Y. (2016). RAS-mitogen activated protein kinase signal is required for enhanced PD-L1 expression in human lung cancers. PLoS ONE 11, e0166626.

Sun, C., and Bernards, R. (2014). Feedback and redundancy in receptor tyrosine kinase signaling: relevance to cancer therapies. Trends Biochem. Sci. 39, 465–474.

Sun, Z., Fourcade, J., Pagliano, O., Chauvin, J.M., Sander, C., Kirkwood, J.M., and Zarour, H.M. (2015). IL10 and PD-1 cooperate to limit the activity of tumorspecific CD8+ T cells. Cancer Res. 75, 1635–1644.

Thommen, D.S., and Schumacher, T. (2018). T cell dysfunction in cancer. Cancer Cell 33. Published online April 9, 2018. https://doi.org/10.1016/j.ccell. 2018.03.012.

Tumeh, P.C., Harview, C.L., Yearley, J.H., Shintaku, I.P., Taylor, E.J., Robert, L., Chmielowski, B., Spasic, M., Henry, G., Ciobanu, V., et al. (2014). PD-1 blockade induces responses by inhibiting adaptive immuneresistance. Nature 515, 568–571.

Twa, D.D., Chan, F.C., Ben-Neriah, S., Woolcock, B.W., Mottok, A., Tan, K.L., Slack, G.W., Gunawardana, J., Lim, R.S., McPherson, A.W., et al. (2014). Genomic rearrangements involving programmed death ligands are recurrent in primary mediastinal large B-cell lymphoma. Blood 123, 2062–2065.

Ugi, S., Maegawa, H., Olefsky, J.M., Shigeta, Y., and Kashiwagi, A. (1994). Src homology 2 domains of protein tyrosine phosphatase are associated in vitro with both the insulin receptor and insulin receptor substrate-1 via different phosphotyrosine motifs. FEBS Lett. 340, 216–220.

Wang, J., Yoshida, T., Nakaki, F., Hiai, H., Okazaki, T., and Honjo, T. (2005). Establishment of NOD-Pdcd1-/- mice as an efficient animal model of type I diabetes. Proc. Natl. Acad. Sci. USA 102, 11823–11828.

Wang,W., Li, F., Mao, Y., Zhou, H., Sun, J., Li, R., Liu, C., Chen, W., Hua, D., and Zhang, X. (2013). A miR-570 binding site polymorphism in the B7-H1 gene is associated with the risk of gastric adenocarcinoma. Hum. Genet. 132, 641–648.

Wang, X., Li, J., Dong, K., Lin, F., Long, M., Ouyang, Y., Wei, J., Chen, X., Weng, Y., He, T., and Zhang, H. (2015). Tumor suppressor miR-34a targets PD-L1 and functions as a potential immunotherapeutic target in acute myeloid leukemia. Cell. Signal. 27, 443–452.

Wang, J., Jia, Y., Zhao, S., Zhang, X., Wang, X., Han, X., Wang, Y., Ma, M., Shi, J., and Liu, L. (2017a). BIN1 reverses PD-L1-mediated immune escape by inactivating the c-MYC and EGFR/MAPK signaling pathways in non-small cell lung cancer. Oncogene 36, 6235–6243.

Wang, X., Yang, L., Huang, F., Zhang, Q., Liu, S., Ma, L., and You, Z. (2017b). Inflammatory cytokines IL-17 and TNF-a up-regulate PD-L1 expression in human prostate and colon cancer cells. Immunol. Lett. 184, 7–14.

Weber, J.S., D'Angelo, S.P., Minor, D., Hodi, F.S., Gutzmer, R., Neyns, B., Hoeller, C., Khushalani, N.I., Miller, W.H., Jr., Lao, C.D., et al. (2015). Nivolumab versus chemotherapy in patients with advanced melanoma who progressed after anti-CTLA-4 treatment (CheckMate 037): a randomised, controlled, open-label, phase 3 trial. Lancet Oncol. 16, 375–384.

Weber, J., Mandala, M., Del Vecchio, M., Gogas, H.J., Arance, A.M., Cowey, C.L., Dalle, S., Schenker, M., Chiarion-Sileni, V., Marquez-Rodas, I., et al.; CheckMate 238 Collaborators (2017). Adjuvant nivolumab versus ipilimumab in resected stage III or IV melanoma. N. Engl. J. Med. 377, 1824–1835.

Wherry, E.J., and Kurachi, M. (2015). Molecular and cellular insights into T cell exhaustion. Nat. Rev. Immunol. 15, 486–499.

Wintterle, S., Schreiner, B., Mitsdoerffer, M., Schneider, D., Chen, L., Meyermann, R., Weller, M., and Wiendl, H. (2003). Expression of the B7-related molecule B7-H1 by glioma cells: a potential mechanism of immune paralysis. Cancer Res. 63, 7462–7467.

Xie, G., Li, W., Li, R.,Wu, K., Zhao, E., Zhang,Y., Zhang, P., Shi, L.,Wang,D., Yin, Y., et al. (2017). Helicobacter pylori promote B7-H1 expression by suppressing miR-152 and miR-200b in gastric cancer cells. PLoS ONE 12, e0168822.

Xiong, H.Y., Ma, T.T., Wu, B.T., Lin, Y., and Tu, Z.G. (2014). IL-12 regulates B7-H1 expression in ovarian cancer-associated macrophages by effects on NF-kB signalling. Asian Pac. J. Cancer Prev. 15, 5767–5772.

Xu, C., Fillmore, C.M., Koyama, S., Wu, H., Zhao, Y., Chen, Z., Herter-Sprie, G.S., Akbay, E.A., Tchaicha, J.H., Altabef, A., et al. (2014). Loss of Lkb1 and Pten leads to lung squamous cell carcinoma with elevated PD-L1 expression. Cancer Cell 25, 590–604.

Xue, J., Chen, C., Qi, M., Huang, Y., Wang, L., Gao, Y., Dong, H., and Ling, K. (2017). Type Ig phosphatidylinositol phosphate kinase regulates PD-L1 expression by activating NF-kB. Oncotarget 8, 42414–42427.

Yamamoto, H., Yamashita, K., and Perucho, M. (2001). Somatic mutation of the beta2-microglobulin gene associates with unfavorable prognosis in gastrointestinal cancer of the microsatellite mutator phenotype. Gastroenterology 120, 1565–1567.

Yamamoto, R., Nishikori, M., Tashima, M., Sakai, T., Ichinohe, T., Takaori-Kondo, A., Ohmori, K., and Uchiyama, T. (2009). B7-H1 expression is regulated by MEK/ERK signaling pathway in anaplastic large cell lymphoma and Hodgkin lymphoma. Cancer Sci. 100, 2093–2100.

Yang, L., Huang, F., Mei, J., Wang, X., Zhang, Q., Wang, H., Xi, M., and You, Z. (2017). Posttranscriptional control of PD-L1 expression by 17b-estradiol via PI3K/Akt signaling pathway in ERa-positive cancer cell lines. Int. J. Gynecol. Cancer 27, 196–205.

Yao, S., Wang, S., Zhu, Y., Luo, L., Zhu, G., Flies, S., Xu, H., Ruff, W., Broadwater, M., Choi, I.H., et al. (2009). PD-1 on dendritic cells impedes innate immunity against bacterial infection. Blood 113, 5811–5818.

Yearley, J.H., Gibson, C., Yu, N., Moon, C., Murphy, E., Juco, J., Lunceford, J., Cheng, J., Chow, L.Q.M., Seiwert, T.Y., et al. (2017). PD-L2 expression in human tumors: relevance to anti-PD-1 therapy in cancer. Clin.CancerRes. 23, 3158–3167.

Yee, D., Shah, K.M., Coles, M.C., Sharp, T.V., and Lagos, D. (2017). MicroRNA- 155 induction via TNF-a and IFN-g suppresses expression of programmed death ligand-1 (PD-L1) inhumanprimary cells. J. Biol.Chem.292, 20683–20693.

Younes, A., Santoro, A., Shipp, M., Zinzani, P.L., Timmerman, J.M., Ansell, S., Armand, P., Fanale, M., Ratanatharathorn, V., Kuruvilla, J., et al. (2016). Nivolumab for classical Hodgkin's lymphoma after failure of both autologous stem cell transplantation and brentuximab vedotin: a multicentre, multicohort, single-arm phase 2 trial. Lancet Oncol. 17, 1283–1294.

Zak, K.M., Kitel, R., Przetocka, S., Golik, P., Guzik, K., Musielak, B., Domling, A., Dubin, G., and Holak, T.A. (2015). Structure of the complex of human programmed death 1, PD-1, and its ligand PD-L1. Structure 23, 2341–2348.

Zaretsky, J.M., Garcia-Diaz, A., Shin, D.S., Escuin-Ordinas, H., Hugo, W., Hu-Lieskovan, S., Torrejon, D.Y., Abril-Rodriguez, G., Sandoval, S., Barthly, L., et al. (2016). Mutations associated with acquired resistance to PD-1 blockade in melanoma. N. Engl. J. Med. 375, 819–829.

Zhang, X., Wrzeszczynska, M.H., Horvath, C.M., and Darnell, J.E., Jr. (1999). Interacting regions in Stat3 and c-Jun that participate in cooperative transcriptional activation. Mol. Cell. Biol. 19, 7138–7146.

Zhang, X., Schwartz, J.C., Guo, X., Bhatia, S., Cao, E., Lorenz, M., Cammer, M., Chen, L., Zhang, Z.Y., Edidin, M.A., et al. (2004).Structural and functional analysis of the costimulatory receptor programmed death-1. Immunity 20, 337–347.

Zhang, N., Zeng, Y., Du, W., Zhu, J., Shen, D., Liu, Z., and Huang, J.A. (2016). The EGFR pathway is involved in the regulation of PD-L1 expression via the IL-6/JAK/STAT3 signaling pathway in EGFR-mutated non-small cell lung cancer. Int. J. Oncol. 49, 1360–1368.

Zhang, J., Bu, X., Wang, H., Zhu, Y., Geng, Y., Nihira, N.T., Tan, Y., Ci, Y., Wu, F., Dai, X., et al. (2017a). Cyclin D-CDK4 kinase destabilizes PD-L1 via Cul3(SPOP) to control cancer immune surveillance. Nature 553, 91–95.

Zhang, X., Zeng, Y., Qu, Q., Zhu, J., Liu, Z., Ning, W., Zeng, H., Zhang, N., Du, W., Chen, C., and Huang, J.A. (2017b). PD-L1 induced by IFN-g from tumor associated macrophages via the JAK/STAT3 and PI3K/AKT signaling pathways promoted progression of lung cancer. Int. J. Clin. Oncol. 22, 1026–1033.

Zhao, Q., Xiao, X., Wu, Y., Wei, Y., Zhu, L.Y., Zhou, J., and Kuang, D.M. (2011). Interleukin-17-educated monocytes suppress cytotoxic T-cell function through B7-H1 in hepatocellular carcinoma patients. Eur. J. Immunol. 41, 2314–2322.

Zhao, L., Yu, H., Yi, S., Peng, X., Su, P., Xiao, Z., Liu, R., Tang, A., Li, X., Liu, F., and Shen, S. (2016). The tumor suppressor miR-138-5p targets PD-L1 in colorectal cancer. Oncotarget 7, 45370–45384.

Zhu, J., Chen, L., Zou, L., Yang, P., Wu, R., Mao, Y., Zhou, H., Li, R., Wang, K., Wang, W., et al. (2014). MiR-20b, -21, and -130b inhibit PTEN expression resulting in B7-H1 over-expression in advanced colorectal cancer. Hum. Immunol. 75, 348–353.

Chapter 6

Identification of CMTM6 and CMTM4 as PD-L1 protein regulators

Riccardo Mezzadra[1*], Chong Sun[1*], Lucas T. Jae[2†*], Raquel Gomez-Eerland[1], Evert de Vries[3], Wei Wu[4,5], Meike E. W. Logtenberg[1], Maarten Slagter[1,6], Elisa A. Rozeman[1,7], Ingrid Hofland[8], Annegien Broeks[8], Hugo M. Horlings[9], Lodewyk F. A. Wessels[6], Christian U. Blank[1,7], Yanling Xiao[3], Albert J. R. Heck[4,5], Jannie Borst[3], Thijn R. Brummelkamp[2,10,11] & Ton N. M. Schumacher[1]

1 Division of Molecular Oncology & Immunology, The Netherlands Cancer Institute, Plesmanlaan 121, 1066 CX Amsterdam, The Netherlands. 2 Division of Biochemistry, The Netherlands Cancer Institute, Plesmanlaan 121, 1066 CX Amsterdam, The Netherlands. 3 Division of Tumor Biology & Immunology, The Netherlands Cancer Institute, Plesmanlaan 121, 1066 CX Amsterdam, The Netherlands. 4 Biomolecular Mass Spectrometry and Proteomics, Bijvoet Center for Biomolecular Research and Utrecht Institute for Pharmaceutical Sciences, Padualaan 8, 3584 CH Utrecht, The Netherlands. 5 Netherlands Proteomics Centre, Padualaan 8, 3584 CH Utrecht, The Netherlands. 6 Division of Molecular Carcinogenesis, The Netherlands Cancer Institute, Plesmanlaan 121, 1066 CX Amsterdam, The Netherlands. 7 Division of Medical Oncology, The Netherlands Cancer Institute, Plesmanlaan 121, 1066 CX Amsterdam, The Netherlands. 8 Core Facility Molecular Pathology & Biobanking, Division of Pathology, The Netherlands Cancer Institute, Plesmanlaan 121, 1066 CX Amsterdam, The Netherlands. 9 Division of Pathology, The Netherlands Cancer Institute, Plesmanlaan 121, 1066 CX Amsterdam, The Netherlands. 10 CeMM Research Center for Molecular Medicine of the Austrian Academy of Sciences, 1090 Vienna, Austria. 11 Cancergenomics.nl, Plesmanlaan 121, 1066 CX Amsterdam, The Netherlands. † Present address: Gene Center and Department of Biochemistry, Ludwig-Maximilians-Universität München, Feodor-Lynen-Straße 25, 81377 Munich, Germany.

* These authors contributed equally to this work.
Correspondence and requests for materials should be addressed to T.R.B. (t.brummelkamp@nki.nl) or T.N.M.S. (t.schumacher@nki.nl)

Nature. 2017 Sep 7;549(7670):106-110

The clinical benefit for patients with diverse types of metastatic cancers that has been observed upon blockade of the interaction between PD-1 and PD-L1 has highlighted the importance of this inhibitory axis in the suppression of tumour-specific T-cell responses[1,2,3,4,5,6,7,8,9]. Notwithstanding the key role of PD-L1 expression by cells within the tumour micro-environment, our understanding of the regulation of the PD-L1 protein is limited[10,11,12,13,14,15]. Here we identify, using a haploid genetic screen, CMTM6, a type-3 transmembrane protein of previously unknown function, as a regulator of the PD-L1 protein. Interference with CMTM6 expression results in impaired PD-L1 protein expression in all human tumour cell types tested and in primary human dendritic cells. Furthermore, through both a haploid genetic modifier screen in CMTM6-deficient cells and genetic complementation experiments, we demonstrate that this function is shared by its closest family member, CMTM4, but not by any of the other CMTM members tested. Notably, CMTM6 increases the PD-L1 protein pool without affecting *PD-L1* (also known as *CD274*) transcription levels. Rather, we demonstrate that CMTM6 is present at the cell surface, associates with the PD-L1 protein, reduces its ubiquitination and increases PD-L1 protein half-life. Consistent with its role in PD-L1 protein regulation, CMTM6 enhances the ability of PD-L1-expressing tumour cells to inhibit T cells. Collectively, our data reveal that PD-L1 relies on CMTM6/4 to efficiently carry out its inhibitory function, and suggest potential new avenues to block this pathway.

Antibodies that block the PD-1–PD-L1 axis are currently evaluated in approximately 800 clinical studies and have been approved for seven different tumour types. In addition, expression of PD-L1 on either tumour cells or on tumour-infiltrating immune cells identifies patients that are more likely to respond to these therapies[16,17]. In view of the limited understanding of the regulation of PD-L1 expression, we set out to identify PD-L1 protein regulators through genetic screening. Interferon-γ (IFNγ)-treated haploid HAP1 cells[18,19] express high levels of PD-L1 on the cell surface (Extended Data Fig. 1a). On the basis of this observation, we performed a fluorescence-activated cell sorting (FACS)-based haploid genetic screen for PD-L1 modulators in IFNγ-treated HAP1 cells (Fig. 1a, experimental design as in ref. 20). The entire IFNγ receptor (IFNγR)-signalling pathway[21] plus IRF1, a known regulator of PD-L1 upon IFNγ exposure[10], were identified as strong hits (Fig. 1a and Supplementary Table 1), demonstrating the validity of the screen setup. In addition, the PD-L1 gene itself (*CD274*) showed a strikingly different integration pattern in PD-L1^{high} and PD-L1^{low} cells. Specifically, whereas PD-L1^{low} cells showed the expected enrichment of integrations towards the 5′ end of the gene, a strong enrichment of integrations in intron 5 and 6 was observed in PD-L1^{high} cells (Extended Data Fig. 1b), fully consistent with the recently described negative regulatory role of the PD-L1 3′ untranslated region (UTR)[11] (Extended Data Fig. 1c).

In addition to the above hits, we identified CMTM6 (CKLF (chemokine-like factor)-like MARVEL transmembrane domain containing family member 6) as one of the most significant hits within PD-L1^{low} cells. CMTM6 was not observed in a similar screen for regulators of IRF1 protein levels[20], suggesting that its role was independent of the IFNγR pathway. CMTM6 is a ubiquitously expressed transmembrane protein that belongs to a family of eight MARVEL-domain-containing proteins[22] for which no clear function has been described. Transcriptome analysis of tumour samples in The Cancer Genome Atlas (TCGA) showed CMTM6 expression in all of the analysed samples distributed across 30 cancer types, and showed that RNA expression levels of *CMTM6* and *CD274* are weakly correlated in the majority of tumour types (Extended Data Fig. 2). Short hairpin RNA (shRNA)-mediated knockdown of *CMTM6* in HAP1 cells reduced IFNγ-induced PD-L1 expression approximately twofold compared to control (Fig. 1b, c). To assess whether CMTM6 also influences PD-L1 cell surface levels beyond the HAP1 system, we examined the effect of CMTM6 knockdown in a series of tumour lines. In A375 melanoma cells, which only show detectable PD-L1 expression after IFNγ exposure, CMTM6 knockdown prevented IFNγ-induced PD-L1 expression to a large extent (Fig. 2a-c, reduction up to 11-fold). CMTM6-deficient A375 clones generated with CRISPR–Cas9 likewise showed reduced cell surface and overall PD-L1 protein levels, whereas lentiviral reconstitution of CMTM6 reverted this phenotype

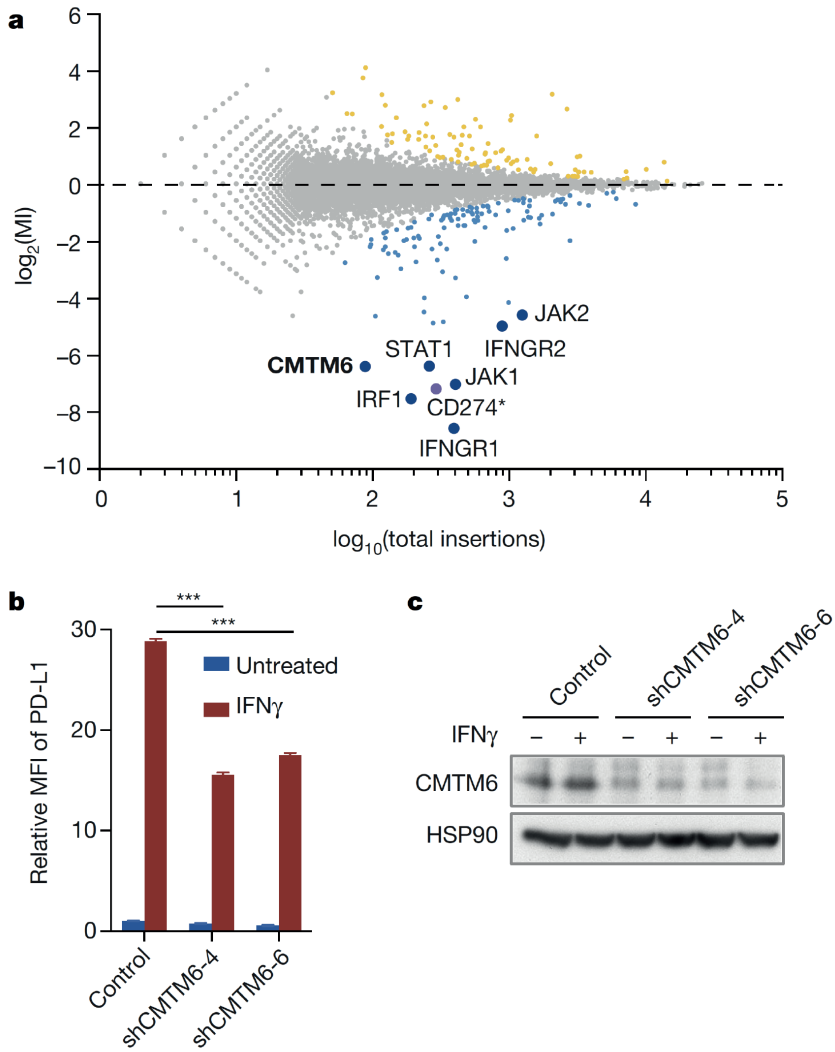

Figure 1: Identification of CMTM6 as a modulator of PD-L1 expression. a, Flow-cytometry-based screen for modulators of PD-L1 cell surface expression in HAP1 cells. Dots represent individual genes; x axis indicates the number of disruptive insertions per gene; y axis shows the frequency of independent insertions in the PD-L1^{high} channel over the frequency of insertions in the PD-L1^{low} channel for each gene. Light-blue and orange dots indicate genes with significant enrichment of insertions (FDR-corrected $P < 10–6$)[27] within the PD-L1^{low} and PD-L1^{high} populations, respectively. Dark-blue circles indicate known components of the IFNγR-signalling pathway plus IRF1 and CMTM6 (in bold). The purple dot represents PD-L1 (CD274*) when excluding integrations downstream of exon 5 (Refseq identifier NM_014143.3). See https://phenosaurus.nki.nl for interactive graphs. b, Relative PD-L1 cell-surface expression in control or independent CMTM6-knockdown HAP1 cells with or without IFNγ exposure. c, Validation of CMTM6 knockdown by western blot. Data are representative of one (a) or at least three (b, c) independent experiments, and were analysed by unpaired t-test (b). Data represent mean ± s.d. of triplicates (b). ***P < 0.001. MFI, median fluorescence intensity; MI, mutation index.

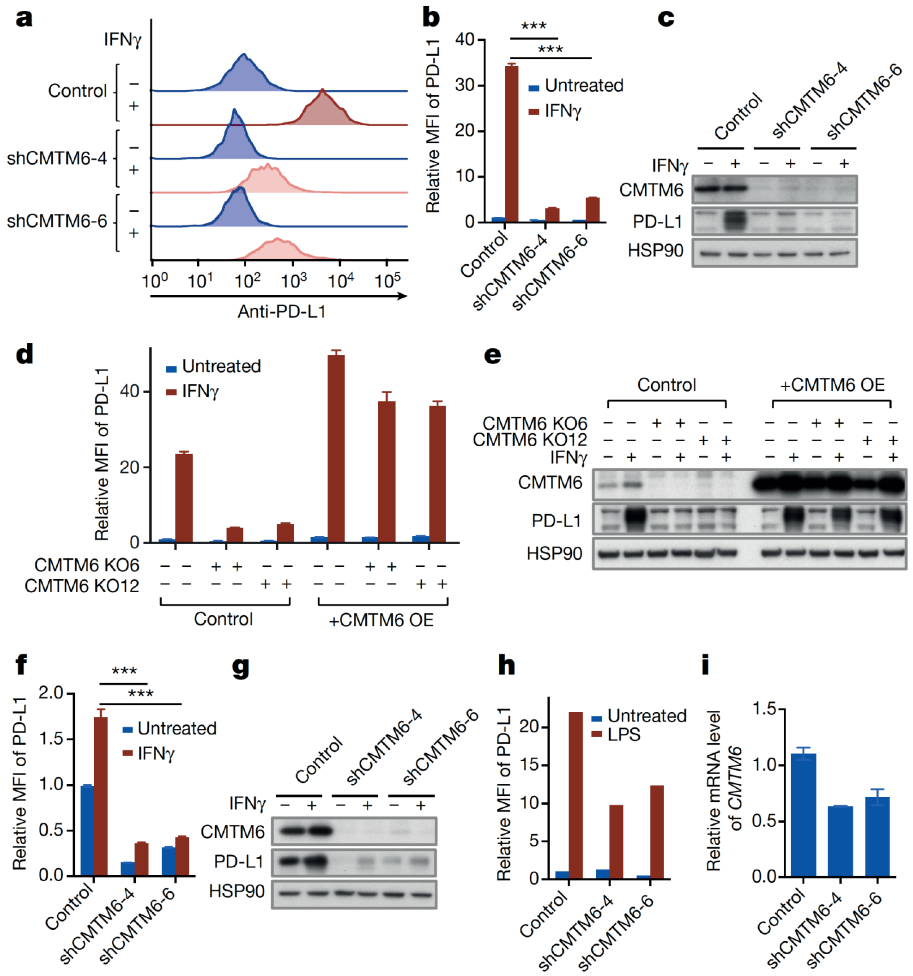

Figure 2: CMTM6 regulates PD-L1 expression in different tumour types and primary dendritic cells. a, b, Relative PD-L1 cell surface expression in control or independent CMTM6-knockdown (shCMTM6-4, shCMTM6-6) A375 melanoma cells with or without IFNγ exposure. c, Western blot analysis of CMTM6 and PD-L1 expression in control or independent CMTM6-knockdown A375 melanoma cells with or without IFNγ exposure. d, e, Flow cytometry (d) and western blot (e) analysis of PD-L1 expression in parental, CMTM6-deficient, CMTM6-overexpressing and CMTM6-reconstituted A375 melanoma cells. f, Relative PD-L1 cell surface expression in control or independent CMTM6-knockdown (shCMTM6-4, shCMTM6-6) 8505C thyroid cancer cells with or without IFNγ exposure. g, Western blot analysis of CMTM6 and PD-L1 expression in control or independent CMTM6-knockdown 8505C thyroid cancer cells with or without IFNγ exposure. h, Flow cytometry analysis of PD-L1 expression in control or independent CMTM6-knockdown primary bone marrow progenitor-derived dendritic cells with or without LPS exposure. i, Knockdown efficiency of CMTM6 in primary bone marrow progenitor-derived dendritic cells. Data are representative of at least three (a–g) or two (h, i) independent experiments and were analysed by unpaired t-test (b, f). Data represent mean ± s.d. of triplicates (b, d, f, i). ***$P < 0.001$. MFI, median fluorescence intensity.

(Fig. 2d, e). In the 8505C thyroid cancer cell line, which has a high basal level of PD-L1 expression, both steady state and IFNγ-induced PD-L1 cell surface and total protein levels were substantially reduced by CMTM6 knockdown (Fig. 2f, g, up to seven- and fivefold, respectively). In total, we assessed the effect of CMTM6 knockdown in 12 human tumour lines, representing melanoma (Fig. 2a–c and Extended Data Fig. 3a–d), thyroid cancer (Fig. 2f, g), colorectal cancer (Extended Data Fig. 3e, f, i, k), lung cancer (Extended Data Fig. 3l, n–p) and chronic myeloid leukaemia (Fig. 1b, c). In addition, we also tested the effect of CMTM6 knockdown in three short-term cultures of melanoma xenografts (Extended Data Fig. 3q). In these different cell systems, we consistently observed decreased expression of PD-L1 (between 2- and 11-fold) upon knockdown of CMTM6. Reduced PD-L1 cell surface levels were likewise observed when cells were stained with recombinant PD-1–Fc protein (Extended Data Fig. 3h, j, m). PD-L1 can be expressed by both cancer cells and infiltrating immune cells, and PD-L1 expression on immune cells may contribute to T-cell inhibition[16,17]. To assess whether CMTM6 also influences PD-L1 levels in primary human dendritic cells, we generated dendritic cells from human bone marrow progenitors[23]. Comparison of lipopolysaccharide (LPS)-induced PD-L1 expression in control and CMTM6-knockdown dendritic cells showed that partial knockdown of CMTM6 resulted in a partial reduction of PD-L1 cell-surface levels (Fig. 2h, i).

The above data establish CMTM6 as a modulator of PD-L1 protein levels. Whereas in some tumour lines, the effect of CMTM6 knockdown is strong (for example, A375, 8505C), in others it is moderate (for example, HAP1), suggesting the possible existence of (an) additional regulator(s). We therefore generated CMTM6-knockout HAP1 cells and performed a modifier screen, with the aim of identifying genetic factors that selectively regulate PD-L1 in the absence of CMTM6. Consistent with the primary screen, genes mediating IFNγR signalling were prominent hits. As expected, in this setting, integrations within the *CMTM6* locus were no longer enriched within the PD-L1^{low} cell population (Fig. 3a and Supplementary Table 2). In CMTM6-deficient HAP1 cells, CMTM4, another member of the CMTM family with 55% homology to CMTM6, was identified as a positive regulator of PD-L1 expression (Fig. 3a). Notably, although CMTM4 is a highly significant hit in CMTM6-deficient HAP1 cells (36.7-fold, false discovery rate (FDR)-corrected $P \leq 10^{-314}$), it is not in CMTM6-proficient HAP1 cells (0.9-fold, FDR-corrected $P = 0.94789$), suggesting that in this system, CMTM4 functions as a back-up regulator of PD-L1 expression.

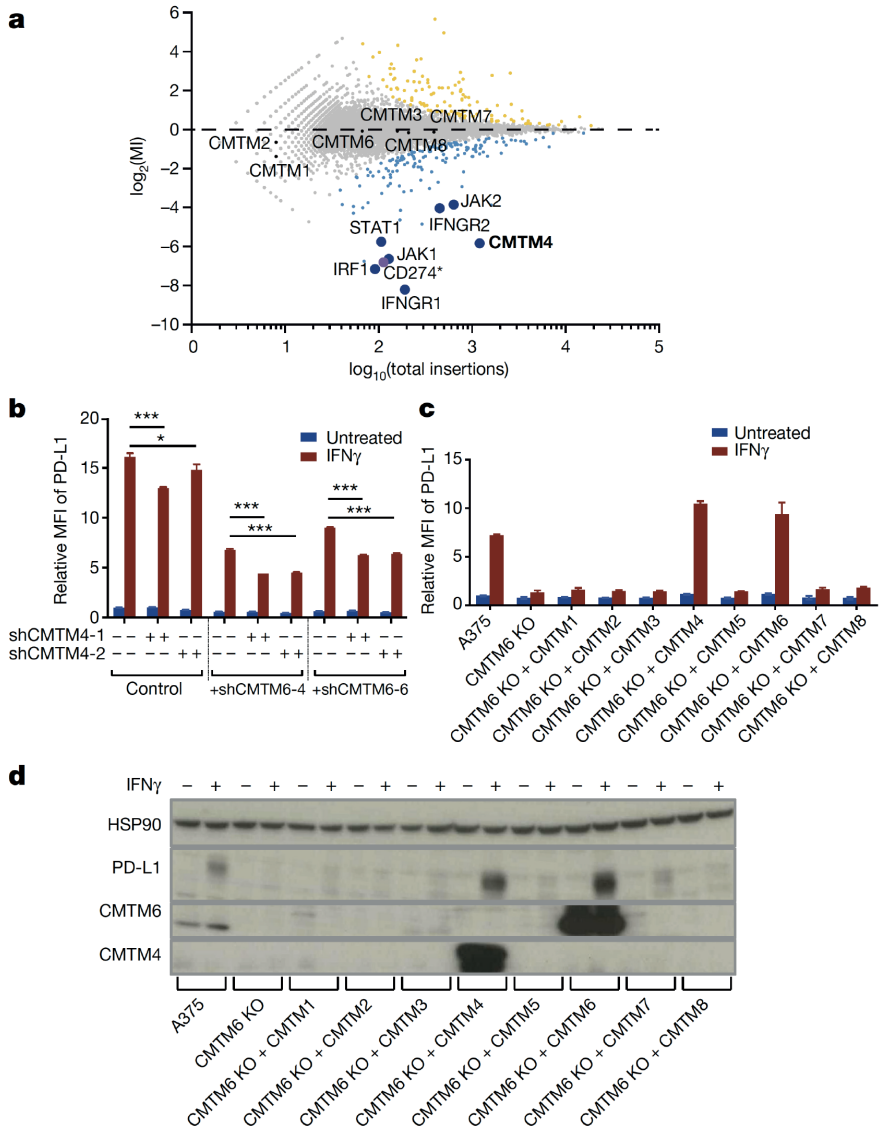

Figure 3: Identification of CMTM4 as a second PD-L1 regulator. a, Haploid genetic screen for modulators of PD-L1 cell surface expression in CMTM6-deficient HAP1 cells. b, PD-L1 surface expression in parental, CMTM6-knockdown, CMTM4-knockdown or double-knockdown H2030 cells with or without IFNγ exposure. c, d, Flow cytometry (c) and western blot (d) analysis of PD-L1 expression in parental A375, CMTM6-knockout A375 cells and CMTM6-knockout A375 cells reconstituted with the indicated CMTM family member with or without IFNγ exposure. Data are representative of one (a), two (b) or three (c, d) independent experiments and were analysed by unpaired t-test (b). Data represent mean ± s.d. of triplicates (b, c). $^{*}P < 0.05$; $^{***}P < 0.001$. KO, knockout; MFI, median fluorescence intensity; MI, mutation index.

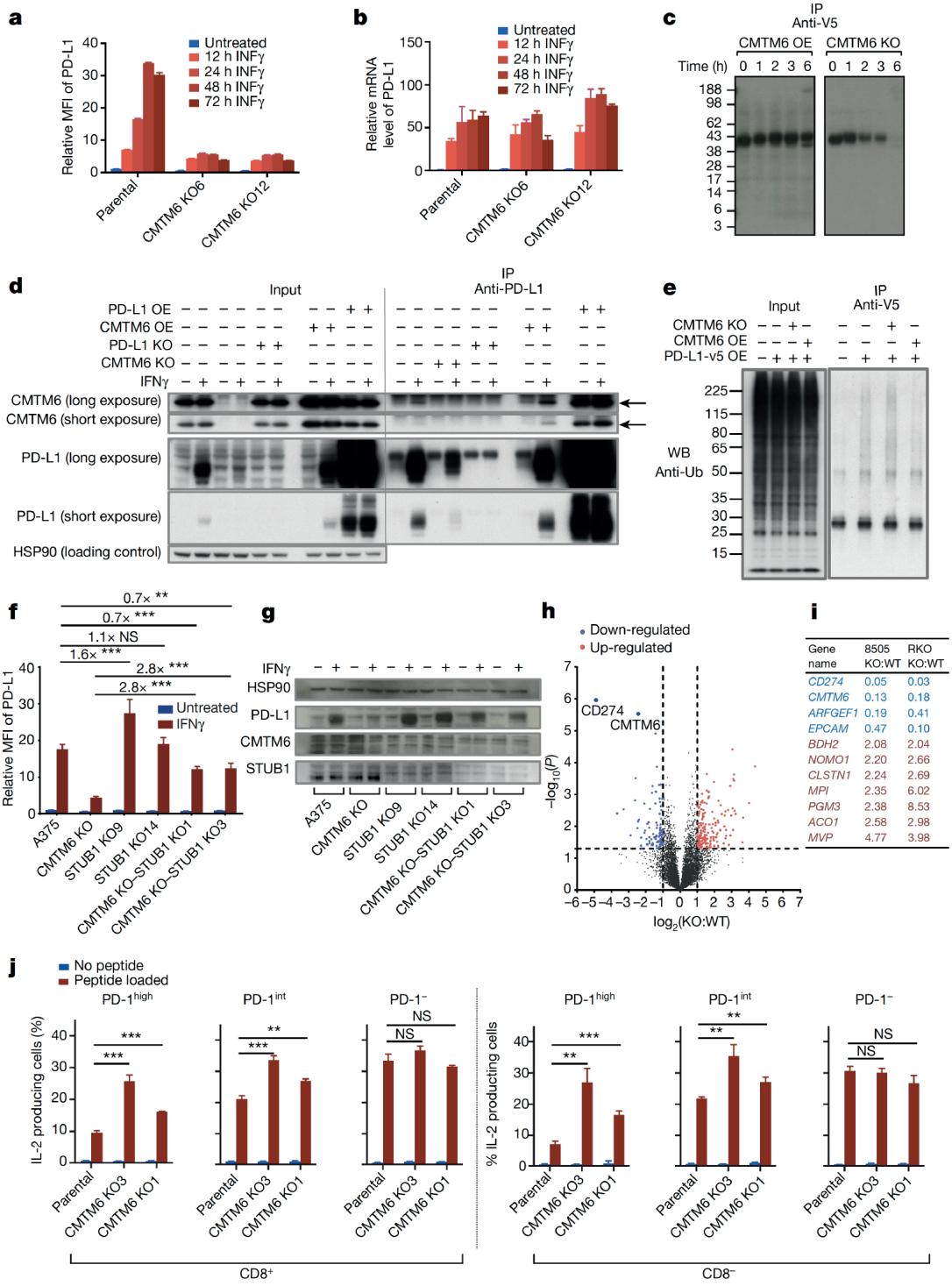
a
Relative MFI of PD-L1
Untreated
12 h INFγ
24 h INFγ
48 h INFγ
72 h INFγ
Parental
CMTM6 KO6
CMTM6 KO12
b
Relative mRNA level of PD-L1
c
IP Anti-V5
CMTM6 OE
CMTM6 KO
Time (h) 0 1 2 3 6
d
Input
IP Anti-PD-L1
PD-L1 OE
CMTM6 OE
PD-L1 KO
CMTM6 KO
IFNγ
CMTM6 (long exposure)
CMTM6 (short exposure)
PD-L1 (long exposure)
PD-L1 (short exposure)
HSP90 (loading control)
e
Input
IP Anti-V5
CMTM6 KO
CMTM6 OE
PD-L1-v5 OE
WB Anti-Ub
f
0.7× **
0.7× ***
1.1× NS
1.6× ***
2.8× ***
2.8× ***
Relative MFI of PD-L1
Untreated
IFNγ
A375
CMTM6 KO
STUB1 KO9
STUB1 KO14
STUB1 KO-STUB1 KO1
CMTM6 KO-STUB1 KO3
g
IFNγ
HSP90
PD-L1
CMTM6
STUB1
h
Down-regulated
Up-regulated
CD274
CMTM6
−log10(P)
log2(KO:WT)
i
Gene name | 8505 KO:WT | RKO KO:WT
CD274 | 0.05 | 0.03
CMTM6 | 0.13 | 0.18
ARFGEF1 | 0.19 | 0.41
EPCAM | 0.47 | 0.10
BDH2 | 2.08 | 2.04
NOMO1 | 2.20 | 2.66
CLSTN1 | 2.24 | 2.69
MPI | 2.35 | 6.02
PGM3 | 2.38 | 8.53
ACO1 | 2.58 | 2.98
MVP | 4.77 | 3.98
j
No peptide
Peptide loaded
PD-1high
PD-1int
PD-1−
IL-2 producing cells (%)
% IL-2 producing cells
Parental
CMTM6 KO3
CMTM6 KO1
CD8+
CD8−

< Figure 4 : CMTM6 forms a molecular partner of PD-L1 and regulates PD-L1 protein stability. a, b, Time course of PD-L1 surface protein (a) or mRNA (b) levels in A375 cells upon IFNγ exposure. c, SDS–PAGE analysis of anti-V5 immunoprecipitates from V5–PD-L1 overexpressing CMTM6-knockout or CMTM6-overexpressing A375 cells at different time points after 35S methionine/cysteine labelling. d, Immunoblots of lysates or anti-PD-L1 immunoprecipitates from the indicated A375 melanoma cells with or without IFNγ exposure. Arrows indicate CMTM6. e, Immunoblots of lysates or anti-V5 immunoprecipitates from V5-PD-L1 overexpressing parental, CMTM6-knockout or CMTM6-overexpressing A375 cells. f, g, PD-L1 surface protein (f) or lysate immunoblots (g) of parental, CMTM6-knockout, STUB1-knockout or double-knockout A375 cells. Numbers in f represent relative PD-L1 MFI. h, Comparative plasma membrane-fractionated mass spectrometry of four CMTM6-proficient and four CMTM6-deficient 8505C clones. i, Overview of proteins consistently found up- (red) or downregulated (blue) upon CMTM6 removal in both 8505C and RKO cells. j, IL-2 production by PD-1high, PD-1int and PD-1– primary human T cells obtained by transduction with the MART-I-specific 1D3 TCR and PD-1, and co-cultured with unloaded or MART-I peptide-loaded parental or CMTM6-knockout 8505C cells. Data are representative of two (a, b), one (c, h) or three (d–g, j) independent experiments and were analysed by unpaired t-test (f, j). Data represent mean ± s.d. of triplicates (a, b, f, j). $^{**}P < 0.01$; $^{***}P < 0.001$; NS, not significant. KO, knockout; IP, immunoprecipitation; MFI, median fluorescence intensity; OE, overexpression; Ub, ubiquitin; WB, western blot.

To validate these data, we transduced H2030 cells, in which CMTM6 depletion modestly suppresses PD-L1 expression and CMTM4 is highly expressed, with shRNAs against *CMTM4* and *CMTM6*, either separately or in combination. In these cells, silencing of *CMTM6* led to repression of IFNγ-induced PD-L1 expression that was further enhanced when *CMTM4* was simultaneously targeted (Fig. 3b and Extended Data Fig. 4a). More directly, ectopic expression of CMTM4 could fully restore IFNγ-induced PD-L1 expression in CMTM6-knockout cells (Extended Data Fig. 4b, c). To understand whether regulation of PD-L1 expression is a specific property of CMTM6 and CMTM4, we individually introduced Flag-tagged versions of all CMTM family members into CMTM6-deficient A375 cells. In contrast to what was observed upon CMTM6 and CMTM4 introduction, expression of other CMTM members (detected for CMTM1, CMTM3, CMTM5 and CMTM7; Extended Data Fig. 4d, e) did not induce a substantial increase in PD-L1 expression, as assessed by either flow cytometry or western blot analysis (Fig. 3c, d).

To study the mechanism by which CMTM6 regulates PD-L1 levels, we first assessed the relationship between CMTM6 expression and *PD-L1* mRNA levels. Comparison of *PD-L1* mRNA levels and cell-surface protein levels at different time points after IFNγ stimulation revealed that whereas CMTM6 depletion greatly reduced PD-L1 cell-surface levels, induction of *PD-L1* mRNA by IFNγ was not substantially altered (Fig. 4a, b and Extended Data Fig. 5d). Notably, both in cell lines (Extended Data Fig. 5a) and in primary dendritic cells (Extended Data Fig. 5b, c), levels of MHC-I and PD-L2 protein were not significantly affected by CMTM6 inhibition, indicating that although CMTM6 regulates PD-L1 at the protein level, it is not a general regulator of protein translation or stability.

To determine where in the PD-L1 protein life cycle CMTM6 exerts its effect, CMTM6-deficient and CMTM6-overexpressing A375 cells were transduced with a V5-tagged PD-L1 gene. Immunoprecipitation of PD-L1–V5 at different time points after a 1-h ^{35}S pulse labelling demonstrated a much more rapid decay of PD-L1 in the absence of CMTM6 (fraction PD-L1 remaining at $t = 6$ h; 94% versus 8%; Fig. 4c and Extended Data Fig. 5e). Notably, acquisition of PD-L1 resistance to deglycosylation by endoglycosidase H, was equally efficient in both cell populations, indicating that CMTM6 influences PD-L1 protein fate after egress from the endoplasmic reticulum (Extended Data Fig. 5f).

To reveal the cellular localization of endogenous CMTM6, we performed mass spectrometry analysis of different subcellular fractions, demonstrating that endogenous CMTM6 is predominantly present within the plasma membrane fraction (Extended Data Fig. 6a) Immunohistochemical analysis confirmed the presence of CMTM6 at the cell membrane (Extended Data Fig. 6b). Furthermore, immunohistochemical analysis of nine melanomas revealed CMTM6 protein expression in human tumours, and also showed that PD-L1 staining in eight of these samples was restricted to areas with clear CMTM6 expression (Extended Data Fig. 6c). Similarly, in three out of five PD-L1$^+$ lung cancer samples, we observed PD-L1 localization in CMTM6$^+$ areas.

A hypothesis arising from the above data is that CMTM6 and PD-L1 could interact molecularly. To test this, we performed immunoprecipitation of PD-L1 followed by western blot analysis of CMTM6, and vice versa. In lysates from A375 cells or 8505C cells, anti-PD-L1 antibody co-immunoprecipitated CMTM6. Likewise, PD-L1 was present in anti-CMTM6 immunoprecipitates. As expected, co-immunoprecipitation of PD-L1 and CMTM6 in A375 was dependent upon PD-L1 induction by IFNγ. As a further control for antibody specificity, co-immunoprecipitation of both CMTM6 and PD-L1 was abrogated upon gene inactivation of the partner molecule (Fig. 4d and Extended Data Fig. 7a, b). Co-immunoprecipitation was likewise observed for PD-L1 and CMTM4, and CMTM4 and CMTM6 (Extended Data Fig. 7c, d).

To understand how CMTM6 influences PD-L1 degradation, wild-type, CMTM6-knockout, and CMTM6-overexpressing A375 were transduced with a V5-tagged PD-L1 gene and ubiquitination of PD-L1 was analysed. In the absence of CMTM6, the amount of ubiquitinated PD-L1 was increased, despite the overall lower PD-L1 levels (Fig. 4e and Extended Data Fig. 8a), suggesting that CMTM4/6 may protect PD-L1 from ubiquitination. Intriguingly, STUB1, an E3 ubiquitin ligase that has, among others, been implicated in the degradation of Foxp3 in regulatory T

cells[24], was identified as a negative regulator of PD-L1 expression in both haploid genetic screens (Extended Data Fig. 8b, c). To assess whether STUB1 affects PD-L1 degradation, we disrupted STUB1 in either CMTM6-proficient or -deficient A375 cells. Deletion of STUB1 resulted in a stronger increase in PD-L1 levels in CMTM6-deficient than in CMTM6-proficient cells, identifying STUB1 as an E3 ligase that causes destabilization of PD-L1 (Fig. 4f, g), either directly, by modification of lysines in the PD-L1 cytoplasmic domain, or indirectly. Consistent with the model that CMTM6 may protect PD-L1 by preventing ubiquitination, cell-surface levels of PD-L1–PD-L2 fusion proteins are only influenced by CMTM6 when carrying the PD-L1 transmembrane and intracellular domain (Extended Data Fig. 8d, e). Exploiting the fact that CMTM6 and PD-L2 do not show detectable association (Extended Data Fig. 8f), we also used PD-L1–PD-L2 fusion proteins to demonstrate that the PD-L1 transmembrane domain is required for efficient interaction (Extended Data Fig. 8g). In line with the role of the PD-L1 transmembrane and intracellular domain in CMTM6-mediated stabilization, orientation mapping of CMTM6 revealed that a large part of the molecule is located within the cytosol and cell membrane (Extended Data Fig. 9).

In view of the broad RNA expression pattern of *CMTM6*, we assessed the effects of CMTM6 on the membrane proteome in an unbiased manner. Mass spectrometric analysis of a series of independent CMTM6-deficient and -proficient clones revealed that, both within the 8505C thyroid cancer cell line and the RKO colorectal cancer cell line, PD-L1 was the most significantly influenced hit (Fig. 4h, i and Extended Data Fig. 10a, b). Expression of PD-L1 affects T-cell responsiveness in a quantitative manner, with higher levels of PD-L1 expression leading to an increased impairment of T-cell survival and/or activity[11,25]. To determine whether CMTM6 influences PD-L1-mediated T-cell suppression, we incubated mixtures of MART-I T-cell receptor (TCR)-transduced T cells that expressed different levels of PD-1 with antigen-loaded CMTM6-deficient or -proficient 8505C or A375 cells. IL-2 production of PD-1^{int} and PD-1^{high} T cells upon encounter of CMTM6-proficient tumour cells was reduced relative to that of PD-1^{-} T cells. However, upon CMTM6 disruption in 8505C or A375 tumour cells, IL-2 production of PD-1-expressing T cells was significantly restored (Fig. 4j and Extended Data Fig. 10c–e).

Recent work has revealed a number of mechanisms of transcriptional and post-transcriptional (dys)regulation of the PD-L1 gene in tumour cells[10,11,12,13,14,15]. Here we identify CMTM6 and CMTM4 as regulators of PD-L1 protein stability. On the basis of the available data we conclude that CMTM6/4, the two most closely related members of the CMTM family (Extended Data Fig. 4f), influence PD-L1 expression across a range of cell types. Furthermore, the observations that (i) CMTM6 affects PD-L1

protein stability at late time points after biosynthesis; (ii) CMTM6, CMTM4 and PD-L1 interact, as shown by co-immunoprecipitation; and that (iii) CMTM6 is largely located at the cell surface, collectively suggest a model in which CMTM6 interacts with PD-L1 at the tumour cell surface and thereby protects it from degradation. In line with this model, CMTM6 influences the levels of PD-L1 ubiquitination and absence of the STUB1 E3 ubiquitin ligase partially reverts the CMTM6-knockout phenotype. Intriguingly, for one of the other CMTM family members, CMTM7, cell surface expression has been described in association with the B-cell receptor (BCR) complex, where it may contribute to BCR signalling[26]. It could be speculated that CMTM6 may also fulfil a similar role in the immunological synapse between T cells and tumour cells or antigen-presenting cells. Finally, the co-localization of PD-L1 and CMTM6 in human tumours and the observation that CMTM6 depletion ameliorates PD-L1-mediated T-cell suppression suggest a potential value of CMTM6/4 as therapeutic targets, either in isolation, or to enhance the effectiveness of the current PD-L1–PD-1 blocking therapies.

Methods

Data reporting

No statistical methods were used to predetermine sample size. The experiments were not randomized and the investigators were not blinded to allocation during experiments and outcome assessment.

Cell lines

A375, DLD1, RKO, H2030 and H2122 cells were purchased from the American Type Culture Collection (ATCC). 8505C was purchased from the Deutsche Sammlung von Mikroorganismen und Zellkulturen GmbH (DSMZ). WM2664 and COLO679 cells were gifts from R. Bernards (The Netherlands Cancer Institute). Short-term cell lines from patient-derived melanoma xenografts were generated as described[28] and were a gift from D. Peeper and K. Kemper. HAP1 cells have been described previously[19]. HAP1 cells were cultured in IMDM (Thermo Fisher Scientific) supplemented with 10% fetal calf serum (FCS, Sigma-Aldrich), 100 U ml^{-1} penicillin–streptomycin (Thermo Fisher Scientific) and l-glutamine (Thermo Fisher Scientific); A375 and short-term melanoma xenograft cultures were maintained in DMEM supplemented with 10% FCS (Sigma-Aldrich) and 100 U ml^{-1} penicillin–streptomycin (Thermo Fisher Scientific). All other cell lines were cultured in RPMI supplemented with 10% FCS (Sigma-Aldrich) and 100 U ml^{-1} penicillin–streptomycin (Thermo Fisher Scientific). IFNγ treatment was performed over a period of 48 h at a concentration of 25 ng ml^{-1}, unless indicated otherwise.

Identification of genetic regulators

The approach described in ref. 20 was followed to identify regulators of PD-L1 abundance. Mutagenized HAP1 libraries (starting with either wild-type cells or CMTM6-deficient HAP1 cells) were expanded to approximately 1.5×10^9 cells and subsequently treated with 0.5 ng ml^{-1} IFNγ (Peprotech) for 24 h to induce expression of PD-L1. Subsequently, approximately 3×10^9 cells were dissociated using trypsin-EDTA (Life Technologies), washed with PBS and stained with FITC-labelled anti-PD-L1 antibody (BD Pharmingen) at 1:20 dilution for 30 min at room temperature in PBS containing 0.5% w/v bovine serum albumin (Sigma-Aldrich) and 0.2% w/v sodium azide (Sigma-Aldrich). Subsequently, cells were washed three times with PBS containing 1% FCS and stained with FITC-labelled polyclonal goat anti-mouse Ig (BD pharmingen) at 1:100 dilution for 30 min at room temperature in PBS containing 0.5% w/v bovine serum albumin (Sigma-Aldrich) and 0.2% w/v sodium azide (Sigma-Aldrich) to allow signal amplification. Following two washes with PBS containing 1% FCS and one wash with PBS, stained cells were passed through a 40-µm strainer (BD FalconTM) and subsequently fixed using BD fix buffer I (BD biosciences) for 10 min at 37 °C, followed by a wash with PBS containing 1% FCS. Subsequently, cells were permeabilized by suspension in cold BD permeabilization buffer (BD Biosciences) while vortexing, and incubated on ice for 30 min before incubation with 100 µg ml^{-1} RNase A (Qiagen) and 10 µg ml^{-1} propidium iodide (Cayman Chemical) at 37 °C temperature for 30 min. Alternatively, cells were subjected to treatment with 3 µM 4′,6-diamidino-2-phenylindole (DAPI) for 30 min. Staining of the cells finished with a final wash in PBS containing 10% FCS. Following staining, cells were sorted on a Biorad S3 Cell sorter (Biorad) or a Moflo Asterios cell sorter (Beckman Coulter) to collect the 1–5% of cells with the highest and lowest PD-L1 staining intensity and 1*n* DNA content. Sorted cells were used for isolation of genomic DNA and retroviral gene-trap insertion sites were retrieved, mapped and analysed as described in ref. 20. For PD-L1, it has been described that alterations of the 3′ portion of the gene can stabilize the gene product and lead to higher PD-L1 proteins levels[11]. As this was also recapitulated by our gene-trap insertion method (gene-trap integrations into the 3′ portion of the gene resulted in increased rather than decreased staining intensity for PD-L1), integrations in the portion of the gene downstream of exon 5 (Refseq identifier NM_014143.3) were disregarded where indicated.

Generation of knockout cell lines

Knockout cell lines were generated using the CRISPR–Cas9 system. To generate knockout HAP1 cells, cells were transfected with a px330 vector (Addgene 42230) encoding a sgRNA for the gene of interest and a vector encoding a sgRNA for the zebrafish TIA gene (5′-GGTATGTCGGGAACCTCTCC-3′), as well as a P2A-blasticidin-

resistance cassette flanked by two TIA target sites. This allows incorporation of the blasticidin-resistance gene into the locus of interest, resulting in a stable knockout, essentially as described[29]. Following blasticidin selection (10 µg ml^{-1}), resistant clones were expanded.

To generate knockout A375 and 8505C cells, cells were transfected with pLentiCRISPR v.2 vector (Addgene 52961) encoding sgRNAs targeting non-overlapping regions of the *CMTM6* gene[30]. Following puromycin selection (2 µg ml^{-1}, for two days), single-cell clones were expanded and gene disruptions were validated by sequencing and western blot analysis.

The sgRNA sequence CCGGGTCCTCCTCCGTAGTG was used to generate the A375 CMTM6-knockout clone CMTM6 KO6, the 8505C CMTM6-knockout clone CMTM6 KO1 and the RKO CMTM6-knockout clone, the sgRNA sequence TCACAATGTACTTTATGTGG was used to generate the A375 CMTM6-knockout clone CMTM6 KO12 and the 8505C CMTM6-knockout clone CMTM6 KO3. The sgRNA sequence ACTGCTTGTCCAGATGACTT was used to generate the A375 PD-L1-knockout clone and the sgRNA sequence GGAGATGGAGAGCTATGATG was used to generate all the *STUB1*-knockout clones.

Immunoprecipitation, SDS–PAGE and western blot analysis

Cells for western blot analysis were seeded in six-well plates and cultured as described in the figure legends. To collect cell lysates, cells were washed with PBS and lysed with RIPA buffer supplemented with freshly added protease inhibitor cocktail (Roche). After incubation on ice for 30 min, cell lysates were centrifuged at 20,000*g* for 15 min at 4 °C. Supernatants were subsequently processed using a Novex NuPAGE Gel Electrophoresis System, according to the manufacturer's instructions (Thermo Fisher Scientific).

Cells for (co)immunoprecipitation experiments were seeded in 15-cm dishes and cultured as described in the figure legends, using 5 million cells per immunoprecipitation reaction. Cells were washed with cold PBS buffer and lysed in CHAPS buffer (1% CHAPS, 50 mM Tris-HCl pH 7.5, 150 mM NaCl). For the detection of protein ubiquitination, cells were lysed in denaturing buffer (50 mM Tris-HCl, 0.5 mM EDTA and 1% SDS) followed by heating at 95 °C for 10 min and then quenched by adding nine volumes of quenching buffer (0.5% Triton X-100, 20 mM Tris-HCl (pH 8.0), 137 mM NaCl, 10% glycerol, 2 mM EDTA). Protease inhibitor cocktail (Roche) was freshly added to all buffers. Cell lysates were incubated on a rotator for 30 min at 4 °C, and then centrifuged at 20,000 *g* for 15 min at 4 °C. Supernatants were subsequently processed using Dynabeads Protein A or Protein G for Immunoprecipitation (Thermo

Fisher Scientific), and the indicated antibodies. The final elute was processed and western blot analysis was performed using a Novex NuPAGE Gel Electrophoresis System, according to the manufacturer's instructions (Thermo Fisher Scientific).

Pulse–chase and EndoH or PNGaseF treatment

V5-tagged PD-L1-transduced CMTM6-overexpressing A375 cells and V5-tagged PD-L1-transduced CMTM6-knockout A375 cells were cultured in methionine- and cysteine-free medium for 1 h at 37 °C. Cells were then pulse labelled with 0.5 mCi ml^{-1} [^{35}S]Cys/[^{35}S]Met (PerkinElmer) for 1 h. Cells were washed with PBS to remove residual [^{35}S]Cys/[^{35}S]Met and then cultured in regular medium with extra 'cold' methionine and cysteine for 0, 1, 2, 3 and 6 h. Cell samples were lysed and used for immunoprecipitation with anti-V5 antibody (Thermo Fisher Scientific) immobilized on protein-A- or protein-G-coated beads (Thermo Fisher Scientific). Immunoprecipitates were either left untreated or treated with EndoH or PNGaseF (New England Biolabs), according to the manufacturer's instructions.

Immunoprecipitates were run on NuPAGE 4–12% gels. Gels were treated with 1 M Na salicylate pH 5.6 before drying, and then analysed on Fujifilm BAS-MP phosphor imager screens. Quantification was performed using a Fujifilm FLA-3000 phosphor imager and AIDA image analyser software. Gels were exposed to film using intensifier screens at −80 °C.

Viral vectors

Lentiviral shRNA vectors were retrieved from the arrayed TRC human genome-wide shRNA collection. Additional information is available at http://www.broadinstitute.org/rnai/public/clone/search using the TRCN number. The following lentiviral shRNA vectors were used: shCMTM6-4: TRCN0000127888; shCMTM6-6: TRCN0000130177; shCMTM4-1: TRCN0000142717; shCMTM4-2: TRCN0000142470.

PD-L1, PD-1, PD-L2, CMTM6, CMTM4 and PD-L1–PD-L2 chimaeras expressing lentiviral vectors were generating by insertion of the relevant gBlock (IDT) into a pCDH-CMV-MCS-EF1-Puro (CD510B-1, System Bioscience)-derived vector in which the puromycin-resistance cassette was substituted with a blasticidin-resistance cassette. PD-L1–PD-L2 chimaeras were generated as follows. Each section in brackets is a separate unit of amino acids (a.a.) from PD-L1 or PD-L2 or the sequence of the Flag-epitope tag (DYDDDDKD): PD-L1–PD-L2 TM (transmembrane): (a.a. 1–18 PD-L1)–(DYDDDDKD)–(a.a. 19–238 PD-L1)–(a.a. 221–242 PD-L2)–(a.a. 263–290 PD-L1). PD-L1–PD-L2 IC (intracellular): (a.a. 1–18 PD-L1)–(DYDDDDKD)–(a.a. 19–262 PD-L1)–(a.a. 246–273 PD-L2). PD-L1–PD-L2 EC (extracellular): (a.a. 1–20 PD-L2)–(DYDDDDKD)–(a.a. 21–221

PD-L2)–(a.a. 232–290 PD-L1). For the generation of chimaeras, isoforms NP_054862.1 (PD-L1) and NP_079515.2 (PD-L2) were used.

V5-tagged PD-L1 was retrieved from the CCSB-Broad Lentiviral Expression Library (ccsbBroad304_15876). CMTM family members were ordered as individual gBlocks (IDT) coding for the different family members using Ensembl gold transcripts ENST00000379500.6 (CMTM1), ENST00000268595.2 (CMTM2), ENST00000361909.8 (CMTM3), ENST00000330687.8 (CMTM4), ENST00000339180.8 (CMTM5), ENST00000205636.3 (CMTM6), ENST00000334983.9 (CMTM7), ENST00000307526.3 (CMTM8) C-terminally fused with a Flag tag, preceded by a short AAV-linker and cloned into the pMX-IRES-Blast vector using restriction enzymes BglII and SalI (CMTM1 and CMTM4), EcoRI and NotI (CMTM2) or BamHI and SalI (CMTM3, CMTM5, CMTM6, CMTM7 and CMTM8). The retroviral vector pBABE-Puro encoding C-terminally Flag-tagged CMTM6 (pBp-CMTM6-Flag) was generated by cloning a gBlock for CMTM6 (ENST00000205636.3) digested with BamHI and XhoI into pBABE-Puro digested with BamHI and SalI.

For production of lentiviral particles, the described plasmids were co-transfected into HEK293T cells along with packaging plasmids (pPAX2, pVSV-G). Two days after transfection, lentiviral supernatant was collected and used for transduction. Retroviral particles were produced and purified as described for HAP1 mutagenesis, except that multiple collections and ultracentrifugation were omitted. Two days after transduction, cells were selected by exposing them to blasticidin or puromycin.

Antibodies

The following antibodies were used for western blot analyses and immunoprecipitation: anti-HSP90: H114 (SantaCruz); anti-CMTM6: HPA026980 (Atlas) or anti-CMTM6 monoclonal antibody (clone RCT8) directed against a peptide in the C-terminal domain of CMTM6 generated by Absea; anti-CMTM4: HPA014704 (Atlas); anti-PD-L1 for western blot analysis: 405.9A11 (Cell Signaling) or immunoprecipitation: E1L3N (Cell Signaling); normal rabbit IgG: 2729 (Cell Signaling); anti-Flag tag: M2 (Sigma-Aldrich); anti-V5 tag: R960-25 (Thermo Fisher Scientific); anti-STUB1 sc133066 (Santa Cruz); anti-ubiquitin antibody: 3933 (Cell Signaling); goat anti-mouse IgG (H + L)-HRP conjugate (BIO-RAD); and goat anti-rabbit IgG (H + L)-HRP conjugate (BIO-RAD). The following antibodies were used for flow cytometry: anti-PD-L1: M1H1 (eBioscience); anti-PD-L2: 24F.10C12 (Biolegend); anti-MHC-I: BB7.2 (BD bioscience); anti-mouse TCRβ: H57-597 (BD Bioscience); anti-CD8: RPA-T8 (BD bioscience); anti-CD3: SK7 (eBioscience); anti-PD-1: eBioJ105 (eBioscience); anti-IL-2: 554567 (BD Bioscience). The following antibodies were used for immunohistochemistry: anti-PD-L1: 22C3

(DAKO); the anti-CMTM6 monoclonal antibody (clone RCT6) directed against a peptide in the C-terminal domain of CMTM6 was generated by Absea.

RNA isolation, first strand cDNA synthesis and RT–qPCR

Total RNA was isolated from cells using the RNeasy Mini Kit (Qiagen). cDNA was obtained by reverse transcription using the Maxima First Strand cDNA Synthesis Kit for RT–qPCR (Thermo Fisher Scientific), according to the manufacturer's instructions. SensiFAST SYBR No-ROX Kit (Bioline) was used for RT–PCR gene expression analysis, carried out on Roche LightCycler 480 platform. Relative mRNA levels were normalized to *GAPDH* mRNA levels. Primer sets used were as follows: *CD274*-F: ATTTGGAGGATGTGCCAGAG; *CD274*-R: CCAGCACACTGAGAATCAACA; *GAPDH*-F: AAGGTGAAGGTCGGAGTCAA; *GAPDH*-R: AATGAAGGGGTCATTGATGG.

IL-2 production assay

Human peripheral blood T cells (Sanquin) were activated and transduced with a retroviral vector encoding the MART-I specific 1D3 TCR as described[31] and with a lentiviral vector encoding PD-1. MART-I TCR and PD-1 expression was validated by flow cytometry. Both 8505C (parental and CMTM6-KO) and A375 cells (parental, PD-L1-overexpressing, and CMTM6-KO PD-L1-overexpressing) were pulsed with 10 ng ml^{-1} MART-I(26–35) peptide for 1 h at 37 °C. Next, 1×10^5 transduced T cells were incubated with 1×10^5 peptide-pulsed tumour cells or non-pulsed tumour cells in the presence of 1 µl ml^{-1} Golgiplug (BD Biosciences). After a 5-h incubation at 37 °C, cells were washed and stained with phycoerythrin (PE)-labelled anti-mouse TCRβ chain, V500-labelled anti-CD8, PerCP Cy5.5-labelled anti-CD3 and PE Cy7-labelled anti-PD-1 and analysed for IL-2 production by intracellular cytokine staining. Activity of T cells with different levels of PD-1 expression was analysed by gating on mouse TCRβ-chain-positive cells expressing low, intermediate or high levels of PD-1.

Membrane fractionation and MS analysis

Snap-frozen cell pellets were lysed by gentle homogenization in isotonic buffers supplemented with phosphatase inhibitor (PhosSTOP, Roche) and protease inhibitor (cOmplete mini EDTA-free, Roche). Cellular disruption of >95% was confirmed by microscopy. Plasma membrane (F4), inner membrane (F3) and cytosolic (F1) fractions were prepared by differential centrifugation using a plasma membrane purification kit (Abcam, ab65400).

From fractions F1, F3 and F4, 20 µg of protein was diluted 20 times in 50 mM ammonium bicarbonate, reduced in 4 mM dithiothreitol (DTT), alkylated in 8 mM iodoacetamide (IAA) and digested sequentially at 37 °C with 1:75 Lys C (Wako) and

1:50 trypsin (Sigma-Aldrich) for 4 and 12 h, respectively. Digested peptides were acidified to 0.1% formic acid (FA) and purified by strong cation exchange (SCX) STAGE tips, using as loading buffer: 80% acetonitrile (ACN), 0.1% FA and as elution buffer: 0.5 M ammonium acetate, 20% ACN, 0.1% FA. Eluted peptides were dried by vacuum and 4 µg equivalent of peptides was analysed in a 3 h reverse-phase separation on the UHPLC 1290 system (Agilent) coupled to an Orbitrap Q Exactive HF mass spectrometer (Thermo Fisher Scientific). SCX flowthrough from cytosolic fraction (denoted F2) was analysed separately to increase proteome coverage.

RP-nanoLC–MS/MS

Proteomics data were acquired using an UHPLC 1290 system (Agilent) coupled to an Orbitrap Q Exactive HF spectrometer (Thermo Scientific). Peptides were first trapped on a 2 cm × 100 µm Reprosil C18 pre-column (3 µm) and then separated on a 50 cm × 75 µm Poroshell EC-C18 analytical column (2.7 µm). Trapping was performed for 10 min in 0.1 M acetic acid (solvent A) and elution with 80% ACN in 0.1 M acetic acid (solvent B) in gradients as follows: 10–40% solvent B in 155 min, 40–100% in 3 min and finally 100% for 1 min. Flow was passively split to 300 nl min^{-1}. MS data were obtained in data-dependent acquisition mode. Full scans were acquired in the *m/z* range of 375–1,600 at the resolution of 35,000 (*m/z* 400) with AGC target 3×10^6. The top 15 most intense precursor ions were selected for HCD fragmentation performed at normalized collision energy (NCE) 25%, after accumulation to target value of 5×10^4. MS/MS acquisition was performed at a resolution of 17,500.

Database search

Raw files were processed using MaxQuant version 1.5.3.30 and searched against the human Swissprot database (version May 2016) using Andromeda.

Cysteine carbamidomethylation was set to fixed modification, while variable modifications of methionine oxidation and protein N-terminal acetylation, as well as up to 2 missed cleavages were allowed. The false discovery rate (FDR) was restricted to 1% in both protein and peptide identification. Label-free quantification (LFQ) was performed with 'match between runs' enabled.

Analysis of *CMTM6* RNA levels and correlation between *CMTM6* and *CD274* RNA levels in TCGA samples

TCGA RNA sequencing data were downloaded from the Broad TCGA genome data analysis centre 1 November 2015 release of the standard runs (http://gdac.broadinstitute.org/runs/stddata). For projects where data from multiple sequencing platforms were available, Illumina HiSeq data was preferentially used. The (RSEM)

normalized read count field was multiplied by 10^6 to arrive at the reported TPM expression values. Correlation coefficients and associated unadjusted *P* values between CMTM6 and CD274 were computed per TCGA-sequencing project with Pearson's method. Two-dimensional kernel density estimates were computed using the MASS::kde2d() function in version 3.3.1 of the R programming language. We computed the correlations between CMTM6 and 10^4 randomly selected genes (identical between sequencing projects) to obtain a reference distribution of correlation coefficients for CMTM6, specific for each TCGA project. The reported empirical *P* values are defined as one minus the quantile of the CMTM6 and CD274 correlation within this reference distribution.

Immunohistochemistry

Immunohistochemistry of the formalin-fixed paraffin-embedded samples was performed on a BenchMark Ultra autostainer (Ventana Medical Systems). In brief, 3 µm paraffin serial sections were cut, heated at 75 °C for 28 min and deparaffinized in the instrument with EZ prep solution (Ventana Medical Systems). Heat-induced antigen retrieval was carried out using Cell Conditioning 1 (CC1, Ventana Medical Systems) for 48 min for PD-L1 and 64 min for CMTM6 antibodies at 95 °C.

PD-L1 clone 22C3 (DAKO) was used at 1:40 dilution, 1 h at room temperature and CMTM6 clone RCT6 was used directly from hybridoma supernatant at either 1:500 or 1:1,000 dilution for tumour samples and 1:100 dilution for cell lines, 1 h at room temperature. Bound antibody was detected using the OptiView DAB Detection Kit (Ventana Medical Systems). Slides were counterstained with Haematoxylin and Bluing Reagent (Ventana Medical Systems).

Patient melanoma samples were obtained (following Institutional Review Board approval) from the NKI-AVL pathology archive biobank and selected for PD-L1 expression.

Statistical analysis

All student *t*-tests were two-tailed under the assumption of equal variance between samples.

Data availability

All sequencing datasets have been deposited in the NCBI Sequence Read Archive under accession number SRP108407. In addition, all processed screen results are accessible in an interactive database (https://phenosaurus.nki.nl/). Source Data for the main and extended data figures are provided in the online version of the paper.

Acknowledgements

We thank F. Scheeren, E. Stickel, V. Blomen, M. Brockmann and the other members of the Schumacher and Brummelkamp laboratories for discussions, J. Grabowska for technical assistance, K. Kemper and D. Peeper for sharing melanoma PDX models and the NKI- AVL flow facility, the NKI-AVL Core Facility Molecular Pathology & Biobanking (CFMPB) for supplying NKI-AVL Biobank material and/or laboratory support. This work was supported by The Queen Wilhelmina Cancer Research Award and European Research Council (ERC) Advanced Grant SENSIT (to T.N.M.S.), NWO Vici Grant (016. Vici.170.033), the Cancer Genomics Center (CGC.nl), and Ammodo KNAW Award 2015 for Biomedical Sciences (to T.R.B.), The Cancer Research Institute (CRI) Irvington Postdoctoral Fellowship (to C.S.), The Landsteiner Foundation for Blood Research, grant 1355 (to J.B.), Proteins@Work, a program of the Netherlands Proteomics Centre financed by NWO, the Netherlands Organisation for Scientific Research (to A.J.R.H.) and The Institute for Chemical Immunology, an NWO Gravitation project (to T.N.M.S. and A.J.R.H.).

Contributions

R.M., C.S. and L.T.J. conceived the project, designed and performed experiments, interpreted data and co-wrote the paper. R.G.-E. designed, performed and interpreted functional assays. W.W. designed, performed and interpreted mass spectrometry analyses, A.J.R.H. designed and interpreted mass spectrometry analyses, E.d.V. designed, performed and interpreted immunoprecipitation experiments, Y.X. designed, performed and interpreted human dendritic cell experiments, M.E.W.L. performed and interpreted melanoma PDX experiments, M.S. performed bioinformatic analyses, L.F.A.W. supervised bioinformatic analysis, E.A.R. and I.H. identified samples and performed immunohistochemistry analyses, A.B. and H.M.H. supervised and scored immunohistochemistry analyses, C.U.B. provided and identified samples for immunohistochemistry analyses, J.B. designed and interpreted immunoprecipitation and human dendritic cell experiments, T.R.B. and T.N.M.S. designed experiments, interpreted data and co-wrote the manuscript.

Competing interests

R.M., C.S., L.T.J., T.R.B. and T.N.M.S. are inventors on a patent application covering the use of CMTM6, CMTM4 and STUB1 as therapeutic and diagnostic targets. T.R.B. is co-founder and shareholder of Scenic Biotech. The other authors declare no competing interests.

References

1 Topalian, S. L. *et al. Safety, activity, and immune correlates of anti-PD-1 antibody in cancer*. *N. Engl.J. Med.* **366**, 2443–2454 (2012)

2 Brahmer, J. R. *et al. Safety and activity of anti-PD-L1 antibody in patients with advanced cancer*. *N. Engl. J. Med.* **366**, 2455–2465 (2012)

3 Ansell, S. M. *et al. PD-1 blockade with nivolumab in relapsed or refractory Hodgkin's lymphoma*. *N. Engl. J. Med.* **372**, 311–319 (2015)

4 Powles, T. *et al. MPDL3280A (anti-PD-L1) treatment leads to clinical activity in metastatic bladder cancer*. *Nature* **515**, 558–562 (2014)

5 Garon, E. B. *et al. Pembrolizumab for the treatment of non-small-cell lung cancer*. *N. Engl. J. Med.* **372**, 2018–2028 (2015)

6 Le, D. T. *et al. PD-1 blockade in tumors with mismatch-repair deficiency*. *N. Engl. J. Med.* **372**, 2509–2520 (2015)

7 Motzer, R. J. *et al. Nivolumab versus everolimus in advanced renal-cell carcinoma*. *N. Engl. J. Med.* **373**, 1803–1813 (2015)

8 Nghiem, P. T. *et al. PD-1 blockade with pembrolizumab in advanced Merkel-cell carcinoma*. *N. Engl. J. Med.* **374**, 2542–2552 (2016)

9 Ferris, R. L. *et al. Nivolumab for recurrent squamous-cell carcinoma of the head and neck*. *N. Engl. J. Med.* **375**, 1856–1867 (2016)

10 Lee, S. J. *et al. Interferon regulatory factor-1 is prerequisite to the constitutive expression and IFN-γ-induced upregulation of B7-H1 (CD274)*. *FEBS Lett.* **580**, 755–762 (2006)

11 Kataoka, K. *et al. Aberrant PD-L1 expression through 3'-UTR disruption in multiple cancers*. *Nature* **534**, 402–406 (2016)

12 Casey, S. C. *et al. MYC regulates the antitumor immune response through CD47 and PD-L1*. *Science* **352**, 227–231 (2016)

13 Dorand, R. D. *et al. Cdk5 disruption attenuates tumor PD-L1 expression and promotes antitumor immunity*. *Science* **353**, 399–403 (2016)

14 Li, C.-W. *et al. Glycosylation and stabilization of programmed death ligand-1 suppresses T-cell activity*. *Nat. Commun.* **7**, 12632 (2016)

15 Lim, S. O. *et al. Deubiquitination and stabilization of PD-L1 by CSN5*. *Cancer Cell* **30**, 925–939 (2016)

16 Herbst, R. S. *et al. Predictive correlates of response to the anti-PD-L1 antibody MPDL3280A in cancer patients*. *Nature* **515**, 563–567 (2014)

17 Ribas, A. & Hu-Lieskovan, S. *What does PD-L1 positive or negative mean? J. Exp. Med.* **213**, 2835–2840 (2016)

18 Carette, J. E. *et al. Haploid genetic screens in human cells identify host factors used by pathogens*. *Science* **326**, 1231–1235 (2009)

19 Carette, J. E. *et al. Ebola virus entry requires the cholesterol transporter Niemann–Pick C1*. *Nature* **477**, 340–343 (2011)

20 Brockmann, M. *et al. Genetic wiring maps of single-cell protein states reveal an off-switch for GPCR signalling*. *Nature* **546**, 307–311 (2017)

21 Platanias, L. C. *Mechanisms of type-I- and type-II-interferon-mediated signalling*. *Nat. Rev. Immunol.* **5**, 375–386 (2005)

22 Han, W. *et al. Identification of eight genes encoding chemokine-like factor superfamily members 1–8 (CKLFSF1–8) by in silico cloning and experimental validation*. *Genomics* **81**, 609–617 (2003)

23 Xiao, Y. *et al. Identification of the common origins of osteoclasts, macrophages, and dendritic cells in human hematopoiesis*. *Stem Cell Rep.* **4**, 984–994 (2015)

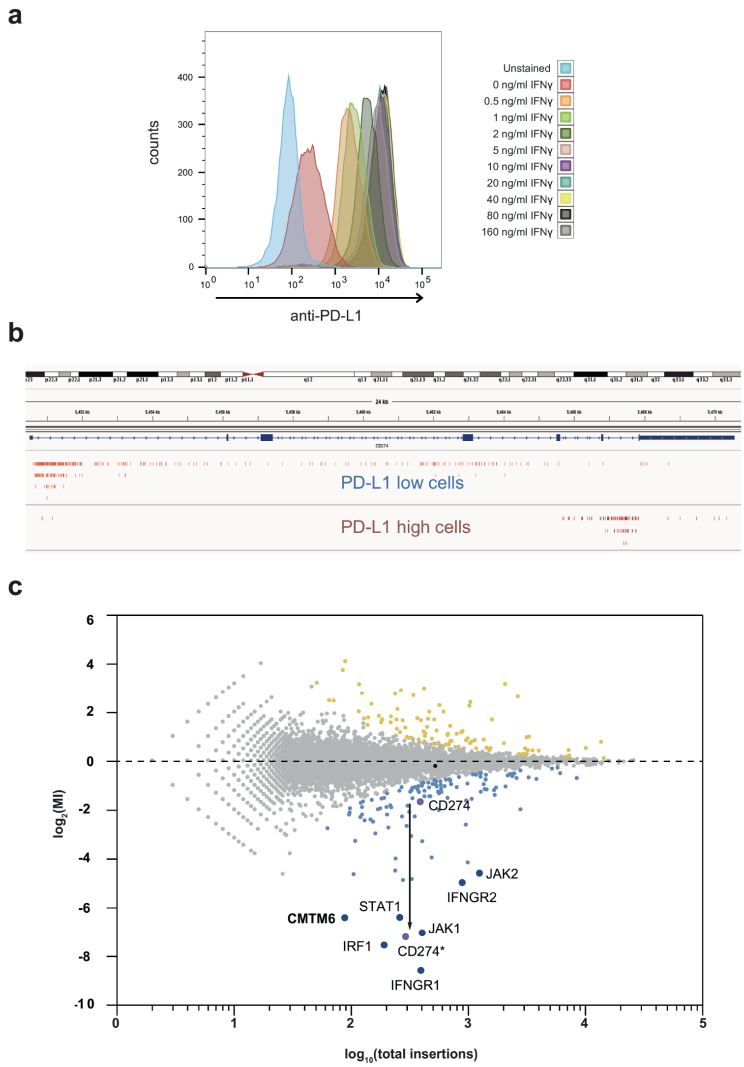

Extended Data Figure 1 : PD-L1 is regulated by IFNγ and by the 3' UTR in HAP1 cells. a, Flow cytometry analysis of PD-L1 expression in untreated HAP1 cells and HAP1 cells treated with the indicated concentrations of IFNγ. An IFNγ concentration of 0.5 ng ml−1 was chosen for the subsequent genetic screen, to allow identification of gene integrations that either enhance or suppress PD-L1 expression. Data are representative of three independent experiments. b, Schematic representation of the PD-L1 gene and of the gene trap insertions observed in HAP1 cells sorted on the basis of either low or high PD-L1 expression. Note the bias towards integrations within introns 5 and 6 in the *PD-L1* gene in PD-L1^{high} cells relative to PD-L1^{low} cells, consistent with the structural variants beyond exon 4 of PD-L1 that have been shown to result in increased PD-L1 expression in a subset of adult T-cell leukaemia, diffuse large B-cell lymphoma and stomach cancers[11]. c, Screen data as depicted in Fig. 1, but now with PD-L1 (*CD274*) data plotted when either including (*CD274*) or excluding (*CD274**) integrations downstream of exon 5 (Refseq identifier NM_014143.3). MI, mutation index.

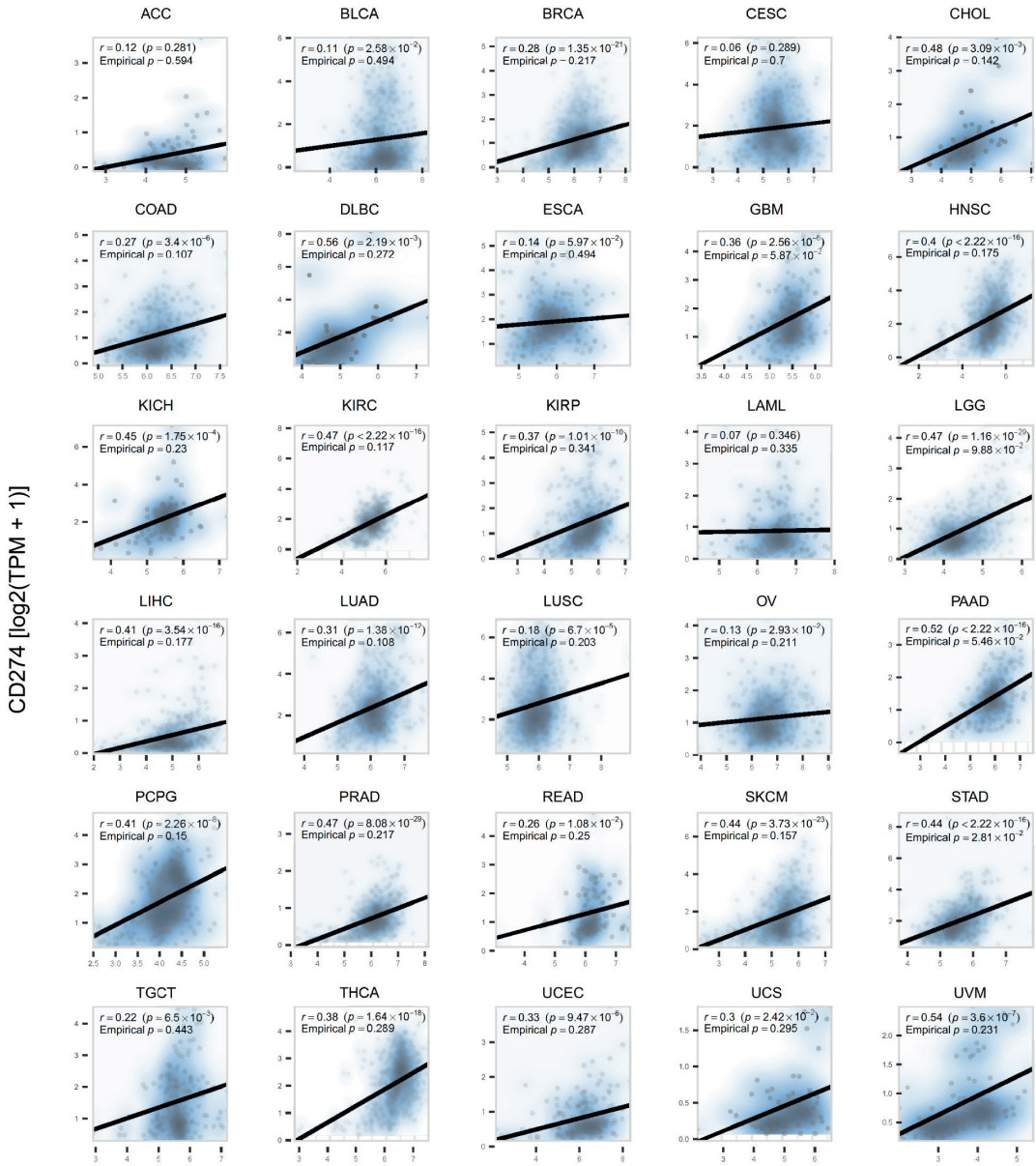
ACC
r = 0.12 (p = 0.281)
Empirical p = 0.594
BLCA
r = 0.11 (p = 2.58 × 10^-2)
Empirical p = 0.494
BRCA
r = 0.28 (p = 1.35 × 10^-21)
Empirical p = 0.217
CESC
r = 0.06 (p = 0.289)
Empirical p = 0.7
CHOL
r = 0.48 (p = 3.09 × 10^-3)
Empirical p = 0.142
COAD
r = 0.27 (p = 3.4 × 10^-6)
Empirical p = 0.107
DLBC
r = 0.56 (p = 2.19 × 10^-3)
Empirical p = 0.272
ESCA
r = 0.14 (p = 5.97 × 10^-2)
Empirical p = 0.494
GBM
r = 0.36 (p = 2.56 × 10^-5)
Empirical p = 5.87 × 10^-2
HNSC
r = 0.4 (p < 2.22 × 10^-18)
Empirical p = 0.175
KICH
r = 0.45 (p = 1.75 × 10^-4)
Empirical p = 0.23
KIRC
r = 0.47 (p < 2.22 × 10^-16)
Empirical p = 0.117
KIRP
r = 0.37 (p = 1.01 × 10^-10)
Empirical p = 0.341
LAML
r = 0.07 (p = 0.346)
Empirical p = 0.335
LGG
r = 0.47 (p = 1.16 × 10^-29)
Empirical p = 9.88 × 10^-2
LIHC
r = 0.41 (p = 3.54 × 10^-16)
Empirical p = 0.177
LUAD
r = 0.31 (p = 1.38 × 10^-12)
Empirical p = 0.108
LUSC
r = 0.18 (p = 6.7 × 10^-5)
Empirical p = 0.203
OV
r = 0.13 (p = 2.93 × 10^-2)
Empirical p = 0.211
PAAD
r = 0.52 (p < 2.22 × 10^-16)
Empirical p = 5.46 × 10^-2
PCPG
r = 0.41 (p = 2.26 × 10^-5)
Empirical p = 0.15
PRAD
r = 0.47 (p = 8.08 × 10^-29)
Empirical p = 0.217
READ
r = 0.26 (p = 1.08 × 10^-2)
Empirical p = 0.25
SKCM
r = 0.44 (p = 3.73 × 10^-23)
Empirical p = 0.157
STAD
r = 0.44 (p < 2.22 × 10^-16)
Empirical p = 2.81 × 10^-2
TGCT
r = 0.22 (p = 6.5 × 10^-3)
Empirical p = 0.443
THCA
r = 0.38 (p = 1.64 × 10^-18)
Empirical p = 0.289
UCEC
r = 0.33 (p = 9.47 × 10^-8)
Empirical p = 0.287
UCS
r = 0.3 (p = 2.42 × 10^-2)
Empirical p = 0.295
UVM
r = 0.54 (p = 3.6 × 10^-7)
Empirical p = 0.231
CD274 [log2(TPM + 1)]
CMTM6 [log2(TPM + 1)]

Extended Data Figure 2 : RNA expression of CMTM6 in human cancers and correlation with PD-L1 mRNA levels. Pearson's correlation coefficients (*r*) are shown along with associated unadjusted *P* values. Because randomly selected genes are on average also weakly positively correlated (not shown), empirical *P* values, which represent one minus the quantile of the *CMTM6*- and *CD274*-expression correlation coefficient among a reference distribution composed of correlation coefficients between *CMTM6* and randomly selected genes, are also depicted. Empirical P values smaller than 0.5 denote a stronger correlation between *CMTM6* and *CD274* than the median observed correlation in the reference distribution. TPM, transcript per million. ACC, adrenocortical carcinoma; BLCA, urothelial bladder carcinoma; BRCA, breast cancer; CESC, cervical squamous cell carcinoma; CHOL, cholangiocarcinoma; COAD, colorectal adenocarcinoma; DLBC, diffuse large B-cell lymphoma; ESCA, oesophageal cancer; GBM, glioblastoma multiforme; HNSC, head and neck squamous cancer; KICH, chromophobe renal cell carcinoma; KIRC, clear cell kidney carcinoma; KIRP, papillary kidney carcinoma; LAML, acute myeloid leukaemia; LGG, lower grade glioma; LIHC, liver hepatocellular carcinoma; LUAD, lung adenocarcinoma; LUSC, lung squamous cell carcinoma; OV, ovarian serous cystadenocarcinoma; PAAD, pancreatic ductal adenocarcinoma; PCPG, pheochromocytoma and paraganglioma; PRAD, prostate adenocarcinoma; READ, rectum adenocarcinoma; SKCM, cutaneous melanoma;, STAD, stomach cancer; TGCT, testicular germ cell cancer; THCA, papillary thyroid carcinoma; UCEC, uterine corpus endometrial carcinoma; UCS, uterine carcinosarcoma; UVM, uveal melanoma.

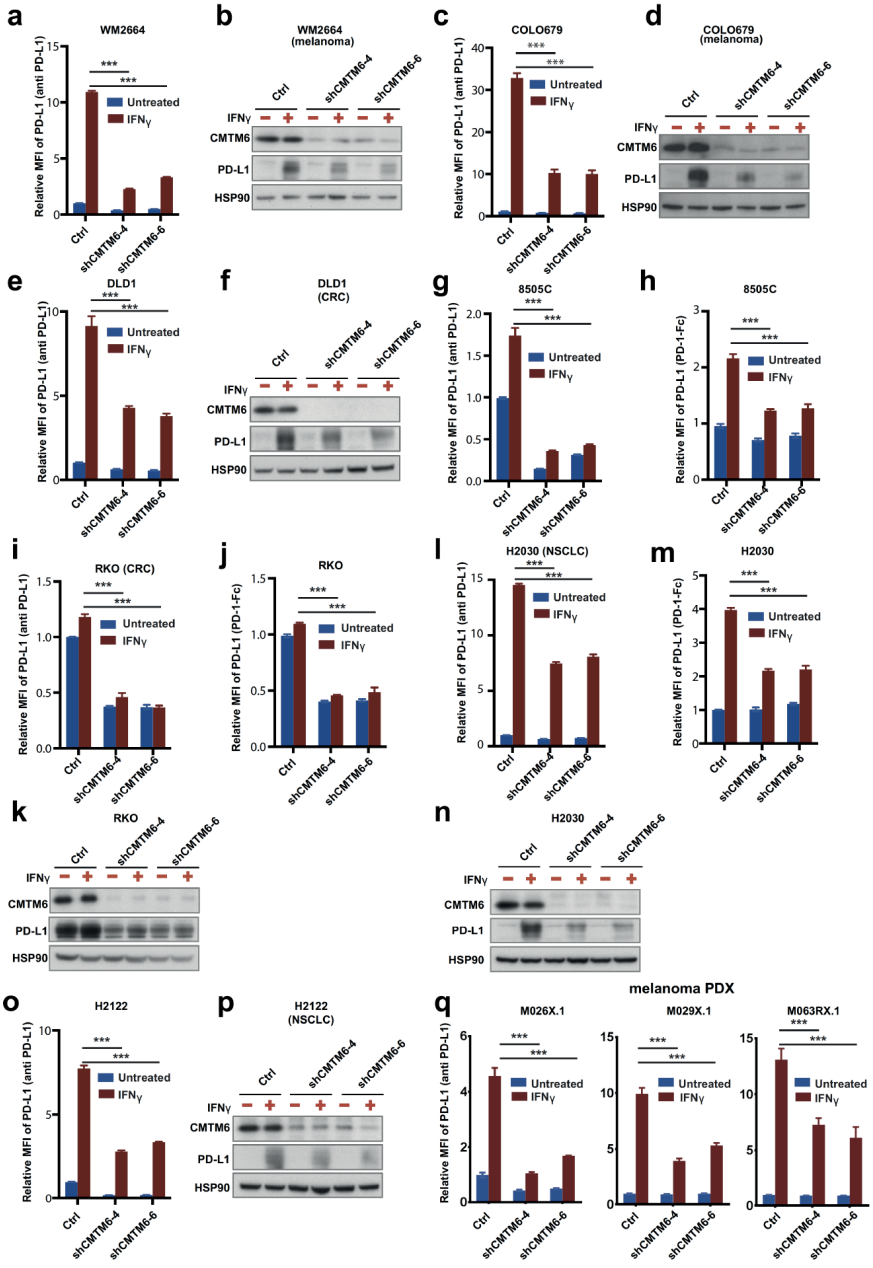
a
WM2664
Relative MFI of PD-L1 (anti PD-L1)
Untreated
IFNγ
Ctrl
shCMTM6-4
shCMTM6-6
b
WM2664 (melanoma)
IFNγ
CMTM6
PD-L1
HSP90
c
COLO679
d
COLO679 (melanoma)
e
DLD1
f
DLD1 (CRC)
g
8505C
h
Relative MFI of PD-L1 (PD-1-Fc)
i
RKO (CRC)
j
RKO
l
H2030 (NSCLC)
m
H2030
k
n
o
H2122
p
H2122 (NSCLC)
q
melanoma PDX
M026X.1
M029X.1
M063RX.1

Extended Data Figure 3 : Regulation of PD-L1 by CMTM6 in different tumour types. a, c, e, o, q, Flow cytometry analysis of PD-L1 expression in WM2664 melanoma cells (a), COLO679 melanoma cells (c), DLD1 colorectal cancer cells (e), H2122 non-small-cell lung cancer cells (o) and three short-term cultures of melanoma xenografts (q). Cells are independently transduced with two vectors expressing different *CMTM6* shRNAs and are compared with cells transduced with the control vector. b, d, f, p, Western blot analysis of *CMTM6* and PD-L1 expression in WM2664 melanoma cells (b), COLO679 melanoma cells (d), DLD1 colorectal cancer cells (f), H2122 non-small-cell lung cancer cells (p). Cells are independently transduced with two vectors expressing different *CMTM6* shRNAs and are compared with cells transduced with the control vector. g–j, l, m, Flow cytometry analysis of PD-L1 expression upon staining with anti-PD-L1 antibody or with PD-1–Fc in 8505C thyroid cancer cells (g, h), RKO colorectal cancer cells (i, j) and H2030 non-small-cell lung cancer cells (l, m). k, n, Western blot analysis of CMTM6 and PD-L1 expression in RKO colorectal cancer cells (k) and H2030 non-small cell lung cancer cells (n). Cells are independently transduced with two vectors expressing different *CMTM6* shRNAs and are compared with cells transduced with the control vector. In all cases, cells treated with IFNγ (25 ng ml−1) or left untreated were compared. g, The graph shown is identical to Fig. 2f, shown again here to facilitate comparison. Data are representative of three (c–n), two (a, b, o, p) or one (q) independent experiments and were analysed by unpaired t-test (a, c, e, g–m, o, q). Data are mean ± s.d. of triplicates (a, c, e, g–m, o, q). ***$P < 0.001$. Ctrl, control; MFI, median fluorescence intensity. CRC, colorectal cancer; NSCLC, non-small-cell lung cancer; PDX, patient-derived xenograft.

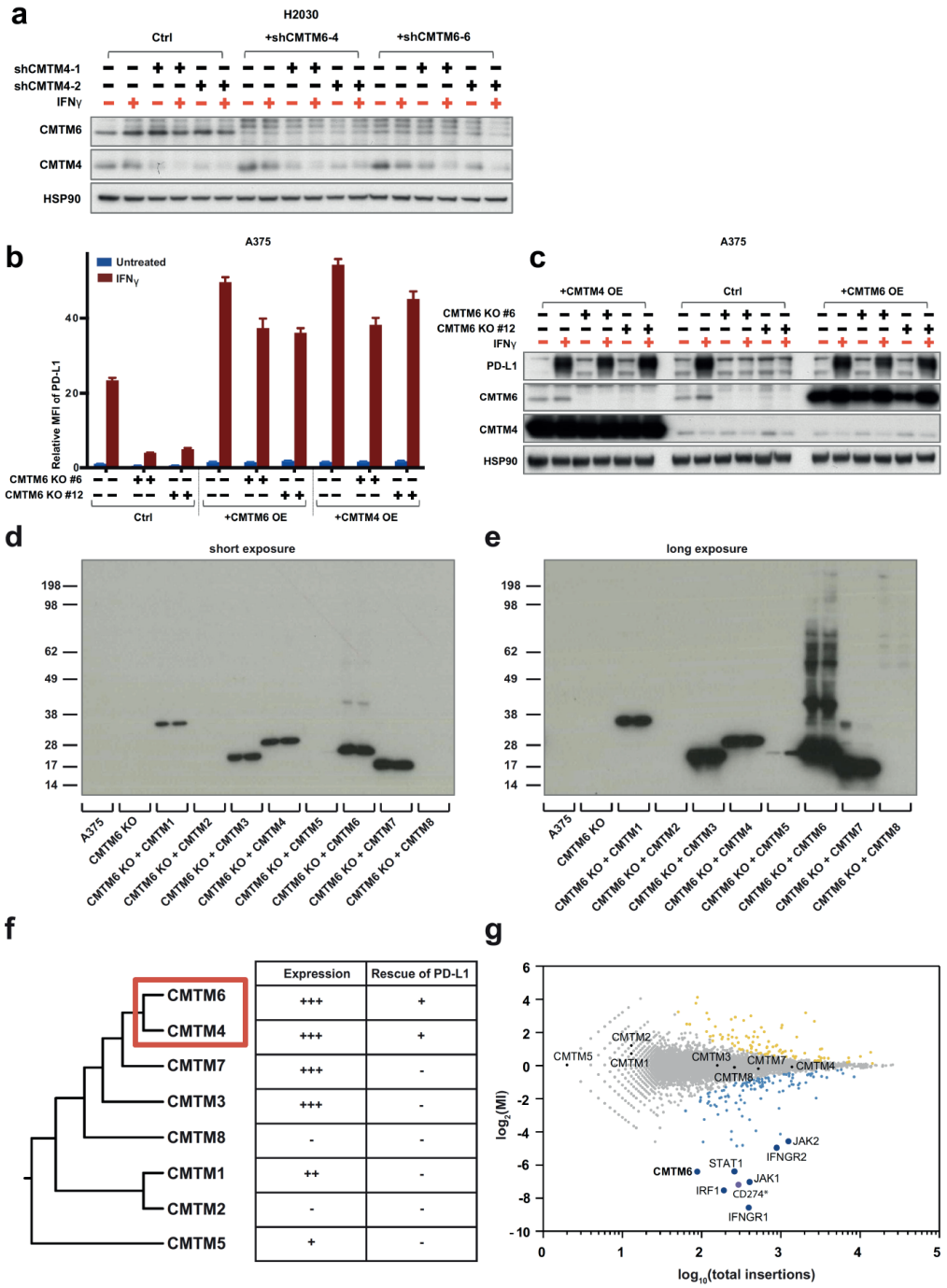
a
H2030
Ctrl
+shCMTM6-4
+shCMTM6-6
shCMTM4-1
shCMTM4-2
IFNγ
CMTM6
CMTM4
HSP90
b
A375
Untreated
IFNγ
Relative MFI of PD-L1
CMTM6 KO #6
CMTM6 KO #12
Ctrl
+CMTM6 OE
+CMTM4 OE
c
A375
+CMTM4 OE
Ctrl
+CMTM6 OE
CMTM6 KO #6
CMTM6 KO #12
IFNγ
PD-L1
CMTM6
CMTM4
HSP90
d
short exposure
198
98
62
49
38
28
17
14
A375
CMTM6 KO
CMTM6 KO + CMTM1
CMTM6 KO + CMTM2
CMTM6 KO + CMTM3
CMTM6 KO + CMTM4
CMTM6 KO + CMTM5
CMTM6 KO + CMTM6
CMTM6 KO + CMTM7
CMTM6 KO + CMTM8
e
long exposure
198
98
62
49
38
28
17
14
A375
CMTM6 KO
CMTM6 KO + CMTM1
CMTM6 KO + CMTM2
CMTM6 KO + CMTM3
CMTM6 KO + CMTM4
CMTM6 KO + CMTM5
CMTM6 KO + CMTM6
CMTM6 KO + CMTM7
CMTM6 KO + CMTM8
f
CMTM6
CMTM4
CMTM7
CMTM3
CMTM8
CMTM1
CMTM2
CMTM5
Expression
Rescue of PD-L1
+++ +
+++ +
+++ -
+++ -
- -
++ -
- -
+ -
g
log2(MI)
log10(total insertions)
CMTM5
CMTM2
CMTM1
CMTM3
CMTM7
CMTM4
CMTM8
JAK2
IFNGR2
STAT1
CMTM6
JAK1
IRF1
CD274*
IFNGR1

Extended Data Figure 4 : CMTM4 and CMTM6, but no other CMTM family members, are regulators of PD-L1. a, Validation of CMTM6 and CMTM4 downregulation by western blot analysis of cells shown in Fig. 3b. b, c, Ectopic expression of CMTM4 restores IFNγ-induced PD-L1 expression in CMTM6-deficient cells. Two clones of CMTM6-deficient A375 cells (CMTM6 KO #6 and CMTM6 KO #12) were transduced with retroviral vectors encoding CMTM4 (CMTM4 OE) or CMTM6 (CMTM6 OE) individually. After blasticidin selection, cells were cultured in the absence (untreated) or presence of 25 ng ml^{-1} IFNγ for 72 h before flow cytometry (b) and western blot (c) analysis. Untransduced A375 parental cells served as controls. d, e, Western blot analysis of expression of the indicated CMTM family members, as determined by staining with an anti-Flag antibody. Two exposures of the same gel are shown. Expression of CMTM2 and CMTM8 is not detected and CMTM5 expression is low compared to that of other CMTM family members. f, Phylogenetic analysis of the CMTM family by CLUSTALW. CMTM6 and CMTM4 form the two most closely related members. In view of the lack of detectable expression/low expression observed for CMTM2, CMTM8 and CMTM5, an effect of these CMTM members on PD-L1 protein fate cannot be excluded. However, the observation that CMTM family members 7 and 3, which are more closely related to CMTM4 and CMTM6, do not influence PD-L1 expression makes this unlikely. g, Results of the flow-cytometry-based screen as shown in Fig. 1a, with the position of all CMTM family members indicated. Data are representative of two independent experiments (a–e). Data are mean ± s.d. of triplicates (b). KO, knockout; MFI, median fluorescence intensity; MI, mutation index; OE, overexpression.

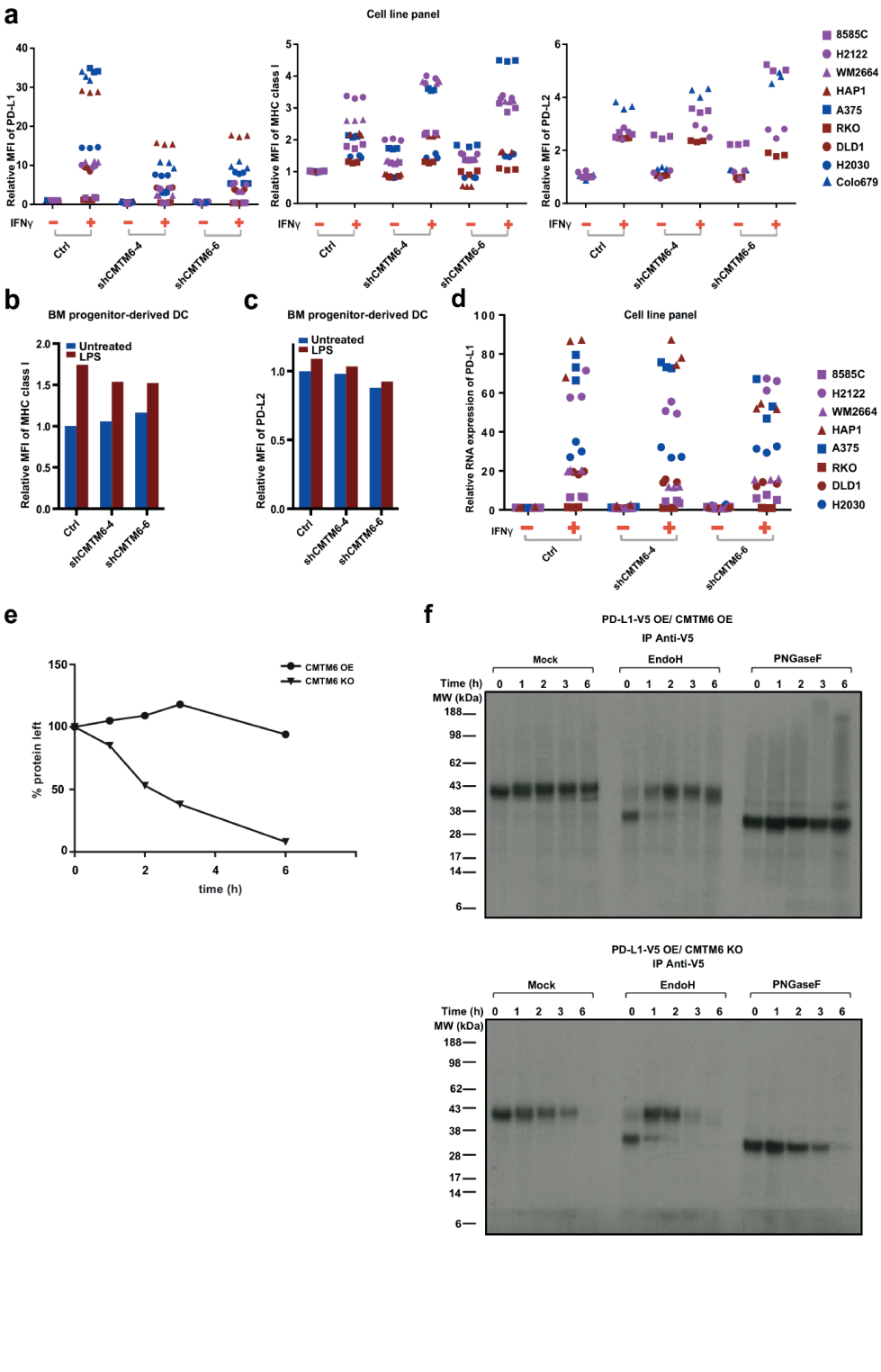
a
Cell line panel
Relative MFI of PD-L1
Relative MFI of MHC class I
Relative MFI of PD-L2
IFNγ
Ctrl
shCMTM6-4
shCMTM6-6
8585C
H2122
WM2664
HAP1
A375
RKO
DLD1
H2030
Colo679
b
BM progenitor-derived DC
Untreated
LPS
Relative MFI of MHC class I
c
BM progenitor-derived DC
Relative MFI of PD-L2
d
Cell line panel
Relative RNA expression of PD-L1
e
CMTM6 OE
CMTM6 KO
% protein left
time (h)
f
PD-L1-V5 OE/ CMTM6 OE
IP Anti-V5
Mock
EndoH
PNGaseF
Time (h)
MW (kDa)
188
98
62
43
38
28
17
14
6
PD-L1-V5 OE/ CMTM6 KO
IP Anti-V5

Extended Data Figure 5 : CMTM6 downregulation does not affect MHC class I and PD-L2 cell-surface levels or PD-L1 mRNA levels and regulates PD-L1 stability after egress from the endoplasmic reticulum. a–c, Flow cytometry analysis of MHC class I and PD-L2 expression in the panel of cell lines tested in Fig. 2 and Extended Data Fig. 3 (a), and in bone marrow progenitor-derived dendritic cells (b, c) in which cells transduced with the control vector are compared with cells independently transduced with two vectors expressing different shRNA directed against *CMTM6*. For cell lines, cells treated with IFNγ (as indicated in the other figure legends) or left untreated were compared, for bone marrow progenitor-derived dendritic cells, cells treated with 500 ng ml^{-1} LPS or left untreated were compared. d, qPCR analyses were performed to quantify relative mRNA levels of PD-L1 in the indicated tumour cell lines. e, Quantification of the experiment shown in Fig. 4c. f, Immunoprecipitates of the samples used in Fig. 4c. Samples were mock-treated, treated with EndoH or with PNGaseF to examine the kinetics of protein maturation. No difference in maturation kinetics was observed between CMTM6-overexpressing and CMTM6-deficient cells. Pulse–chase experiments were performed three times, once comparing CMTM6-overexpressing and CMTM6-deficient cells (a) and twice comparing wild-type and CMTM6-deficient cells. Other data are representative of at least two independent experiments. BM, bone marrow; DC, dendritic cell; EndoH, endoglycosidase H; KO, knockout; MFI, median fluorescence intensity; OE, overexpression; PNGaseF, peptide-N-glycosidase F.

a

Cell line	Uniprot accession	Protein name	Gene name	Unique peptides	Mol. weight [kDa]	Sequence length	MS/MS count					Sequence coverage [%]	LFQ intensity
							[F1] Cytosolic	[F2] Cytosolic SCX FT	[F3] Inner memb	[F4] Plasma memb	Total in 4 fractions		
8505c_WT	Q9NX76	CKLF-like MARVEL transmembrane domain-containing protein 6	CMTM6	3	20.419	183	1	2	4	7	14	21.3	6.49E+08
	Q9NZQ7	Programmed cell death 1 ligand 1	CD274	6	33.275	290	10	2	14	38	64	32.1	9.54E+09
RKO_WT	Q9NX76	CKLF-like MARVEL transmembrane domain-containing protein 6	CMTM6	3	20.419	183	1	0	2	6	9	21.3	2.77E+08
	Q9NZQ7	Programmed cell death 1 ligand 1	CD274	6	33.275	290	5	4	20	20	49	32.1	6.70E+09

b

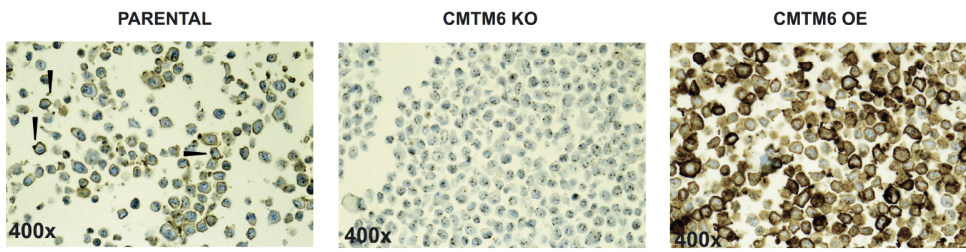

c

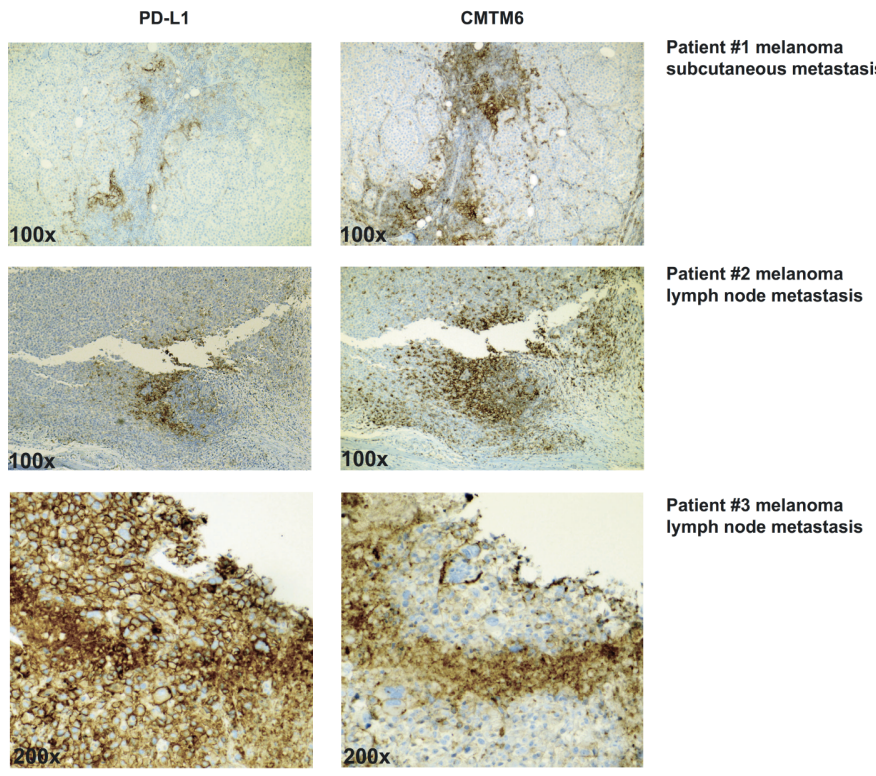

Extended Data Figure 6 : Specificity and membrane localization of CMTM6, and co-localization with PD-L1 in human tumours. a, Membrane-fractionated proteome of 8505C and RKO cells. CMTM6 and PD-L1 were detected by LC–MS/MS predominantly from the plasma membrane fractions. Label-free quantification (LFQ) performed by intensity-based normalization of four fractions together across different cell lines is depicted. b, A375 parental cells, CMTM6-knockout or CMTM6-overexpressing cells were fixed and formalin embedded, and stained for CMTM6 with a monoclonal antibody (clone RCT6) generated against a peptide from the C-terminal domain of CMTM6. Analysis shows a mainly membranous stain, as indicated by the arrowheads. c, Sequential slides from lymph node and subcutaneous metastases from three melanoma patients were stained for PD-L1 (left) or CMTM6 (right), showing frequent localization of PD-L1 within $CMTM6^{+}$ areas. In total, samples from nine melanoma patients and five $PD\text{-}L1^{+}$ lung cancer samples were analysed. KO, knockout; OE, overexpression.

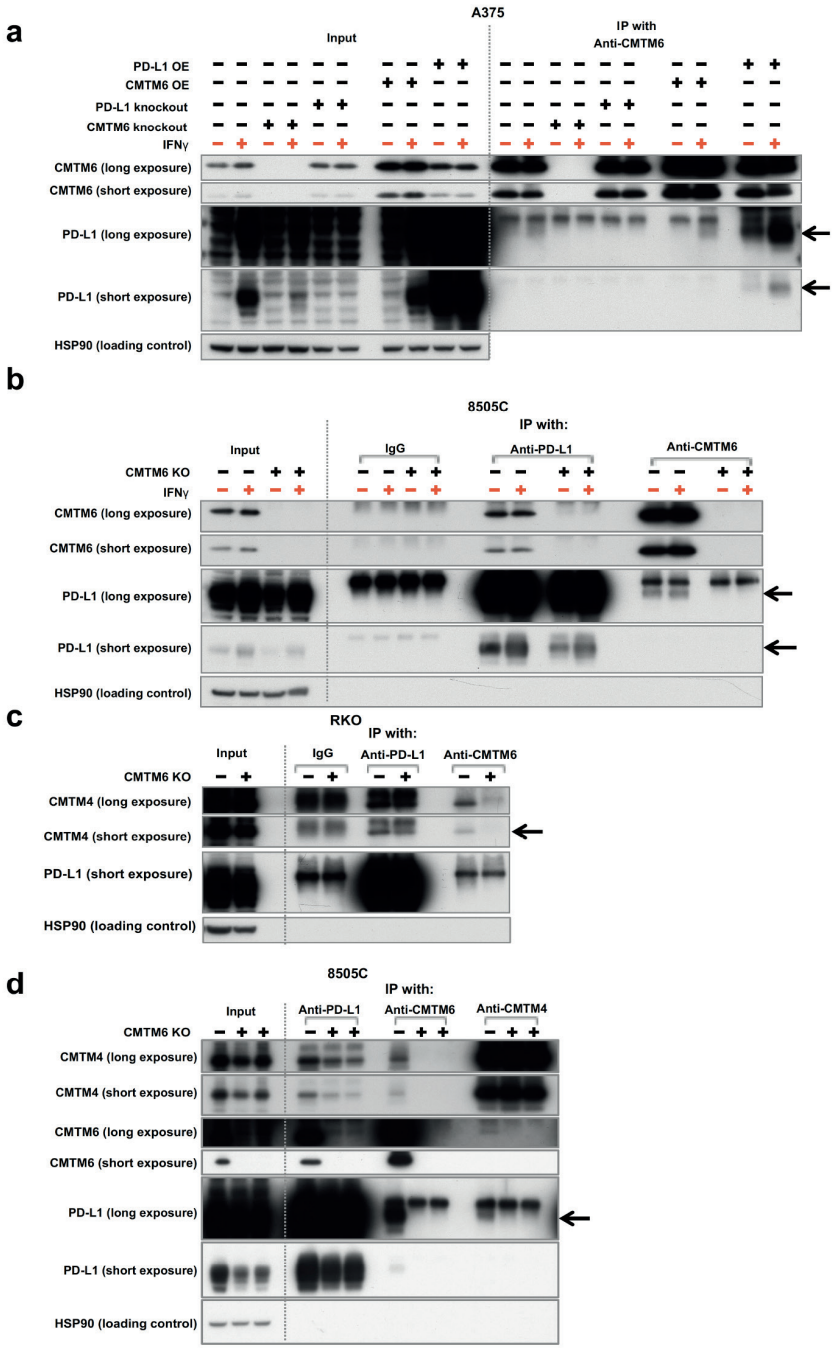
a
A375
Input
IP with
Anti-CMTM6
PD-L1 OE
CMTM6 OE
PD-L1 knockout
CMTM6 knockout
IFNγ
CMTM6 (long exposure)
CMTM6 (short exposure)
PD-L1 (long exposure)
PD-L1 (short exposure)
HSP90 (loading control)
b
8505C
IP with:
Input
IgG
Anti-PD-L1
Anti-CMTM6
CMTM6 KO
IFNγ
CMTM6 (long exposure)
CMTM6 (short exposure)
PD-L1 (long exposure)
PD-L1 (short exposure)
HSP90 (loading control)
c
RKO
IP with:
Input
IgG
Anti-PD-L1
Anti-CMTM6
CMTM6 KO
CMTM4 (long exposure)
CMTM4 (short exposure)
PD-L1 (short exposure)
HSP90 (loading control)
d
8505C
IP with:
Input
Anti-PD-L1
Anti-CMTM6
Anti-CMTM4
CMTM6 KO
CMTM4 (long exposure)
CMTM4 (short exposure)
CMTM6 (long exposure)
CMTM6 (short exposure)
PD-L1 (long exposure)
PD-L1 (short exposure)
HSP90 (loading control)

Extended Data Figure 7 : Interactions between CMTM6, PD-L1 and CMTM4, and effect of CMTM6 on PD-L1 stability. a, A375 parental cells, CMTM6-deficient cells, PD-L1-deficient cells and cells ectopically expressing CMTM6 or PD-L1, were cultured in the absence or presence of 25 ng ml^{-1} IFNγ for 48 h before preparation of cell lysates. Immunoprecipitation was performed using a CMTM6-specific antibody immobilized on protein-A-coated beads. Immunoprecipitates and whole cell lysate were subjected to SDS–PAGE and immunoblotted for CMTM6 and PD-L1. Two exposures of the same western blot are shown. Arrows indicate PD-L1 bands. b, Parental and CMTM6-deficient 8505C cells were cultured in the absence or presence of 50 ng ml^{-1} IFNγ for 72 h before preparation of cell lysates. Immunoprecipitation was performed using $CMTM6^{-}$ or PD-L1-specific antibodies immobilized on protein-A-coated beads. Immunoprecipitates and whole cell lysates were subjected to SDS–PAGE and immunoblotted for CMTM6 and PD-L1. Two exposures of the same western blot are shown. Normal IgG served as a control. Arrows indicate PD-L1 bands. c, d, Parental and CMTM6-knockout RKO cells (c) and 8505C cells (d) were lysed and immunoprecipitation was performed using antibodies immobilized on protein-G-coated beads as indicated. Immunoprecipitates and whole-cell lysates were subjected to SDS–PAGE, and western blot analysis of CMTM4 and PD-L1 expession was carried out. Two exposures of the same western blots are shown. Arrows indicate CMTM4 (c) or PD-L1 (d). Data are representative of three independent experiments. KO, knockout; OE, overexpression.

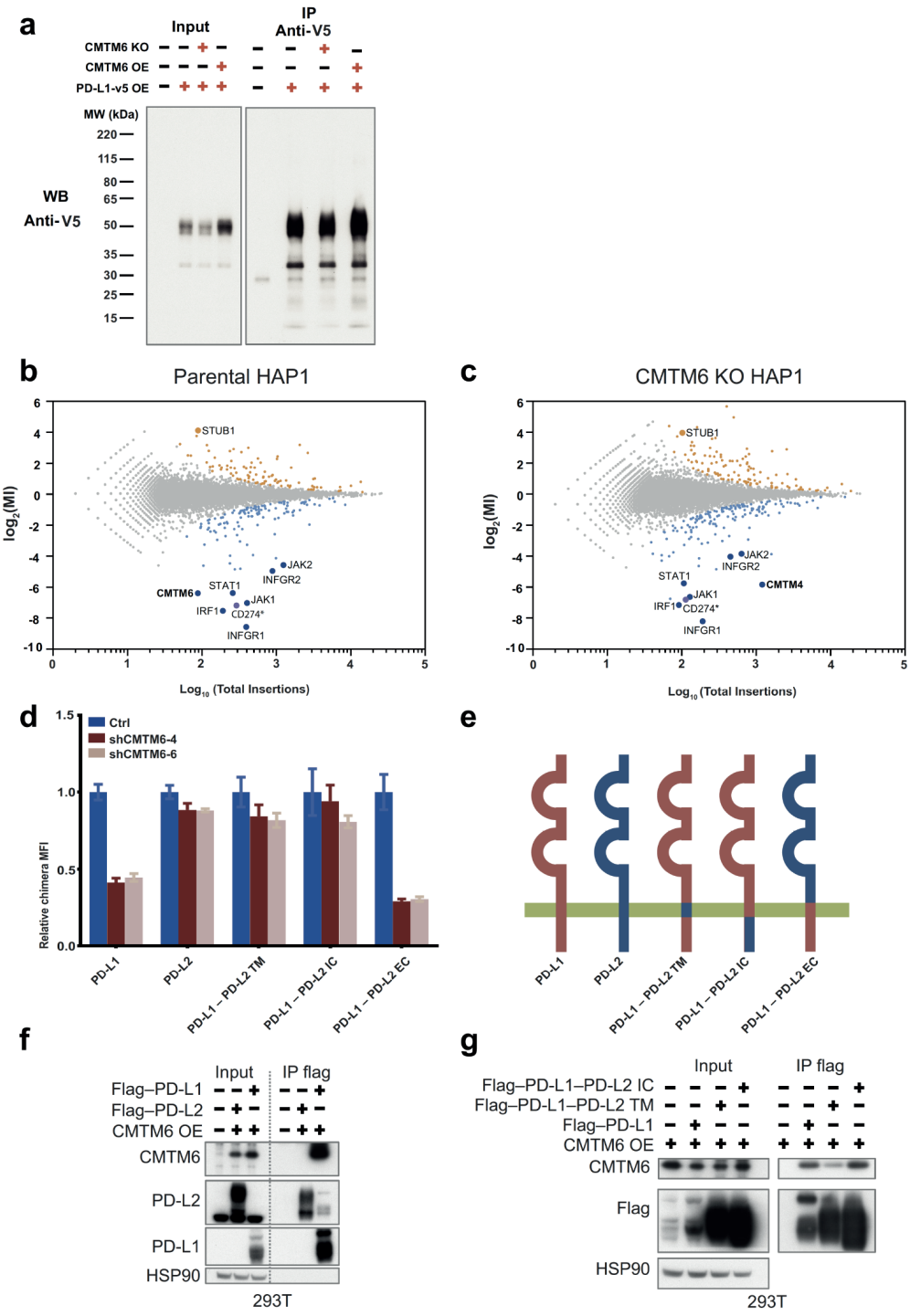
a
Input
IP
Anti-V5
CMTM6 KO
CMTM6 OE
PD-L1-v5 OE
MW (kDa)
220
115
80
65
50
35
30
25
15
WB
Anti-V5
b
Parental HAP1
log2(MI)
Log10 (Total Insertions)
STUB1
JAK2
INFGR2
STAT1
CMTM6
JAK1
IRF1
CD274*
INFGR1
c
CMTM6 KO HAP1
log2(MI)
Log10 (Total Insertions)
STUB1
JAK2*
INFGR2
STAT1
CMTM4
JAK1
IRF1
CD274*
INFGR1
d
Ctrl
shCMTM6-4
shCMTM6-6
Relative chimera MFI
PD-L1
PD-L2
PD-L1 – PD-L2 TM
PD-L1 – PD-L2 IC
PD-L1 – PD-L2 EC
e
PD-L1
PD-L2
PD-L1 – PD-L2 TM
PD-L1 – PD-L2 IC
PD-L1 – PD-L2 EC
f
Input
IP flag
Flag–PD-L1
Flag–PD-L2
CMTM6 OE
CMTM6
PD-L2
PD-L1
HSP90
293T
g
Input
IP flag
Flag–PD-L1–PD-L2 IC
Flag–PD-L1–PD-L2 TM
Flag–PD-L1
CMTM6 OE
CMTM6
Flag
HSP90
293T

Extended Data Figure 8 : Aspects of PD-L1 regulation by CMTM6 and STUB1. a, V5-tagged PD-L1 was introduced into parental, CMTM6-overexpressing and CMTM6-deficient A375 cells. Cell lysates were denatured and then subjected to immunoprecipitation with anti-V5 antibody immobilized on protein-G-coated beads. Immunoprecipitates were then analysed by immunoblotting with an anti-V5 antibody as a control for the experiments shown in Fig. 4e. b, c, Results of the FACS-based genetic screens in CMTM6-expressing and CMTM6-deficient HAP1 cells as shown in Fig. 1a (b) and in Fig. 3a (c), with the position of STUB1 indicated. d, Relative expression of PD-L1, PD-L2 and the indicated PD-L1–PD-L2 chimaeric proteins in CMTM6 knockdown A375 cells compared to matched control. Chimaeras were detected with an anti-PD-L1 or an anti-PD-L2 antibody. e, Schematic overview of the chimaeric proteins analysed. f, g, HEK293T human embryonic kidney cells were co-transfected with a vector encoding either PD-L1, PD-L2 or the indicated chimaeric protein, together with a vector encoding CMTM6. Cell lysates were denatured and subjected to immunoprecipitation with anti-Flag antibody immobilized on protein-G-coated beads. Lysates and immunoprecipitates were then analysed by immunoblotting with the indicated antibodies. Data are representative of three (a, d), one (f) or two (g) independent experiments. Data represent mean ± s.d. of triplicates. EC, extracellular; IC, intracellular; KO, knockout; MFI, median fluorescence intensity; OE, overexpression; TM, transmembrane.

a

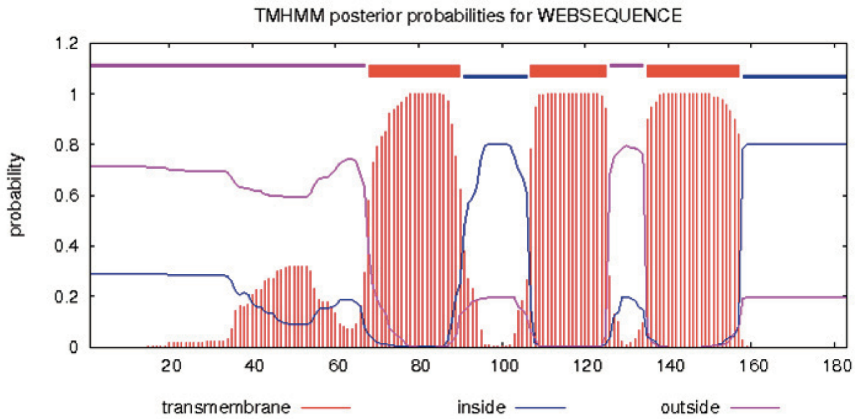
TMHMM posterior probabilities for WEBSEQUENCE
probability
1.2
1
0.8
0.6
0.4
0.2
0
20
40
60
80
100
120
140
160
180
transmembrane
inside
outside

b

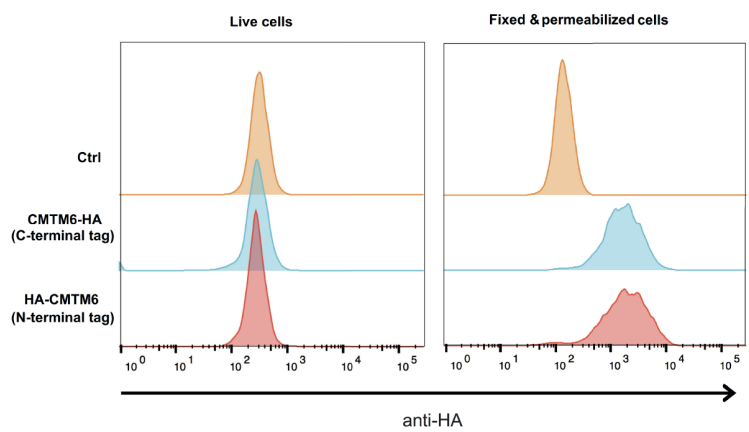
Live cells
Fixed & permeabilized cells
Ctrl
CMTM6-HA
(C-terminal tag)
HA-CMTM6
(N-terminal tag)
anti-HA

c

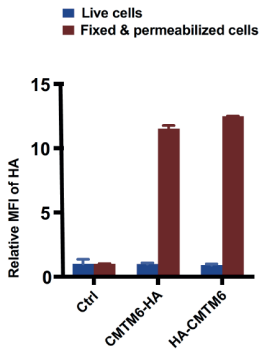
Live cells
Fixed & permeabilized cells
Relative MFI of HA
15
10
5
0
Ctrl
CMTM6-HA
HA-CMTM6

Extended Data Figure 9 : Orientation mapping of CMTM6. a, Predicted domain topology of CMTM6 according to TMHMM Server v. 2.0 (http://www.cbs.dtu.dk/services/TMHMM/). b, c, A375 cells were transduced with C- or N-terminal haemagglutinin (HA)-epitope-tagged CMTM6. HA-epitope tag staining was performed in both live cells and fixed and permeabilized cells followed by flow cytometry analysis and quantified in c. Data represent mean ± s.d. of triplicates. MFI, median fluorescence intensity.

a

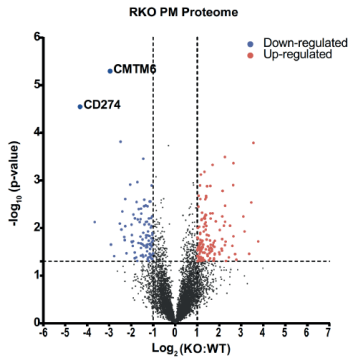

b

No.	Uniprot Accession	Protein name	Gene name	8505 Ave Log2 Intensity [4WT]	8505 Ave Log2 Intensity [4KO]	8505 Fold change [KO:WT]	8505 T.Test p-value [KO:WT]	RKO Ave Log2 Intensity [4WT]	RKO Ave Log2 Intensity [4KO]	RKO Fold change [KO:WT]	RKO T.Test p-value [KO:WT]
1	Q9NZQ7	Programmed cell death 1 ligand 1	CD274	27.05	22.72	0.05	2.84E-05	23.45	28.35	0.03	1.09E-06
2	Q9NX76	CKLF-like MARVEL transmembrane domain-containing protein 6	CMTM6	25.56	22.60	0.13	5.10E-06	22.91	25.35	0.18	2.96E-06
3	A0A024R7X0	Brefeldin A-inhibited guanine nucleotide-exchange protein 1	ARFGEF1	25.74	23.34	0.19	4.50E-03	26.25	27.52	0.41	2.89E-02
4	B5MCA4	Epithelial cell adhesion molecule	EPCAM	23.74	22.64	0.47	6.22E-03	22.92	26.22	0.10	2.91E-03
5	A0A024RDG9	3-hydroxybutyrate dehydrogenase type 2	BDH2	22.62	23.68	2.08	4.27E-02	23.28	22.25	2.04	3.32E-02
6	A0A0G2JN29	Nodal modulator 1	NOMO1	22.94	24.08	2.20	2.47E-03	23.24	21.83	2.66	1.20E-02
7	B4E3Q1	Calsyntenin-1	CLSTN1	22.49	23.65	2.24	7.58E-04	23.64	22.21	2.69	2.16E-02
8	H3BPB8	Mannose-6-phosphate isomerase	MPI	25.32	26.55	2.35	1.85E-02	25.13	22.54	6.02	4.51E-03
9	B3KN28	Phosphoacetylglucosamine mutase	PGM3	24.19	25.44	2.38	4.27E-02	25.18	22.09	8.53	3.26E-04
10	V9HWB7	Aconitate hydratase	HEL60	27.52	28.89	2.58	2.51E-03	24.78	23.20	2.98	4.25E-02
11	X5D2M8	Major vault protein	MVP	28.64	30.90	4.77	3.23E-04	24.11	22.11	3.98	4.12E-02

c

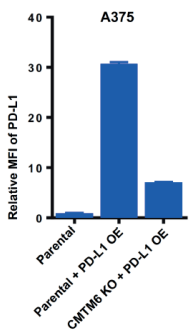

d

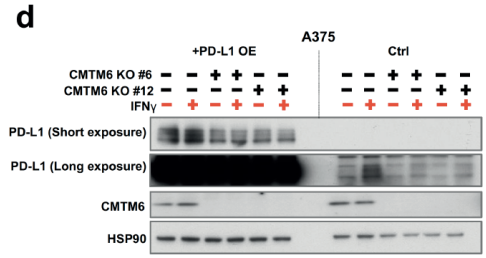

e

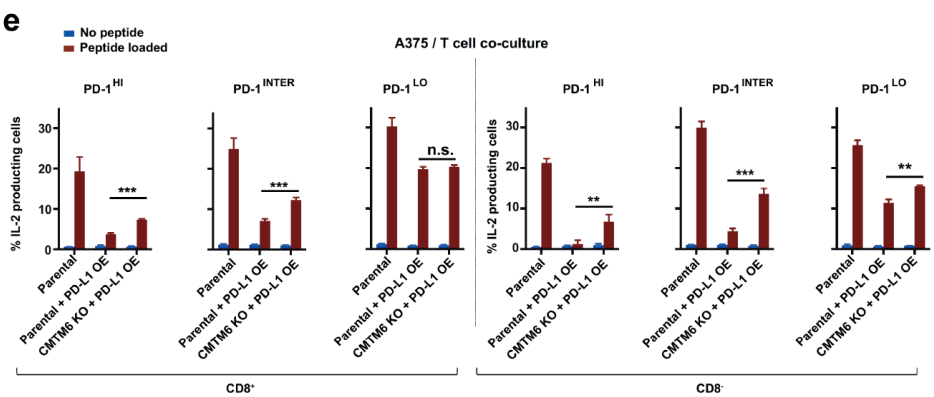

Extended Data Figure 10 : Selectivity of CMTM6 and CMTM6 loss alleviates PD-L1-mediated T-cell suppression. a, Comparative membrane-fractionated mass spectrometry of CMTM6-proficient or -deficient RKO cells. Four wild-type and four CMTM6-knockout RKO clones were analysed by LC–MS/MS and differential protein abundance is shown in a volcano plot. b, Proteins found up- or downregulated upon CMTM6 removal in both 8505C and RKO cells. c, d, Flow cytometry (c) and western blot (d) analysis of CMTM6 and PD-L1 expression in parental A375 or CMTM6-deficient A375 clones in which PD-L1 is ectopically expressed by lentiviral transduction. e, Primary human T cells were transduced with the MART-1-specific 1D3 TCR[31] and PD-1. Transduced T cells were co-cultured with unloaded or MART-I peptide-loaded PD-L1-overexpressing A375 cells (Parental + PD-L1 OE), parental A375 cells (Parental) or CMTM6-deficient A375 cells that overexpressed PD-L1 (CMTM6 KO + PD-L1 OE). IL-2 production in T cells that expressed high (PD-1high), intermediate (PD-1^{inter}) or low (PD-1^{low}) levels of PD-1 were analysed by flow cytometry. Untransduced A375 cells (Parental) served as controls. Data are representative of three independent experiments and were analysed by unpaired t-test (c). Data represent mean ± s.d. of triplicates. $^{**}P < 0.01$; $^{***}P < 0.001$; NS, not significant. KO, knockout; OE, overexpression; PM, plasma membrane; TM, transmembrane; WT, wild type.

Chapter 7

SLFN11 can sensitize toward T cell-dependent IFN-γ-induced toxicity

Riccardo Mezzadra[*,1], Marjolein de Bruijn[*,1], Lucas T Jae[2,3], Raquel Gomez-Eerland[1], Thijn R. Brummelkamp[2,4] and Ton N. Schumacher[1,#]

[1] Division of Molecular Oncology & Immunology, The Netherlands Cancer Institute, Plesmanlaan 121, 1066 CX Amsterdam, The Netherlands
[2] Division of Biochemistry, The Netherlands Cancer Institute, Plesmanlaan 121, 1066 CX Amsterdam, The Netherlands
[3] Present address: Gene Center and Department of Biochemistry, Ludwig-Maximilians-Universität München, Feodor-Lynen-Straße 25, 81377 Munich, Germany.
[4] CeMM Research Center for Molecular Medicine of the Austrian Academy of Sciences, 1090 Vienna, Austria
[5] Cancergenomics.nl, Plesmanlaan 121, 1066 CX Amsterdam, The Netherlands.

[*] These authors contributed equally to this work.
[#] Correspondence to t.schumacher@nki.nl

Submitted for publication

Experimental and clinical observations have highlighted the role of cytotoxic T cells in human tumor control. However, the parameters that control tumor cell sensitivity to T cell attack remain incompletely understood. To identify modulators of tumor cell sensitivity to T cell effector mechanisms, we performed a whole genome haploid screen in HAP1 cells. Selection of tumor cells by exposure to tumor-specific T cells identified components of the interferon-γ (IFN-γ) receptor (IFNGR) signaling pathway, and tumor cell killing by cytotoxic T cells was shown to be in large part mediated by the pro-apoptotic effects of IFN-γ. Notably, we identified schlafen 11 (SLFN11), a known modulator of DNA damage toxicity, as a regulator of tumor cell sensitivity to T cell-secreted IFN-γ. SLFN11 does not influence IFNGR signaling, but couples IFNGR signaling to the induction of the DNA damage response (DDR) in a context dependent fashion. In line with this role of SLFN11, loss of SLFN11 can reduce IFN-γ mediated toxicity. Collectively, our data indicate that SLFN11 can couple IFN-γ exposure of tumor cells to DDR and cellular apoptosis. Future work should reveal the mechanistic basis for the link between IFNGR signaling and DNA damage response, and identify tumor cell types in which SLFN11 contributes to the anti-tumor activity of T cells.

Introduction

Immunotherapeutic approaches are emerging as a revolutionary class of cancer therapeutics with clinical benefits across a series of cancer types. Specifically, infusion of antibodies blocking the action of the T cell inhibitory molecules CTLA-4 and PD-1 has shown clinical benefit in, amongst others, melanoma, non-small cell lung cancer, and urothelial carcinoma (1,2). Furthermore, direct evidence for T cell-mediated tumor regression comes from adoptive T cell transfer studies using tumor-infiltrating lymphocytes (TIL) for melanoma (3), and chimeric antigen receptor (CAR)-modified T cells for B cell malignancies (4). Despite these impressive clinical results, a large fraction of patients does not benefit from current immunotherapies and relapses are common, motivating a search for mechanisms that influence tumor cell sensitivity to T cell effector mechanisms. In recent work, selection of inactivating mutations in genes in the IFNGR signaling pathway and antigen presentation pathway was shown to occur in tumors that relapsed after PD-1 blockade (5). Likewise, mutations in the IFNGR pathway have been observed in tumors not responding to CTLA-4 (6) and PD-1 (7) blockade. In line with these data, inactivation of components of the IFNGR pathway and antigen presentation machinery were identified in recent CRISPR-based genetic screens aimed at the unbiased exploration of tumor cell resistance mechanisms towards T cell attack (8-11). The loss of components of the antigen presentation machinery is readily explained by the selective survival of tumor cells that no longer present T cell-recognized antigens. However, loss of components of the IFNGR signaling pathway may be explained in different ways. First, by modulating the expression of genes in the antigen processing and antigen presentation pathway, impaired IFNGR signaling may reduce presentation of tumor antigens (12). Second, IFN-γ has also been shown to have direct cytopathic effects on a subset of human cells, but mechanisms that lead to this effect have only partly been elucidated (13).

In this study, we performed a haploid genetic screen to identify tumor cell resistance mechanisms to T cell killing. Using this approach, we identified the direct cytotoxic effect of IFN-γ as a major effector mechanism of T cells in this system. Surprisingly, we identified SLFN11, an IFN-inducible gene previously shown to influence tumor cell sensitivity to DNA damaging agents (DDA), as a modulator of HAP1 sensitivity to T cell attack (14,15). Notably, interference with SLFN11 expression reduced sensitivity of HAP1 to both IFN-γ and DNA damaging agents. In contrast, in cell lines that showed a much lower sensitivity to IFN-γ-induced cell death, interference with SLFN11 expression reduced their sensitivity to DNA damaging agents but not IFN-γ. Evidence for a link between IFNGR signaling and DDR was provided by the observation of IFN-γ-induced phosphorylation of H2AX. Collectively, our data reveal an unexpected link

between a known DNA damage response modulator and sensitivity of tumor cells to cytotoxic T cell attack.

Results

A haploid genetic screen for resistance mechanisms to T cell killing

In order to identify cancer cell-intrinsic mechanisms of resistance to T cell-mediated cytotoxicity, we set up a whole-genome loss-of-function haploid cell screen. To generate a system in which tumor cells can be exposed to defined T cell pressure, the HLA-A2-positive haploid human cell line HAP1 (16) was modified to express the HLA-A2-restricted MART-1$_{(26\text{-}35,\ 27\ A>L)}$ epitope. Subsequently, a library of loss-of-function mutant cells was generated by transduction with a gene-trap vector, and this mutant cell library was exposed to T cells transduced with the MART-1$_{(26\text{-}35,\ 27\ A>L)}$-specific 1D3 TCR (17). After 24h of co-culture, T cells were removed and surviving cells were expanded. Subsequently, gene-trap vector integration sites were sequenced in order to identify genes whose loss conferred resistance to T cell attack, as depicted in figure 1A. In line with recent data obtained in patients developing resistance to T cell checkpoint blockade and data obtained in CRISPR-based in vitro and in vivo screens (5-11), all canonical components of the IFNGR pathway (18) were identified as dominant hits. In addition, a single IFN-γ-induced gene was identified as a recurrent integration site in T cell resistant HAP1 cells, the putative DNA/RNA helicase SLFN11 (schematized in Fig 1B and data not shown (15)). Notably, contrary to other studies, none of the components of the antigen presenting machinery was identified as a dominant hit, suggesting that in this system impaired presentation of antigen by a tumor cell clone forms less of a selective advantage than impaired IFNGR signaling.

IFN-γ-mediated T cell toxicity is alleviated by SLFN11 loss in HAP1 cells

To directly test the contribution of the IFNGR pathway on T cell mediated killing of HAP1 cells, we generated IFNGR1 KO HAP1 cells using CRISPR-Cas9 and exposed these cells to T cells at different effector: target cell ratios. In line with the results from the haploid genetic screen, HAP1 cell sensitivity to T cells was highly reduced by IFNGR deficiency (Fig 2A). To evaluate whether SLFN11 also influences sensitivity of HAP1 cells towards T cell-mediated toxicity, SLFN11 deficient HAP1 cells were generated and exposed to tumor-specific T cells. Comparison of survival of SLFN11-deficient and -proficient clones demonstrated that the SLFN11 putative DNA/RNA helicase enhances sensitivity of HAP1 cells to T cell-mediated cytotoxicity (Fig 2B). To subsequently assess through which pathway SLFN11 determines the outcome of T cell recognition of tumor cells, we first exposed either SLFN11-proficient or SLFN11-

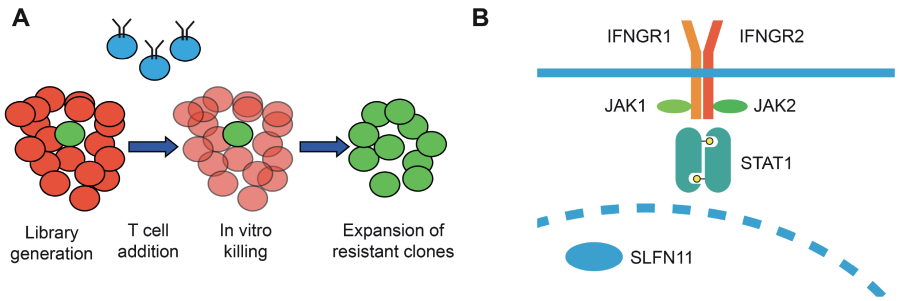

Figure 1. A haploid genetic screen for resistance to T cell mediated killing.
A) Experimental scheme: A library of gene trap-mutagenized haploid HAP1 cells was generated, in which most cells harbor irrelevant mutations (red) and rare cells harbor mutations that reduce their sensitivity towards T cell killing (green). Upon exposure to T cells (depicted in blue), cells with reduced sensitivity are positively selected and, following expansion, integration sites in the surviving cell population are analyzed. B) List of most significantly enriched hits. Yellow: components of the IFNGR signaling pathway; green: SLFN11.

deficient HAP1 cells to IFN-γ. Both in a 7-day clonogenic assay (Fig 2C), and in a short-term cell survival assay (Fig 2D), the dose-dependent toxicity of IFN-γ in HAP1 cells was mitigated by inactivation of SLFN11. By the same token, knockdown (KD) of SLFN11 using shRNA resulted in increased cell survival following IFN-γ exposure (Fig 2E-F). To evaluate whether the sensitivity toward T cell cytotoxicity that is conferred by SLFN11 is fully explained by IFN-γ-mediated toxicity, we disrupted SLFN11 in IFNGR1 KO cells. In cells with impaired IFNGR signaling, inactivation of SLFN11 did not influence sensitivity to T cells, indicating that SLFN11 exclusively operates by sensitizing tumor cells toward IFN-γ-mediated toxicity (Supplementary Fig 1). SLFN11 has previously been shown to block DNA replication in situations of replication stress (19,20). However, the substantial drop in cell numbers in a short time frame following IFN-γ exposure of SLFN11-proficient cells was more suggestive of active programmed cell death. To test this, HAP1 cells were exposed to IFN-γ in the presence or absence of either necrostatin, a RIPK1 inhibitor that prevents necroptosis, or Q-VD-OPh, a pan-caspase inhibitor that prevents apoptosis. Whereas necrostatin treatment did not noticeably enhance cell survival upon IFN-γ exposure, Q-VD-OPh almost completely prevented IFN-γ-induced toxicity, indicating that caspase-dependent programmed cell death is a dominant mechanism of IFN-γ in this context (Fig 2G). Subsequently, we tested whether IFN-γ can still impact long-term tumor cell proliferation when apoptosis is blocked. To this purpose, we exposed HAP1 cells to IFN-γ in the presence or absence of Q-VD-OPh for a 24 hour period and evaluated growth kinetics (experimental scheme in Fig. 3A). When cells were left untreated or exposed to Q-VD-OPh only, exponential cell expansion was observed. When cells were exposed to IFN-γ for 24 h in the absence of the caspase

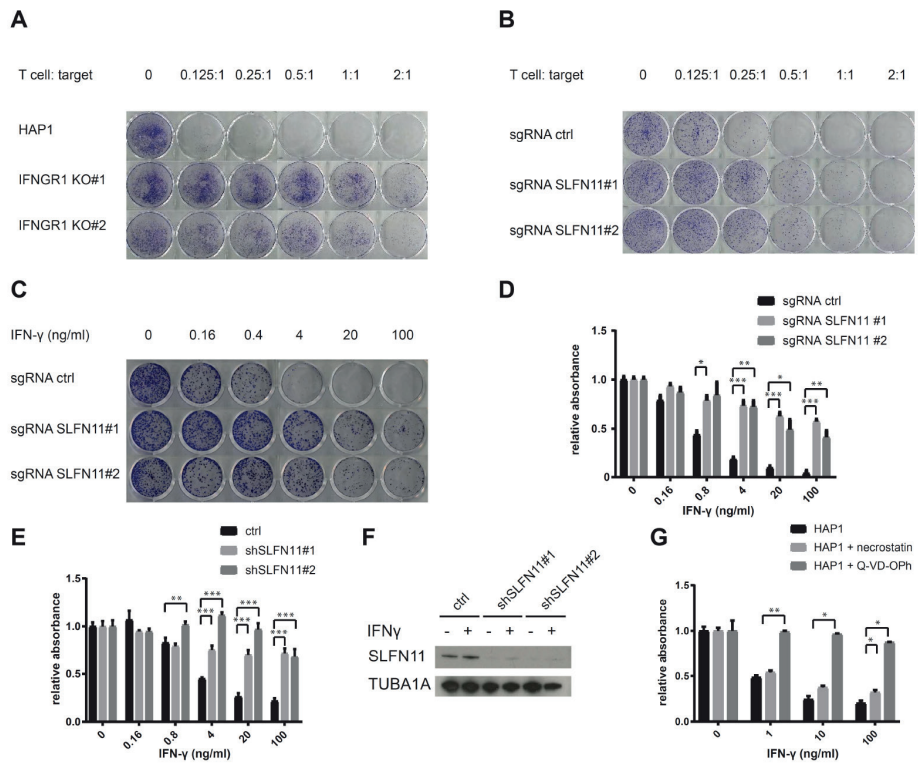

Figure 2. Interference with the IFNGR pathway and SLFN11 protects HAP1 from T cell- and IFNγ-mediated toxicity.

A) Parental HAP1 or two IFNGR1 KO clones were exposed to T cells at the indicated effector: target ratio for 24 h. 7 days after T cell exposure, surviving cells were stained with crystal violet. B-C) HAP1 cells transduced with a Cas9-encoding lentiviral vector with either a non-targeting sgRNA (sgRNA ctrl) or two independent sgRNA targeting SLFN11 (sgRNA SLFN11#1 and#2) were exposed to either T cells at the indicated effector: target ratio for 24 h (B), or to IFN-γ at the indicated concentrations for the whole duration of the experiment (C). 7 days after T cell or IFN-γ exposure, surviving cells were stained with crystal violet. D) HAP1 cells transduced with a Cas9-encoding lentiviral vector with either a non-targeting sgRNA (sgRNA ctrl) or two independent sgRNA targeting SLFN11 (sgRNA SLFN11#1 and#2) were exposed to the indicated concentrations of IFN-γ. 48 hours after IFN-γ exposure, cell viability was assayed by analysis of metabolic activity. E) HAP1 cells transduced with a control lentiviral vector or with two independent lentiviral vectors encoding SLFN11-targeting shRNA were exposed to the indicated concentrations of IFN-γ. 48 hours after IFN-γ exposure, cell viability was assayed by analysis of metabolic activity. F) Validation of SLFN11 KD by western blot analysis of untreated or IFN-γ treated (10 ng/ml, 24 h) HAP1 cells. G) HAP1 cells that were either untreated or pre-incubated for 1 h with the indicated compounds (20 μM for necrostatin, 10 μM for Q-VD-OPh) were exposed to the indicated concentrations of IFN-γ. 48 hours after IFN-γ exposure, cell viability was assayed by analysis of metabolic activity.

inhibitor Q-VD-OPh, relative cell expansion at day 18 was approximately 4.6×10^6 fold lower than for untreated controls. Interestingly, IFN-γ exposure in the presence of caspase blockade resulted in a delay in expansion that lasted for approximately a week after IFN-γ removal, after which cells resumed expansion with a similar kinetic as untreated controls (Fig. 3B).

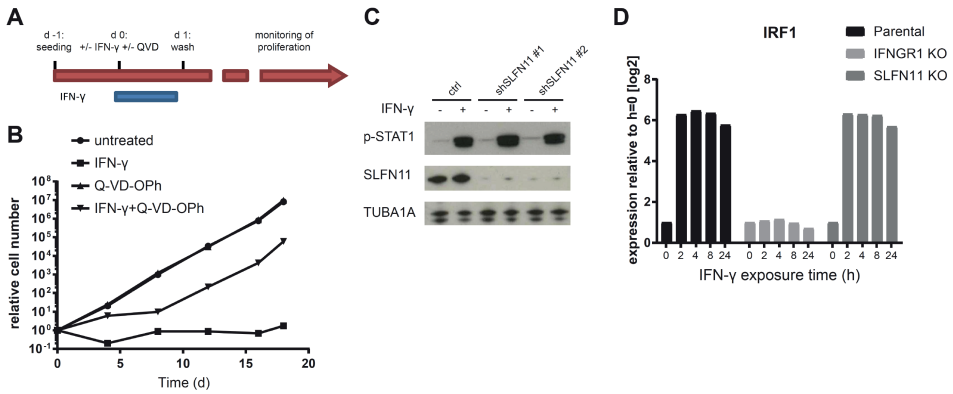

Figure 3. SLFN11 does not regulate IFNGR signaling and evaluation of IFN-γ effects in HAP1.
A) Schematic overview of experimental design in B. B) Growth kinetics of cells left untreated or treated with 10 ng/ml of IFN-γ for 24 h, in the presence or absence of Q-VD-OPh. C). Western blot analysis of phosphorylated STAT1 in HAP1 cells transduced with a control lentiviral vector or with lentiviral vectors encoding independent SLFN11-targeting shRNA, either left untreated or exposed to 10 ng/ml of IFN-γ for 24h. D) IRF1 transcript levels following exposure to 10 ng/ml of IFN-γ for the indicated times in parental, IFNGR1 KO, and SLFN11 KO cells.

To obtain mechanistic insight into the regulation of IFN-γ sensitivity by SLFN11, we first evaluated whether SLFN11 influences the magnitude of IFNGR signaling. First, analysis of phosphorylated STAT1 in WT and SLFN11 KD HAP1 cells following IFN-γ exposure demonstrated that SLFN11 levels do not detectably influence proximal IFNGR signaling (Fig. 3C). As phosphorylation of STAT genes by itself does not necessarily imply IFN-γ -induced transcriptional activity (21), we also exposed parental, SLFN11 KO, or IFNGR1 KO cells to IFN-γ and evaluated the transcriptional induction of a series of IFN-γ inducible genes. As expected, IFNGR deficiency abolished induction of all genes tested (IRF1 (Fig. 3D), IDO1, HLA-A, PD-L1 and IFIT3 (Supplementary Fig. 2A-D)). In contrast, induction of all these genes was fully maintained in SLFN11 KO cells. Consistent with these data, SLFN11 was not a hit in two independent haploid screens for regulators of IRF1 and PD-L1 upon IFN-γ treatment (22,23). Collectively, these data imply that SLFN11 regulates IFN-γ-mediated toxicity without altering IFNGR signaling activity but rather influences the functional outcome of IFNGR signaling.

SLFN11 regulates sensitivity toward IFN-γ in a context dependent fashion

SLFN11 has been implicated as a key determinant of tumor cell sensitivity to DNA damaging agents, but not other types of chemotherapeutics (15). Subsequent work has provided evidence for a role of SLFN11 in blocking replication forks under conditions of DNA replication stress (19,20). We sought to assess whether the role of SLFN11 as a mediator of T cell- and IFN-γ-induced cell death is linked to its role in mediating cell death induced by DNA damaging agents. We generated SLFN11 deficient HAP1 clones, and exposed these to different types of chemotherapeutic agents or to IFN-γ. As also observed for SLFN11 KD clones, HAP1 clones deficient in SLFN11 showed a decreased sensitivity toward IFN-γ-mediated toxicity (Fig 4A). Furthermore, in line with the data from Pommier and colleagues (15), loss of SLFN11 resulted in decreased sensitivity towards the DNA damaging agents cisplatin and doxorubicin (Fig 4B, C), whereas sensitivity to the microtubule disrupting agent docetaxel was unaffected (Fig 4D).

To assess whether SLFN11 influences IFN-γ- and DDA-induced cell death in a parallel manner in different cell systems, we generated SLFN11 KD variants of the prostate cancer cell line DU145 and the melanoma cell line WM2446, chosen because of their high levels of SLFN11 expression. Notably, interference with SLFN11 expression failed to show a consistent protective effect against IFN-γ exposure in these lines (Fig 5A-D). As in DU145 we observed that one of the shRNAs confer reduced sensitivity and the other increased sensitivity toward IFN-γ, despite similar efficiency in SLFN11 KD, we conclude that those effects are SLFN11-unrelated (Fig 5A, C). As a control, sensitivity towards both cisplatin and doxorubicin was reduced upon SLFN11 KD in both cell lines, consistent with prior data (Fig 5E-H). Thus, whereas the effect of SLFN11 on DDA-induced cell death is invariant between these cell systems, the role of SLFN11 in IFN-γ-induced cell death shows context dependency. Lack of SLFN11 involvement in the inhibitory effects of IFN-γ on DU145 and WM2664 may potentially be explained by reliance on distinct pathways of cell inhibition. Indirect support for this notion was provided by the observation that, as compared to the effect on HAP1 cells, IFN-γ-induced inhibition of cell proliferation was a) more modest (see Fig. 2D, E and Fig. 4A for comparison) and b) took substantially longer to manifest (48 hours for HAP1 vs. 7 days for the other lines). To directly test whether IFN-γ inhibits cell expansion by different mechanisms in HAP1 versus DU145 and WM2664, we exposed DU145 and WM2664 to increasing amounts of IFN-γ in the presence or absence of Q-VD-OPh. Contrary to what was observed for HAP1, DU145 and WM2664 cells were not protected from IFN-γ by caspase inhibition (Fig. 5I, J, see Fig. 2G for comparison). Given the role of SLFN11 in sensitization of tumor cells toward DDA-mediated toxicity,

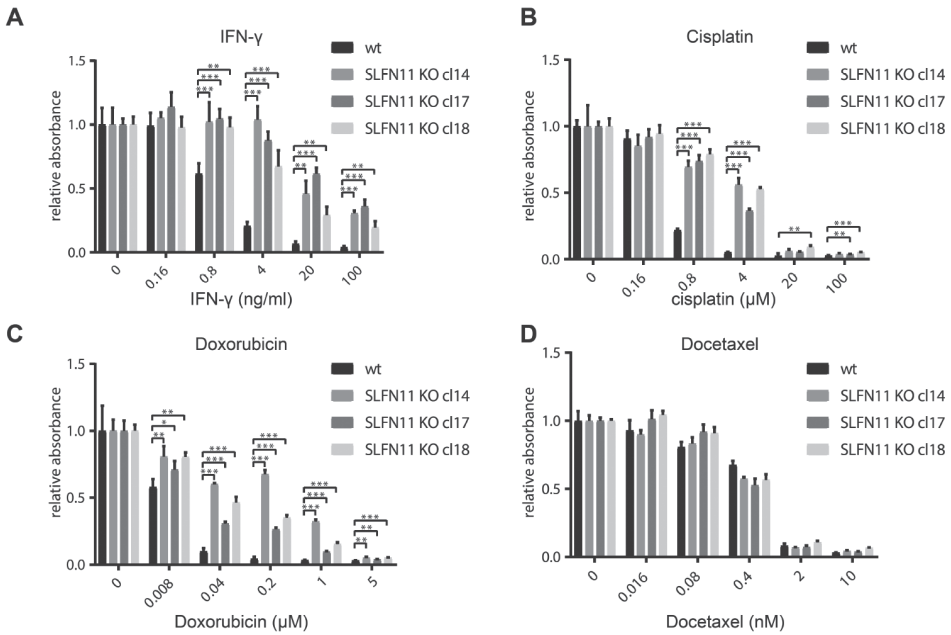

Figure 4. Interference with SLFN11 expression protects HAP1 from IFN-γ and DDA.
A-D) Parental HAP1 cells or three SLFN11 KO clones were exposed to the indicated concentrations of IFN-γ (A), cisplatin (B), doxorubicin (C), or docetaxel (D). 48 hours after IFN-γ or chemotherapy exposure, cell viability was assayed by analysis of metabolic activity.

7

we also sought to assess whether there is an association between IFN-γ exposure and induction of a DNA damage response. To this purpose, SLFN11-proficient or -deficient HAP1 cells were exposed to IFN-γ. Within 8 hours following exposure an induction of DDR was observed, as revealed by a minor increase in phosphorylated ATM and a major increase in phosphorylated histone H2AX (γ-H2AX, Fig. 6).

Restoration of a functional SLFN11 locus reverts the phenotype of SLFN11-deficient HAP1 cells

Genetic complementation of SLFN11 deficient cells with a lentiviral vector expressing SLFN11 cDNA did not revert the phenotype of SLFN11 deficient cells (data not shown), either suggesting that SLFN11 function may rely on a distinct transcript, or that transient SLFN11 deficiency may result in a permanent reduction in IFN-γ sensitivity. To address whether renewed expression of the *SLFN11* locus in cells in which the *SLFN11* gene has previously been inactivated restores their sensitivity to IFN-γ, we generated a gene trap vector encoding a GFP-puromycin N-acetyltransferase fusion protein flanked by lox-p sites and homology arms for a genomic region in the first exon of SLFN11. Integration of this vector by CRISPR-mediated knock-in

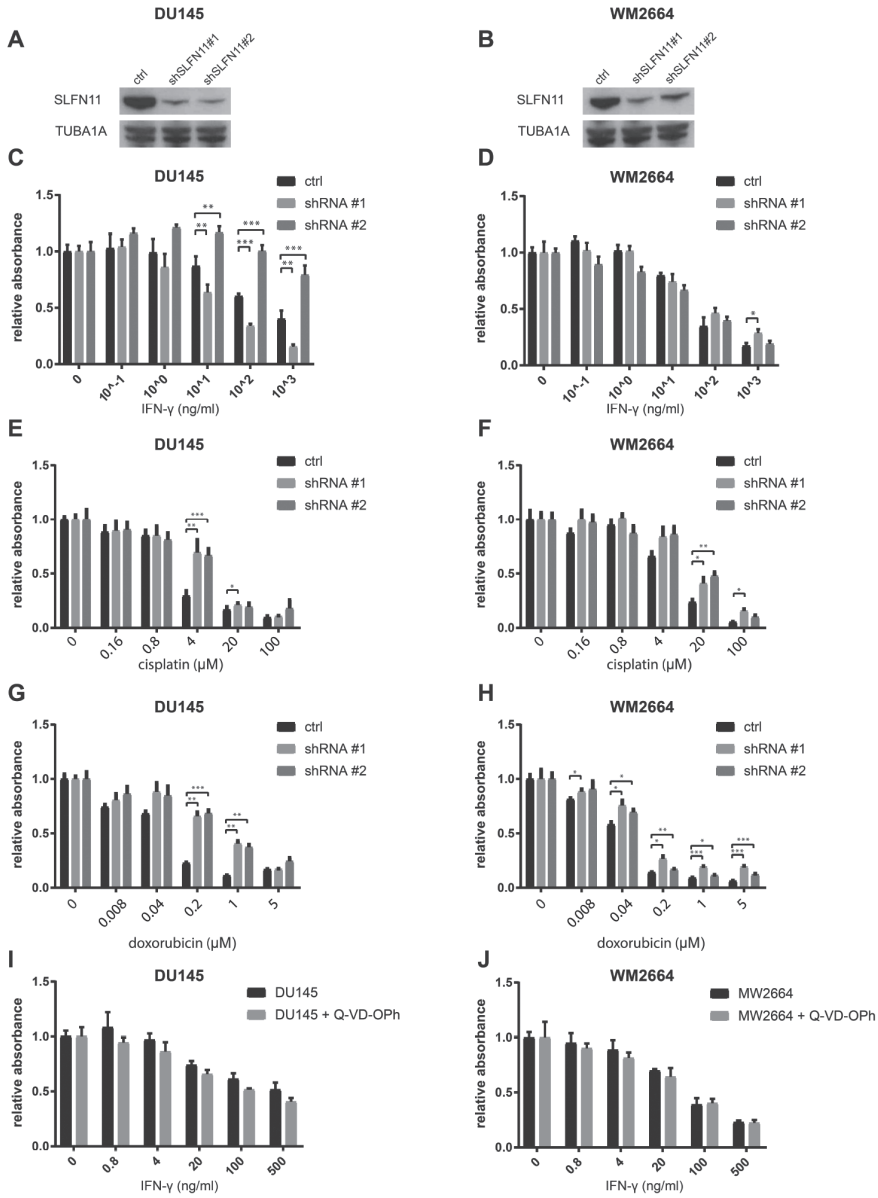

Figure 5. Sensitization of melanoma and prostate cancer cells to DDA but not IFN-γ.
A-B) Validation of SLFN11 KD by western blot in DU145 (A) and WM2664 (B). C-D) DU145 (C) and WM2664 cells (D) transduced with a control lentiviral vector or with independent SLFN11-targeting shRNA were exposed to the indicated concentrations of IFN-γ. 7 days after IFN-γ exposure, cell viability was assayed by analysis of metabolic activity. E-H) DU145 (E, G) and WM2664 (F, H) cells transduced with a control lentiviral vector or with independent vectors encoding SLFN11-targeting shRNA were exposed to the indicated concentrations of cisplatin (E, F) or doxorubicin (G, H). 48 hours after exposure, cell viability was assayed by analysis of metabolic activity. I-J) DU145 (I) and WM2664 (J) cells that were either untreated or pre-incubated for 1 h with Q-VD-OPh (10μM) were exposed to the indicated concentrations of IFN-γ. 7 days after IFN-γ exposure, cell viability was assayed by analysis of metabolic activity.

allows disruption of the SLFN11 coding frame, tracking and selection of the gene-modified cells by visualization of GFP and puromycin treatment, respectively, and the reactivation of SLFN11 by excision of the gene trap using Cre recombinase (Fig. 7A). We co-transfected HAP1 cells with the vector encoding the excisable gene trap, together with a vector expressing Cas9 and sgRNA targeting the first exon of SLFN11. Notably, subsequent exposure of the transfected cells to IFN-γ resulted in an approximately 100-fold increase in GFP^+ cells (Fig. 7B, C), indicating a selective enrichment for SLFN11 deficient cells consistent with our prior observations. In order to assess whether reactivation of the *SLFN11* locus restores sensitivity toward IFN-γ, we first exposed gene trap-transfected HAP1 cells to puromycin, in order to select for those cells in which the gene trap is active, yielding a population of >95% modified cells (Fig. 7D). Furthermore, site-specific integration of the gene trap vector was shown by PCR using one primer binding on the gene trap and one primer binding on the SLFN11 genomic region (Fig. 7A, E) and by sequencing of the PCR product (data not shown). After 10 days, transfection of Cre was used to induce excision of the gene trap vector, thereby restoring the *SLFN11* locus in a fraction of the cells. Importantly, exposure of this cell mixture to IFN-γ resulted in the preferential killing of cells with restored SLFN11 expression (Fig. 7F, G). Thus, IFN-γ sensitivity of HAP1 is a property that toggles with activity of the *SLFN11* gene.

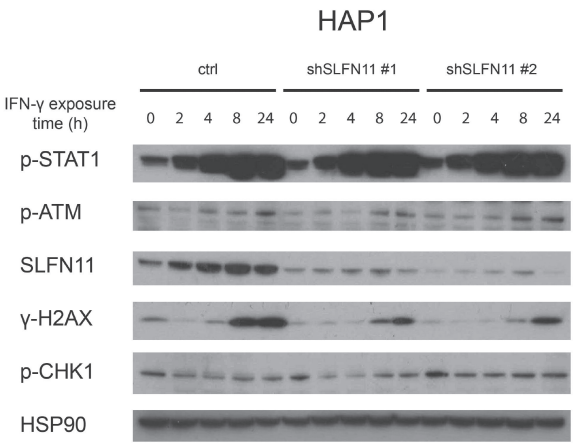

Figure 6 DDR in IFN-γ-treated HAP1
Western blot analysis of the indicated proteins in control or SLFN11 KD HAP1 cells following exposure to 10 ng/ml of IFN-γ for the indicated time periods.

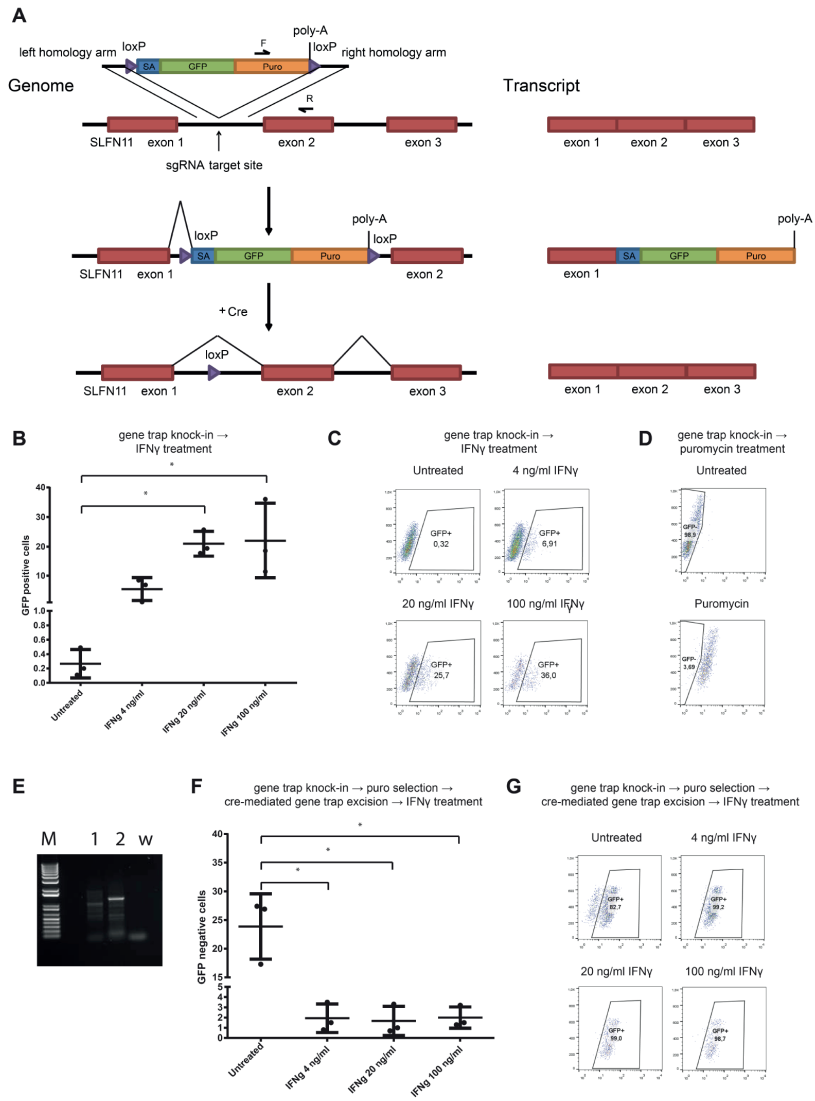

Figure 7. Reversible inhibition of IFN-γ sensitivity by inactivation of the SLFN11 locus.
A) Schematic overview of experimental design. A promoterless gene trap vector was inserted into the first intron of the SLFN11 gene. SLFN11 exons are indicated in red, GFP and puromycin N-acetyltransferase coding sequences in green and orange, and loxP sites in purple. Left part of the panel depicts the genomic locus, right part depicts the resulting transcripts. B-C) Cells with integrated gene trap vector were either left untreated or exposed to the indicated IFN-γ concentrations. Technical replicates (B) and representative flow plots (C) are depicted. D) Puromycin treatment results in homogeneous selection of cells with integrated gene trap vector. E) Detection of the integrated gene trap vector in the SLFN11 locus by PCR. Used primers are depicted in panel A (F and R). 1: untransfected HAP1; 2: transfected and puromycin-selected HAP1; w: water control. F-G) Excision of the gene trap vector results in re-sensitization of HAP1 cells to IFN-γ. Cells from panel D were transfected with a cre expressing vector and either left untreated or exposed to the indicated IFN-γ concentrations. Technical replicates (E) and representative flow plots (F) are depicted.

Discussion

We designed a whole-genome loss-of-function screen to identify mechanisms of tumor cell escape from T cell-mediated toxicity in haploid HAP1 cells (Fig. 1A). Similar to what has been observed for CRISPR-based screens in other cell systems (8-11), we identified the IFNGR pathway as a major pathway of tumor cell resistance. In contrast to other studies, no significant enrichment of cells with mutations in components of the antigen presentation pathway was observed (Fig. 1B). This observation was surprising, as it suggested that loss of sensitivity to IFN-γ provided a greater selective advantage than impaired antigen presentation. Subsequent experiments indeed demonstrated that, in HAP1, IFN-γ is a major source of toxicity upon T cell recognition, as interference with the IFNGR pathway is strongly protective against T cell-mediated toxicity (Fig. 2A). The mechanism of IFN-γ-induced cell death in HAP1 appears distinct from that in other cell systems. First, cell death induction by IFN-γ is observed at >10 fold lower concentrations in HAP1 than in DU145 and WM2664. Second, whereas exposure to IFN-γ mainly results in growth impairment for DU145 and WM2664 (Fig. 5C,D), it rapidly induces caspase-dependent cell death in HAP1 (Fig 2G). As IFN-γ is not directionally released in the immunological synapse (24), the differential sensitivity of tumors to IFN-γ may determine the relative importance of direct tumor cell killing versus bystander killing in T cell-mediated tumor control, and it will be important to identify characteristics of tumors with IFN-γ hypersensitivity.

SLFN11 was identified as the sole major hit in our screen that was known to be IFN-regulated (25). SLFN11 is a putative DNA-RNA helicase that has been shown to sensitize tumor cells toward DNA damage-induced cell death (14,15). In addition, SLFN11 has been implicated in inhibition of HIV protein synthesis in a codon-usage-dependent manner (26). However, to date SLFN11 expression has not been linked to IFN-γ-induced toxicity or resistance to tumor-specific T cells. Here we demonstrate that SLFN11 expression can regulate IFN-γ-mediated toxicity (Fig. 2C-E, 4A) and, as a consequence, sensitivity of tumor cells to T cell attack (Fig. 2B). This role of SLFN11 is independent of regulation of IFNGR signaling, as shown by unaltered induction of a series of IFNGR target genes (Fig. 3D and Supplementary Fig. 2). We observed that in HAP1 SLFN11 also functioned as a modulator of sensitivity towards DDA (Fig. 4B, C), as previously described in other cell systems (15). Furthermore, evidence for a possible link between IFNGR signaling and DNA damage response pathways was obtained by the observed induction of a γ-H2AX upon IFN-γ exposure of HAP1 (Fig. 6). While the role of SLFN11 as a modulator of sensitivity to DDA was shared in all cell systems analyzed here, the role of SLFN11 as a mediator of IFN-γ-mediated toxicity was specifically observed in HAP1. Future work should reveal the mechanistic basis for

the context dependency of SLFN11 as a modulator of IFN-γ but not DDA sensitivity. Related to this, a number of recent studies have demonstrated that the mechanism of action of SLFN11 in DDR response involves recruitment to sites of DNA damage and subsequent blockade of fork progression during replication stress (19,20,27). It will be of interest to assess whether a similar mode of action is responsible for its role in regulation of IFN-γ-mediated toxicity. A better understanding of the mechanisms that allow SLFN11-mediated toxicity following IFN-γ exposure should be of value to enhance the anti-tumor effect of T and NK cell-based cancer immunotherapies.

Acknowledgements

We would like to thank Chong Sun and Meike Logtenberg for valuable discussions and the NKI genomic core facility for RNA sequencing experiments. This work was supported by ERC AdG SENSIT to T.N.S. and by KWF grant NKI-2014-7474 to A.D.

Materials and methods

Cell lines

HAP1 cells have been described previously (28). DU145 were a kind gift of J. Neefjes (Leiden University), WM2664 were a kind gift of R. Bernards, and were authenticated by STR from the source. HAP1 cells were maintained in IMDM (Thermo Fisher Scientific) supplemented with 10% fetal calf serum (FCS, Sigma-Aldrich), 100 U ml^{-1} penicillin–streptomycin (Thermo Fisher Scientific) and L-glutamine (Thermo Fisher Scientific); DU145 and WM2664 were maintained in DMEM supplemented with 10% FCS (Sigma-Aldrich) and 100 U ml^{-1} penicillin–streptomycin (Thermo Fisher Scientific). Cells were tested for mycoplasma by PCR. To generate a MART-$1_{(26\text{-}35,\ 27\ A>L)}$ epitope expressing HAP1 variant, the coding sequence of MLNA (aa 18-38, 27 A>L) was cloned in front of the coding sequence of the Katushka protein with the two open reading frames linked by P2A coding sequence, and was subcloned into pCDH-CMV-MCS-EF1-copGFP (System Bioscience) using XbaI - SalI sites.

Generation of MART-1-specific T cells

Retroviral transduction of T cells to generate MART-1-specific T cells has been described previously (17). In brief, retroviral particles were produced by transfecting the pMP71-1D3 vector that encodes the MART-1-specific 1D3 TCR (17) into FLYRD18 packaging cells. Leucocytes were purified from healthy donor buffy coats (Sanquin) using Ficoll density gradients (Sigma-Aldrich), T cells were activated and magnetically isolated using Human T-Activator CD3/CD28 dynabeads (Thermo Fisher Scientific). 48 h after activation, T cells were spin transduced (90', 2,000 RPM) on retronectin-coated plates (Takara).

Haploid genetic screen for resistance to T cell pressure

Procedures for the generation of gene-trap retrovirus and HAP1 mutagenesis have been described previously (29). To select Hap1 variants resistant to T cell pressure, approximatively 10^8 HAP1 cells (>90% haploid) were exposed to 1D3 transduced T cells for 24 hours, at a ratio of 0.5 TCR transduced T cell/ HAP1 cell). Subsequently, T cells were removed by 3 washes with PBS and surviving HAP1 clones were expanded for 7 days. Integration sites were amplified and analyzed as described in (29).

Generation of knockout and knockdown cell lines

Knockout cell lines were generated using the CRISPR–Cas9 system. To generate bulk knockout HAP1 cells, cells were transduced with pLentiCRISPR v.2 vector (Addgene 52961) encoding two independent sgRNAs targeting SLFN11. 48 h after transduction, cells were selected with puromycin (2 µg ml−1, for two days). In order to generate knockout clones, cells were transfected with px459 vectors (Addgene 48139) encoding either sgRNAs targeting SLFN11 or IFNGR1. Following puromycin selection (2 µg ml−1, for two days), single-cell clones were expanded and gene disruptions were validated by sequence analysis and western blot analysis (SLFN11), or by flow cytometry (IFNGR1). The sgRNA sequence acatgaaccctatcgtatat was used for generating IFNGR1 KO clones. The sgRNA sequences tgtcagctgagtctatctag (sgRNA SLFN11#1) and tacactggtctgctaagggg (sgRNA SLFN11#2) were used to generate bulk populations of SLFN11 KO cells. The sgRNA sequence acggaggctaagcgtcgcaa (sgRNA ctrl) served as non-targeting control. Lentiviral shRNA vectors were retrieved from the arrayed TRC human genome-wide shRNA collection. Additional information is available at http://www.broadinstitute.org/rnai/public/clone/search using the TRCN number. The following lentiviral shRNA vectors were used: TRCN0000152057 (shSLFN11#1) and TRCN0000148990 (shSLFN11#2). For production of lentiviral particles, indicated plasmids were co-transfected into HEK293T cells along with packaging plasmids (pPAX2, pVSV-G). Two days after transduction, transduced cells were selected by exposure to puromycin.

Excisable gene trap

The vector for the excisable gene trap experiment was custom synthesized by Thermo Fisher Scientific. The left homology arm spanned genomic region 35370581-35371183 and right homology arm spanned genomic region 35369965-35370580 of chromosome 17 (assembly Dec.2013 GRCh38/hg38). In between these homology arms, a loxP site, a splicing acceptor sequence, a codon optimized GFP-puromycin N-acetyltransferase fusion protein, an SV40 polyA site, and another loxP site were inserted in this order. To introduce this DNA segment into the SLFN11 locus, >90% haploid HAP1 cells were transfected together with the vector px458 (addgene 48138)

expressing the sgRNA agttatctggtatagtcttt, designed such that the majority of the genomic sequence recognized by the sgRNA is located on one of the homology arms and the PAM on the other, in order to avoid Cas9 activity against the transfected plasmid or after integration of the DNA segment.

MTT and colony forming assays

For experiments involving IFN-γ or chemotherapeutics, 5,000 HAP1/well or 500 DU145 or WM2664/well were plated in 100 µl/well in 96 well plates 24 hours before addition of IFN-γ or chemotherapeutics. Compounds were added in 100 µl of medium to reach the indicated final concentration, and cell viability was assessed after either 2 days (chemotherapeutics or IFN-γ exposed HAP1), or 7 days (IFN-γ exposed DU145 and WM2664). To assess cell viability, supernatants were discarded and cells were incubated with 50 µl of 2.4 mM MTT 3-(4,5-dimethylthiazol-2-yl)-2,5-diphenyltetrazolium (Thermo Fisher Scientific) for 30' at 37°C. Subsequently, supernatant was removed and cells were incubated in DMSO at room temperature for 15'. 540 nm absorbance was used as a measure of cell viability. For colony forming assays, 25,000 cells/ well (6 well plates) or 5,000 cells/ well (24 well plates) were seeded 24 h before addition of T cells or IFN-γ. Cells were exposed to T cells at the indicated ratio for 24 h, or to IFN-γ at the indicated concentration for the entire duration of the experiment. 7 days after T cell or IFN-γ exposure, cells were washed once with PBS, fixed in ice-cold methanol for 15', and stained with 0.05% (w/v) crystal violet solution in water.

Western blot analysis

Cell lysates for western blot analysis were prepared by washing cells with PBS and subsequent lysis in RIPA buffer supplemented with freshly added protease inhibitor cocktail (Roche). After incubation on ice for 30 min, cell lysates were centrifuged at 20,000g for 15 min at 4 °C. Supernatants were subsequently processed using a Novex NuPAGE Gel Electrophoresis System, according to the manufacturer's instructions (Thermo Fisher Scientific). The following antibodies were used for western blot analysis: anti-HSP90: H114 (SantaCruz); anti-TUBA1A: 2144s (Cell Signaling Technology); anti-phosphorylated STAT1 7649s (Cell Signaling Technology); anti γ-H2AX 2577s (Cell Signaling Technology); anti-phosphorylated CHK1 12302s (Cell Signaling Technology); anti-phosphorylated ATM 10H11.E12 (Millipore); anti-SLFN11 HPA023030 (Atlas).

RNA seq and gene expression

Total RNA was extracted using TRIzol reagent (Ambion life technologies) according to the manufacturer's instructions. Quality and quantity of total RNA was assessed on

a 2100 Bioanalyzer using a Nano chip (Agilent). Total RNA samples having RIN values >8 were subjected to library generation. Strand-specific libraries were generated using the TruSeq Stranded mRNA sample preparation kit (Illumina Inc.) according to the manufacturer's instructions. Libraries were sequenced on a HiSeq2500 using V4 chemistry (Illumina Inc.), and reads (65bp single-end), were aligned against the human reference genome (hg38) using TopHat (version 2.1.0), allowing the spanning of exon-exon splice junctions. TopHat was supplied with a known set of gene models (Ensembl version 77). Samples were generated using a stranded library preparation protocol, in which TopHat was guided to use the first-strand as the library-type. Tophat was run with bowtie 1 version 1.0 and the additional parameters "--prefilter-multihits" and "--no coverage". In order to count the number of reads per gene, a custom script (ItreeCount) was used. This script is based on the same concept as HTSeq-count and has comparable output. ItreeCount generates a list of the total number of uniquely mapped sequencing reads for each gene that is present in the provided Gene Transfer Format (GTF) file.

Author contributions

R.M., conceived the project, designed and performed experiments, interpreted data and co-wrote the paper. M.d.B. and R.G.-E. designed and performed experiments. L.T.J. designed and performed experiments and analyzed the screen results. A.D. performed, designed and interpreted DDR experiments. F.A.S. had critical input in and interpreted the excisable gene trap experiments. T.R.B. co-supervised the project and interpreted experiments. T.N.S. conceived the project, designed and interpreted experiments and co-wrote the manuscript.

References

1. Ribas A, Wolchok JD. Cancer immunotherapy using checkpoint blockade. Science **2018**;359(6382):1350-5 doi 10.1126/science.aar4060.
2. Sun C, Mezzadra R, Schumacher TN. Regulation and Function of the PD-L1 Checkpoint. Immunity **2018**;48(3):434-52 doi 10.1016/j.immuni.2018.03.014.
3. Hinrichs CS, Rosenberg SA. Exploiting the curative potential of adoptive T-cell therapy for cancer. Immunol Rev **2014**;257(1):56-71 doi 10.1111/imr.12132.
4. June CH, Riddell SR, Schumacher TN. Adoptive cellular therapy: a race to the finish line. Sci Transl Med **2015**;7(280):280ps7 doi 10.1126/scitranslmed.aaa3643.
5. Zaretsky JM, Garcia-Diaz A, Shin DS, Escuin-Ordinas H, Hugo W, Hu-Lieskovan S, *et al.* Mutations Associated with Acquired Resistance to PD-1 Blockade in Melanoma. N Engl J Med **2016**;375(9):819-29 doi 10.1056/NEJMoa1604958.
6. Gao J, Shi LZ, Zhao H, Chen J, Xiong L, He Q, *et al.* Loss of IFN-gamma Pathway Genes in Tumor Cells as a Mechanism of Resistance to Anti-CTLA-4 Therapy. Cell **2016**;167(2):397-404 e9 doi 10.1016/j.cell.2016.08.069.
7. Shin DS, Zaretsky JM, Escuin-Ordinas H, Garcia-Diaz A, Hu-Lieskovan S, Kalbasi A, *et al.* Primary Resistance to PD-1 Blockade Mediated by JAK1/2 Mutations. Cancer Discov **2017**;7(2):188-201 doi 10.1158/2159-8290.CD-16-1223.
8. Manguso RT, Pope HW, Zimmer MD, Brown FD, Yates KB, Miller BC, *et al.* In vivo CRISPR screening identifies Ptpn2 as a cancer immunotherapy target. Nature **2017**;547(7664):413-8 doi 10.1038/nature23270.
9. Patel SJ, Sanjana NE, Kishton RJ, Eidizadeh A, Vodnala SK, Cam M, *et al.* Identification of essential genes for cancer immunotherapy. Nature **2017**;548(7669):537-42 doi 10.1038/nature23477.
10. Kearney CJ, Vervoort SJ, Hogg SJ, Ramsbottom KM, Freeman AJ, Lalaoui N, *et al.* Tumor immune evasion arises through loss of TNF sensitivity. Sci Immunol **2018**;3(23) doi 10.1126/sciimmunol.aar3451.
11. Pan D, Kobayashi A, Jiang P, Ferrari de Andrade L, Tay RE, Luoma AM, *et al.* A major chromatin regulator determines resistance of tumor cells to T cell-mediated killing. Science **2018**;359(6377):770-5 doi 10.1126/science.aao1710.
12. Fruh K, Yang Y. Antigen presentation by MHC class I and its regulation by interferon gamma. Curr Opin Immunol **1999**;11(1):76-81.
13. Schroder K, Hertzog PJ, Ravasi T, Hume DA. Interferon-gamma: an overview of signals, mechanisms and functions. J Leukoc Biol **2004**;75(2):163-89 doi 10.1189/jlb.0603252.
14. Barretina J, Caponigro G, Stransky N, Venkatesan K, Margolin AA, Kim S, *et al.* The Cancer Cell Line Encyclopedia enables predictive modelling of anticancer drug sensitivity. Nature **2012**;483(7391):603-7 doi 10.1038/nature11003.
15. Zoppoli G, Regairaz M, Leo E, Reinhold WC, Varma S, Ballestrero A, *et al.* Putative DNA/RNA helicase Schlafen-11 (SLFN11) sensitizes cancer cells to DNA-damaging agents. Proc Natl Acad Sci U S A **2012**;109(37):15030-5 doi 10.1073/pnas.1205943109.
16. Duncan LM, Timms RT, Zavodszky E, Cano F, Dougan G, Randow F, *et al.* Fluorescence-based phenotypic selection allows forward genetic screens in haploid human cells. PLoS One **2012**;7(6):e39651 doi 10.1371/journal.pone.0039651.
17. Jorritsma A, Gomez-Eerland R, Dokter M, van de Kasteele W, Zoet YM, Doxiadis, II, *et al.* Selecting highly affine and well-expressed TCRs for gene therapy of melanoma. Blood **2007**;110(10):3564-72 doi 10.1182/blood-2007-02-075010.
18. Platanias LC. Mechanisms of type-I- and type-II-interferon-mediated signalling. Nat Rev Immunol **2005**;5(5):375-86 doi 10.1038/nri1604.

19. Mu Y, Lou J, Srivastava M, Zhao B, Feng XH, Liu T, *et al.* SLFN11 inhibits checkpoint maintenance and homologous recombination repair. EMBO Rep **2016**;17(1):94-109 doi 10.15252/embr.201540964.
20. Murai J, Tang SW, Leo E, Baechler SA, Redon CE, Zhang H, *et al.* SLFN11 Blocks Stressed Replication Forks Independently of ATR. Mol Cell **2018**;69(3):371-84 e6 doi 10.1016/j.molcel.2018.01.012.
21. Xiao Q, Wu J, Wang WJ, Chen S, Zheng Y, Yu X, *et al.* DKK2 imparts tumor immunity evasion through beta-catenin-independent suppression of cytotoxic immune-cell activation. Nat Med **2018**;24(3):262-70 doi 10.1038/nm.4496.
22. Brockmann M, Blomen VA, Nieuwenhuis J, Stickel E, Raaben M, Bleijerveld OB, *et al.* Genetic wiring maps of single-cell protein states reveal an off-switch for GPCR signalling. Nature **2017**;546(7657):307-11 doi 10.1038/nature22376.
23. Mezzadra R, Sun C, Jae LT, Gomez-Eerland R, de Vries E, Wu W, *et al.* Identification of CMTM6 and CMTM4 as PD-L1 protein regulators. Nature **2017**;549(7670):106-10 doi 10.1038/nature23669.
24. Sanderson NS, Puntel M, Kroeger KM, Bondale NS, Swerdlow M, Iranmanesh N, *et al.* Cytotoxic immunological synapses do not restrict the action of interferon-gamma to antigenic target cells. Proc Natl Acad Sci U S A **2012**;109(20):7835-40 doi 10.1073/pnas.1116058109.
25. Mavrommatis E, Fish EN, Platanias LC. The schlafen family of proteins and their regulation by interferons. J Interferon Cytokine Res **2013**;33(4):206-10 doi 10.1089/jir.2012.0133.
26. Li M, Kao E, Gao X, Sandig H, Limmer K, Pavon-Eternod M, *et al.* Codon-usage-based inhibition of HIV protein synthesis by human schlafen 11. Nature **2012**;491(7422):125-8 doi 10.1038/nature11433.
27. Murai J, Feng Y, Yu GK, Ru Y, Tang SW, Shen Y, *et al.* Resistance to PARP inhibitors by SLFN11 inactivation can be overcome by ATR inhibition. Oncotarget **2016**;7(47):76534-50 doi 10.18632/oncotarget.12266.
28. Carette JE, Raaben M, Wong AC, Herbert AS, Obernosterer G, Mulherkar N, *et al.* Ebola virus entry requires the cholesterol transporter Niemann-Pick C1. Nature **2011**;477(7364):340-3 doi 10.1038/nature10348.
29. Jae LT, Raaben M, Riemersma M, van Beusekom E, Blomen VA, Velds A, *et al.* Deciphering the glycosylome of dystroglycanopathies using haploid screens for lassa virus entry. Science **2013**;340(6131):479-83 doi 10.1126/science.1233675.

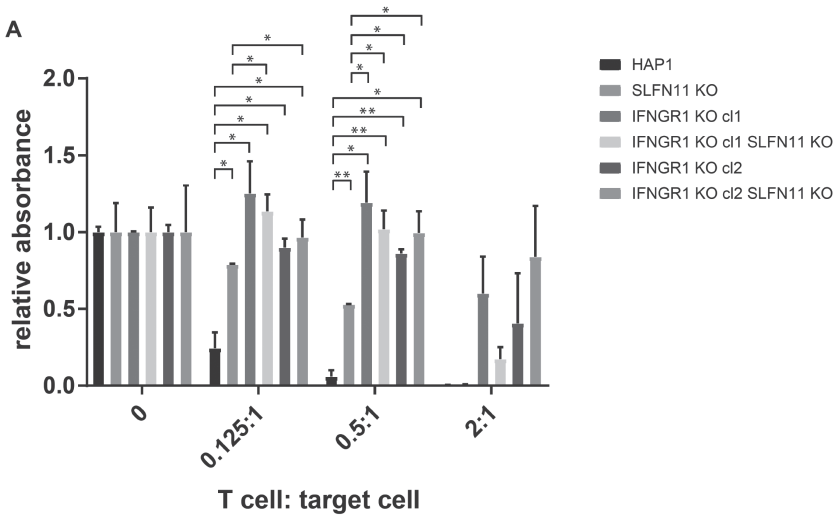

Supplementary Figure 1. SLFN11-mediated sensitization of HAP1 to T cell pressure is dependent on IFNGR signaling

Parental, SLFN11 KO, two independent IFNGR1 KO clones, or the same IFNGR1 KO clones in which SLFN11 was subsequently disrupted were exposed to T cells at the indicated effector: target ratio. Viability was assessed by analysis of metabolic activity 7 days after T cells exposure.

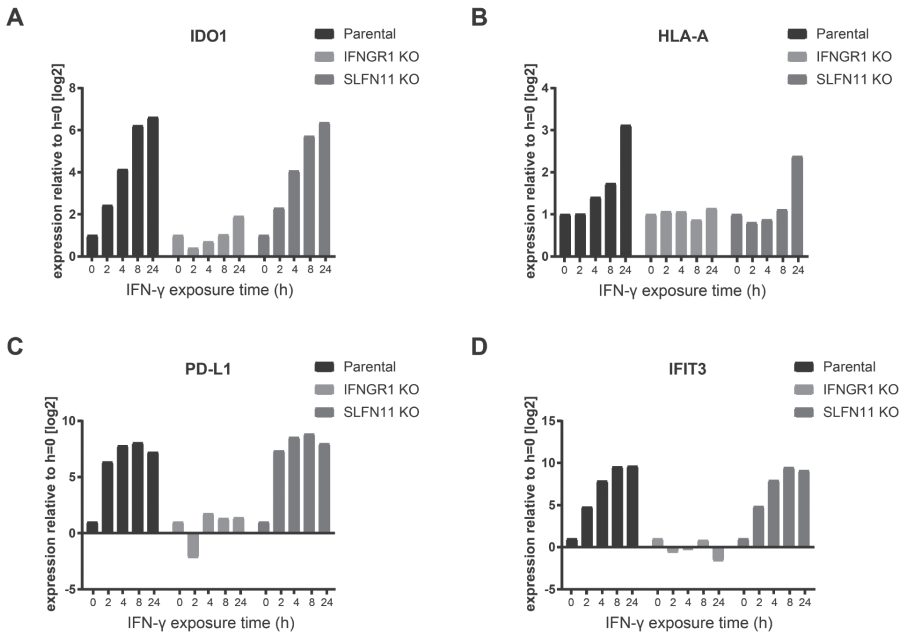

Supplementary Figure 2. SLFN11 does not modulate induction of IFNGR-induced genes
A-D) Transcript levels of IDO1 (A), HLA-A (B), PD-L1 (C) and IFIT3 (D) following exposure to 10 ng/ml of IFN-γ for the indicated times in parental, IFNGR1 KO, and SLFN11 KO cells.

Chapter 8

Discussion

The work described in this thesis reflects my interest in genetic manipulation, and employs a series of genetic manipulation techniques in order to approach relevant questions in the field of cancer immunology. The first part of this thesis (**Chapters 2, 3 and 4**) focuses on redirecting T cells by TCR gene transfer, in order to generate novel populations of tumor reactive T cells, an approach that may either be utilized to introduce T cell reactivities that were absent from the endogenous repertoire, or to 'transplant' tumor reactive TCRs that are present in a patient from exhausted T cells into fresh T cells. The second part (**Chapters 5, 6 and 7**) focuses on understanding different mechanisms of tumor resistance towards T cell attack, using genetic screens as an experimental approach. While united by the use of genetic manipulation, the research in this thesis covers a rather broad series of topics, and in this discussion I would like to outline my views on a series of questions that I consider relevant for the field and that my work touched upon over the past years.

What is the best approach to redirect T cells?

The tools that are used for gene transfer can be divided into virally-derived and non-virally-derived vectors, and additionally into integrating and non-integrating vectors. Given the proliferative potential of hematopoietic tissue, gene transfer into cells of the hematopoietic system, including T cells, will generally require the use of tools that are able to stably integrate into the host genome.

The field of T cell redirection (i.e. the generation of CAR- and TCR-modified T cells) is currently dominated by the use of retrovirus-derived gene transfer tools, including HIV-derived lentiviral vectors. This bias can in large part be explained by historical and practical reasons. Vectors derived from retroviruses were developed starting from the 80's, and have since then become a very frequently used research tool. The first report of infusion of retrovirally modified cells in humans was published already in 1990[1] and a large amount of preclinical and clinical experience with retroviral vectors has emerged over the years. Retroviral vectors represent a reliable and generally safe approach for genetic manipulation[2], in particular when the target of genetic manipulation is formed by differentiated cells, such as T cells, for which the risk of transformation due to insertional mutagenesis is substantially lower than for hematopoietic stem cells[3].

Possibly, the most significant issues with the use of retroviral vector-based approaches are formed by the costs and by the regulatory requirements for their use, calling for extensive validation of each viral batch before use in patients. When using the same viral vector for a larger patient group, as has thus far been done when employing T cells redirected either with chimeric receptors or with TCRs directed against shared

antigens[4], these issues are burdensome but surmountable. However, for the now foreseen development of gene-modified cell therapies that employ patient-specific transgenes, these two issues have become a major hurdle. Specifically, over the past years it has become apparent that neoepitopes that are formed as a consequence of DNA damage represent a highly attractive target for immunotherapeutic approaches[5]. Furthermore, the bulk of neoepitopes in human cancers is derived from private mutations. For these reasons, it is plausible that the field will move towards the redirection of T cells with neoepitope-specific TCRs that target mutant epitopes that are specific to the tumor of an individual patient (discussed in **Chapter 2**). In this, at present still hypothetical, scenario, the current regulation would become a major limiting factor in further development of the field. With this issue in mind, it makes sense to look for alternative platforms, such as plasmid-based transposon systems[6]. As at present every single viral batch has to be tested to meet regulatory standards, the current regulation creates time and cost concerns that would make viral vectors, but not plasmid-only based platforms, impractical for personalized TCR gene therapy. At this moment, the use of non-viral approaches is hampered by two practical limitations, i.e. their toxicity and low efficiency, that are described in **Chapter 2** and that constitute the rationale for the research carried out in **Chapters 3 and 4**. In the work described in this thesis, I have aimed to reduce these issues. However, even with the optimized strategies that have been developed to date, the degree of toxicity that is observed upon DNA electroporation remains a significant barrier towards clinical application. To resolve this issue, a large research effort that aims to understand how cellular stress and toxicity is induced following introduction of DNA into T cells would be of value. Conceivably the type of genetic screens that I have used in the second part of my thesis could provide an experimental approach towards this goal. A related point that will have to be addressed is whether those cells that survive DNA electroporation are hampered in their fitness. Once these issues have been resolved, I believe transposon-based gene transfer systems will be ready to move towards widespread clinical application, and may become a cornerstone in the development of personalized TCR gene therapies.

Which immunotherapeutic approach is preferentially used?

T cell-centered immunotherapeutic approaches can conceptually be divided in two classes:

1) Approaches that aim at generating T cell responses that are absent in the natural T cell repertoire (e.g. TCR or CAR gene transfer[4]) or that have not been adequately primed by the expanding tumor (e.g. vaccination[7,8], CTLA-4 blockade[9]).

2) Approaches that aim at reverting the dysfunction of existing T cell responses and/or counteracting suppressive mechanisms (e.g. TIL therapy[10], PD-1–PD-L1 blockade[11], CTLA-4 blockade[12]).

A simple flow for determining which immunotherapeutic approach a given patient could benefit from would be to first establish if there is an ongoing T cell response to the tumor. In absence of this, the initial strategy should be aimed at those approaches that generate new reactivities. On the contrary, if a response exists, but it is locally suppressed, the strategy should aim to revert the immunosuppressive mechanism(s) precluding tumor clearance.

At present, a series of strategies exist that can be utilized to infer the likelihood of of an ongoing T cell response being present, but these methods are unfortunately hampered by limited specificity and sensitivity. These strategies are represented by analysis of mutational load[13-15], immunohistochemical detection of PD-L1, which is strongly upregulated by interferons (IFN, discussed in **Chapter 5**), detection of several IFN-induced genes[16,17] or presence of tumor-infiltrating T cells[18], including T cells with defined differentiation states[19-21] (see also **Chapter 5**). Although providing some useful indications, these methods do not unambiguously identify patients that either have or do not have a tumor-specific T cell response for a series of reasons. For example, a high mutational burden increases the likelihood of generation of neoepitopes, but gives no guarantee of a response (or of the absence of one). As other examples, intratumoral expression of PD-L1 can be driven by non-immunological factors (see **Chapter 5**), IFN can be produced by other cells than T cells and T cell infiltration can be driven by inflammatory phenomena that are not necessary reflective of tumor recognition (see Table 1).

On top of the aforementioned limitations, these methods have to date mostly been used to predict clinical response to agents that block the PD-1–PD-L1 axis. As an ongoing antitumoral response is likely to be a prerequisite for response to PD-1–PD-L1 blocking therapies, it is sensible that responding patients are to be sought among those with tumor-specific T cells. However, it is probable that the PD-1–PD-L1 axis is one of at least a few drivers of local suppression of the antitumoral activity[22]. Observations in support of this hypothesis are for example the existence of tumor types that respond particularly poorly to PD-1–PD-L1 blockade in view of their mutational load, the most notable of these being microsatellite stable colorectal cancer[23]. As a series of studies have indicated that presence of infiltrating T cells has a very strong prognostic value in colorectal cancer [24], in line with a role of the adaptive arm of the immune system in controlling it, it is plausible that in those tumors alternative or additional immunosuppressive

mechanisms are active. As a recent example of an additional local immunosuppressive mechanism, it has been shown that TGF-β is a microenvironmental component that can impair the response to PD-L1 blocking agents[22]. These data support the notion that even in those cases in which an antitumoral immune response is being suppressed by the tumor, blockade of the PD-1–PD-L1 axis may not always be the optimal strategy to promote tumor control.

Detection method	False positive	False negative	Comments
Mutational load	High mutational load in absence of tumor-reactive T cells	Low mutational load in presence of tumor-reactive T cells	Increasing mutational load increases the likelihood of a response, exceptions can exist on both sides
PD-L1 expression	Non immunologically-related PD-L1 expression, non T cell-mediated IFN secretion	Mutations in IFN pathways, inability of T cells to secrete IFNs because of ongoing suppression	
IFN signature	Non T cell-mediated IFN secretion	Mutations in IFN pathways, inability of T cells to secrete IFNs because of ongoing suppression	
T cell infiltration	Inflammatory environment, infiltration can be an epiphenomenon	Immune excluded phenotype, e.g. because of TGF-β	

Table 1: potential explanation for the occurrence of false positives and false negatives when inferring the presence of a tumor-specific T cell response using the indicated methodologies

In conclusion, two main issues limit our ability to select the optimal therapy for each patient. The first is the inability to unambiguously identify those patients that would not benefit from reinvigoration of locally suppressed T cells, in order to direct them toward therapies that can generate new responses. The second is the inability to distinguish, for those patients with an ongoing tumor-specific T cell response, which mechanism(s) is preventing tumor eradication. This second issue is complicated by the fact that it is likely that some of these mechanisms are yet to be fully elucidated, and that it is plausible that in many cases the antitumoral response is suppressed by a combination of factors. In order to solve these issues, a more in-depth understanding of tumor immunobiology is required, and I think the field is rapidly achieving this, by combining studies on clinical samples and in appropriate animal models. In addition, we require sensitive and affordable diagnostic strategies that can be applied in a clinical setting for better patient stratification. As recent evidence suggests that tumor-reactive T cells are rare within the tumor microenvironment[25] (and Wouter Scheper, personal communication), I can envision this to happen in the future by developing methods for interrogating single cells for both their antigenic exposure history and for their suppressive signature. This could potentially happen by developing single cell sequencing technologies into a diagnostic platform.

What is the biological driver for PD-L1 regulation by CMTM6?

In order to understand the biology of a given protein, it is important to reveal how its abundance is regulated. A comprehensive overview of the known PD-L1 regulatory mechanisms is described in **Chapter 5**. In **Chapter 6** of this thesis I described our discovery (simultaneously with the lab of Mark Dawson[26]) of an unexpected posttranslational layer of regulation of PD-L1 by the, until then, functionally orphan protein CMTM6. In all cell systems tested, we observed that the magnitude of cell surface expression of PD-L1 is dependent on the presence of CMTM6, that CMTM6 associates with PD-L1 and by doing so regulates its stability.

With respect to the biological role this layer of regulation we can at present only speculate. In such speculation, it may be useful to consider why evolutionary pressure did not push to have a more stable PD-L1 protein, but rather to have it stabilized by another protein. In my opinion there are two, non-exclusive, ways of interpreting this observation.

The first is that, similarly to what happens for other proteins, PD-L1 cell surface levels may need to be regulated rapidly under certain conditions, and that CMTM6 serves this function. This could be done by degrading or physically segregating CMTM6 from PD-L1. Also, it is possible that CMTM6 is regulating, next to PD-L1, other protein(s) and co-regulation of these proteins may be beneficial. As counterarguments, our data suggest that CMTM6-mediated regulation of PD-L1 is relatively specific and also show that in certain cell systems the effect of CMTM6 on PD-L1 cell surface levels is modest, so other explanations should also be considered.

A second explanation for the existence of the CMTM6–PD-L1 complex is that CMTM6 is relevant for the functional activity of PD-L1, in addition to its PD-L1 stabilizing role through which it was identified. CMTM6 has a number of features in common with tetraspanins, a class of membrane proteins involved in cell membrane organization, such as having four transmembrane domains with intracellular N- and C-termini and the fact of being associated with at least one molecular partner[27,28]. Furthermore, a number of similarities exist between how PD-L1 interacts with CMTM6 and the way the tetraspanin CD81 interacts with its partner CD19. CD81 is required for efficient expression of CD19[29-31] and biochemical experiments suggest that the mechanism of CD81-mediated regulation of CD19[32] is similar to the mechanism of CMTM6-mediated regulation of PD-L1. In light of these observation, it would seem useful to explore if other known features of CD81 are shared with CMTM6. Tetraspanins are a class of structurally related surface protein that are involved in the organization of their molecular partners on the cell membrane in so-called tetraspanin-enriched

microdomains. Additionally, they can connect their molecular partners with cytoskeletal components, proteins involved in cell-cell or cell-matrix interactions, such as integrins and they can also supramolecularly organize surface receptors in order to facilitate signaling. Finally, many tetraspanins are described to be able to interact with more than one molecular partner (reviewed in[27,28]).

A first point to be addressed could be whether CMTM6 has additional interaction partners, next to PD-L1. In addition, it will be of importance to understand whether CMTM6 also organizes PD-L1 in supramolecular complexes, and whether such putative complexes require an interaction with the cytoskeleton. If this is the case, it may also be useful to assess whether CMTM6 is required for regulating the availability of PD-L1 in the immunological synapse upon T cell recognition of target cells, in order to increase its availability for its ligand. To test this, one possible experimental approach could be to determine whether CMTM6 can also qualitatively, and not only quantitatively, alter the efficiency of PD-L1-mediated suppression of T cells.

Requirement to address these questions will be the availability of biochemical and microscopy approaches to detect possible interactions and to analyze membrane dynamics. In addition, sensitive assays to measure the inhibitory effects of PD-L1, in order to be able to detect even subtle changes in its suppressive capacity will be required. The thus-far proposed experiments aim at exploring the role of CMTM6 in relation to its role in PD-L1, but in future it will also be of importance to explore the function of CMTM6 in an unbiased manner, e.g. in CMTM6 KO mice. It such mice, it will be important to not only assess PD-L1-related immunological phenotypes, such as sensitivity toward experimentally-induced autoimmunity, or maternal-fetal tolerance, but also to understand whether these mice display any non PD-L1-related phenotype(s). Clearly, these kind of discoveries will be by their nature serendipitous, as there are no indications yet on what to expect, but standard mouse pathological evaluation of organs, analysis of representation of different immune populations in various body compartment, and analysis of adaptive immune responses could result in interesting leads.

How much more can we learn about immunotherapy from genetic screens in tumor cells?

When comparing immunotherapies with conventional therapies, such as chemotherapy, radiotherapy and targeted therapy, it may be posed that immunotherapies are more complex in the way they work and also in the way(s) that cancer cells become resistant to them. Arguments in favor of this notion could be both that the immune system works through several effector mechanisms and that during their development

cancerous cells already have had to face the pressure of the immune system. When trying to understand how T cell-centered immunotherapies work and how tumors can evade from them, it is important to keep in mind that the immune system has evolved in order to fight pathogens in such a way that the likelihood of escape is minimized, and this is achieved by two levels of redundancy. The first is 'cellular redundancy', the existence of different immune cell types that carry out distinct effector functions, reducing the likelihood of escape from different immune effector cell arms. As an example, NK cells are able to recognize those tumor cells that escape from cytotoxic T cell recognition by loss or downregulation of MHC-I. The second level of redundancy is represented by 'molecular redundancy', the notion that immune cells with cytolytic function can kill target cells by inducing cell death through parallel pathways, such as FAS/FASL and granzymes. The presence of these parallel pathways implies that loss of a given pathway will not suffice to prevent elimination of the target cell by the immune system. Conceivably, these built-in redundancies explain the observation that acquired resistance after an initial profound therapy response upon PD-1 or CTLA-4 blockade is relatively rare, as compared to acquired resistance after targeted therapy.

Over the past years, genetic screens have been widely used to understand tumor cell resistance or vulnerability to targeted cancer therapies[33]. Recently, the use of loss-of-function genetic screens has also become popular for interrogating tumor-intrinsic mechanisms of resistance to immunotherapeutic approaches. A series of screens has been performed, both *in vitro*, by co-culturing a library of tumor cells with redirected T cells[34-36] and **Chapter 7** of this thesis, and *in vivo* by inducing endogenous tumor-specific T cell responses against a library of cancer cell variants in a transplantable tumor model[37]. In these different studies a number of genes have been identified that act as modulators of tumor cell sensitivity towards T cell effector mechanisms. Part of these genes are involved in broad cellular functions, such as cellular metabolism, basal transcription, or they are modulators of different kinds of cellular stress. Pinpointing which function(s) of those genes, among the many they are involved in, contributes to the altered sensitivity to T cell pressure is difficult. A large part of the other identified genes belongs to or modulate the antigen presentation machinery, the IFN-γ signaling pathway or the TNF signaling/NF-κB activation pathway. Implication of these pathways in resistance mechanisms towards T cell centered immunotherapeutic approaches is of major importance. Furthermore, the relevance of the acquired resistance mechanisms identified in these studies is underscored by the observation that both defects in antigen presentation[38,39] and in IFN-γ signaling[39-41] have been associated with unresponsiveness or resistance to checkpoint blockade in patients. On the other hand, all the identified pathways were already known as being relevant for T cell-mediated target killing, as antigen presentation is required

for target recognition, IFN-γ signaling has for long been known as a determinant of immunological rejection of tumors[42] and the involvement of TNF in T cell-mediated killing of targets was also previously established. In this sense, these genetic screens have perhaps brought less surprises than may have been expected.

As the screens that have been performed so far mainly highlighted the relevance of those three pathways, I think that in future screens should address other aspects related to the escape from immunotherapeutic approaches. As a first point, it is likely that only part of the resistance toward T cells-based immunotherapeutic approaches is due to a reduced sensitivity toward T cell effector mechanisms, as soluble factors and the action of microenvironmental components can both have immunosuppressive roles. Identification of those mechanisms by pooled genetic screens can be challenging, as emergence of a single clone able to secrete an immunosuppressive factor can fail to confer a sufficient selective advantage in an environment where the surrounding cells are not secreting it. This can be especially true in an *in vitro* setting, where soluble factors are free to diffuse. Also, the microenvironmental components are absent in *in vitro* screens, and in *in vivo* screens it is unlikely that a clone harboring a given genetic alteration could be able to alter the surrounding microenvironment to a level conferring it a selective advantage. Another point of relevance is that, as compared to targeted therapies, acquired resistance to cancer immunotherapy is less frequent, and this may be due, at least in part, to the need to overcome the redundant effector mechanisms that are employed by the immune system. It is therefore plausible that cancer cells would need two independent mutations to overcome T cell pressure. Screening for two concomitant events at a whole-genome scale would require experiments of a complexity that is unlikely to be achieved with current technologies, so identifying mechanisms that have to act in parallel to confer resistance in a screen would be extremely difficult at present.

Summarizing, I believe that, despite their value in revealing some of the genetic mechanisms that mitigate target cell sensitivity toward T cell-mediated killing, the current genetic screening systems fail to be informative on other aspects that may be equally relevant, and the insights they have provided thus far can only partially explain clinical immunotherapy resistance mechanisms. I foresee that in the future a number of studies will describe additional modulators of target cell sensitivity to T cell effector mechanisms, but the current strategies for analyzing cancer cell-intrinsic mechanisms of sensitivity toward T cell effector mechanisms will not elucidate aspects such as the contribution of non-cancerous tumor cells in suppression of T cell activity or the co-occurrence of multiple genetic events in resistant cells. Rather, I would expect them to identify more modulators of the known pathways.

A series of potential approaches may be utilized to overcome at least some of the limitations of the current genetic screens. For example, in order to reveal unknown soluble factors able to suppress T cell activity, pooled screens are likely not the ideal setup. A conceivable approach to identify such factors would be to perform a series of screen in an arrayed format, by for example plating a small number of cells derived from a library (either a loss-of-function or a gain-of-function library) in multiwell plates, exposing them to T cells and pooling the surviving cells to understand whether those cells had induced a soluble factor. To understand molecules that are involved in regulating known suppressive factors, such as IL-10, IL-1β or TGF-β, a possible approach could be to perform flow-based haploid genetic screens in HAP1 in a similar fashion as has been described by Brockmann et al.[43]. The fact that HAP1 are derived from KBM7, a myeloid cell line could make this cell system well-suited to screen for at least some of these soluble immunosuppressive factors. Another potentially useful, although technically difficult, approach to identify strategies that overcome resistance mechanisms would be to perform *in vivo* genetic screens by manipulating different kind of suppressive cells, such as in regulatory T cells or suppressive myeloid cells, in order to understand which factors contribute to their recruitment to the tumor site. Downside of the last two approaches, is that they would only identify modulators of known pathways, rather than the discovery of novel ones. An additional potentially valuable approach would be to perform screens in T cells for factors that would either cause or prevent a dysfunctional phenotype.

What is the cancer cell-intrinsic role of IFN-γ signaling in immunotherapy?

Over the past few years, a number of collectively very convincing pieces of evidence have accumulated showing that impairment in the IFN-γ signaling pathway is associated with acquired and intrinsic resistance toward checkpoint blockade therapies in patients and T cell attack in experimental systems. In a first study, mutations in the IFN-γ signaling pathway have been found in two out of four patients developing resistance to PD-1 blockade after an initial prolonged response[39]. Moreover, patients with mutations in genes associated with the IFN-γ signaling pathway have been found to be enriched among non-responders to both CTLA-4 and PD-1 blockade[40,41]. As discussed above, this association was functionally validated by genetic screens in which loss of IFN-γ signaling confers resistance to T cell-mediated cytotoxicity[34,35,37] and in **Chapter 7** of this thesis. In the previous paragraph I discussed that it is plausible that there are several ways, both involving cancer cell-intrinsic and -extrinsic mechanisms, for a tumor to escape from T cell pressure. Of those, the IFN-γ pathway is linear and non-redundant, so it can easily be lost by cancerous cells and in genetic screens. Additionally, it is a widely studied and well-known pathway, so

identified mutations could be readily linked to it. Moreover, it is important to note that because the IFN-γ pathway is a cancer cell-intrinsic pathway, mutational analysis could be informative, in contrast to microenvironmental factors, such as recruitment of suppressive cells or secretion of soluble mediators where mutational analysis would not be helpful.

At present, the reasons why cancer cell-intrinsic IFN-γ receptor signaling appears so important (apart from the technical reasons listed above) have not been yet fully elucidated. IFN-γ is one of the most abundantly produced cytokines following T cell activation, and it has a described pro-inflammatory and antiviral role. In **Chapter 7** of this thesis, I describe our data in which we provide evidence that IFN-γ can have a direct cytotoxic effect, in a context-dependent manner. Nevertheless, together with others in the lab, I have observed that in most cell lines IFN-γ does not have a strong cytopathic effect, but rather a mild anti-proliferative effect. These observations lead me to conclude that IFN-γ is in general not used by T cells as a key molecule to kill target cells, even if it has this effect in certain cases. Which parameters control the ultimate outcome of IFN-γ receptor signaling still needs to be revealed. As one putative model, it appears possible that certain types of cellular stress could synergize with IFN-γ and increase its toxicity. If this model is correct, a better understanding of these signals could open the path toward combinatorial therapies. On top of its anti-proliferative effect, IFN-γ enhances tumor cell visibility by increasing antigen presentation, both by inducing the immunoproteasome and by increasing the cell surface expression of MHC molecules. IFN-γ can also induce the secretion of the chemokines CXCL9, CXCL10 and CXCL11 that attract T cells by signaling through their receptor CXCR3[44].

Evidence so far strongly indicate that loss of the cancer cell-intrinsic IFN-γ receptor signaling is involved in tumor escape from T cell-based immunotherapies. Still, I think there are some aspects of this phenomenon that are incompletely understood. Firstly, it is unclear which one of the aforementioned effects is the most important in contributing to T cell-mediated tumor control. Moreover, it is currently unclear whether the sole loss of the pathway would be sufficient to explain tumor escape from T cell-based immunotherapeutic approaches. Our observations that in different cell types the cytopathic effect of IFN-γ is highly dissimilar would suggest that in some situations this pathway has major relevance. Nevertheless, in other situations, loss of IFN-γ signaling can be one of the events contributing in shifting the balance from sensitivity to insensitivity to T cell-based immunotherapeutic approaches. Another interesting observation is that in some cases patients develop resistances towards immunotherapies in which there are no known mutations in the pathway[39,45]. It would be of great importance to understand whether loss of this pathway has the

same importance for different tumors in order to develop resistance. If not, it would be very important to understand what the reasons for this are, and if this is due to specific cancer cell-intrinsic aspects such as the type of oncogenic aberrations of a given tumor or to cancer cell-extrinsic aspects, such as the type of milieu a tumor is subjected to.

At the moment a priority in the field is to further understand resistance mechanisms and the relative importance among those of the IFN-γ pathway. To identify other resistance pathways in an unbiased manner, it will be valuable to analyze large datasets of mutational and transcriptional data of patients that develop immunotherapy resistance. Possibly the insights emerging from these analyses, and also from more refined genetic screening systems, will allow us to generate novel lines of therapies that aim at counteracting the backup suppressive mechanisms that limit the activity of the current generation cancer immunotherapies.

Concluding remarks and future perspective

Throughput my PhD work, I have been fascinated by the power and rapid development of genetic engineering techniques, and I think that the potential of these technologies when applied to complex problems is in large part what drove me to explore the various field of biology I have worked on. Together with my colleagues, I have firstly applied gene transfer technologies to the redirection of T cell specificity, by trying to overcome limitations related to non-viral gene transfer systems. In the second part of my PhD work, I focused on genetic screens, which, again in collaboration with others, I applied to understanding molecular mechanisms of escape from T cell attack and to reveal mechanisms of PD-L1 regulation. In this effort, we identified a previously unappreciated, IFN-γ-mediated cytotoxic mechanism of T cells and we discovered the strong dependency of PD-L1 on the proteins CMTM6 and CMTM4 for its surface expression. The work presented in this thesis may on the one hand facilitate the clinical application of non-viral-based gene transfer systems in T cells. On the other hand, the more fundamental discoveries related to IFN-γ-mediated tumor cell killing and PD-L1 regulation may help to further understand resistance toward immunotherapies and how to overcome them.

References

1 Rosenberg, S. A. *et al.* Gene transfer into humans--immunotherapy of patients with advanced melanoma, using tumor-infiltrating lymphocytes modified by retroviral gene transduction. *N Engl J Med* **323**, 570-578, doi:10.1056/NEJM199008303230904 (1990).

2 Naldini, L. Gene therapy returns to centre stage. *Nature* **526**, 351-360, doi:10.1038/nature15818 (2015).

3 Newrzela, S. *et al.* Resistance of mature T cells to oncogene transformation. *Blood* **112**, 2278-2286, doi:10.1182/blood-2007-12-128751 (2008).

4 June, C. H., Riddell, S. R. & Schumacher, T. N. Adoptive cellular therapy: a race to the finish line. *Sci Transl Med* **7**, 280ps287, doi:10.1126/scitranslmed.aaa3643 (2015).

5 Schumacher, T. N. & Schreiber, R. D. Neoantigens in cancer immunotherapy. *Science* **348**, 69-74, doi:10.1126/science.aaa4971 (2015).

6 Peng, P. D. *et al.* Efficient nonviral Sleeping Beauty transposon-based TCR gene transfer to peripheral blood lymphocytes confers antigen-specific antitumor reactivity. *Gene Ther* **16**, 1042-1049, doi:10.1038/gt.2009.54 (2009).

7 Ott, P. A. *et al.* An immunogenic personal neoantigen vaccine for patients with melanoma. *Nature* **547**, 217-221, doi:10.1038/nature22991 (2017).

8 Sahin, U. *et al.* Personalized RNA mutanome vaccines mobilize poly-specific therapeutic immunity against cancer. *Nature* **547**, 222-226, doi:10.1038/nature23003 (2017).

9 Kvistborg, P. *et al.* Anti-CTLA-4 therapy broadens the melanoma-reactive CD8+ T cell response. *Sci Transl Med* **6**, 254ra128, doi:10.1126/scitranslmed.3008918 (2014).

10 Dudley, M. E. *et al.* Randomized Selection Design Trial Evaluating CD8+-Enriched Versus Unselected Tumor-Infiltrating Lymphocytes for Adoptive Cell Therapy for Patients With Melanoma. *Journal of Clinical Oncology* **31**, 2152-2159, doi:10.1200/jco.2012.46.6441 (2013).

11 Ribas, A. & Wolchok, J. D. Cancer immunotherapy using checkpoint blockade. *Science* **359**, 1350-1355, doi:10.1126/science.aar4060 (2018).

12 Arce Vargas, F. *et al.* Fc Effector Function Contributes to the Activity of Human Anti-CTLA-4 Antibodies. *Cancer Cell* **33**, 649-663 e644, doi:10.1016/j.ccell.2018.02.010 (2018).

13 Hellmann, M. D. *et al.* Tumor Mutational Burden and Efficacy of Nivolumab Monotherapy and in Combination with Ipilimumab in Small-Cell Lung Cancer. *Cancer Cell*, doi:10.1016/j.ccell.2018.04.001 (2018).

14 Rizvi, N. A. *et al.* Cancer immunology. Mutational landscape determines sensitivity to PD-1 blockade in non-small cell lung cancer. *Science* **348**, 124-128, doi:10.1126/science.aaa1348 (2015).

15 Snyder, A. *et al.* Genetic basis for clinical response to CTLA-4 blockade in melanoma. *N Engl J Med* **371**, 2189-2199, doi:10.1056/NEJMoa1406498 (2014).

16 Seiwert, T. Y. *et al.* Safety and clinical activity of pembrolizumab for treatment of recurrent or metastatic squamous cell carcinoma of the head and neck (KEYNOTE-012): an open-label, multicentre, phase 1b trial. *Lancet Oncol* **17**, 956-965, doi:10.1016/S1470-2045(16)30066-3 (2016).

17 Ayers, M. *et al.* IFN-gamma-related mRNA profile predicts clinical response to PD-1 blockade. *J Clin Invest* **127**, 2930-2940, doi:10.1172/JCI91190 (2017).

18 Tumeh, P. C. *et al.* PD-1 blockade induces responses by inhibiting adaptive immune resistance. *Nature* **515**, 568-571, doi:10.1038/nature13954 (2014).

19 Gros, A. *et al.* Prospective identification of neoantigen-specific lymphocytes in the peripheral blood of melanoma patients. *Nat Med* **22**, 433-438, doi:10.1038/nm.4051 (2016).

20 Gros, A. *et al.* PD-1 identifies the patient-specific CD8(+) tumor-reactive repertoire infiltrating human tumors. *J Clin Invest* **124**, 2246-2259, doi:10.1172/JCI73639 (2014).

21 Thommen, D. S. *et al.* A transcriptionally and functionally distinct PD-1(+) CD8(+) T cell pool with predictive potential in non-small-cell lung cancer treated with PD-1 blockade. *Nat Med*, doi:10.1038/s41591-018-0057-z (2018).

22 Mariathasan, S. *et al.* TGFbeta attenuates tumour response to PD-L1 blockade by contributing to exclusion of T cells. *Nature* **554**, 544-548, doi:10.1038/nature25501 (2018).

23 Yarchoan, M., Hopkins, A. & Jaffee, E. M. Tumor Mutational Burden and Response Rate to PD-1 Inhibition. *N Engl J Med* **377**, 2500-2501, doi:10.1056/NEJMc1713444 (2017).

24 Pagès, F. *et al.* International validation of the consensus Immunoscore for the classification of colon cancer: a prognostic and accuracy study. *The Lancet*, doi:10.1016/S0140-6736(18)30789-X.

25 Simoni, Y. *et al.* Bystander CD8(+) T cells are abundant and phenotypically distinct in human tumour infiltrates. *Nature* **557**, 575-579, doi:10.1038/s41586-018-0130-2 (2018).

26 Burr, M. L. *et al.* CMTM6 maintains the expression of PD-L1 and regulates anti-tumour immunity. *Nature* **549**, 101-105, doi:10.1038/nature23643 (2017).

27 Hemler, M. E. Tetraspanin functions and associated microdomains. *Nat Rev Mol Cell Biol* **6**, 801-811, doi:10.1038/nrm1736 (2005).

28 Levy, S. & Shoham, T. The tetraspanin web modulates immune-signalling complexes. *Nat Rev Immunol* **5**, 136-148, doi:10.1038/nri1548 (2005).

29 Maecker, H. T. & Levy, S. Normal lymphocyte development but delayed humoral immune response in CD81-null mice. *J Exp Med* **185**, 1505-1510 (1997).

30 Miyazaki, T., Muller, U. & Campbell, K. S. Normal development but differentially altered proliferative responses of lymphocytes in mice lacking CD81. *EMBO J* **16**, 4217-4225 (1997).

31 Tsitsikov, E. N., Gutierrez-Ramos, J. C. & Geha, R. S. Impaired CD19 expression and signaling, enhanced antibody response to type II T independent antigen and reduction of B-1 cells in CD81-deficient mice. *Proc Natl Acad Sci U S A* **94**, 10844-10849 (1997).

32 Shoham, T. *et al.* The tetraspanin CD81 regulates the expression of CD19 during B cell development in a postendoplasmic reticulum compartment. *J Immunol* **171**, 4062-4072 (2003).

33 Bernards, R. Finding effective cancer therapies through loss of function genetic screens. *Curr Opin Genet Dev* **24**, 23-29, doi:10.1016/j.gde.2013.11.007 (2014).

34 Patel, S. J. *et al.* Identification of essential genes for cancer immunotherapy. *Nature* **548**, 537-542, doi:10.1038/nature23477 (2017).

35 Pan, D. *et al.* A major chromatin regulator determines resistance of tumor cells to T cell-mediated killing. *Science* **359**, 770-775, doi:10.1126/science.aao1710 (2018).

36 Kearney, C. J. *et al.* Tumor immune evasion arises through loss of TNF sensitivity. *Sci Immunol* **3**, doi:10.1126/sciimmunol.aar3451 (2018).

37 Manguso, R. T. *et al.* In vivo CRISPR screening identifies Ptpn2 as a cancer immunotherapy target. *Nature* **547**, 413-418, doi:10.1038/nature23270 (2017).

38 Sade-Feldman, M. *et al.* Resistance to checkpoint blockade therapy through inactivation of antigen presentation. *Nat Commun* **8**, 1136, doi:10.1038/s41467-017-01062-w (2017).

39 Zaretsky, J. M. *et al.* Mutations Associated with Acquired Resistance to PD-1 Blockade in Melanoma. *N Engl J Med* **375**, 819-829, doi:10.1056/NEJMoa1604958 (2016).

40 Gao, J. *et al.* Loss of IFN-gamma Pathway Genes in Tumor Cells as a Mechanism of Resistance to Anti-CTLA-4 Therapy. *Cell* **167**, 397-404 e399, doi:10.1016/j.cell.2016.08.069 (2016).

41 Shin, D. S. *et al.* Primary Resistance to PD-1 Blockade Mediated by JAK1/2 Mutations. *Cancer Discov* **7**, 188-201, doi:10.1158/2159-8290.CD-16-1223 (2017).

42 Shankaran, V. *et al.* IFNgamma and lymphocytes prevent primary tumour development and shape tumour immunogenicity. *Nature* **410**, 1107-1111, doi:10.1038/35074122 (2001).

43 Brockmann, M. *et al.* Genetic wiring maps of single-cell protein states reveal an off-switch for GPCR signalling. *Nature* **546**, 307-311, doi:10.1038/nature22376 (2017).

44 Groom, J. R. & Luster, A. D. CXCR3 ligands: redundant, collaborative and antagonistic functions. *Immunol Cell Biol* **89**, 207-215, doi:10.1038/icb.2010.158 (2011).

45 Donia, M. *et al.* Acquired Immune Resistance Follows Complete Tumor Regression without Loss of Target Antigens or IFNgamma Signaling. *Cancer Res* **77**, 4562-4566, doi:10.1158/0008-5472.CAN-16-3172 (2017).

Chapter 9 - Addenda

English Summary

The notion that tumors are not exclusively composed by cancerous cells has been appreciated for more than 150 years[1-6], even if the importance of the non-cancerous cells in tumor development and progression has been controversial until the 1990s. Up to that point, cancer research was largely dominated by research aiming to decipher the molecular mechanisms that lead to cellular transformation[7-9]. Nowadays, it is appreciated that cancerous cells can only survive in a favorable environment, and that cancer cell-intrinsic and -extrinsic aspects of tumors are two faces of the same coin[10]. Indeed, a large body of literature has shown that tumor-resident non-cancerous cells have a series of tumor-promoting and tumor-suppressing functions[7]. Of the non-cancerous tumor-resident cells, special attention has been given to tumor-infiltrating immune cells[11], and evasion from selective pressure exerted by the immune system is now acknowledged as one of the hallmarks of cancer[12]. Among the cells of the immune system, cytotoxic T cells are considered particularly able to counteract cancer cell growth[13]. A series of studies have provided indirect and direct evidence for a role of T cells in tumor control: tumor cells can be recognized by T cells[14-17], T cell can shape the tumor in highly immunogenic mouse models[18] and therapeutic interventions able to reinvigorate T cells can lead to objective clinical benefit in cancer patients[19,20].

In order for a patient to achieve an adequate antitumoral T cell response, two conditions need to be met. First, the presence of a population of T cells able to recognize the tumor is required. Second, these cells need to be able to effectively eliminate cancer cells once they reach the tumor site. In order to do this, T cells not only need to be insensitive to local suppressive mechanisms at the tumor site, but tumor cells also need to be sensitive to T cell effector mechanisms. The work presented in this thesis is centered around genetic manipulation approaches that on the one hand aim at improving non-viral gene transfer-based approaches to redirect T cells, and on the other hand at the use of genetic screens in order to understand the conditions under which T cells are able to effectively kill tumor cells.

Transposon-based T cell redirection

In **Chapter 2** of this thesis we discuss the intratumoral TCR repertoire of infiltrating T cells, and we propose ways to use it for T cell redirection, in order to increase the pool of tumor reactive T cells. We suggest that the use of transposon-mediated gene transfer may have a number of advantages over the currently used technologies. The main issues related to redirection of T cells using non-viral gene transfer systems, such as transposons, are formed by their high level of toxicity and by their low efficiency

in generating stably modified cells. In **Chapter 3** of this thesis we generate a system that allows efficient enrichment of transposon-redirected T cells in a traceless way, and in **Chapter 4** we identified a compound that to some extent mitigates the toxicity induced in T cells upon transposon-based gene transfer.

Regulation of PD-L1 expression

One of the mechanisms that cancer cells employ to escape from T cell pressure is expression of PD-L1 on their surface. Because of its ability to bind to its ligand PD-1 that is expressed on T cells, PD-L1 is able to suppress T cell effector function. In **Chapter 5** of this thesis we extensively review the literature on PD-L1 function and regulation of expression, and we discuss its utility as a predictive marker. In **Chapter 6** we used a genetic screen-based approach to discover novel regulators of PD-L1 expression, and we identified two previously undescribed post-translational regulators of PD-L1 expression, CMTM6 and CMTM4.

Cancer cell-intrinsic resistance to T cell effector mechanisms

In order to explore whether loss of expression of certain genes can confer resistance towards T cell mediated killing, in **Chapter 7** of this thesis we performed a loss-of-function genetic screen, in which we interrogated genes for their effect on sensitivity of tumor cells to cytotoxic T cells. We identified that, in the HAP1 cell system that was used, interferon (IFN)-γ is the main driver of toxicity, and that loss of the SLFN11 gene mitigates IFN-γ mediated toxicity. We observed that this effect is context-specific, and we note that these data indicate a link between DNA damage response and IFNGR signaling that deserves further attention.

Concluding remarks and future perspective

This thesis is focused on the use of genetic manipulation techniques to approach immunologically relevant issues. The first part of this thesis focuses on the development of approaches that can help to overcome limitations related to non-viral gene transfer systems. The second part of this thesis focuses on the use of genetic screens to identify a previously unappreciated, IFN-γ-mediated, cytotoxic mechanism of T cells and to identify two previously undescribed post-translational regulators of PD-L1, CMTM6 and CMTM4.

As such, the work presented in this thesis may facilitate the clinical application of non-viral-based gene transfer systems in T cells and increases our understanding of resistance mechanisms towards cancer immunotherapies and approaches to overcome them.

Nederlandse Samenvatting

Het feit dat tumoren niet enkel bestaan uit kankercellen is al ruim 150 jaar bekend[1-6]. Desondanks bleef de rol die niet-neoplastische cellen spelen in de ontwikkeling van tumoren onduidelijk tot de jaren '90. Tot die tijd was kankeronderzoek voornamelijk gericht op het ontcijferen van de moleculaire mechanismen die leiden tot de transformatie van een kankercel[7-9]. Tegenwoordig weten we echter dat kankercellen enkel kunnen overleven in een omgeving die dat toestaat, en dat de intrinsieke en extrinsieke aspecten van kankercellen in tumoren als twee zijden van dezelfde medaille zijn[10]. Een grote hoeveelheid studies heeft aangetoond dat de niet-neoplastische cellen in de tumor zowel een positieve als negatieve invloed kunnen hebben op de progressie van kanker[7]. Veel aandacht is daarbij uitgegaan naar immuun cellen die aanwezig zijn in de tumor[11]. Als gevolg daarvan is het ontwijken van de selectiedruk die het immuunsysteem uitoefent op de tumor nu erkend als algemeen kenmerk van kanker[12]. Van de verschillende immuun cellen worden voornamelijk de cytotoxische T cellen beschouwd als het celtype dat de groei van kankercellen kan remmen[13]. Een reeks studies heeft zowel direct als indirect aangetoond dat T cellen een belangrijke rol spelen in het in toom houden van de tumor: zo kunnen kankercellen worden herkend door T cellen[14-17], kunnen T cellen tumorgroei voorkomen of remmen in immunogene muismodellen voor kanker[18], en blijken therapieën die gericht zijn op het activeren van T cellen succesvol in de behandeling van sommige kankerpatiënten[19,20].

Om een goede anti-tumor T cel activatie te krijgen moet er aan twee voorwaarden voldaan worden. Ten eerste moet er een populatie T cellen aanwezig zijn in de tumor die de kankercellen kan detecteren, en ten tweede moeten deze cellen in staat zijn de kankercellen op te ruimen. Hiertoe moeten de T cellen niet alleen de aanwezige immunosuppressieve mechanismen in het tumor milieu weerstaan, maar moet de tumor ook gevoelig zijn voor de effector mechanismen van de T cellen. Het onderzoek in dit proefschrift behelst het verbeteren van non-virale gentransfer methoden om T cellen aan te passen met behulp van genetische manipulatie, alsmede het door middel van genetische screening in kaart brengen onder welke omstandigheden T cellen de kankercellen effectief kunnen doden.

Aanpassing van T cellen met behulp van transposons

In **Hoofdstuk 2** van dit proefschrift bespreken we het TCR repertoire van de in de tumor aanwezige T cellen, en opperen we manieren om dit te moduleren, opdat de hoeveelheid tumor-reactieve T cellen vergroot kan worden. We laten zien dat gentransfer met behulp van transposons een aantal voordelen heeft op de huidige technologieën. Het grootste probleem met betrekking tot T cel modulatie met

non-virale gentransfer systemen, zoals transposons, is de hoge toxiciteit en lage efficiëntie van het genereren van stabiel gemodificeerde cellen. In **Hoofdstuk 3** van dit proefschrift beschrijven we een methode die gebruikt kan worden om door transposons aangepaste T cellen te kunnen verrijken. In **Hoofdstuk 4** beschrijven we de identificatie van een molecuul welke de toxiciteit van transposon gentransfer in T cellen voor een deel kan verminderen.

Regulatie van de expressie van PD-L1

Een van de mechanismen waarmee kankercellen de aanval van T cellen kunnen ontwijken is expressie van PD-L1 op het celmembraan. Omdat PD-L1 kan binden aan PD-1, wat tot expressie wordt gebracht door T cellen, kan PD-L1 zorgen voor onderdrukking van effector functies van T cellen. In **Hoofdstuk 5** van dit proefschrift geven we een overzicht van de literatuur op het gebied van de functie en de regulatie van expressie van PD-L1, en bespreken we de bruikbaarheid van dit molecuul als voorspellende marker. In **Hoofdstuk 6** gebruiken we genetische screens om nieuwe regulatoren van PD-L1 expressie te identificeren, welke hebben geleid tot de ontdekking van twee voorheen onbekende post-translationele regulatoren van PD-L1, CMTM6 en CMTM4.

Kankercel-intrinsieke resistentie tegen T cel effector mechanismen

Om te achterhalen of het verlies van expressie van bepaalde genen resistentie tegen T cel effector mechanismen teweeg kan brengen, hebben we in **Hoofdstuk 7** van dit proefschrift een loss-of-function genetische screen uitgevoerd, waarbij we hebben gekeken naar genen die betrokken zijn bij gevoeligheid van kankercellen voor aanvallen van T cellen. We laten zien dat in het HAP1 cel modelsysteem interferon (IFN)-γ het belangrijkste effector molecuul is, en dat verlies van het SLFN11 gen dit toxische effect afzwakt. We laten zien dat dit effect context-specifiek is en dat er een verband bestaat tussen de DNA schade respons van de cel en IFNGR signalering, welke verder onderzocht dient te worden.

Conclusies en toekomstperspectieven

Dit proefschrift beschrijft hoe genetische manipulatie gebruikt kan worden voor immunologisch onderzoek. Het eerste deel gaat over de ontwikkeling van manieren die kunnen helpen bij het verbeteren van non-virale gentransfer systemen. Het tweede deel van dit proefschrift gaat over het gebruik van genetische screens om een voorheen ondergewaardeerd, IFN-γ-gemedieerd, cytotoxisch mechanisme van T cellen te ontrafelen en om twee voorheen onbekende post-translationele regulatoren van PD-L1, CMTM6 en CMTM4, te identificeren.

Als zodanig zou het onderzoek dat in dit proefschrift wordt beschreven gebruikt kunnen worden voor klinische toepassingen van non-virale gentransfer systemen in T cellen en verhoogd het ons begrip van resistentiemechanismen tegen immuuntherapieën voor kanker en manieren om deze te overwinnen.

References

1 Jodele, S., Blavier, L., Yoon, J. M. & DeClerck, Y. A. Modifying the soil to affect the seed: role of stromal-derived matrix metalloproteinases in cancer progression. *Cancer metastasis reviews* **25**, 35-43, doi:10.1007/s10555-006-7887-8 (2006).

2 Mueller, M. M. & Fusenig, N. E. Friends or foes - bipolar effects of the tumour stroma in cancer. *Nature reviews. Cancer* **4**, 839-849, doi:10.1038/nrc1477 (2004).

3 Paget, S. The distribution of secondary growths in cancer of the breast. 1889. *Cancer metastasis reviews* **8**, 98-101 (1989).

4 Schmidt, A. & Weber, O. F. In memoriam of Rudolf virchow: a historical retrospective including aspects of inflammation, infection and neoplasia. *Contrib Microbiol* **13**, 1-15, doi:10.1159/000092961 (2006).

5 Talmadge, J. E. & Fidler, I. J. AACR centennial series: the biology of cancer metastasis: historical perspective. *Cancer research* **70**, 5649-5669, doi:10.1158/0008-5472.can-10-1040 (2010).

6 Witz, I. P. & Levy-Nissenbaum, O. The tumor microenvironment in the post-PAGET era. *Cancer letters* **242**, 1-10, doi:10.1016/j.canlet.2005.12.005 (2006).

7 Maman, S. & Witz, I. P. A history of exploring cancer in context. *Nature reviews. Cancer*, doi:10.1038/s41568-018-0006-7 (2018).

8 Vogelstein, B. & Kinzler, K. W. The multistep nature of cancer. *Trends in genetics : TIG* **9**, 138-141 (1993).

9 Vogelstein, B. & Kinzler, K. W. Cancer genes and the pathways they control. *Nature medicine* **10**, 789-799, doi:10.1038/nm1087 (2004).

10 Wellenstein, M. D. & de Visser, K. E. Cancer-Cell-Intrinsic Mechanisms Shaping the Tumor Immune Landscape. *Immunity* **48**, 399-416, doi:10.1016/j.immuni.2018.03.004 (2018).

11 Junttila, M. R. & de Sauvage, F. J. Influence of tumour micro-environment heterogeneity on therapeutic response. *Nature* **501**, 346-354, doi:10.1038/nature12626 (2013).

12 Hanahan, D. & Weinberg, R. A. Hallmarks of cancer: the next generation. *Cell* **144**, 646-674, doi:10.1016/j.cell.2011.02.013 (2011).

13 Schreiber, R. D., Old, L. J. & Smyth, M. J. Cancer immunoediting: integrating immunity's roles in cancer suppression and promotion. *Science (New York, N.Y.)* **331**, 1565-1570, doi:10.1126/science.1203486 (2011).

14 Kvistborg, P. *et al.* TIL therapy broadens the tumor-reactive CD8(+) T cell compartment in melanoma patients. *Oncoimmunology* **1**, 409-418 (2012).

15 van der Bruggen, P. *et al.* A gene encoding an antigen recognized by cytolytic T lymphocytes on a human melanoma. *Science (New York, N.Y.)* **254**, 1643-1647 (1991).

16 van Rooij, N. *et al.* Tumor exome analysis reveals neoantigen-specific T-cell reactivity in an ipilimumab-responsive melanoma. *J Clin Oncol* **31**, e439-442, doi:10.1200/JCO.2012.47.7521 (2013).

17 Wolfel, T. *et al.* A p16INK4a-insensitive CDK4 mutant targeted by cytolytic T lymphocytes in a human melanoma. *Science (New York, N.Y.)* **269**, 1281-1284 (1995).

18 Shankaran, V. *et al.* IFNgamma and lymphocytes prevent primary tumour development and shape tumour immunogenicity. *Nature* **410**, 1107-1111, doi:10.1038/35074122 (2001).

19 Ribas, A. & Wolchok, J. D. Cancer immunotherapy using checkpoint blockade. *Science (New York, N.Y.)* **359**, 1350-1355, doi:10.1126/science.aar4060 (2018).

20 Rosenberg, S. A. *et al.* Durable complete responses in heavily pretreated patients with metastatic melanoma using T-cell transfer immunotherapy. *Clinical cancer research : an official journal of the American Association for Cancer Research* **17**, 4550-4557, doi:10.1158/1078-0432.ccr-11-0116 (2011).

Acknowledgements

The work of this thesis could not have been possible without the people I had around. I had wonderful time at the NKI, and I owe much to many people I was very fortunate to work and interact with.

At first, Ton, I feel enormously privileged about the opportunity I've had of working with you. I could not have wished any better and more inspiring mentorship. You have been a unique example for me. Thanks for teaching me critical thinking and scientific creativity, for the great support and freedom you gave me, and thanks for believing in me even in the more difficult periods of my PhD.

An important part of my PhD work was focused on applying genetic screens in cancerous cell to address immunologically relevant questions. This work could not have been possible without the precious and stimulating collaboration with Thijn and his laboratory. Thijn, thanks for being such an inspiring and dedicated collaborator.

I was very fortunate to interact with many inspiring PIs, whose advice and suggestions where very instrumental to my work. Jannie, Karin, Sjaak, Daniel, Wouter, Kees, Heinz, Christian, John, Leila, and Pia, thanks a lot for all the comments and discussions.

Andreas, when I joined the lab you guided me, it was great working with you and from you I have learned scientific rigor and method. More importantly, you have been a great friend during those years.

Raquel, during my PhD we have done an enormous amount of work together. I have always loved working and discussing results with you and the quantity of pipetting you have done for this thesis is impressive!

Chong, I feel very lucky I had the opportunity of collaborating so closely with you. Working with you had been fantastic and you have become a great friend for me. I feel together we did something really special by pushing our work to our limits. It was extremely intense, but I loved the long hours working side by side with you till late in the night.

Marjolein, I had real great time in working with you. You have been very perseverant and dedicated and I am sure you will keep on doing great.

Lucas, the collaboration with Thijn's laboratory would not have been possible without you, I really had great time in working with such a brilliant scientist as you are. Astrid, even if we only collaborated briefly I really enjoyed it!

Meike, it was really fun to work with you at the beginning of your time here. Anne, Paula had been really great to share the office with you.

Max, my dear friend! You have no idea how much I am missing the daily afternoon coffee and the late-night-drinking with you. I really hope you and Tessa will move to New York.

To the whole KdV group, thanks for adopting me, when I was keeping on invading your offices for drinking coffee and chitchatting.

Also, I would not have loved my time in Amsterdam so much without the many friend I have, Maarten, Jules, Joost, Anna, KK, Lorenzo B., Lorenzo S., Feline, Ferenc, Leila, Wouter, Luca Brasi, Kong, Marit, Sander, Laura, Carsten, Gavin, Bo, and many others, thanks for the great time!

Thanks to everyone else at B3 and B6, past and present. Interacting with so many bright people made my time at the NKI awesome.

Mamma, papa, Alfredo, e Guglielmo, anche se torno sempre troppo poco in Italia, grazie per il supporto e per aver sempre creduto in me.

Camilla, questi anni sono stati fantastici, ma senza di te niente sarebbe stato lo stesso. Grazie per aver reso speciale ogni momento. Mi manchi tantissimo e non vedo l'ora che arrivi a New York.

Curriculum vitae

Riccardo Mezzadra was born on February, the 5th 1985 in Milan, Italy. In 2004 he completed secondary education at the scientific high school "Alessandro Volta" in Milan, Italy. The same year he started his bachelor studies in medical and pharmaceutical biotechnology at Vita-Salute San Raffaele University, in Milan, Italy. He graduated in 2007 with a thesis work based on the analysis of integration sites of lentiviral vectors in hematopoietic stem cells, in order to understand potential genotoxicity aspect of gene therapy approaches for β thalassemia under the supervision of Professor Giuliana Ferrari. Also in 2007, he started his master in in medical, molecular and cellular biotechnology still at Vita-Salute San Raffaele University. He graduated in 2010 with a work once again performed under the supervision of Professor Giuliana Ferrari, in which he was exploring how lentiviral integration can affect the expression of neighboring genes, still to understand potential genotoxicity aspect of gene therapy approaches for β thalassemia. From 2006 till the end of his undergraduate studies, he constantly attended the laboratory of Giuliana Ferrari as a volunteer student, in which he developed a strong fascination for genetic manipulation. Also during that time, he contributed to the identification of aberrant splicing as a previously unappreciated mechanism of potential gene therapy-related genotoxicity. In 2010 he started his PhD work in the lab of Ton Schumacher at the Netherlands Cancer Institute in Amsterdam, the Netherlands. Results of his PhD studies are presented in this thesis. Riccardo will follow his interest for genetic manipulation, cancer and immunology in the laboratory of Scott Lowe, at Memorial Sloan Kettering Cancer Center, in New York, USA, where he will be studying microenvironmental components of tumor in spontaneous models of cancer.

Publications

Low and variable tumor-reactivity of the intratumoral TCR repertoire in human cancers.
Scheper W, Kelderman S, Fanchi LF, Linnemann C, Bendle G, de Rooij MAJ, Hirt C, **Mezzadra R**, Slagter M,Dijkstra K, Kluin R, Snaebjornsson P, Milne K, Nelson BH, Zijlmans H, Kenter G, Voest E, Haanen JBAG, and Schumacher TN
Nat Med., Accepted for publication

Regulation and Function of the PD-L1 Checkpoint.
Sun C*, **Mezzadra R***, Schumacher TN*.
Immunity. 2018 Mar 20;48(3):434-452.
* These authors contributed equally

Identification of CMTM6 and CMTM4 as PD-L1 protein regulators.
Mezzadra R*, Sun C*, Jae LT*, Gomez-Eerland R, de Vries E, Wu W, Logtenberg MEW, Slagter M, Rozeman EA, Hofland I, Broeks A, Horlings HM, Wessels LFA, Blank CU, Xiao Y, Heck AJR, Borst J, Brummelkamp TR#, Schumacher TNM#.
Nature. 2017 Sep 7;549(7670):106-110.
* These authors contributed equally, # Corresponding authors

Mutations Associated with Acquired Resistance to PD-1 Blockade in Melanoma.
Zaretsky JM, Garcia-Diaz A, Shin DS, Escuin-Ordinas H, Hugo W, Hu-Lieskovan S, Torrejon DY, Abril-Rodriguez G, Sandoval S, Barthly L, Saco J, Homet Moreno B, **Mezzadra R**, Chmielowski B, Ruchalski K, Shintaku IP, Sanchez PJ, Puig-Saus C, Cherry G, Seja E, Kong X, Pang J, Berent-Maoz B, Comin-Anduix B, Graeber TG, Tumeh PC, Schumacher TN, Lo RS, Ribas A.
N Engl J Med. 2016 Sep 1;375(9):819-29.

A Traceless Selection: Counter-selection System That Allows Efficient Generation of Transposon and CRISPR-modified T-cell Products.
Mezzadra R, Hollenstein A, Gomez-Eerland R, Schumacher TN.
Mol Ther Nucleic Acids. 2016 Mar 22;5:e298.

TCR repertoires of intratumoral T-cell subsets.
Linnemann C, **Mezzadra R**, Schumacher TN.
Immunol Rev. 2014 Jan;257(1):72-82. doi: 10.1111/imr.12140. Review.

Lentiviral vector integration in the human genome induces alternative splicing and generates aberrant transcripts.
Moiani A, Paleari Y, Sartori D, **Mezzadra R**, Miccio A, Cattoglio C, Cocchiarella F, Lidonnici MR, Ferrari G, Mavilio F.
J Clin Invest. 2012 May;122(5):1653-66.

Correction of beta-thalassemia major by gene transfer in haematopoietic progenitors of pediatric patients.
Roselli EA, **Mezzadra R**, Frittoli MC, Maruggi G, Biral E, Mavilio F, Mastropietro F, Amato A, Tonon G, Refaldi C, Cappellini MD, Andreani M, Lucarelli G, Roncarolo MG, Marktel S, Ferrari G.
EMBO Mol Med. 2010 Aug;2(8):315-28.